

# Petrophysical and geomechanical characterization of a marginal (Wabi) field reservoir in north-central Niger Delta.

ZORASI, C.B.

2019

The author of this thesis retains the right to be identified as such on any occasion in which content from this thesis is referenced or re-used. The licence under which this thesis is distributed applies to the text and any original images only – re-use of any third-party content must still be cleared with the original copyright holder.

**PETROPHYSICAL AND GEOMECHANICAL CHARACTERIZATION OF  
A MARGINAL (WABI) FIELD RESERVOIR IN NORTH CENTRAL  
NIGER DELTA**

**ZORASI, COLLINS BARIBOR**

**BSc, MSc (Applied Geophysics)**

**1417713**

PETROPHYSICAL AND GEOMECHANICAL CHARACTERIZATION OF A  
MARGINAL (WABI) FIELD RESERVOIR IN NORTH CENTRAL NIGER  
DELTA

ZORASI, COLLINS BARIBOR

BSc, MSc (Applied Geophysics)

1417713

A thesis submitted in partial fulfillment of the  
requirements of the  
Robert Gordon University  
for the degree of Master of Research

This research programme was carried out in  
Collaboration with Schlumberger, Aberdeen.

September 2019

## **Dedication**

I hereby dedicate this thesis to Almighty God for his provisions of life, unmerited favour and wisdom to accomplish this research work and; to my grandmother Mrs. Leyorma Tanen who had given me words of encouragement and had been keen for my success in life. This thesis is also dedicated to my lovely wife Mrs. Zorasi Happy Barineka.

## **Acknowledgements**

It is rare and almost impossible for a research work such as this to be carried out successfully without meaningful contributions from others by way of moral, academic, financial as well as spiritual encouragement and support. It is in this light that I wish to pay tribute to Almighty God for his gracious gift of health, provision and wisdom for completing this thesis in his Glory.

I wish to express my sincere thanks and appreciation to my supervisory team Dr. Nadimul Faisal, Dr. Sheikh Islam and Dr. Gbenga Oluyemi whose advice, constructive criticism, positive suggestions and materials contributed so much to the success of this thesis. Thanks to my Lecturers/academic staff, Prof. Bab, Oyeneyin, Dr. Colin Thompson, Dr Gelareh Holbrook, Dr. James Cunningham and Prof. Richard Laing for their academic advice and support. I really appreciate Dr. Fabian Krzikalla Schlumberger Aberdeen for his advice and materials support.

It is my pleasure to acknowledge. Mr. Huub Strengh of Total Exploration and Production Nigeria Limited for the provision of data used in this research and Mr. Adeyiga Adeyemi of the Department of Petroleum Resources for his kind consideration towards the data collection. My heartfelt gratitude also goes to Dr. Mammah Sylvester for his assistance through various means to ensure that I am successful in my endeavour and the special joy he has added to my life.

It was an honour to be chosen as a recipient of the most prestigious Petroleum Technology Development Fund (PTDF) scholarship award, without their financial support I would not be able to complete this study on time. I really acknowledge your support.

I will remain grateful to my family members especially Mrs. Tanen Sila Rose, Uncle Zorasi John and all well-wishers who contributed in one way or the other toward the success of this thesis I say thank you. I also wish to acknowledge my colleague Mr. Abbey Dearson for the time spent to proofread this report.

**ZORASI, Collins Baribor**

## ABSTRACT

The aim of this study is to evaluate marginal field petrophysical and geomechanical parameters and to develop a model for analysis of geomechanical problems to mitigate stress related issues in drilling, development and reservoir management for Wabi field, onshore Niger Delta.

The increase in oil and gas demand globally has necessitated the re-evaluation of mature depleted and marginal fields for enhancement of hydrocarbon recovery and development in the Niger delta province. These oil and gas fields are situated in the young sedimentary rocks known as shaly-sand formation basin called Tertiary Niger delta. Tertiary Niger Delta is an unconsolidated formation which depositional environment had led to production and development difficulties due to related geomechanical issue possibilities such as weak reservoir rocks, low pressure (depleted reservoir), stack or multiple reservoirs with thick net pay and high porosity. The methodology leverage on integrated approach (seismic, core, wireline logs and DST in-situ stress measurements), for continuous and static measurements along the borehole record of mechanical properties of the rock penetrated for petrophysical and geomechanical characterization of Wabi field.

To understand the current condition of this field of study, identification of stress state and mechanical rock properties was investigated for reservoir development and management. Therefore, this research focuses on geomechanical characterisation for development of geomechanical model for predicting fault reactivation, fractures and sand production which leads to compaction and subsidence.

In summary, the followings conclusions are made: Wabi field has pockets of potential hydrocarbon reserves at different intervals with good reservoir qualities to enhance its development for production. Also, rock strength estimation in this field shows that the reservoir is stable; however, production of hydrocarbon from these zones may lead to subsidence. To mitigate for this futuristic event reservoir pressure maintenance should be plan for. If injection will be anticipated the appropriate pressure should be used not to fracture or cause fault reactivation in the wells. The results of this study show the estimation of hydrocarbon reserve and help to avoid and predict geomechanical related problems and devise a mitigating strategy for sanding management. Finally, the results should be beneficial to marginal field's operators who may venture into acquisition of marginal fields with limited resources and needs to maximize profits.

## TABLE OF CONTENTS

Title Page	i
Dedication	iii
Acknowledgement	iv
Abstract	v
Table of Contents	vi
List of Figures	x
List of Tables	xiii
Nomenclature	xiii

### CHAPTER 1: INTRODUCTION

1.1	Research context	1
1.2	Motivation of the study/statement of the problems	5
1.3	Research aims	5
1.4	Objectives	6
1.5	Contribution to knowledge/justification of the study	6
1.6	Thesis layout	7

### CHAPTER 2: LITERATURE REVIEW

2.1.	Rock and rock mechanics	8
2.2.	Sand production management	10
2.2.1.	Fault and fractures of rock	14
2.3.	Review of the Niger Delta geology	16
2.3.1.	Tectonic settings of the Niger Delta	16
2.3.2.	Regional Geology of the Niger Delta	20
2.3.3	Stratigraphy of the Niger Delta	22
2.3.4	Location of the study area	25

2.4.	Conceptual framework	26
2.4.1.	Stress field pattern of the Niger Delta	30
2.4.2.	Petroleum basin geomechanical characterisation	34
2.5.	Estimation of in situ stress	36
2.5.1.	Description of principal stresses	38
2.6.	Theoretical framework (Behavior of rock)	38
2.6.1.	Linear elasticity	38
2.6.2.	Poro-elasticity	40
2.6.3.	Plasticity	40
2.6.4.	Visco-elasticity	40
2.7.	Rock strength and rock failure	41
2.7.1.	Factors affecting rock strength	41
2.7.2.	Rock failure and fracture mechanics	43
2.7.3.	Basic rock model	44
2.8.	Empirical review	45
2.8.1.	Sand production	45
2.8.2.	Geomechanical methodology	48
2.8.5.	Previous work on Wabi field.	53

### **CHAPTER 3: MATERIALS AND METHODS**

3.1	Materials and methods	55
3.1	Method of data collection and instrumentation	55
3.2	Research design (workflow)	55
3.2.1	Procedures to carry out this analysis	57
3.3.	Geomechanical properties estimation	58
3.3.1.	Elastic properties of rock	58
3.3.2.	In situ stress measurement of mechanical properties	60
3.3.3.	Geophysical tools (acoustic and density logs)	61
3.3.4.	Determination of elastic constants	65
3.4.	In situ stress estimation	68

3.4.1. Vertical stress determination	68
3.4.2. Minimum horizontal stress determination	69
3.4.3. Maximum horizontal stress	70
3.4.4. Pore pressure estimation	71
3.4.5. Stress (pressure/depth) gradient determination	72
3.5 Rock strength determination	73
3.5.1 Unconfined compressive strength (UCS)	73
3.5.2 Cohesive strength ( $C_o$ )	74
3.5.3 Tensile strength ( $T_o$ )	74
3.6 Failure mechanisms	75
3.6.1 Shear failure mechanism	75
3.6.2 Tensile failure mechanism	76
3.7 Failure criteria	76
3.7.1. Mohr criterion	77
3.7.2. Mohr Coulomb failure criterion	77
3.9. Cost and Limitation of the study.	78

## **CHAPTER 4 : RESULT PRESENTATION AND DISCUSSION**

4. Data analysis presentation and discussion	80
4.1. Data sources (inventory)	80
4.1.1. Regional correlation	81
4.1.2. Depositional environment	82
4.1.3. Reservoir delineation for sand production/failure	82
4.2. Petrophysical evaluation analysis	88
4.2.1. Reservoir delineation and petrophysical characterization.	89
4.2.2. Reservoir analysis for hydrocarbon types and fluid contacts	92
4.2.3. Quantitative analysis	94
4.3. Seismic interpretation of Wabi field	110
4.3.1. Time structural map	112

4.3.2. Structural analysis	112
4.4. Stress distribution from geologic map of seismic section	115
4.4.1. Stress direction	115
4.4.2. Magnitude of principal stresses	116
4.4.3. Pore pressure and overburden gradient	120
4.5. Mechanical properties estimation	123
4.5.1. Young's modulus of the field	123
4.5.2. Poisson's ratio of the Wabi field	126
4.5.3. Unconfined compressive strength	127
4.5.4. Influence of rock strength	127
4.5.5. Fracture and Fault stability analysis	128
4.5.6. 3D Mohr diagram of the field.	129

## **CHAPTER 5: CONCLUSION AND RECOMMENDATIONS**

5.1 Summary of research	132
5.2 Conclusion	133
5.3 Recommendations	137
References	138
Appendices	155

## LIST OF FIGURES

<i>Fig</i>	<i>Title</i>	<i>No</i>
2.1	Rock contact and terminology	9
2.2	Geomechanics through the life of a field	11
2.3	Sand productions.	13
2.4	Simplified geologic map of the Nigeria and surrounding areas showing main drainage into the Gulf of Guinea.	19
2.5	Map of the Niger Delta showing faulting system	20
<b>2.5b:</b>	Shows a section illustrating the depositional setting of the Niger Delta basin	24
2.6.	Map of the study area showing spatial well locations.	26
2.7	The normal and shear stress components on an infinitesimal cube. b) The stress tensor, a second- order tensor	27
2.8(a)	Generalized world stress map	29
2.8(b).	World stress map. Heidbah <i>et al.</i> , 2008, showing stress direction, source and regimes.	29
2.9	Schematic diagram of Attached and detached Stress regimes	32
2.10	Andersonian's classification scheme for types of faulting regimes	34
2.11.	Shows load sharing by pore pressure. Pore fluids support a portion of the total applied	36
2.12.	Mohr Coulomb failure envelope.	44
3.1	Workflow design	56
3.2	The sonic logging tool	62
3.3	Formation density tool.	64
4.1	Regional correlation of the Wabi field	81
4.2	Slowness profile for Wabi 5A	85
4.3	Slowness profile Wabi 5B	86
4.4	$V_P/V_S$ profile for lithology delineation of Wabi 5A	86

4.5	$V_P/V_S$ profile for lithology delineation Wabi 5B	87
4.6	Interval transit time for lithology delineation in Wabi 11	87
4.7	X-ray computerized tomography scan of core showing cracks (induce fractures)	88
4.8a	Wabi 5A reservoir delineation	90
4.8b	Wabi 5B reservoir delineation	90
4.9a	Wabi 11A reservoir delineation	91
4.9b	Wabi 11B reservoir delineation	91
4.10a	Wabi 5A fluid contact analysis	92
4.10b	Wabi 5B fluid contact analysis	93
4.11a	Wabi 11 fluid contact analysis	93
4.11b	Wabi 11B fluid contact analysis	94
4.12a	Wabi 5 A quantitative analysis	98
4.12b	Wabi quantitative analysis	98
4.13a	Wabi 11 A quantitative analysis	99
4.13b	Wabi 11B quantitative analysis	99
4.14	Wabi 5 histogram	100
4.15	Wabi 11 histogram	101
4.16a	Wabi 5A lithology cross plot	102
4.16b	Wabi 5B lithology cross plot	102
4.17	Wabi 11 lithology cross plot	103
4.18a	Seismic fault and horizon interpretation.	110

4.18b	Fault system of the field.	111
4.19	Wabi field broken into 3 major blocks (map captured at 2.212sec)	112
4.20	Depth contour maps for shallow and deep reservoir with interval of 10m/s.	113
4.21	Pillar gridding of Wabi field showing well trajectories	114
4.22	Structural framework	114
4.23a	Estimated stress profile model for Wabi 5 shallow reservoir	118
4.23b	Estimated stress profile model for Wabi 5 deep reservoir	119
4.24	Estimated stress profile model for Wabi 11 reservoir	120
4.25a	Pore pressure gradient/stress gradient for Wabi 5 shallow reservoir	121
4.25b	Pore pressure gradient/stress gradient Wabi 5 deep reservoir	122
4.26	Pore pressure gradient/stress gradient Wabi 11 reservoir	122
4.27a	UCS derived from Young's modulus for Wabi 5 shallow reservoir	124
4.27b	UCS derived from Young's modulus for Wabi 5 deep reservoir	124
4.28a	UCS derived from Poisson's ratio for Wabi 5 shallow reservoir	125
4.28b	UCS derived from Poisson's ratio for Wabi 5 deep reservoir	125
4.29a	Poisson's ratio in Wabi 5 for shallow reservoir	126
4.29b	Poisson's ratio in Wabi 5 for deep reservoir	127

## LIST OF TABLES

<i>Table</i>	<i>Title</i>	<i>No</i>
2.1	Failure theory for ductile and brittle materials	51
3.1	Sonic interval transit time and velocities for different matrices	62
4.1	Data inventory for this study (data source)	81
4.2	Summary report on identification of reservoir of interest in Wabi wells	104
4.3	Summary table for Wabi wells showing fluid type and the fluid constant	105
4.4.	Summary table for Wabi wells showing fluid type and the fluid constant	105
4.5	Average summary report on Wabi 05	106
4.6	Average summary report on Wabi 11	107
4.7	Average summary report on Wabi 06	108
4.8	Average summary report on Wabi 07	109

## NOMENCLATURE

$C_o$	-	Cohesion
UCS	-	Unconfined compression strength
$C_p$	-	Compaction factor for sonic log
$C_r$	-	Rock matrix compressibility
GR	-	Gamma ray
h	-	Reservoir thickness
K	-	Parameter related to cohesion
Kb	-	Bulk modulus
L <sub>OT</sub>	-	Leak off test
m,n	-	Hoek constant
NPHI	-	Neutron log
P <sub>p</sub>	-	Pore pressure
$\Delta P$	-	Drawdown pressure
RHOB	-	Density log
$S_o$	-	Peak strength parameters related to cohesion
(t)	-	time
$\Delta v$	-	Change in volume
$V_o$	-	Initial volume
$V_p$	-	Pore volume
$K_r$	-	Bulk rock constituents
$C_b$	-	Rock bulk compressibility
$K_b$	-	Bulk modulus of the material
$\sigma_t$	-	Tensile strength

$R_t$	-	Resistivity of uninvaded zone
$V_S$		Volume of shale
$a$	-	Tortuosity factor
$R_W$	-	Resistivity of formation water
$S_W$	-	Water saturation
$R_S$	-	Resistivity of adjacent shale
DRHO	-	Bulk density correction
$C_P$	-	Compaction factor for sonic log
$\sigma_s$	-	Shear stress
$\sigma_v$	-	Overburden (vertical stress)
$\sigma$	-	Minimum horizontal stress
$K_O$	-	Calibration factor or rock stiffness
$S_{11}$	-	The overburden stresses
$S_{22}$	-	The international horizontal stress
$S_{33}$	-	The minimum horizontal stress
$\sigma^I$	-	Effective stress
$\sigma$	-	Total applied stress
$\rho_r$	-	The rock density
$h$	-	The depth of burial
$g$	-	Acceleration due to gravity (gravitational) constant
$V_S$	-	Shear velocity (S – wave)
$V_P$	-	Compressional velocity (P – wave)
$d$	-	Magnitude constant
$f$	-	Shape constant
$a$	-	Constant

$b$	-	Constant
$Sh_{min}$	-	Minimum horizontal stress
$Sh_{max}$	-	Maximum horizontal stress
$E_{Stat}$	-	Static elastic constant
$Fg$	-	Fracture gradient
$F$	-	Force
$A$	-	Area
$D$	-	Depth
$E$	-	Young modulus
$G$	-	Shear Modulus
$l$	-	Original length
$h$	-	Depth
$V$	-	Original volume
$\Delta d$	-	Change in diameter
$\Delta l$	-	Change in length
$PF$	-	Pore pressure
$\mu$	-	Coefficient of internal friction
$T_o$	-	Tensile strength
$\tau_{max}$	-	Maximum shear stress
$\theta$	-	Angle of surface sliding
$\phi$	-	Frictional angle
LAS file	-	Industry standard binary format for storing data.
SEG Y	-	Society of Exploration Geophysicists standard for storing Geophysical data.

### **Greek symbol**

$\alpha$	-	Biot constant
$\beta$	-	High velocity coefficient
$\epsilon_x$	-	Strain in x direction
$\epsilon_y$	-	Strain in y direction
$\epsilon$	-	Elastic strain
$\epsilon_V$	-	Volumetric strain
$\theta$	-	Angle of internal friction
$\nu$	-	Poisson ratio
$\rho_b$	-	Bulk density of that formation
$\rho_{log}$	-	Density read off bulk density log
$\rho_f$	-	Fluid density in a wellbore
$\rho_{ma}$	-	Density of the matrix material
$\phi_D$	-	Density derived porosity
$\phi_{Sonic}$	-	Sonic derived porosity
$\Delta t_{log}$	-	Interval transit time of formation
$\Delta t_{ma}$	-	Interval transit time of formation matrix
$\Delta t_{fl}$	-	Interval transit time of fluid in borehole
$\Delta t_{sh}$	-	Transit time of adjacent shale
C	-	Constant (1)
$V_{ma}$	-	Velocity matrix of material
$\sigma_h^l$	-	Effective minimum horizontal stress
$\sigma_1$	-	Maximum stress
$\sigma_2$	-	Intermediate stress
$\sigma_3$	-	Minimum stress

$\sigma_1, \sigma_2, \sigma_3$	-	Principal stresses
$\sigma_H$	-	Maximum horizontal stress
$\sigma_h$	-	Minimum horizontal stress
$\sigma_f$	-	Normal stress at failure
$\sigma_n$	-	Normal stress
$\tau_0$	-	Cohesive strength
$\tau_f$	-	Shear stress at failure
$\phi$	-	Porosity
$T_S$	-	Slip tendency
$D_S$	-	Dilation tendency



# CHAPTER 1

## INTRODUCTION

### 1.1 Research context

Interestingly, we are in a dispensation of hydrocarbon prospecting which marks the gradual end of the era of readily available hydrocarbon discovery with decline in extractable oil from existing reserves (Tunio *et al.*, 2011). This coupled with the increase in energy demand worldwide, prompted the government, multinational and indigenous oil industries to look inward for hydrocarbon production from undeveloped discovery herein referred to as marginal or depleted mature field, for the reassessment of upside potential of the field. Again, some hydrocarbon discoveries that are unsuccessful to go with the preferred or conventional production pace may underline set of reasons for reservoir issues (i.e. geomechanical problems) which need to be carefully and critically examined (Hugo and Ian, 2014).

In Petroleum prospecting surveys, exploration geophysics is conducted in a sequential order of relative cost, starting with magnetic, gravity and seismic to find commercial hydrocarbon accumulation. Less expensive methods are utilized first to narrow down the prospect to be explored by more expensive methods. In geophysical prospecting the physical properties measured are density, electrical conductivity, magnetism, radioactivity and elasticity. Interpretation involves much inferential reasoning to provide information about the structure and distribution of rock types (Martey, 2000).

Authors such as, Adetoba (2008) and Offia (2011) cited previous studies conducted in the prolific Niger Delta region by the Department of Petroleum Resources (1999) which shows that there are about 116 marginal fields identified to be lying redundant and unproductive, which transverse the southern part of Nigeria called the Tertiary Niger delta basin. According to the research work by Newcross Petroleum (2010), the vast hydrocarbon deposits in such fields account for about 1.3 Billion barrels, (Ajayi, 2017).

Marginal field identifies a prospect with questionable overall economic viability. These marginal fields mean diverse things to different operating companies worldwide (e.g. what international Oil Company sees as marginal would not be considered by indigenous companies as marginal). In

other words, multinational oil companies focus on the development of their large reserves against smaller ones (Fee and O'Dea, 1986).

Furthermore, Kulasinga *et al* (2014) defined Marginal field as hydrocarbon discoveries that may or may not possess the technical characteristics of a conventional oil field discovered by multinational oil and gas companies and have not developed it for over a decade.

As the high energy demand grows worldwide, it is undeniably accompanied by the increasing rate of oil production, prompting prospecting for oil and gas activities in frontier harsher environmental degradation, where there are geomechanical stress related challenges facing reservoir during oil and gas exploration and production.

Ajayi (2017) reported that to achieve the desired daily crude oil production rate to meet the world energy demand and boost the country's economy, farm out of undeveloped or marginal fields was circulated for their allocation to home-grown oil companies in Nigeria. In addition, Adamu *et al.* (2013) emphasized on the strategic importance of developing marginal fields in the prolific Niger Delta by the Federal Government of Nigeria as may serve as a drive towards improving reserve and production capacity enrichment.

According to Nouri *et al.* (2003), over 70% of developed hydrocarbon fields globally are found in sediments that are unconsolidated (e.g. sandstone and carbonate formations). Therefore, they are evidently very prone to unwanted sand production (Udebhulu and Ogbe, 2015). Regions of the world with continual sand production problems have been recognized in young sediments such as in: Nigeria, Venezuela, Canada-Tar sands, Indonesia, California and US Gulf coast. These sediments serve as reservoirs for the world's hydrocarbon reserves (Osisanya, 2010).

The Tertiary Niger Delta formation is an unconsolidated formation of which sand control is of major geomechanical problem, especially in geologically complex or difficult areas where some oil reservoirs and marginal fields are found (Schlumberger, 1985). In their submission, Oluyemi (2007) and notably, Otti and Woods (2005) has it that the typical characteristics of these formations/fields include strong degree of unconsolidation, high porous formation with thick net pay, high rock instability and high depletion rate. Economides and Nolte (2000) opined that the existence of any two of the characteristics mentioned above, may eventually subject the formation

to structural failure because reservoirs that are located underneath the earth crust suffer tectonic stresses. Several geological activities may have been responsible from the inception of the original deposition.

Besides, due to scarcity of reliable relevant data from operating oil and gas companies in the Niger delta, stress pattern of the region is not well understood. However, Tingay *et al* (2005) illustrated that the result of world stress map (WSM) conducted so far correlate with global and regional stress patterns. This WSM is quite helpful when working in areas with none or trivial pre-existing knowledge particularly, in attempting to comprehend the relative stress orientation and magnitude from a known area to unknown area. Hence, information of present-day tectonic stress is necessary for several applications in oil and gas industry (Tingay *et al.*, 2005).

In rock formation, three basic internal stresses are identified Tiab and Donaldson (2012), these are compressive, shear, and tensile. Reservoir formations are affected by the collective load of the overlying strata which causes vertical compressive stress, together with lateral (horizontal) stresses thereby creating imbalance upon the extraction of hydrocarbon (Rasouli *et al.*, 2011). Hence, anisotropy (variations of stress in materials) occurs as the in-situ principal stresses are united vertically and horizontally (Zimmerman, 2006; Jamshidian *et al.*, 2017). Principal stresses are defined as those normal components of stress that act on planes that have shear stress components with zero magnitude. Stress states in a formation are not always hydrostatic that is, being equal in all directions, because of the balanced system of the stresses which could be influence by either tension or compression stresses (Wilson and Cosgrove, 1982). Hence, these in-situ stresses are aligned into three most important stresses. These three states of stresses exist in subsurface formation and are described in descending order of magnitude as: vertical or overburden, sigma 1 ( $\sigma_1$ ), maximum or intermediate horizontal, sigma 2 ( $\sigma_2$ ) and minimum or least horizontal, sigma 3 ( $\sigma_3$ ). The directions and magnitudes of these formation stresses are used to characterize reservoir conditions for various geomechanical applications (Sinha *et al.*, 2008). For instant, the bearing and size of these stresses are requisite for forecasting geomechanical issues such as borehole stability, hydraulic fracturing for enhanced production and for discerning intervals of perforation for sand management (Sinha *et al.*, 2008). Hence, they play important roles in petroleum prospecting for oil and gas and reservoir development (Sinha *et al.*, 2008).

Langhi (2014) succinctly affirmed that stresses and deformations have potential to adversely impact on exploration activities, field development and production operations. Therefore, evaluating these stresses is critical to comprehending the mechanical performance of a reservoir rock to make optimal decision throughout the field's lifespan. Archer and Rasouli (2012) assert that precise estimation of the state of stresses will necessarily aid proper understanding of the formation to avoid risk.

To achieve optimum development results and produce reasonable quantities of these hydrocarbons from marginal or mature fields, these formations/fields will require detailed and comprehensive assessment or reassessment of the reservoir petrophysical and geomechanical/mechanical properties of the field such as; the rock strength, present day/in situ stress, and elastic moduli for development of reservoir geomechanical model for predicting fault reactivation, wellbore instability, compaction that leads to subsidence and sand production meant to be used for development plan strategy. Geomechanical characterization of hydrocarbon reservoir rock gives the description of mechanical parameters based on the physical and chemical composition (Dusseault, 2011) of rock mass of the geologic formation.

This research will furnish and address geomechanical stress related problems and recommend mitigating strategy for well completion design and infill drilling in Wabi, in the study area. It shall employ both quantitative and qualitative approaches/methods that are in accordance with best industry practices and adopt existing empirical correlations, using seismic and wire line logs parameters as an input data depending on the initiate stage in the life cycle of the field with the aim of developing a geomechanical model. Geomechanical model is meant for characterising stress at depth as well as for solving wide range of geomechanical in-situ stress related to development problems in the field of study such as fractures, fault reactivation, compaction, sand production prediction and wellbore instability (Herwanger and Koutsabeloulis, 2011). It can also be used to devise or design a mitigating strategy for longevity of the field. The integration of Petrophysics and Geomechanics characterization is paramount for assessment of stresses in the reservoir, prediction of sand failure, failure in seal, fault reactivation, recommendation for perforation location and casing for reservoir management. The results obtained from detailed geomechanical

analysis shall enhance longevity of well management and ultimately add value to or increase the daily hydrocarbon production.

## **1.2 Motivation of the study /Statement of problem**

Many researchers have studied new discovery, brownfield (mature depleted reservoirs), undeveloped discoveries and marginal fields in the Niger Delta based on their upside potentials, economic viability, wax deposition, water coning, high gas/oil ratio with little or no emphasis on rock geomechanics properties for well engineering; that is, the original in-situ stress state and the alteration this stress state may have on the reservoir, whether it is close to failure envelope of the reservoir rocks (Herwanger and Koutsabeloulis, 2011). The Tertiary Niger Delta is an unconsolidated formation faced with naturally fractured petroleum reservoirs, this creates geomechanics challenges which affected well development, drilling and completion, production and enhancement of recovery.

The unconsolidated nature of the Niger Delta depositional environment has led to production and development difficulties due to weak reservoir rocks, stack or multiple reservoirs with thick net pay, highly porous and low pressure due to depleted reservoir (Schlumberger, 1985).

The occurrence of these phenomena at the same time compounds the overall stress-related geomechanics problems which is damaging to production and development. Hence, identifying the consequence of initial stress state and what its changes may impact on the reservoir strength during development and production is vital for reservoir engineering management (Herwanger and Koutsabeloulis, 2011). This research focuses on geomechanical and petrophysical characterization of hydrocarbon reservoir rock for optimal development and production of oil and gas. This is vital for forecasting sand production occurrence for well completion design.

## **1.3 Research Aim**

The aim of this research is to characterize marginal field petrophysical and geomechanical parameters and develop 3D Mohr Circle geomechanical model for analysis of geomechanical problems in Wabi, onshore Niger Delta.

#### **1.4 Objectives:**

The objectives of this research are as follows:

1. To investigate and estimate the field's mechanical behavior and mechanical properties of the formation rocks.
2. To carry out Petrophysical interpretation to ascertain Wabi field reservoirs quality.
3. To investigate and model stress (pressure/depth) gradient in the field.
4. To estimate and model the elastic properties, rock strength, and in-situ stress field that exist in Wabi field from geophysical logs
5. To develop 3D Mohr Circle Geomechanical model to predict rock strength, fault reactivation, wellbore instability, sand production fractures, wellbore instability and sand failure during production.

#### **1.5. Contributions to knowledge and justification of the study**

This research contributes to knowledge as follows: Geomechanics as at today had not been fully implemented in most fields in the Niger Delta, especially, it is lacking in field development plan (FDP) submission by operators to Government regulating agency. Sequel to the above, the author has carried out petrophysical and geomechanical evaluation known as reservoir geomechanics and wellbore stability investigations of Wabi field using an integrated approach with data sets comprising of seismic data, petrophysical logs and core x-ray computerized tomography (CT scan) to guide and assure stable wellbore, choice of completion intervals and prediction of onset sand production. This research finding predicted in-situ rock stresses, Poisson's ratio, modulus of elasticity, porosity, pay zones (reservoirs with hydrocarbons), volume of shale, hydrocarbon saturation and rock strength for proper characterization of Wabi reservoirs, these are the claimed contributions by the author in Wabi field. The applications of the findings are relevant in well intervention programs, infill drilling and injectivity for enhancement of hydrocarbon recovery to profer better engineering design to reduce risks associated with oil and gas development for production optimization. This is very helpful to marginal field's operators who may venture into

acquisition of marginal fields for optimum profitability and high investment returns as financial resources is a barrier to their operation.

## **1.6 Thesis layout**

*Chapter 1:* This introductory chapter gives an insight into the background of this study and explained the general overview of mechanical behavior of reservoir bearing formation and related stress states that exist beneath the earth crust including their effects on oil and gas production. It goes forward to highlight the reasons and significance of this study.

*Chapter 2:* This section is dedicated to related studies and introduces the concept of rock mechanics, in situ stress state, geology of Niger delta, sand production, fault reactivation leading to compaction and fracture of reservoirs. This review identifies the missing gap to be investigated for mitigation strategy for optimization of hydrocarbon.

*Chapter 3:* This chapter highlights the theories of rock failure, field approach of evaluating petrophysical and geomechanical parameters of the hydrocarbon reservoir of interest and presents the data set and materials required for the actualization of the objectives of this research.

*Chapter 4:* Presents the results of this research findings and discussion of the hydrocarbon potential including related geomechanical characteristics issues in the field.

*Chapter 5:* The conclusions of the research studies are presented in this chapter followed by the remarks and recommendation for further studies.

## CHAPTER 2

### LITERATURE REVIEW

The aim of the present literature review is not to consolidate the entire research, but to pick a handful of articles that are either closely related to the research or which, if studied might lead to a conclusion that might help in further justifying the necessity and validity of the research. This includes literatures concerning geomechanics and petrophysical characterization as appeared in several publications. This is based on conceptual framework, theoretical framework and empirical review to identify the gap to be addressed particularly in Wabi field, Niger Delta, Nigeria.

#### 2.1 Rock and rock mechanics

Rock mechanics generally concentrate on the theoretical and applied mechanical behavior of rock; where rocks responses due to stress field are studied within its surrounding environment for engineering and geological purposes (Sorough, 2013). Rock is a natural substance known not to be a continuum rather a regulated discontinuum **Figure 2.1**. They are composed of discontinuity (separation in the rock continues having effectively zero tensile strength) and intact matrix (Norouzi, Baghbanan and Khani, 2013). Xie and Gao (2014) stated that the existence of various defects (i.e. pores, crystal boundaries, fissures, dislocations secondary phases, twin crystallites, inclusions and precipitate made rock to be complex. These defects caused the discontinuous, inhomogeneous, nonlinear and anisotropic in mechanical behavior and properties of rocks due to irregularity of scale and cracks distribution. Therefore, decrease in physical and mechanical properties occurs (Xie and Gao, 2014). The priority of rock mechanics is to understand the mechanical behavior and mechanical properties of a given rock about its deformation, strength and failure when subjected to external force (Xie and Gao, 2014).

The structural and textural characteristics, minerals composition including fracturing, porosity, mineral strength constituents and degree of cement bond are some of the factors upon which rock strength determination are based (Sygala, Bukowski and Janoszek, 2014).

The uppermost crust is an inhomogeneous material in nature that is filled with flaws, fractures and pre-existing cracks (Duan, Kwok and Tham, 2014; Hazzard, Young and Maxwell, 2000).

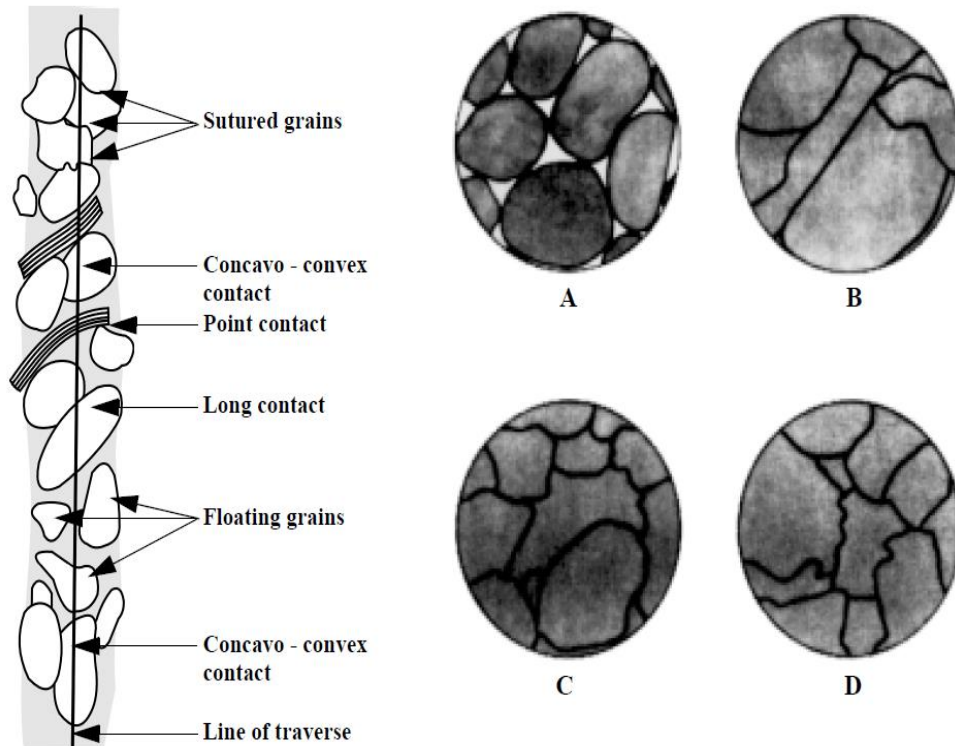


**Figure 2.1** Rock contact and terminology (Baker Huges, 1999).

These are the characteristics that cause brittle material (e.g. rock) to deviate from being a pure elastic medium. The term brittle rock described the property of fracturing or rupturing with slight or no plastic flow occurrence within the earth upper crust (Hucka and Das, 1974). Therefore, understanding the rock geometry and the size of these cracks and their effect on the mechanical behavior and rock properties are essential for engineering operations and geological processes (Hazzard, Young and Maxwell, 2000). The strength of brittle rock undergoing compression depends on the formation existing cracks, growth and the interaction of flaws including how they propagate into bigger shear faults (Duan, Kwok and Tham, 2014).

The distinction between macro-mechanical and micro-mechanical properties of rock can be defined as follows: macro-mechanical properties of a formation are the rock macro-scale properties

such as Young modulus, Poisson's ratio and peak strength whereas the micromechanical properties are the rock micro-scale properties such as pores, cracks, fissures and flaws (Jumiski, 1983). The knowledge of mechanisms of ruptures (fracture) and populates of deformation in micro and macro mechanical properties of rocks have practical and theoretical significant (Xie and Gao, 1999).

Initiation and propagation of fracture/deformation are caused by micro cracks in the formation; this can be illustrated by a sample that is loaded to a peak stress, cracks are visible as the sample attained peak stress and at the edge of the sample a small process zone of crack is form. This is followed by propagation of macro shear fault in the brecciate zone through the mechanisms of kinking or buckling (Hazzard, Young and Maxwell, 2000). As rock density increases it cause dislocations which depend on the increased in applied load resulting in to micro-cracks formation (Hazzard, Young and Maxwell, 2000). Again, micro-cracks are form during the convergence of two groups of dislocations, secondary phase particles or crystal boundary resulted to a local zone that is concentrated with high stress (Xie and Gao, 1999). Pores in both high and weak stressed region extent and converge respectively to form macro fracture (Xie and Gao, 1999). Cracks in brittle rocks are known to be predominantly tensile and orientate sub parallel to compressive stress direction (Duan, Kwok and Tham, 2014).

Initiation in rock failure and deformation was conducted by Nolen-Hoesema who reported that rock process of propagation of cracks increases with applied force/load in a marble (Xie and Gao, 1999). Wu and Chudnovsky (1993) cited in Xie and Gao (1999) attributed the influence of micro-cracks distribution on the macro cracks to stress factor in the rock formation.

Petroleum exploration is conducted within the upper crust (brittle material) which ranges from 10  $\pm$  5km, this depth is of a particular interest for petroleum prospecting and other activities such as storage of waste or carbon sequestrations and earthquakes studies (Allmendinger, 2015). At this depth, the application of Mohr Coulomb failure criteria can determine rock failure.

## **2.2 Sand Production Management**

Herwanger and Koutsabeloulis (2011) explained that rock failure leads to sand production, compaction and subsidence in a reservoir. Economides *et al.* (2013) defined sand production as the production of solid particles especially, rock grains with oil, gas, and water from the reservoir.

The occurrence of this observable fact in an unconsolidated and sometimes from consolidated formation is unwanted. Gholami *et al.* (2016) credited sand production failure to shear stress and fluid flow forces. Over the years, several methods have been established to forecast sand production and to avoid it by altering drilling or production strategies. This has been a setback associated with petroleum industry worldwide. This problem is more severe in loose young sedimentary formations for instant Tertiary Niger Delta.

Isehunwa and Farotade (2010), described sand production as a progression that develops in three scenarios, that is , in the formation, cavity and wellbore **Figure 2.3**. Balarabe and Isehunwa (2017) identified the collapse of surrounding rock formations in perforated wells from which liberated grains are generated due to changes in stress, sand grains dislodgment from failed rocks and fluid flow transportation of these grains into the well bore and up to the surface facility, as notable causes of sanding occurrence. Hence, sand production is the production of rock particles along with oil, gas and water (Economides *et al.*, 2013). **Figure 2.2** explained geomechanical related issues associated with exploration, appraisal, development, production and abandonment of oil field. (Zoback, 2016; Hugo and Ian, 2014).

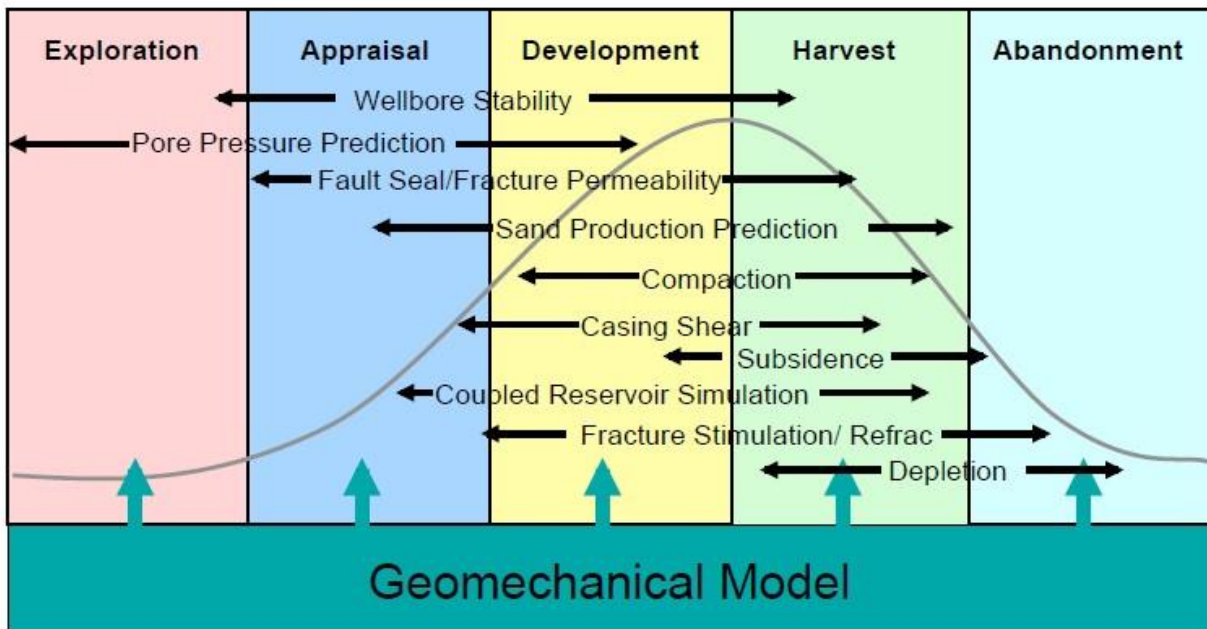


**Figure 2.2.** Geomechanics through the life of a field (Zoback, 2016)

This has been a major problem faced during hydrocarbon exploration and production because any invasion of sand may cause wellbore instability and blockage in flow line respectively (Economics *et al.*, 2000). Numerous oil and gas fields are been affected by its occurrence, wherever it is found especially in young sedimentary basins around the world. Sand production has the capability to damage both producing formation and the production equipment (Zhang, Rai and Sondergeld, 2000).

According to Tiab and Donaldson (2012), the prerequisite data needed for evaluation of sand production in any reservoir are; uniaxial compressive strength, production history, and formation fluid pressure. Therefore, predicting its occurrence beforehand is the best practice embraced by virtually most producing companies. This implies that accurate and comprehensive formation's mechanical strength, rock failure criterion and in situ stresses need to be investigated. These geomechanical parameters of a reservoir formation are the most essential information desired for the prediction of sand production and advice for sand control completion (Zhang, Rai and Sondergeld, 2000).

Almisned (1995) explained that one pathway to controlling sand production problem is the ability to successfully predict its occurrence before the well is completed. Sand production management refers to well engineering planning designs to monitor, control and prevention of sand production from occurring during exploration and production activities. It also involves the provision of proactive strategies to manage its existence in a well. Petroleum geomechanics discipline is well known for handling rock associated problems such as sand production, fault reactivation, compaction, subsidence, wellbore instability etc.

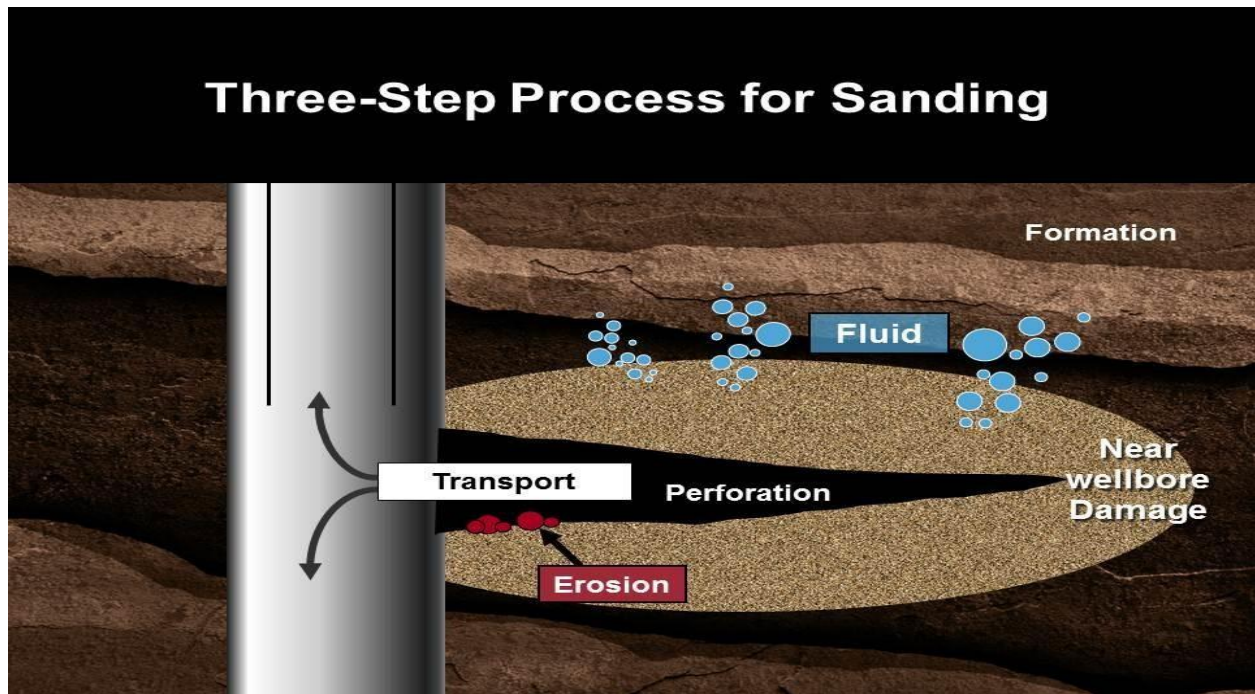


**Figure 2.3.** Sand productions (‘Halliburton ‘Amos, 2012).

Geomechanics is essential to give description of rock deformations due to in situ stress, pore pressure and formation temperature changes ensuing from hydrocarbon production and fluid injection pressure (Gutierrez, 1998).

Cerveny *et al.* (2004) submitted that when rock layers are subjected to tectonic stress, it may lead to contraction or extension induced shear failure, in this case, the rock is fractured or faulted. A fault is defined as a shear fracture or surface failure in a geological rock caused by relative displacement of a fracture plane (Jaeger and Cook, 1979). Thus, hydrocarbon reserve accumulated in this faulted siliciclastic (clayey) reservoir may become difficult to develop and produce as the properties of rock developed within these faulted zones affect the fault’s potential to seal. The analyses of fault seal improve the prediction of fault behavior in the subsurface and lessen the uncertainty in exploiting faulted siliciclastic.

### 2.2.1 Fault and fracture of rocks

In their well-articulated work, Sorkhabi and Tsuji (2005) posited that the current approaches used for fault seal analysis mostly proffer solution to normal fault in classic reservoirs where the integration of fault seal and in situ stress analyses had been proven as an innovative technology breakthrough in the petroleum industry. Thus, fault investigation becomes necessary as petroleum traps have developed along two separate and successive lines of deliberation such as fault rock seal and fault closures. This approach is basically concerned with structural geology development applications, utilizing quantitative fault analysis methods for kinematic and geometric investigation of sedimentary basins, which concluded that plate tectonics presented an integrated tool to show a relationship between faults and basins been dependent on the far field (i.e. plate boundary produce stress) (Sorkhabi and Tsuji, 2005).

The importance of the geometric diagnoses is obvious from identification of various sealing processes in fault zones, architectures and quantitative appraisal of petrophysical properties. Generally, faulted rock has been being detrimental for exploration of fault traps because of their high-capillarity and low permeability features in sedimentary basins. However, recent studies conducted have changed the previous polarized observation of faults as either seals or leaks into rationale of more complex fault fluid flow behavior (Sorkhabi and Tsuji, 2005).

Ferrill *et al.* (1999) suggested an algorithm known as Slip tendency ( $T_s$ ) and dilation tendency ( $T_d$ ) to evaluate the relative strength or weakness of fault seal under in-situ stress conditions. They described slip tendency as a shear failure, defined as the ratio of shear stress to normal stress. It is expressed mathematically as:

$$T_s = \sigma_s / \sigma_n \quad (2.1)$$

Similarly, Dilation tendency (i.e. failure by extension fracturing) is given by:

$$T_d = \frac{\sigma_1 - \sigma_n}{\sigma_1 - \sigma_3} \quad (2.2)$$

where,  $T_s$  is the slip tendency,  $T_d$  is the dilation tendency,  $\sigma_s$  is shear stress,  $\sigma_n$  is normal stress, and  $\sigma_1$  is the overburden or vertical stress,  $\sigma_2$  is the intermediate stress and  $\sigma_3$  is the minimum

horizontal stress acting on the fault surface. The values of  $\sigma_s$  and  $\sigma_n$  can be calculated from equation as follows:

$$\sigma_n = \sigma_v \sin^2 \alpha + \sigma_h \cos^2 \alpha \quad (2.3)$$

$$\sigma_s = \frac{(\sigma_v - \sigma_h) \sin 2\alpha}{2} \quad (2.4)$$

where,  $\sigma_v$ , is the vertical stress;  $\sigma_h$  is the horizontal stress and  $\alpha$  is the angle between  $\sigma_n$  and the fault or fracture plane.

From stress regimes description of faults, in normal faults,  $\sigma_1$  vertical stress or the maximum principal stress ( $\sigma_v$ ) exerted overlying weight/ overburden thickness and the horizontal stress ( $\sigma_h$ ) was considered as the minimum principal stress ( $\sigma_3$ ) (Kachi *et al.*, 2005) which could be calculated as follows;

$$\sigma_h = K_o \sigma_v \quad (2.5)$$

where  $K_o$  is the coefficient of earth pressure at depth and it is a calibration factor

Sims *et al.* (2005) explained the extensional fault system development and reservoir connectivity and concluded that it depends on whether fault transverse reservoir acts as conduits for flow in fracture carbonate reservoirs or as barrier to flow (in highly porous sandstone reservoir). They inferred from their study that fault system evolution or growth has effects on the extent to which rock coupled between and around faults and fault network connectivity. As fault system advances, rock mass connection decreases and network connectivity increase concurrently (Sims *et al.*, 2005).

Yamada *et al.* (2005) postulated that regional scale stress has a major impact on fault expansion during the formation of geological structures. Also, faults created after stress conversion is affected by pre-existing faults; therefore, the consequential geometry of the faults is determined by the order of the stresses.

Normal faulting field analysis demonstrated that synthetic layer dip related to normal faults is a familiar feature of extensional fault systems, developed where layers up thrown and down thrown

in the opposite direction (antithetic) or both sides of a normal fault dip toward the down thrown side of the fault (Ferrill *et al.*, 2005).

Aydin (1978) defined deformation bands in sedimentary rocks as thin (millimeter-wide) planar structures in faulted sandstones from study conducted in Utah. Deformation band transpire as single planar structures in host formation (e.g. sandstone) away from weak zones (Sorkhabi and Haasegawa, 2005). In the perspective of Sorkhabi and Hasegawa (2005), deformation bands increase noticeably in bulk and connectivity toward the fault plane, signifying that faulting develops from entity bands to a high- deformational zone described as anastomosing cataclastic slip bands (Fowles and Burley, 1994) and culminating/assembles in the slip fault plane. Thus, reactivation of bedding perpendicular due to shear faults caused major normal faults development.

Davatzes and Aydin (2005) interned from their examination of the distribution of fault rock and rupture structures in shaly-sand formation that rupture zones are found along strike and dip. Consequently, these are caused by variations in the fault geometry, lithology, fault slip and fault mechanism.

## **2.3 Review of the Niger Delta geology**

### **2.3.1 Tectonic setting of the Niger Delta**

The drifting apart of the continental crust of Africa and South America plates during the late Jurassic rift (Doust and Daukoru, 1990; Etu-Efeotor, 1997) marked the origin of tectonic setting in the Niger Delta and the entire Gulf coast of Guinea **Figure 2.4**. According to Tuttle, Brownfield and Charpentier (1999) the tectonic framework of the plate margin beside the coast of West Africa shield was controlled by mid-oceanic ridges and Cretaceous fracture zones articulated as trenches in the deep Atlantic, which subdivides the plate boundary into entity basins. These amount to the formation of triple junction or the rift-ridge system (i.e. RRR) during the Cretaceous era which arms are known as; the Atlantic arm, Gulf of Guinea transforms complex and the Abakaliki-Benue trough (Tuttle, Brownfield and Charpentier, 1999; Schlumberger, 1985). Two arms of this triple junction followed the Southeastern and southwestern coasts of Cameroun and Nigeria and developed into collapsed continental margins (Doust and Omatsola, 1990), while the third arm, failed and developed into the Abakaliki–Benue trough (Doust and Omatsola, 1990; Weber and

Daukoru, 1975) known to be the oldest sedimentary basin. Along the Nigerian coast, the Benue-Abakaliki trough is seen up to West African shield (Tuttle, Brownfield and Charpentier, 1999). These three arms (RRR) known as the triple junction rift-ridge system opened at different rates and different times initiated the continental drift that separated Africa from South America (Weber and Daukoru, 1975; Doust and Omatsola, 1990). This rifting ceased totally in the late Cretaceous and gravity tectonism became the main deformation process in the Niger Delta complex (Tuttle, Brownfield and Charpentier, 1999). After the separation between Africa and the South Atlantic, the Gulf of Guinea was created now occupied by Niger delta basin.

In the mid Cretaceous (Albian) time, marine deposits or incursion took place in Anambra–Benue trough known as the fail arm of the triple junction (Doust and Omatsola, 1990; Short and Stauble, 1967) and this was recognized as the first sedimentary deposits in the Niger delta basin which end in the Santonian time known as Akata Formation. Subsequently, paralic clastics deposits sequences were deposited on top the older under compacted marine shale (clay) as the growth of the proto Niger delta in the late Cretaceous which ended during the transgression of Paleocene marine known as Agbada Formation. During the Eocene to recent the final phase of the depositional sequence was deposited which ended the deposit and manifested the present-day Niger delta progradation (Short and Stauble, 1967; Doust and Omatsola, 1990). The third phase was deposited, after the occurrence of gravity tectonism has ceased. The successions of the marine and paralic clastics thickness deposits were deposited in series of regressive and transgressive phases (Doust and Omatsola, 1990).

The actual development of the present day Niger Delta commenced in late Paleocene/Eocene, as sediments built out afar the Benue-Abakaliki trough southward against the crust of the Atlantic Ocean, where it assume the current convex to sea morphology (Doust and Omatsola, 1990). This growth has been dependent between the rate of sedimentation and subsidence balance, caused by tectonics of the basement and structural configuration **Figure 2.5**. In general, the regressive classic sequence has the maximum thickness of about 30,000 to 40,000ft or 9,000 to 12,000 m (Evamy *et al.*, 1978).

Weber and Daukoru (1989) asserted that the Niger Delta expansion is affected by basement faulting which in turn influences the thickening of the sediment distribution. The majorities of these faults affect different parts of the Agbada formation and flatten/even out into detachment plane adjacent to overpressure Akata Formation (Doust and Omatsola, 1990; Weber and Daukoru, 1975). However, the associated faults in the basin act as stratigraphic traps to accumulate hydrocarbons and serve as hydrocarbon migration paths from Akata over pressured formation to Agbada sand (Weber and Daukoru, 1975). These associated growth faults are roll over anticline, close space flank faults, collapse growth fault crest, shale diapirs, back to back features and diapirs and abruptly (Evamy *et al.*, 1978). Growth faults of the Niger delta signifies that their formation is active and allows faster sedimentation in normal faulting that is, in down thrown relative to reverse or upthrown (Weber and Daukoru, 1975, Weber, 1971).

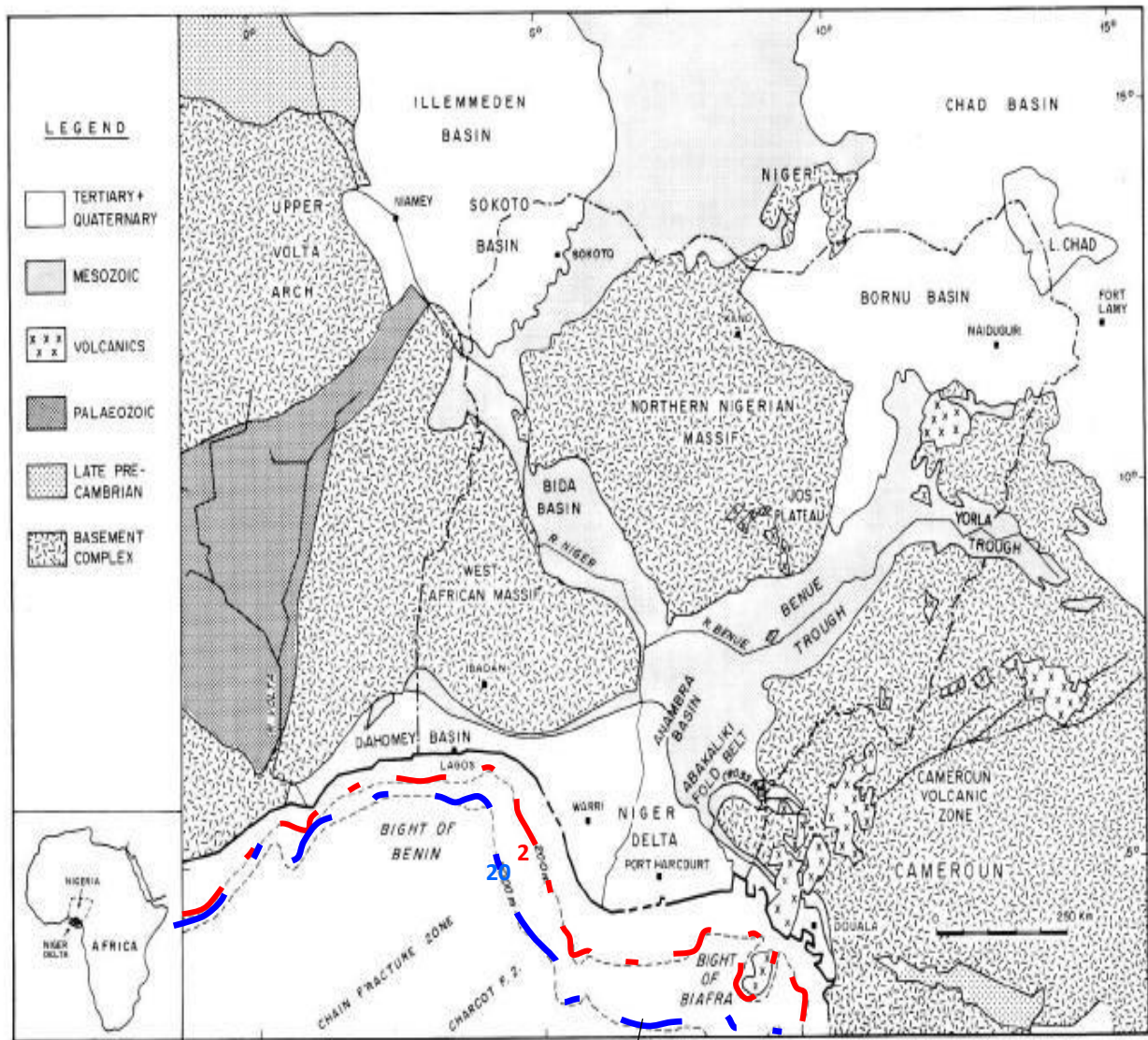


**Figure 2.4.** Simplified geologic map of the Nigeria and surrounding areas showing main drainage into the Gulf of Guinea. The dash red and blue lines demarcate different depobelts (Whiteman, 1982; Allen, 1965).

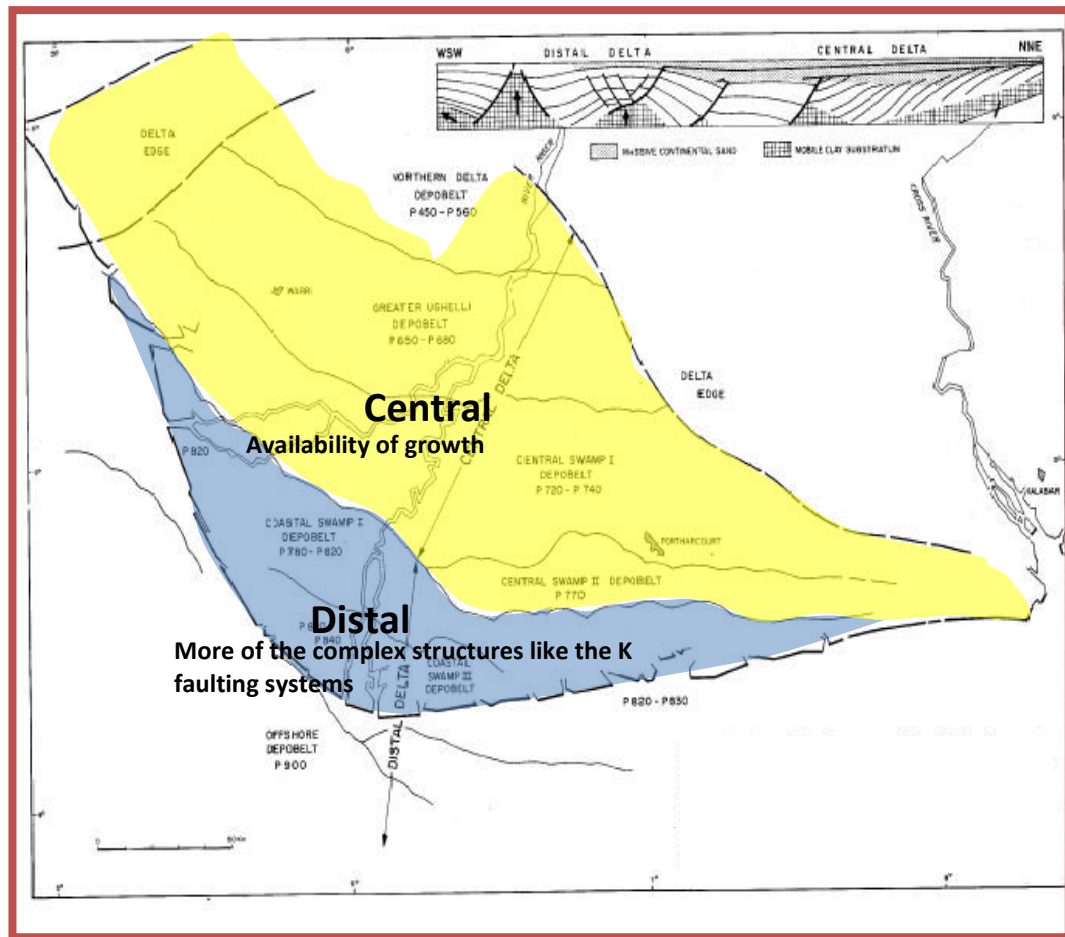


**Figure 2.5.** Map of the Niger Delta showing faulting system (Evamy *et al.*, 1978)

### 2.3.2. Regional Geology of the Niger Delta

The Tertiary Niger delta basin is located at the apex of Gulf of Guinea on the Western coastline of Africa (Doust and Omatsola, 1990) and it is well known as one of the prolific hydrocarbon deltaic province in the world today (Haack, 2000). The coordinates of this region are roughly situated between longitude 4° and 8°E and latitude 3° and 6°N (Zorasi *et al.*, 2017). Three igneous and metamorphic rocks onshore constitute the basement complex of the Niger delta, and bounded by the Northern Nigerian massif, Western Africa massif and Eastern Nigeria massif. These basement complexes are dated Precambrian and early Paleocene (Schlumberger, 1985). The lower exposed Cretaceous (Albian) of the Abakaliki and Benue rift basins have the oldest dated sedimentary

rocks. Similarly, older sediments sequence may also exist in the offshore Miogeoclinal basins underneath the Niger Delta complex formed on the sea floor during the first opening of the Gulf of Guinea and resulted to the drifting apart of the continent (Schlumberger, 1985).

The Niger Delta complex today, covers an area of about 100,000 sq.km, of which less than 20% is considered as prospective. 100% of the Nigerian hydrocarbon production is from this great petroliferous Delta complex. Niger Delta basin is located in the southern part of the country and the host of the vast known petroleum (hydrocarbon) potential of the country. These oil and gas reserves are found precisely underneath the onshore (inland) and shallow to deep water of the Niger Delta province especially, in the Agbada Formation (Short and Stauble, 1967; Weber and Daukoru, 1990). Three Formations are known in the Niger Delta. These are Akata, Agbada and Benin. Akata Formation is known as the source rock, Agbada Formation is a paralic clastics sequence, which consists of sand, siltstone; interbedded high energy deltaic sandstones with intercalation of shales generated in several offlap cycles (Short and Stauble, 1967). These features made the Agbada formation the objective target of most exploration activities in the region due to its reservoir quality with the beneath marine shales serving as the source rock /petroleum system (Tuttle *et al.*, 1999). The Benin Formation is known as sandy and potable water formation.

The vast quantities of sediments supplied to the Niger Delta complex were partly generated and eroded from the hinterland and especially from the thermal uplift blocks in Cameroun Mountain (Schlumberger, 1985) and by eustatic changes in sea level. Most of the Oil and Gas produced from the Niger Delta are in the Agbada sand reservoirs where the hydrocarbons are trapped in mostly rollover anticlines and other associated structures (Schlumberger, 1985). There are huge undiscovering that may exist in both the onshore and offshore Niger Delta.

The commonly fault found in the Niger Delta is the synsedimentary fault or growth fault. They are initiated around local depocentres at the time of formation and grow faster during sedimentation. Growth fault offsets active surface of sedimentary deposition and flattening with depth are common (Weber and Daukoru, 1985).

### **2.3.3. Stratigraphy of the Niger Delta**

In the Niger delta three lithofacies have been identified by the oil and gas industry as Akata, Agbada and Benin Formations. These three depositional sequence are laid down from the subsurface basement complex to surface outcrop (Short and Stauble 1967; Avbovbo, 1978).The order of their deposition in an upward direction signifies the age of each formation from oldest to the youngest (i.e marine shale, transitional and continental environments).

#### **1) Akata Formation**

This formation age ranges from Eocene to recent. It is a basal unit of the Cenozoic Niger delta basin, composed of mainly marine shales deposited in the advanced delta into deep water or offshore (Weber and Daukoru, 1985).It is an under compacted clay with locally sandy, silty beds with some plant remains at the top, deposited as turbidities and continental slope channel fills (Schlumberger, 1985). Between the adjacent Agbada and top of Akata formations sandstone lenses occur, this development makes prospecting for oil and gas at the top of Akata formation viable due to the presence of planktonic foraminifera content that may account for over 50% of the rich micro fauna and the benthonic assemblages indicating that its deposition is on the shallow marine shelf environment and slope (Short and Stauble 1967; Avbovbo, 1978).Hence, it is referred to as the main source rock for the Niger delta complex. This formation thickness depends on the shale diapirism and or it subjection to permeability (flowage). Weber and Daukoru (1985) estimated its thickness to range from 600 to over 6000m.

#### **2) Agbada Formation**

The overlying paralic sequence, on top of the under compacted clays constitute the Agbada formation. It consists of alterations of sandstones, sands, shales and siltstones. The sandy upper unit of this formation is the hydrocarbon reservoir, while at the base significant sandstones' unit is evidence which are very coarse to fine in grain size with intercalation of shales (Schlumberger, 1985; Weber and Daukoru, 1985; Short and Stauble, 1967). It is slightly consolidated and have calcareous matrix (cementation), bulk of this formation is unconsolidated. This unconsolidated nature of the Agbada formation is what affect and caused most of the completion and production issues (geomechanical problems) seen in the Niger Delta till date (Schlumberger,1985). The sandstone are poorly sorted with variation in grain sizes ranging from fine to coarse. Shale content

increases downward as the formation passes or grades into Akata Shales. Lignite streaks, limonite, shell fragments and glauconites are present. The formation is built up of various offlap rhythms that cut across the entire subsurface of the Niger delta basin (Doust and Omatsola, 1990). The age is from Eocene to Oligocene. Weber and Daukoru (1985) estimated its thickness to range from 300 to about 4500m.

### **3) Benin Formation**

Among the three sedimentary deposits, Benin formation is the youngest and the uppermost unit of the Tertiary Niger delta basin. It is composed of gravels and nonmarine sand deposited in an alluvial or fluvial environment (Weber and Daukoru, 1985; Doust and Omatsola, 1990). The formation is known for its high percentage of sand as it cut across the entire Niger delta. It has few minor streaks and lacks the presence of marine fauna and blackish water (Schlumberger, 1985). The sandstones and sands are coarse to fine, poorly sorted, sub-angular to well-rounded and has granular texture. Lignite streaks occurs and feldspars and Hematite are common (Schlumberger, 1985). Its shale content consists of sandy to silty and has plant remains. Structural features associated with this formation are; Oxbow fills, channel fills, point bars and natural levees back swamp. Its age is from Miocene to recent. According to Weber and Daukoru (1990), the thickness of this formation especially within the central Niger delta is 2100m. Till date only little oil and gas has been found in the Benin formation. Hence, it is known for its potable water bearing (Short and Stauble, 1967).

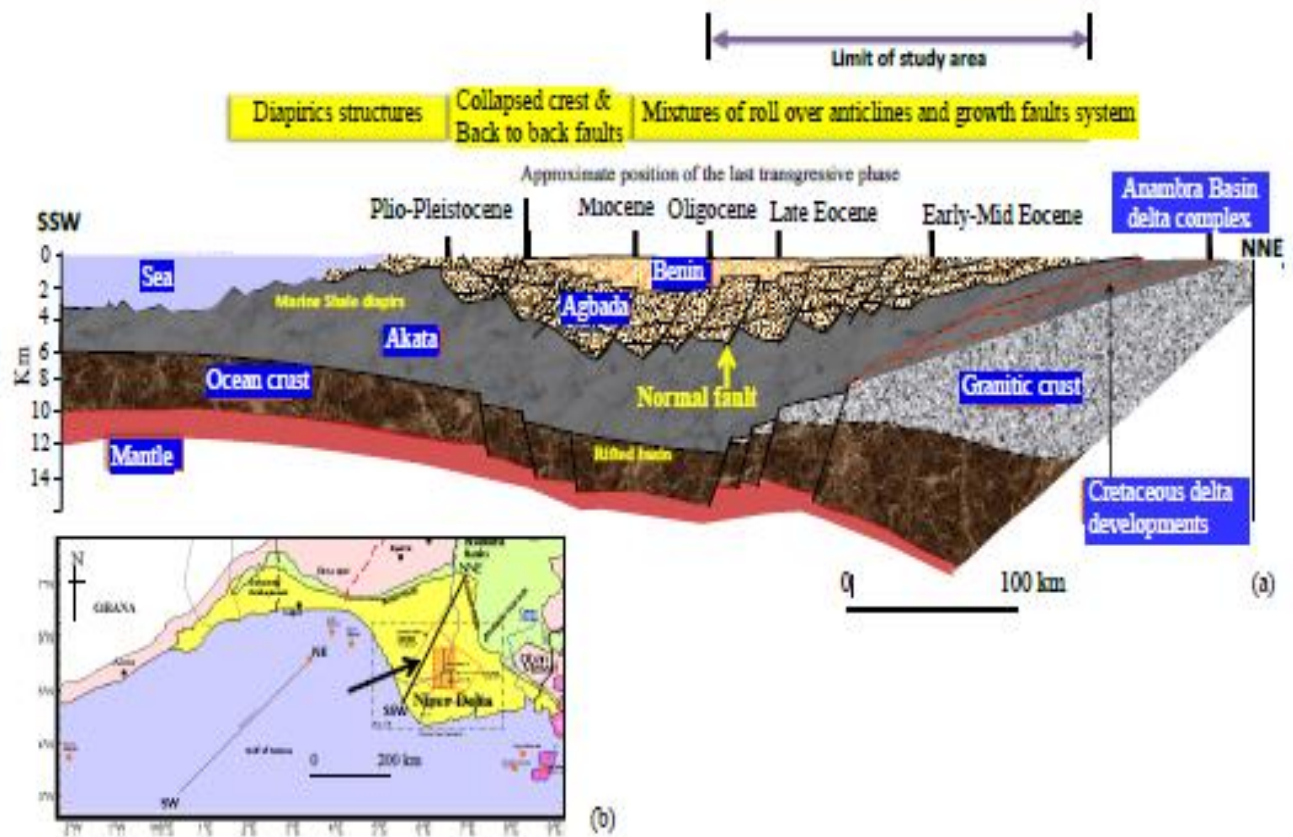


**Figure 2.5b:** Shows a section illustrating the depositional setting of the Niger Delta basin from Anambra in the far NNE to offshore Niger Delta at the SSW end (Merki, 1972, Weber and Daukoru, 1975; Whiteman, 1982).

#### 2.3.4. Location of the study area

This study area is located in the North central onshore Niger Delta with codename OML Wabi. Its coordinates are 5° 13' 50.88''N and 6° 39'56.88'' E. The field is situated in the greater Ughelli depobelts. **Figure 2.6** with sedimentary deposits sequence ranging from Oligocene to lower Miocene based on biostratigraphical study (Baulac, Grosdidier and Boutet, 1986). The first discovery was made in 1982 by Wabi 11 which encountered about 355.5m of gas (Scf.) and 11m of oil (bbl.) both gross pays were found in eleven distinct reservoirs. The well was tested at shallow and deeper levels. Therefore, the field has multiple reservoirs. A total of 5 well have been drilled into the Wabi structure which encountered different reservoirs between the depth of 2070 m and 4400 m. One of the Wabi well was tested at four (4) gas/condensate reservoir levels, completed and suspended as gas and condensate producer. However, production in some intervals commenced. The Wabi structure (trapping) style confirmed the dominance of synthetic growth fault system with possible sequential down the basin trending style that is, NESW (Zorasi *et al.*, 2017). Fault plays impact in the structural trapping mechanism; hence faulted assisted closure resulted in the hydrocarbon accumulation within the field.

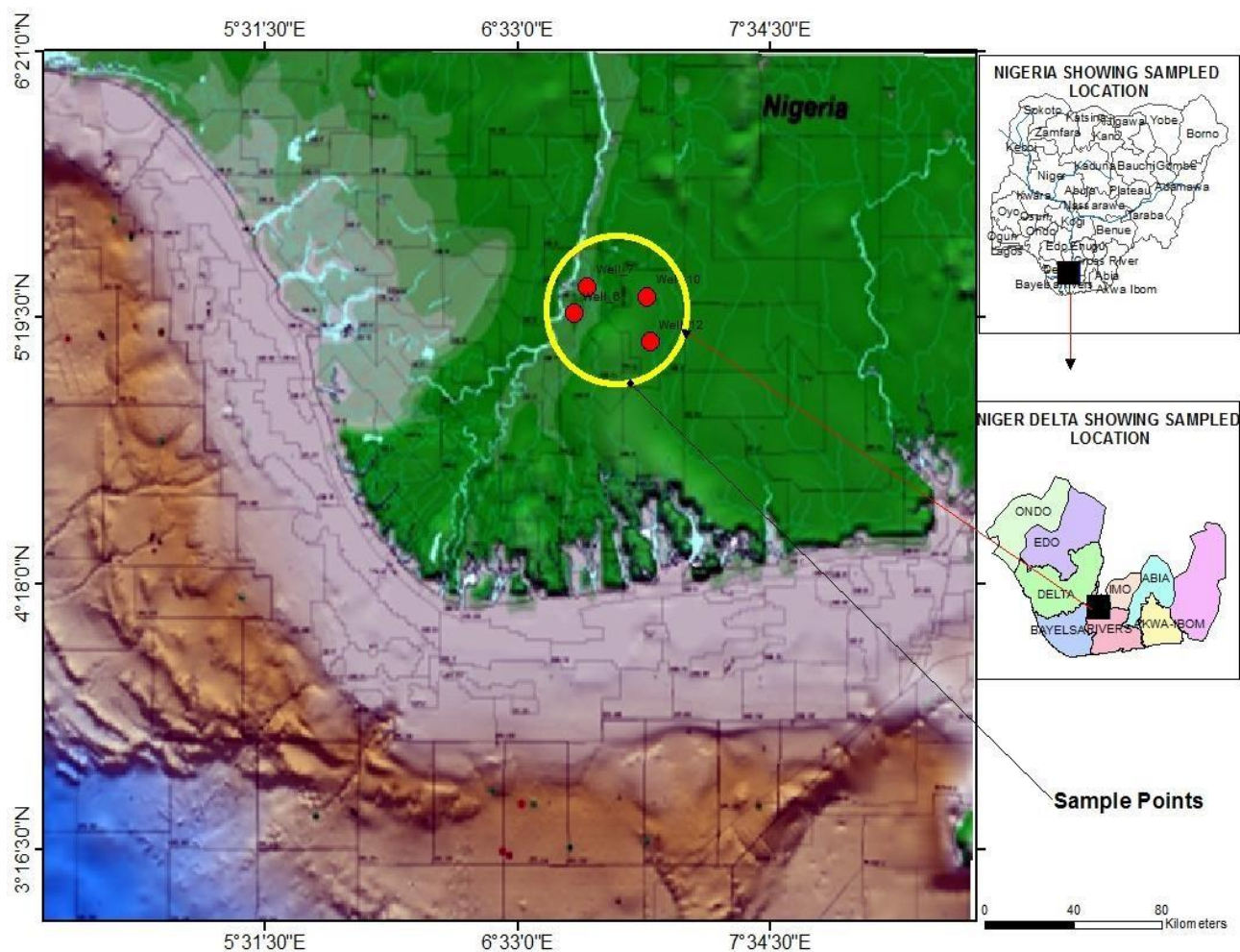


**Figure 2.6.** Map of the study area showing spatial well locations (Modified by Zorasi, 2017)

## 2.4 Conceptual framework

Zoback (2007) stated that to completely understand and resolve the state of stresses acting within or at some point in the subsurface called reservoir and to know its effect which could be positive or negative to operators, we need to understand stress as it relates to rock mechanics. The term stress is defined as the force acting over a given area. Sometimes, since stress is a tensor, stress tensor is used to depict the density of forces acting upon a surface in a continuum at a given point (Tingay, 2009; Zoback, 2007). Rocks have both anisotropic and isotropic properties. For anisotropic or heterogenous rocks, the values of rock properties measured in all directions differ from one another while in isotropic or homogenous rocks the values of rock properties measured in all directions are equivalent. Jaeger *et al.* 2007 asserted that materials whose response is independent of the applied

stress is Isotropic materials. According to Hudson and Harrison (1997), continuum mechanics describes the stresses acting on a homogenous isotropic body as a second-rank tensor, having nine components. Three out of these nine stresses are normal while six are shear **Figure 2.7** (Tiab and Donaldson, 2012) which completely define the state of stress acting on the cubic element at any point or given depth as shown in equation (2.6).

$$S = \begin{bmatrix} \sigma_{11} & \tau_{12} & \tau_{13} \\ \tau_{21} & \sigma_{22} & \tau_{23} \\ \tau_{31} & \tau_{32} & \sigma_{33} \end{bmatrix} \quad (2.6)$$

where, the subscripts of the second order rank tensors denote the direction of force components and the surface it is acting. Hence stress components represent force acting in a precise direction on a unit area of given orientation. To completely depict the condition of stress at depth in the reservoir, one must describe these six shear stress magnitudes and the three normal stress magnitudes including their angles of orientations in 3D coordinate system (Zoback, 2007).

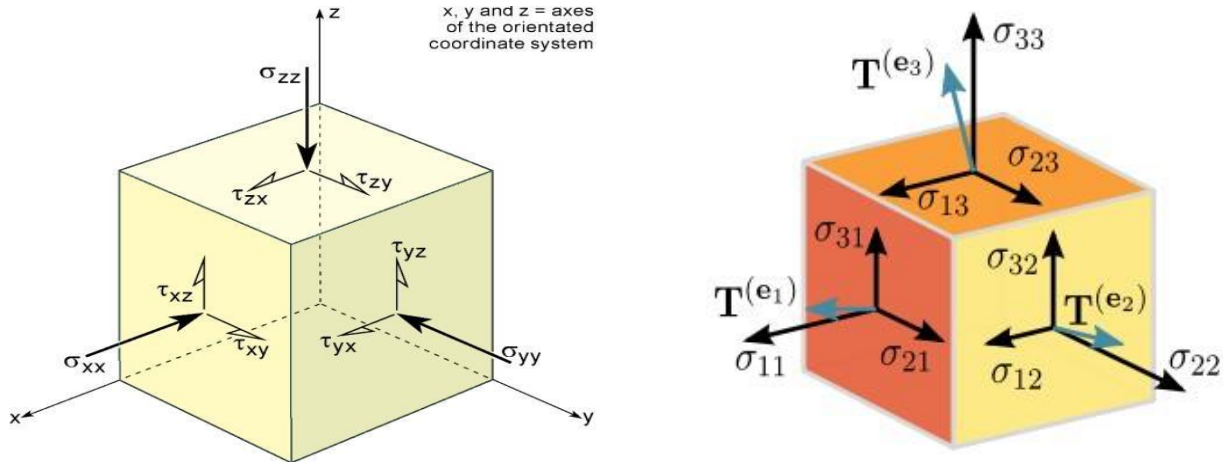


**Figure 2.7.** a) The normal and shear stress components on an infinitesimal cube. b) The stress tensor, a second- order tensor (Hudson and Harrison, 1997).

There are sets of axes along which all shear stresses become zero while the normal stresses are at their extreme values. These axes define the three mutually- perpendicular planes and the normal stresses acting on these planes are called principal stresses (Tiab and Donaldson, 2012). All states of stress help to understand the principal stresses. The principal stress tensor is represented as;

$$S = \begin{bmatrix} \sigma_1 & 0 & 0 \\ 0 & \sigma_2 & 0 \\ 0 & 0 & \sigma_3 \end{bmatrix} \quad (2.7)$$

where  $\sigma_1$  is the overburden,  $\sigma_2$  is the intermediate horizontal and  $\sigma_3$  is the minimum horizontal stress.

Sorough (2013) explicitly explained that geomechanics engineers utilize theoretical and applied science for the evaluation of mechanical behavior of subsurface rocks within the force fields of their physical environment. In other words, it is the application of engineering principles to mechanics of rock design and construction of any kind either on or in the rock. The concept of geomechanics was originally developed to enhance mining activities as well as to aid in civil engineering design purposes. However, because of its efficacy it was implemented into the oil and gas industry over three decades ago for improvement of drilling, fault reactivation, stress evolution and hydraulic fracturing. Geomechanical characterization is executed both for well scale analysis for wellbore stability, sand production, hydraulic and field scale such as fault reactivation, subsidence or heave, cap rock integrity, and effect of reservoir flow or match (Schlumberger, 2017) The main rationale behind the practice of geomechanical analysis is to calculate approximately the rock properties and stresses acting on a wellbore.

Moreover, Tingay *et al.* (2005) revealed that understanding of the present-day tectonic stress is crucial for various applications such as improving the stability of the wellbore to enhance hydrocarbon recovery through natural or induced fracture. The key insight into earth's stress state is made possible by global stress map studies which uncover the controlled forces causing regional and local stress fields as tectonic activities at plate boundaries (Tingay *et al.*, 2009) in particular mid-ocean ridges and continental converging zone. Hence, the knowledge of stress distribution and redistribution, rock distribution and deformation history are revealed from the present day stress field understanding, mostly in sedimentary basin (Tingay *et al.*, 2005). Thus, local and regional scale stresses have significant implications on petroleum exploration and exploitation **Figure 2.8 (a-b).**

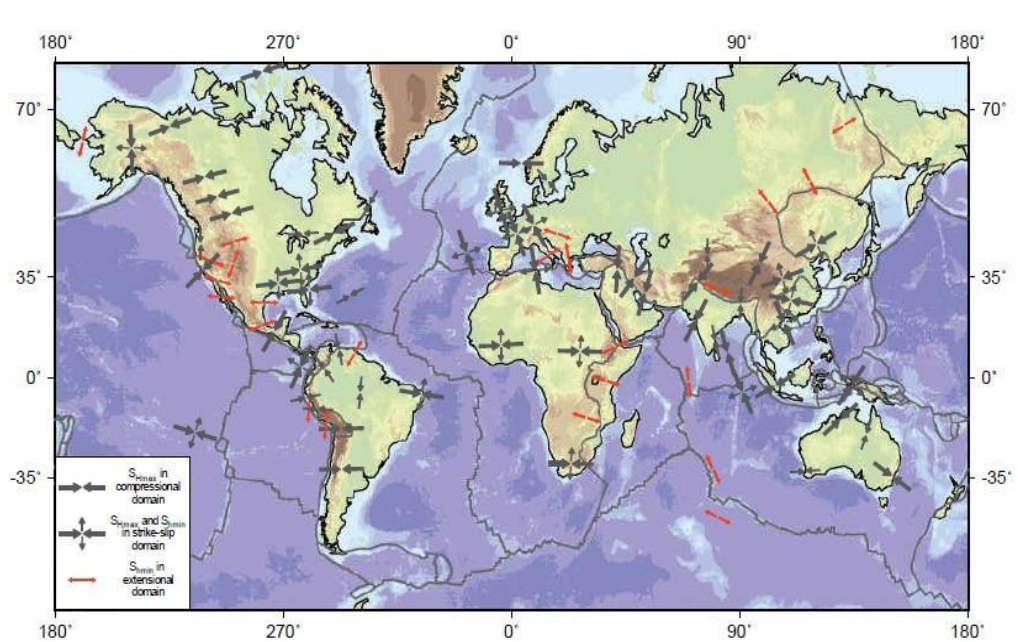


**Figure 2.8a** Generalized world stress Map (Zoback, 1992)

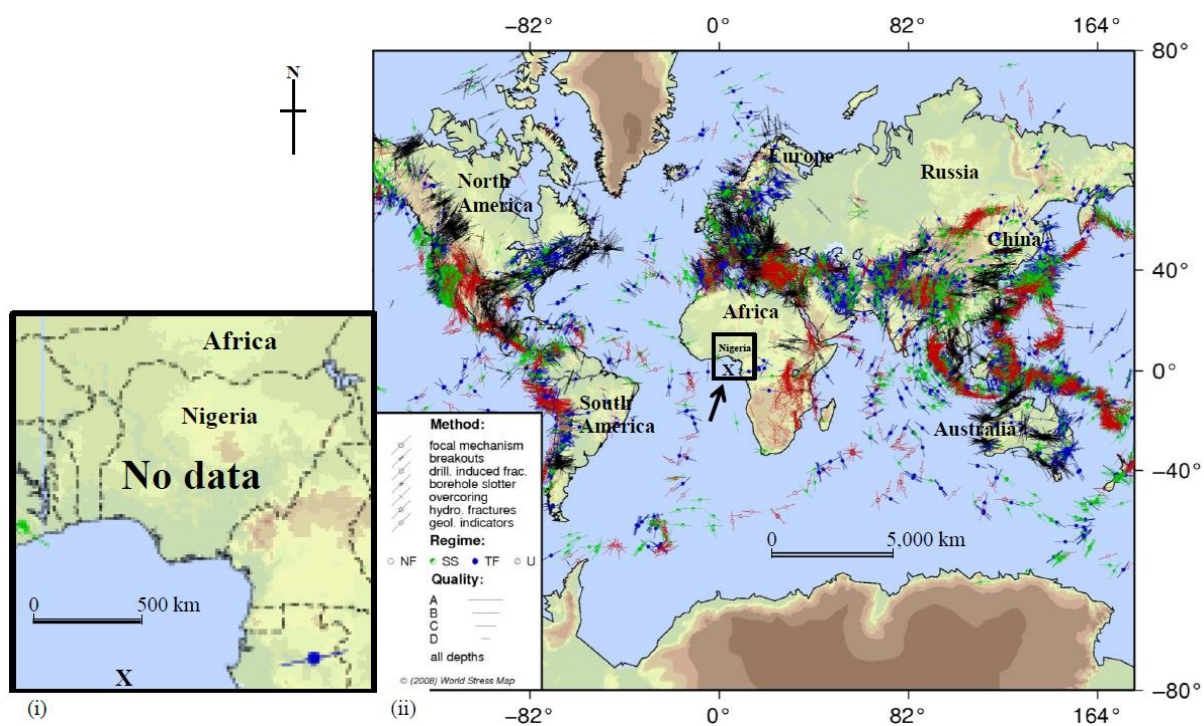


**Figure 2.8b:** World stress map. Heidbah *et al.*, 2008, showing stress direction, source and regimes.

### 2.4.1 Stress field pattern of the Niger Delta

The concept of subsurface stress in the lithosphere has been reviewed and documented by (Zoback, 1989; Tingay *et al.*, 2005; Bell, 1996; Magnenet, Cornet and Fond, 2007). In the Niger delta, the issue of in situ stress is considered mostly as overpressure development which is very common in the west and central Niger delta fields due to numerous extensive growth faults and associated roll over anticline that concentrate in the Agbada formation (Ojo *et al.*, 2017) which varies with depths. Far field stress or basement stress, regional and local stress are what contributes to stress pattern of any region globally (Tingay, 2009; Zoback, 2007). In other words, the summation of these stresses provides an insight into the Niger delta stress field pattern. The understanding of the state of stress beneath the earth's crust can be made available through the world stress map (WSM) (Tingay, 2009) **Figure 2.9**. This is a map showing the relative magnitudes of horizontal principal stress and their orientations (Zoback, 2002). Tingay (2009) inferred from this map that forces exerted at mid-oceanic ridges, subduction zones and continental collision zones are the causes responsible for plate-scale stress and the reason for the sub parallel motion in regional stress orientation. Rifting and gravity tectonism played major roles for the formation of secondary structures in the Niger delta, that is, structures that are related to the tectonic rock's deposition and regional stress field (Verner, 2007).

Knowledge of this present day (in-situ stress) state facilitates good understanding of deep-seated geological processes that occur in the earth's interior and it is vital for mining activities, understanding basin evolution due to plate tectonic motion, investigation of rock distribution and deformation history and petroleum exploration and exploitation (Tingay, 2009; Zoback, 2007; Rajabi, Tingay and Heidbach, 2016).

#### **i. Attached regimes**

In sedimentary basins the first deposits of young sedimentary Cretaceous rocks that overlain the basement complex mechanically and has low strength rocks intervals (e.g. evaporates, over pressured shale or mechanically weak spot) that can interfere and disrupt the original laid down sediment to cause mechanical detachment in the basin is referred to as Attached regimes (Bell, 1996; Tingay, 2009). This regime has primary structure associated with the origin of rocks

deposition. The stress field, magnitudes and orientations in this region are influenced by far field stresses (plate scale forces and intra-basins forces) acting from afar or within the basement complex (Tingay, 2009). The stress pattern displays in this attached region depict the underlying rock pattern and show regional consistency in their orientations (Bell, 1996; Tingay, 2009) which are predictable in the whole basin.

Based on global comparison and correlation made, Bell (1996) and Zoback (2007) further state and confirm that attached stress regimes demonstrates uniformity in directional homogeneity of stress orientations with other similar studies conducted elsewhere in the world.

## **ii. Detached regimes**

This is the mechanical separation of the basal unit from the overlying sedimentary sequence. Overpressure shale of the Niger delta basin forms a detachment folds, detachment zone for normal fault and thrust structures in a linked extensional contractional systems (Wiener *et al.*, 2010). Doust and Omatsola (1990) Asserted that basin deposited with intervals of low strength rocks such as evaporites, over pressured, halite and ductile marine shales with slope instability are weak geomechanical zones which would trigger development of growth faults structures known as detached fault (Bell, 1996; Tingay, 2009). Detachment fault is a low angle normal fault along which a basal strata shears at an inclined surface (Howard and John, 1987).

By deep mechanical detachment, far field stresses (acting in the basement) are partially and/or completely removed from the paralic clastic sequence overlying on the basal unit (Tingay, 2009). The stress patterns of this region are complicated or random because of the dominance of local (intra-basin) sources of stress mentioned above and exhibit vastly different and compound stress orientations. In other words, stresses in detached regimes are basically controlled by small or local sources of stress (Bell, 1996; Tingay, 2009). However, Bell and Babcock (1986) revealed that there is less orientation consistency found in other part of the world sediments.

Consequently, there exist some variations in horizontal stresses which depend on the sedimentary basin of interest. Similarly, Becker *et al.* (1987) maintained that stress orientations can differ between thrust plates due to multi-level detachment, forming the surfaces of detachment. The most spectacular of detachment case is the appealing to conclude that stress regime which reflect

basement stresses of Mesozoic and Cenozoic sequences is attached base on the coincident of regional stress direction of the Scotian shelf and North American plate (Zoback and Zoback, 1991; Yassir and Bell, 1994).

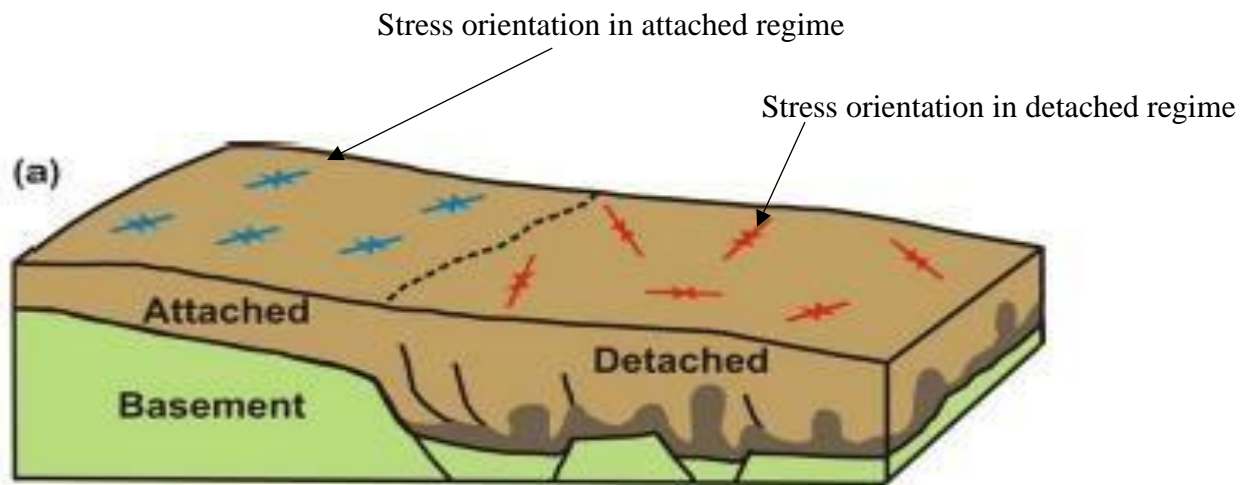


**Figure 2.9.** Schematic diagram of Attached and detached Stress regime (Bell, 1996; Tingay, 2009).

### iii. Anderson classification scheme

Besides, Anderson (1951) and Cervený *et al.* (2004) unanimously agreed that three stress regimes are identifiable if rock fails in shear. These stress regimes are associated with the three classifications of fault regimes by Anderson hypothesis of faulting is extensively used as a basis to describe the basics of fault failure and orientation. Stress state is defined by three principal stresses which are mutually perpendicular to each other (Twiss and Moores, 1992). Anderson did this description using a hypothesis which assumes that one of the principal stresses is the greatest, followed by intermediate and the least (i.e.  $\sigma_1 > \sigma_2 > \sigma_3$ ) in descending order of magnitude. The lithostatic load is constantly vertical and should be identified first since the other two are orthogonal and horizontal **Figure 2.10**. This automatically defines the orientations of the two horizontal stresses (Cervený *et al.*, 2004; Economides and Nolte, 2000). Anderson's theory of faulting predicts the type of developed fault at any given area to form in two conjugate planes

depending on any three of the principal stresses that becomes vertical with the other two being orthogonal (Twiss and Moores, 1992; Jaeger and Cook, 1979; Zoback, 2007) as follows:

- 1) Faults are expected to form at  $+60^{\circ}$  to the minimum horizontal stress  $\sigma_3$  direction.
- 2) Faults are expected to form at  $\pm 30^{\circ}$  to the vertical principal stress  $\sigma_1$  direction.
- 3) The line created by connection of conjugate fault planes will be parallel to  $\sigma_2$ .

Following the orientations of the stresses defined above, Anderson (1951) described the classification of fault in an area as Normal fault; when dip is  $60^{\circ}$ , Thrust fault; when dip is  $30^{\circ}$  and strike slip; when dip is an angle of  $30^{\circ}$  (Twiss and Moores, 1992). His theory assumes and characterize maximum principal stress (overburden) to be vertical in normal faulting, the minimum horizontal stress as vertical in the thrust faulting and intermediate horizontal stress as vertical in the strike slip faulting (Zoback, 2007).

Moreover, the work of Bell (1996) reviewed the in situ stresses in sedimentary rocks for geological and petroleum geomechanical engineering applications and elaborated on the generally used measurements methods for determination of in situ stress in sedimentary rock especially in terms of the three principal stresses; vertical, intermediate and minor horizontal stresses (Bell, 1996). Consequently, he mentioned the sources where these three principal stresses, which are relative can be obtained from, as density log for vertical stress determination, leak off test or hydraulic fracture test for minor horizontal stress, core monitoring techniques for minor and intermediate stresses including micro and mini fracture data.

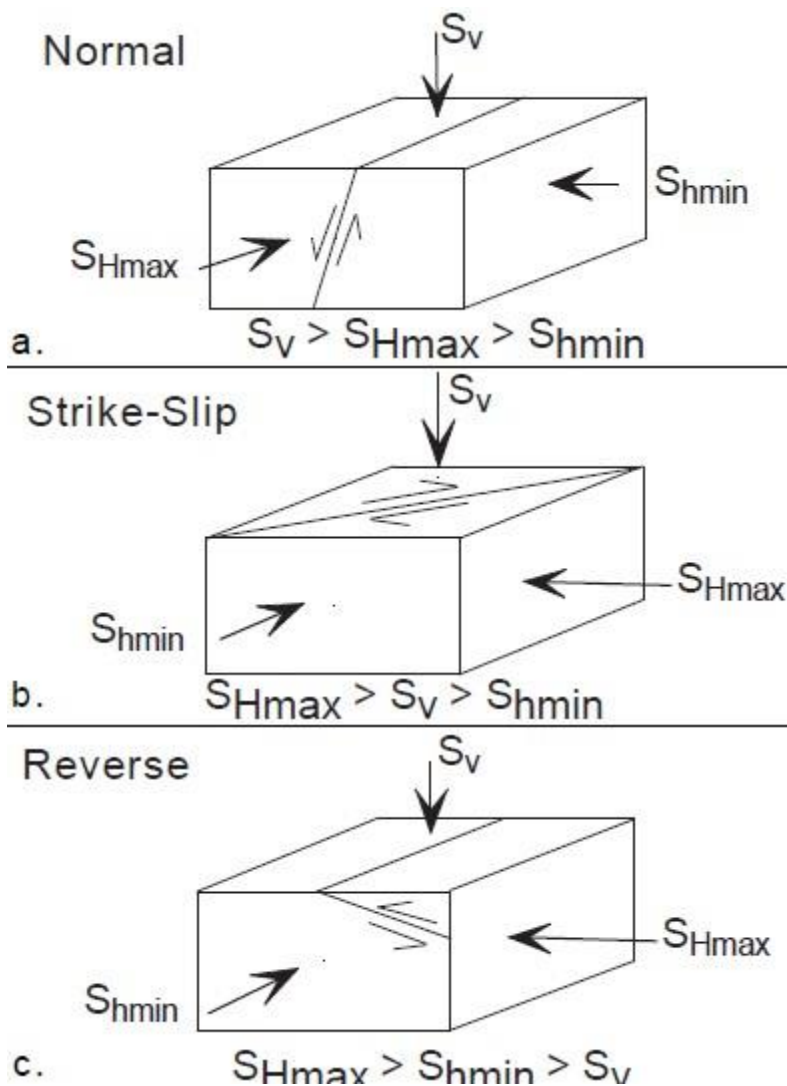


**Figure 2.10.** Andersonian's classification scheme for types of faulting regimes (Zoback, 2016)

#### 2.4.2. Petroleum basin geomechanical characterization.

Hudson and Harrison (1997) asserted that petroleum and geomechanics engineers evaluate rocks to ascertain the pre-existing state of stresses in the ground/rock for the purposes of design and completion applications. Hence, good grasp of the fundamental of stress tensor is vital for comprehension of stress magnitudes and orientations in the subsurface.

Meanwhile, Bell (1993, 1996) disclosed that understanding of the stress state of a basin for its characterization requires measurements of in situ stress in the basin in terms of its overall

geomechanics, which incidentally includes the relationship between the sediments and the overlying rocks.

In addition, Zoback (2007) submitted that sedimentary basins are found in stress regimes with normal strike-slip and reverse faulting environments. Thus, data gathered during drilling and hydrocarbon production, provide necessary information on stress orientations and magnitudes (Zoback, 2007). These data are required and acquired as a function of depth to address geomechanical stress related issues if the reservoir has geomechanical challenge (Dusseault, 2011). The understanding of stress magnitude and distribution in the earth interior can be combined with mechanical, thermal and rheological constraints to examine a broad range of geologic processes (Tingay *et al.*, 2005).

Zoback (2007) and Bell (1996) asserted that in some regions, consistent stress field exists all over the upper brittle crust as indicated by constant orientations observed in part of North Sea and western Canada. However, change in in-situ stress as a result of production, injection and drilling activities make it difficult for the existence of uniform present-day stress from the different measurement techniques sampling very different rock volumes and depth ranges (Zoback, 2007).

In the account of Schneider (1985), Bell (1996) and Yale (2003) demonstrated that present day stress orientations are strongly influence by mechanical properties contrasts of rock unit present in the basin. In other words, geologic structures such as diapirs, folds and faults deflected the horizontal principal stress in an order of few meters to kilometers (Tingay, 2009) and are known to be the controlling factor in local stress field. Examples have been cited around the world where these local stress variations have been observed (Tingay, 2009; Bell, 1996), a weak fault or fracture zones cannot uphold shear stresses hence, act as a free surface. Hence, the stress field within this faulted or fracture zones are re-oriented locally so that  $S_{h_{max}}$  is deflected to be sub- parallel to the faults or fracture, this suggests that the weak zones are soft relative to the surrounding rocks. Similarly, in a stiff structure  $S_{h_{max}}$  is deflected to be perpendicular to the fault trace or igneous intrusive (Bell, 1996; Tingay, 2009). These anomalous local stress orientations are the consequences of near geologic structures and/or mechanical properties contrasts of the rocks. How much horizontal principal stresses are deflected depends on the scale (i.e greater, larger and small) nature of the interface and the geomechanical property contrast (Zhang *et al.*, 1994).

## 2.5. Estimation of in-situ stress

The diagram below showed that rock is porous to some extent and the pore space are filled with in-situ fluids (water, oil, gas or rock melt) under pressure. These pore fluids may affect rock failure due to mechanical effect (tensile stress) of the pore pressure and due to chemical interactions between the rock and in-situ fluids (Jaeger *et al.*, 2007).

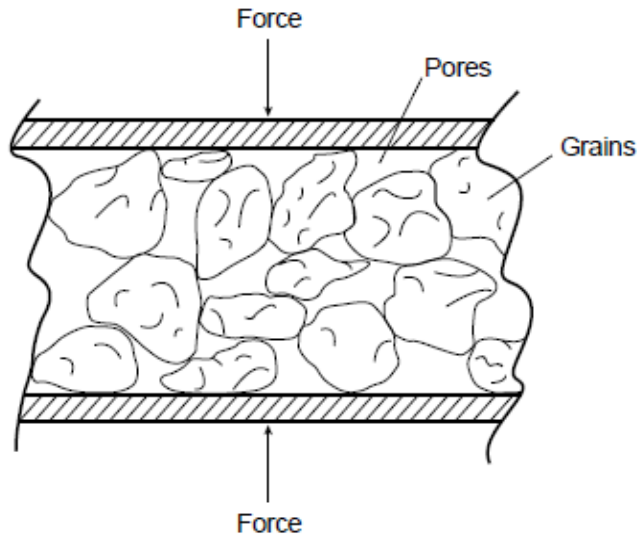


**Figure 2.11.** Show load sharing by pore pressure. Pore fluids support a portion of the total applied stress and only a portion of the total stress (effective stress) is carried by the rock.

The first concept of effective stress was introduced in 1923 by Terzaghi with a mathematical relation as follow:

$$\sigma^l = \sigma - P \quad (2.8)$$

where,  $\sigma$  is the total applied stress,  $\sigma^l$  is the effective stress governing consolidation of the material and  $P$  is the pore pressure. Following the proposed equation by Terzaghi, Biot between 1941 and 1956 came up with a consistent theory that accounts for the coupled distribution/deformation processes that are observed in elastic materials. He expressed this for poroelastic elastic materials as;

$$\sigma^l = \sigma - \alpha p \quad (2.9)$$

where,  $\alpha$  is the poroelastic (Biot) constant which varies between (0 and 1). Terzaghi (1923) effective stress equation governs rock deformation.

Worldwide, oil and gas hydrocarbon reservoirs are found at various depths (shallow and deep reservoirs) below the earth's surface, that is, within few hundred to several thousand meters/feet (Jones *et al.*, 1992). As the depth to hydrocarbon discoveries increases, so the weight of the overlying rock column increases and acts as overburden stress on the reservoir. To estimate stress state generated, we assume that the rock is a semi – infinite isotropic medium subjected to gravitational loading where there is no horizontal strain. Vertical stress is generated by the weight of the overburden and it is referred to as maximum principal stress (Economides, 2000).

$$\sigma_v = \int_0^H \rho(H)g dH$$

or

2.10

$$\sigma_v = \int_0^h \rho_r g h$$

where,  $\sigma_v$  is the overburden stress,  $g$  is the gravitational constant,  $H$  is the depth of burial and  $\rho_r$  is the rock density. The integration of density log gives us the vertical stress. In young sediment formation over burden gradient varies from about 0.8psi/ft to about 1.25psi/ft in high density formations.

Sedimentary rocks are known for its porous nature which host fluid such as oil, water and gas in a formation. Considering a cross section of the hydrocarbon reservoir; generally, the whole rock columns on top of the hydrocarbon reservoir down to the reservoir ideally will also be saturated with (oil, condensate, brine or water) and/or gases (natural gas or air). These liquids, thus, form a continuous column from surface of the earth down to the reservoir interval and the load of this column is accountable for another stress component acting in the hydrocarbon reservoir this is known as the hydrostatic pressure or component of pore fluid pressure expressed by (Jones *et al.*, 1992) as:

$$P_p = \int_0^h \rho_f g h$$

(2.11)

Where,  $P_p$  is the pore pressure and  $\rho_f$  is the pore fluid pressure,  $g$  is the gravitational constant and  $h$  is depth.

Tingay *et al.* (2005) explained that the present-day stress field is been controlled by the deflection caused by geologic structures such as faults and diapirs. Thus, the present-day stress pattern, geologic setting and type of rock in a basin also subject hydrocarbon reservoir to horizontal stresses (Jones *et al.*, 1992).

### **2.5.1 Description of principal stresses**

Economides and Nolte (2000) asserted that a complete account of the state of stress is of significance because hydraulic fractures promulgate perpendicular to the minimum principal stress. This aids hydraulic fracturing design as follows: if  $\sigma_3$  is horizontal, a vertical fracture will be created (recommended for the reservoir). If  $\sigma_3$  is vertical, a horizontal fracture will be created (recommended for the reservoir) and if  $\sigma_3$  is inclined, an incline fracture normal to it will be created (recommended).

### **2.6 Theoretical framework (mechanical behavior of rock)**

Rock deforms when subjected to load due to high stress level and more strain experience.

Jones *et al.* (1992) posited that sedimentary rocks consist of porous media, grains and minerals that eventually cemented (bonded) these rock properties together. These sedimentary rocks are the hub for hydrocarbon generation, storage and transmissivity by their intrinsic nature. The theories of rock behavior that is, elastic, nonlinear or inelastic which determine the relationship between stress and strain provide the basis for interpretation of geomechanical parameters for well construction design. These theories are referred to as constitutive laws.

Rocks are not completely elastic they are brittle with negligible plasticity; the awareness of elastic parameters is of enormous importance for engineering applications. At low effective stresses rock samples subjected to load behave elastically while at high effective stresses rocks deform or rupture (Cerveny *et al.*, 2004; Jones *et al.*, 1992). When a rock sample or an element of the earth is submitted to load, it exhibits elastic behavior at low stresses but at high effective stresses, it deforms, yield or give way in service. Thus, rock behavior depends on the existing stress conditions. The description of the behavior of rock undergoing deforming force is governed by constitutive laws which determines the relationship between stress and strain and describes the deformation (Zoback, 2007). There are three types of these laws namely; Elasticity, plastic and Viscous (Serra, 1984)

### **2.6.1 Linear elasticity**

For an ideal rock, it is assumed that rock behaves as an elastic material this gives it significant advantages (Serra, 1984). In elastic theory, it is assumed that there is a one-to-one association between stress and strain when subjected to an applied force and upon the removal of the force the rock behavior becomes reversible. This display linear elasticity behavior and Hooke's law is obeyed, that is, it assumed a linear and unique relationship between stress and strain. Once more, taking into account the strength of the materials the deformation will be elastic until the point of failure is reached. Beyond the elastic limit, any small degree of inelastic deformation leads to failure of material (Tiab and Donaldson, 2012). This is valid for well cemented rocks but for weak and poorly cemented rocks the applicability of the above strength of material approach is more questionable (Zoback, 2007). This theory is applied to non-linear and anisotropy materials. As mentioned above, the rock returning to initial shape is not necessarily immediate and may take some time; this is known as Elastic-plastic (non-linear elastic). This defines rock behavior which responds elastically to the stress level at which it yields and then deforms plastically; without limit upon unloading of the applied force the rock would again behave elastically. In this case there is nonlinear relationship between stress and strain, but it recovers strain attained upon unloading. Anisotropic material has properties that differ in different directions and these properties can be

characterized by five young moduli, Poisson's ratio, compressibility, bulk modulus and shear modulus (Economides and Nolte, 2000).

### **2.6.2 Poroelasticity**

Poroelastic theory explains the deformation in a porous rock saturated with fluid where, the stiffness of a fluid saturated rock will depend on the rate (i.e. time dependent deformation) at which external force is applied. Therefore, the deformation of a poroelastic material is time dependent. It is a property shared with viscoelastic materials.

### **2.6.3 Plasticity**

Soft rocks are usually weak and manifest larger deformation features (creep), creep is a time dependent deformation that occur in materials under constant stress, its originates from visco-elastic effect and occur in both saturated or dry rocks, that is, they flow. Plasticity theory deals with the reaction of rock to load further than elastic limit. Rock deformation becomes permanent above a certain threshold (Serra, 1984). It behaves elastically prior to the point of threshold attainment and deformation occur because of inter-granular movements and recrystallization processes. The theory of plasticity deals with the complex rock behavior particularly in compression. Therefore, it is used for predicting stress concentration around a borehole and the behavior of soft materials in a depleted reservoir (Economides and Nolte, 2000).

### **2.6.4 Visco-elasticity**

Visco-elastic theory is one in which the deformation of rock is in response to an applied stress or strain, it is time rate dependent. The deformational stress required to cause a certain amount of strain in the rock depends on the perceptible viscosity  $\eta$  of the rock (Serra, 1984). Viscosity is the internal resistance offered against the free flow of fluid material. It is equal to the ratio of shear stress  $\tau$ , to the rate of shear strain,  $\dot{\gamma}$ . Viscous material can deform, and the strain is unrecoverable (Serra, 1984). A viscous material that exhibits permanent deformation after application of a load describes visco-plastic. The above theories describe the constitute behavior of rock in elastic, poroelastic, elastic-plastic and viscoelastic media (Zoback, 2007).

## **2.7. Rock strength**

The strength of a reservoir rock is the stress at which the rock fails (i.e. loses its integrity) either in shear, compression and tension depending on load configuration, geometry and stress distribution. The strength of rock can be obtained from various laboratory test methods. These test methods are; triaxial compressive and extension, hydrostatic compressive, uniaxial compressive, uniaxial tension, and polyaxial or true triaxial. The general strength of rocks is a connection between the principal effective stress mechanism as articulated by (Terzaghi, 1923; Economides and Nolte, 2000). Rock strength are dependent on the following factors: rock type and composition, rock weathering, rock density, rock grain size, rock porosity, confining stresses, rock anisotropy, rate of loading, rock geometry, shape and size, time, temperature, pore fluid pressure and fluid saturation (Amadei, 2007).

### **2.7.1 Factors affecting rock strength**

The intrinsic properties of reservoir rocks (i.e. texture and mineralogy) coupled with the geomechanical behavior of rocks are controlled by the following factors:

#### **i. Influence of pore pressure**

Pore fluids in a formation provide some support to portion of the total applied stress, besides, a portion of the effective vertical stress is also supported by the rock matrix. The effective stress of a formation varies across the life span of the reservoir (Economides and Nolte, 2000). Furthermore, the fluid response is modified by the mechanical performance of the porous rock in two ways: an increase of pore pressure which reduces normal reservoir stress and induces rock dilation and compression of the rock which produces pore pressure increase causing a time dependent characteristic to the mechanical properties of the rock (Detournay and Cheng, 1993).

#### **ii. The effect of water**

Han and Dusseault (2005) reported that the increase of water saturation during production leads to sand failure. Formation water act in different ways to cause sand failure: by chemical deterioration

of cementing materials which weaken the strength of the crystal structure rock and; by pressure solution caused by dissolves soluble minerals deposited locally in low stress environment which are prone to complete flush out (Allmendinger, 2015). A sandstone will addition of water or fully saturated may typically lose its strength by 15% (Goodman, 1989). On the other hand, the consequence of fissure water and pore pressure influences the rock strength.

### **iii. The effect of size on strength**

Rocks are composed of crystals and intact grain to grain, principally characterized by joints, cracks, fissures, shistosity, cavities and other possible discontinuity (Jumikis, 1983). To understand the components that influence rock strength, large samples are required for test, these samples suggest pre-existing cracks, but when the test specimen sample is small in size such that relatively, few cracks are present. This sample failure involves new crack growth. Therefore, rock strength is size dependent (Goodman, 1989). Rock strength decreases with the size of the test specimen and a finer size grain leads to high fracture (Amadei, 2007).

### **iv. Anisotropic rock**

Rock anisotropy describes the continuous directional variations of principal stresses and mechanical properties of compressive strength (Bidgoli and Jing, 2014; Goodman, 1989). It occurs in so many formations with interlayer mixtures components such as sandstones/shale intercalation, chert/shale alteration and banded gneisses. The characteristic of strong anisotropy is established in rocks with parallel arrangement of flat minerals like chlorite, mica and long mineral like hornblende or clay (Goodman, 1989). Deformation and rock strength anisotropy has significant role for well engineering design and assessment in geomechanics as rock exhibiting anisotropy may leads to strong strength anisotropy (Goodman, 1989).

### **v. Confining pressure**

All rocks deform slightly by some few percentages prior to their rupture or fracture at low confining pressure (Serra, 1986). This mean that at high confining pressure rock mechanical property behavior variation is observed. Hence, at reservoir depth confining pressure increases the rock strength (Amadei, 2007).

## vi. Time

Rocks generally exhibit elastic behavior except in few cases where they have nonlinearity. When the rocks are subjected to very short time or duration stresses they behave elastically and become plastic when they are exposed to stresses applied over long duration of time. Thus, time played a significant role in the behavior of rocks (Tiab and Donaldson, 2012)

## vii. Temperature

Elasticity limit of rock is observed to decrease as the formation temperature increases; therefore, when temperature increases less stress is required to produce deformation or strain in a reservoir.

### 2.7.2 Rock failure and fracture mechanics

Rock failure means the gross loss of reliability in a rock sample specimen to carry out its proposed function as regard to civil engineering context (Jumikis, 1983). A rock fails as soon as the state of stress is such that the criterion is met along one plane, which is also the failure plane. For instance, in the case of Mohr circle this means that the state of stress at failure is represented by a Mohr circle that touches the failure envelop. To comprehend failure, certain compactable failure criterion needs to be employed because sand fails in shear, while clay fails as plastic, these have been documented as their respective failure mechanisms (Economides, Watters and Dun-Norman, 1998). Other failure mechanisms are; tensile, cohesive, creeping and pore collapse. These criteria are used to generate envelopes which separate unstable from stable zones.

The empirical relations for rock failure criteria are terminology of physical hypotheses derived from laboratory experiments, which indicate how temperature, time effects and in situ stress including other factors affect rock strength (Goodman, 1989). There are numerous rock failure criteria for different rock types.

Thus, they are used to evaluate if a rock will fail or not for engineering design. These relationships are called the failure criterion, and its graphical representation is called the failure envelope. In this study because of the well-established background and simplicity of Mohr Coulomb's and Mohr's criteria, its use is therefore adopted **Figure 2.12**. The figure below explained Mohr diagram, shear

failure occurs if the stress state produces a shear stress that falls outside the stability envelope while tensile failure occurs if the stress state falls to the left shear stress axis and exceeds the tensile strength of the rock.

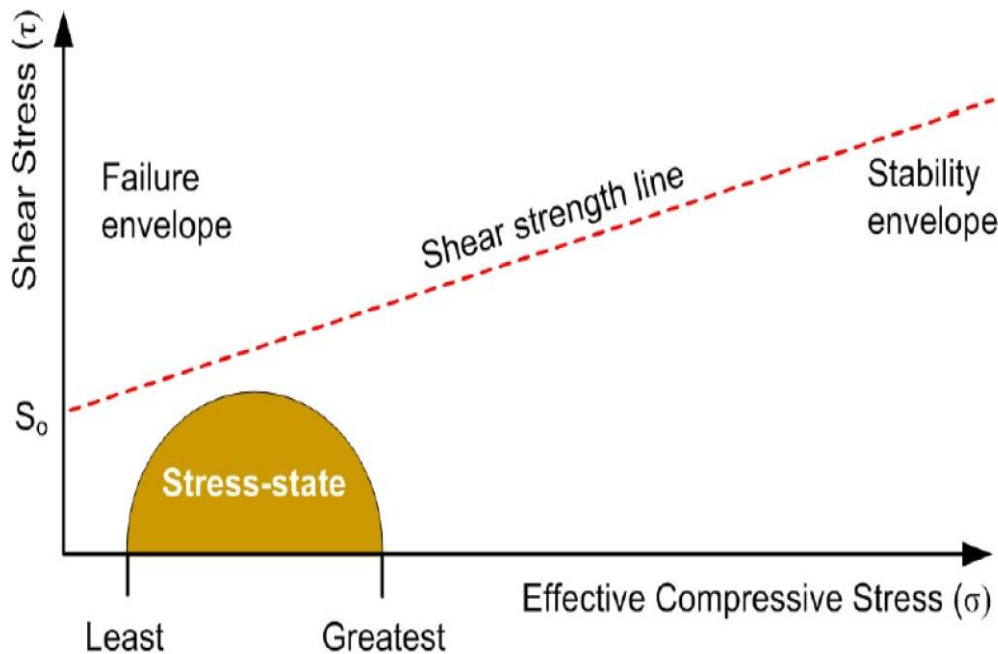


**Figure 2.12.** Mohr Coulomb failure envelope.

### 2.7.3 Basic rock failure model

Models developed to predict rock failure can be divided into four categories namely; Empirical correlation model, analytical analysis model, numerical analysis model and probabilistic model.

- i. Empirical correlation models are developed based on exact field data. They describe the physical behavior of a reservoir rock failure based on field observations. They rely on establishing an empirical correlation with relationships between onset sand product, well data and field parameters which are responsible for causing sanding development in a hydrocarbon reservoir (Gholami *et al.*, 2016).
- ii. Analytical models: are theoretical model applied for the prediction of rock failure which focuses on stress state analysis in the formation, wellbore and/or perforation intervals for

which critical condition has reached for the initiation of rock failure. These simplify the rock mechanic properties and geometry problem and are very realistic for screening purposes and are deployed over a broad range of circumstances (Oyenehin, 2015). As the name implies analytical mathematical equations are used to estimate rock failure or sanding potential (Oyenehin, 2015; Gholami *et al.*, 2016). Thus, they are widely used for sand production evaluation in subsurface engineering, although suffer from assumptions used (Gholami *et al.*, 2016).

- iii.** Numerical analysis models: These are the best model to be employed in solving precise geomechanical problems because they proffer great details of rock failure development as a result of various combinations of input data used for their simulation analysis than their counterparts. The acquisition of all these parameters as input for reservoir simulation suffers some drawback because varied procedures are required, and their corrections must be affected accordingly (Gholami *et al.*, 2016).
- iv.** Probabilistic models: These statistical models developed which utilizes analytical models in conjunction with numerical models to evaluate and predict statistical variation underlying field parameters with reference to satisfactory range of uncertainty.

## **2.8 Empirical analysis review**

Rock formation may become loose after shear volume or tensile failure. When rock fails by shearing or in tensile it led to sand production.

### **2.8.1 Rock Failure and Sand production**

Udebhulu and Ogbe (2015) asserted that the Niger Delta formation is a poorly consolidated and friable region which makes it prone to sand production. This necessitated the need for proper geomechanical analysis to be carried out to understand the in-situ stress, rock strength and elastic properties for field development.

Osisanya (2010) confirmed that poor consolidation reservoirs have always proved difficult which warrants sand production issues to be expected when completing wells in these formations. The

reduction of in situ stress due to poor completion practices also results in consolidation rock failure in mature and brown fields globally. A lot of factors influence sand failure. They include fluid production rate, formation strength and changing in in-situ stresses; just to mention but a few. Sand production is one of foremost problems usually encountered by producing companies for several decades now (Osisanya, 2010).

According to particles together Nouri *et al.* (2003), sand production is the phenomenon that is associated with the production of solid with reservoir fluid. The volumetric failure model which he puts forward argues that pore collapse is a significant source of sanding in a reservoir through induced disintegrated material exposure to the cavity's face.

Soroush (2013) and Majidi *et al.* (2015) confidently maintained that when the virgin state of stress is disturbed by different oil and gas exploration activities, pore fluid pressure in the reservoir is reduced. This reduction may eventually instigate a redistribution of stress in the reservoir and surrounding rocks; thereby leading to a variety of potential issues such as compaction, subsidence, fault reactivation and other forms of strain localization

Oyeneyin (2015) stated and explained that reservoir management for sand production needs an accurate acquaintance of the likelihood of rock failure and the amount of sand it will produce. Conducting a geomechanical analysis is a vital step to assess and prevent costly problems during oil and gas exploration and production (Hoedeman and Hughes, 2015).

Moreover, Jones *et al.* (1992) reiterated that in order to comprehend the mechanical behavior of hydrocarbon reservoir rocks, a sound knowledge of geomechanical properties is indispensable.

The understanding of a reservoir rock may influence the well design strategy. Three approaches are used in geomechanics for its evaluation. They are theoretical, experimental and best industry practices. They emphasized that the productive capacity of a field is affected by the in-situ stress and deformation of rocks due to pressure drop in the reservoir.

The key objectives of geomechanical assessment of reservoir rocks are essentially for economic development, better well engineering, evaluation of the probability of deformational problem occurring in the subsurface, estimation of cost and impact on environmental safety, prediction of

drilling and wellbore stability problems, design of effective well completions and the prompt provision of geomechanical data for mass balances of simulations (Jones *et al.*, 1992).

Pak and Chan (2008) and Hibbeler and Rac (2005) explained that petroleum reservoir having low permeability for the flow of fluid requires hydraulic fracturing to make it commercially feasible. The study justified real time sanding model with minimal input parameters from geophysical logs. Cartson *et al.* (1992) asserted that detailed understanding of reservoir formation, mechanical strength, rock failure mechanism and present-day stress state is necessary for predicting sanding potential for mitigation strategy.

Benetatos *et al.* (2015) succinctly submitted that the notable sources of stress in the subsurface could be categorized as natural and anthropogenic processes. The former is, as a matter of fact, occasioned by tectonic loading, sediment compaction, sediment loading and post-glacial rebound. However, the latter process of stresses formation is basically triggered by man-made activities such as drilling operations, fluid exploitation and local hydrocarbon production.

Abija and Tse (2016) explained the significance of in situ stress level and direction for oil and gas field development planning for optional well placement, especially, in deviated wells for safe and stable drilling to lessen nonproductive time.

In addition, Hubert and Willis (1957) clearly established that the direction of propagation of hydraulic fracturing in a reservoir should be perpendicular to the minimum horizontal principal stress orientation. This was further revealed analytically through the work done to open an amount of a fracture when compared to the product of the stress acting vertically to the fracture plane and/or times the fracture opening amount.

A well is said to be poorly planned or designed when there is inadequate geomechanical data or information about it. The required information about such well may include the elastic properties and the strength of the rock, in-situ stress and well bore stresses around the wellbore wall. Sometimes, production activities may lead to geomechanical problems such as wellbore collapse, kick, lost circulation, side tracking and even well abandonment particularly during an infill and extended wells drilling (Abija and Tse, 2016). The review behind the development of a

geomechanical model of a field is to sustain the lifetime of the reservoir (Hegazy and Lakshmikantha, 2014).

### **2.8.2 Geomechanical methodologies (theories and methods)**

Considering the separate works of Chin and Ramos (2002) and; Udebhulu and Ogbe (2015) reveals that there is a wide variety of empirical, numerical and analytical models for sand production prediction because of the efforts that have been spent in developing these models for geomechanical prediction of sand failure over the years, to assist in several ways of field development and management.

Udebhulu and Ogbe (2015) developed a general mechanistic model that incorporates the theory of dimensionless quantities related with sanding and concluded that nearly all reservoirs have distinctive sand production rate (SPR) relationship index which represents its susceptibility to produce sand or its sanding characteristics.

Abdideh and Ahmadifar (2013) designed methodological workflow for geomechanical model with a primary aim to predict appropriate layers for hydraulic fracturing operation in hydrocarbon reservoir rock using geomechanical model. Their geomechanical model followed an outline which includes five main steps to estimate and calculate elastic properties of rock: in-situ stresses, design for safe mud window, selection of hydraulic suitable layers for fracturing and failure prediction from stress. They concluded that geomechanics provides the key understanding for the investigations and interpretation of the earth response against stresses, which may be natural and anthropogenic.

As a step towards addressing related geomechanical problems for well stability, Darvisa *et al.* (2015) described hydraulic fracturing as a well stimulation treatment and/or enhancement of hydrocarbon production that requires desirable technical deployment. Geomechanical model established for a field enhances the detailed comprehension of the field development options to improve well liberation through an optimized and incorporated method (Xiao *et al.*, 2016). Balarabe and Isehunwa (2017) developed a geomechanical model, whose purpose is to reliably estimate critical pressure below which sand production can occur in a reservoir.

McDermott and Kolditz (2006) put forward a geomechanical model which characterizes fracture closing as a function of effective stress and the variations in petrophysical reservoir parameters which include aperture, permeability and porosity. The changes in normal effective stress cause fracture closure and can be used to formulate an analytical elastic deformation solution to compute the buckle reaction to changes in effective stress (McDermott and Kolditz, 2006). Their model provides an imminent key process to determining the closing of a fracture and serve as a substance input function for numerical models involving the effects of the stress field disparity.

Moreover, Zoback and Khaksar (2006) reiterated the existing empirical equations developed worldwide to estimate rock strength from geophysical logs. These equations have been proven to be very useful in the oil exploration and production industry for estimating and solving a wide range of geomechanical problems; especially, when direct strength information from core is not available. However, some of these equations work practically well for strength-porosity relationships in sandstone and shale formations. The variation of rock strength in individual physical property, shown that published or unpublished empirical correlations designed for estimation of rock strength at a particular region could not adequately fit another region.

Meanwhile, Kang *et al.* (2009) brilliantly and reliably introduced a new approach based on grainscale discrete element to mimic the realistic rock condition. Their well-articulated and presented work revealed the limitations inherent in conventional models and the potential usefulness of a new approach based on a discrete element method (DEM).

In his contribution Hoedeman (2015) compared the different geomechanical model such as 1D, 3D, 4D finite element models for state of stress and asserted the model that gives a more precise and reliable present-day stress among its counterpart as 1D geomechanical models.

Besides, Archer and Rasouli (2012) applied log derived methodology to estimate rock strength through the calculation of the elastic properties and in-situ stress magnitudes from vertical, major and minor horizontal stresses.

Woehrl *et al.* (2010) presented meaningful comparison between the different methods used to obtain rock mechanical properties from petrophysical logs using empirical relations and algorithms. The petrophysical logs allow for computation of continuous presentation of

mechanical properties with depth. These log-derived petrophysical data were correlated with laboratory-derived rock mechanical properties for validation of result.

In their work, Fidelis and Akaha (2016) further stated that geomechanical analysis and its modeling is a tool employed to generate data for well planning and reservoir engineering. These properties are the elastic constants such as bulk modulus, shear modulus, Young's modulus and Poisson's ratio including the in-situ stress. These geomechanical properties account for hydrocarbon reservoir stress profile which is critical to any reservoir development. Thus, they play a key role in the assessment and development of a field by predicting and mitigating the effects of stress and pressure changes for resultant strains on the reservoir, wellbore and completion design in the formation.

In an anticipation to get a better reservoir performance Zhou *et al.* (2005) applied two methods which are based on mapping and radial basis function to estimate rock strength from high-quality nuclear spectrometric tools, comprises of prompt gamma Neutron activation, natural gamma and conventional geophysical logs.

Hudson and Harrison (2000) stated two approaches as direct and indirect for the determination of  $\sigma_{hmin}$ . The direct method as the name implies involves direct stress measurements using either of the tests methods: micro-frac, mini-frac, leak-off test and step rate tests (Zoback, 2007; Fang and Khaksar, 2011; Carnegie *et al.*, 2002).

Jamshidian *et al.* (2017) submitted in their studies that, various models have been anticipated for the indirect method of determining minimum horizontal stress ( $\sigma_{hmin}$ ) parameter and listed these models to include: Newberry, Huang, Terzaghi, Anderson and horizontal poroelastic strain models (Jamshidian *et al.*, 2017). Basically, this indirect method requires various data sets from wireline logs data, core, pore pressure, static Young's modulus, Poisson's ratio and shear sonic transit time (Jamshidian *et al.*, 2017).

Bieniawski (1974) also proposed two comprehensible and easy-to-use methods primarily designed for the prediction of the behavior of rock materials and the estimation of the strength of the rock (i.e uniaxial and triaxial). He validated his methods with some 700 representative specimens from five different rock types.

The deformations of porous rock have been reported by (Carbognin *et al.*, 1978; Yin *et al.*, 2006, 2007; Taheri, 2015) as major concern in some reservoir that affects not only the surface facilities but also cause blockage in the tubing and reduced production rate.

In another contribution, Zoccarato *et al.* (2016) succinctly declared that the prediction of the subsurface compaction of producing oil and gas fields is an imperative issue for accurate reservoir management.

According to Darvish *et al.* (2015), in order to effectively address stress associated issues of reservoir rocks, it is essential to carry out some vital rock mechanical test on different reservoir rock (core) samples for physical and mechanical properties information of the reservoir rock.

Sengupta *et al.* (2011) highlighted on the importance of the extent to which seismic driven earth model can be incorporated into the domain of geomechanics and drilling. The impact of formation parameters from seismic data on well design was duly emphasized. Mention was also made on the fact that seismic inversion parameters improve the resolution and quality of a 3D Mechanical earth model (MEM).

To comprehend failure phenomenon, a specific and compatible criterion must be employed, while some materials such as sand, fail in shear, others, such as clay, may fail due to plastic deformation. Many empirical criteria have been developed to predict rock and formation failure (Aadnoy and Looyeh, 2011). Most of them consider only minimum ( $\sigma_3$ ) and maximum ( $\sigma_1$ ) principal stresses. (Konietzky *et al.*, 2017). However, more advanced ones include the intermediate principal stress ( $\sigma_2$ ). Below are some failure theories and UCS model adopted in rock mechanics. **Table 2.1** Failure theories for ductile and brittle materials

**Table 2.1:** Failure theories for ductile and brittle materials

	<b>Equation/Model</b>	<b>Name of Failure theories</b>	<b>Comment</b>
1.	$\tau = S_o - \sigma_n \mu_1$ $\sigma_1 = C_o + q \sigma_3$	Mohr Coulomb	This criterion relates the shearing resistance to the contact forces and friction to the physical bonds that exist among the rock grains.
2.	$\sigma I_1 + \sqrt{J_2} - B = 0$	Drucker-Prager	This criterion allows evaluation of a given problem related to rock formation failure and its fits for high stress level.
3.	$\sqrt{J_2} = \frac{1}{3}(\sigma_1 - \sigma_3)$	Von Mises	It is used to separate materials into regions i.e. safe and failed or stable and unstable region.
4.	$(\sigma_1 - \sigma_3)^2 = 8\sigma_t(\sigma_1 + \sigma_3)$	Griffith	This failure criterion is applicable to materials which break in tension due to presence of existing microcrack.
5.	$\sigma_1 = \sigma_3 + \sqrt{I_f} \sigma_c \sigma_3 + I_i(\sigma_c * \sigma_c)$	Hoek-Brown Failure Criterion	This criterion is entirely empirical and usually applied to naturally fractured reservoir.
6.	$\sigma_{oct} = \frac{1}{3}(\sigma_1 + \sigma_2 + \sigma_3)$	Mogi-Coulomb Criterion	It utilizes the intermediate stress to give a best fit as against M.C.

### **2.8.5 Previous work on Wabi field**

Adewole and Healy (2013) obtained the directions and magnitudes of two principal stresses namely maximum and minimum horizontal stress components in the Niger Delta from petroleum exploration data and recommended that the maximum horizontal stress is the intermediate principal stress in the basin. Also using two approaches which depict function of vertical stress and over pressure at depths they quantified the magnitude of horizontal. Hence, proposed the existence of inhomogeneous stress in the Northern Niger Delta and suggested different sources of stress field in the study basin base on analyses of 32 borehole breakouts recorded in six wells.

Abija *et al.* (2016) carried out investigation of in situ stress orientation and magnitude for determination of stress pattern in Wabi field Niger delta for well engineering particularly, for directional drilling trajectory optimization for actualization of safe drilling operation of infill wells in the field.

Uzorhukwu (2016) conducted a critical evaluation of the different existing correlations employed for estimation and analysis of geomechanical parameters of rocks adopting three approaches; namely, ranking and cross plots to obtain the best correlation that fits the Niger Delta region and recommends the best correlation that can be applied to evaluate rock strength in the Niger Delta reservoir as the Sharma and Singh approach.

Abija and Tse (2016) examined the geomechanical properties of an onshore field in the north central Niger Delta for geosteering, wellbore stability, hydraulic fracturing in directional wells for implementation in infill well using data from Oil and gas producing company.

Salawu, Sanaee and Onabanjo (2017) determined the rock strength (unconfined compressive strength) of core samples collected from across the Niger Delta basin at different depths to obtain an empirical correlation equation for the region and compared the derived UCS correlation equation with other best industry existing correlations to verify if any existing correlation correlate well in the Niger Delta region and concluded that known of the obtainable correlations built for other regions of the world fits the Niger Delta.

Besides, Zorasi et al (2017) also embarked on a detailed and comprehensive seismic, petrophysical, sequence/stratigraphic and geochemical evaluation of a mature onshore field (Wabi) in the Niger Delta for reservoir characterization and upside hydrocarbon potential determination using seismic, wire line logs, Drill stem test (DST), core and geochemical data, and identified bypassed pay zone deeper in the field for reservoir development.

## CHAPTER 3

### MATERIALS AND METHODS

This chapter presents the materials, data sets and practical methodologies that were used or employed for the evaluation of Wabi field petrophysical and geomechanical parameters through oil and gas company best practices and empirical relations to understand the mechanical behaviour of rocks for mitigation strategy and development. The materials used in this study includes: (i) petrophysical logs such as gamma ray, resistivity, density, neutron and sonic logs, and (ii) processed seismic data acquired by serving company.

#### 3.1 Method of data collection and instrumentation

Data sets from Brown Mature/Marginal field reservoirs were collected from an oil producing company in the Niger Delta with the assistance of the Department of Petroleum Resources (DPR). These data include:

1. Digitize 3D seismic data (in Seg-Y data format).
2. Digitize conventional logs: Gamma ray, sonic, density, neutron, resistivity in LAS format
3. Repeat formation tester/ Drill stem test data for Pore pressure measurement.
4. Core x-ray scan for Wabi 5.
5. Check shots.

The following software: Schlumberger Petrel, interactive petrophysics and MS Excel were employed for the analyses and interpretation of these data.

#### 3.2 Research design (workflow)

The workflow designed for this study help to optimize both Wabi reservoir petrophysical and geomechanical characterisation **Figure 3.1**. The step by steps workflow includes: Seismic interpretation which gives lateral resolution of the subsurface, petrophysical evaluation gives vertical resolution of wellbores, sequence stratigraphy analysis depicts the depositional environment and geomechanics gives estimation of mechanical rock properties and the formation strength to support completion design.

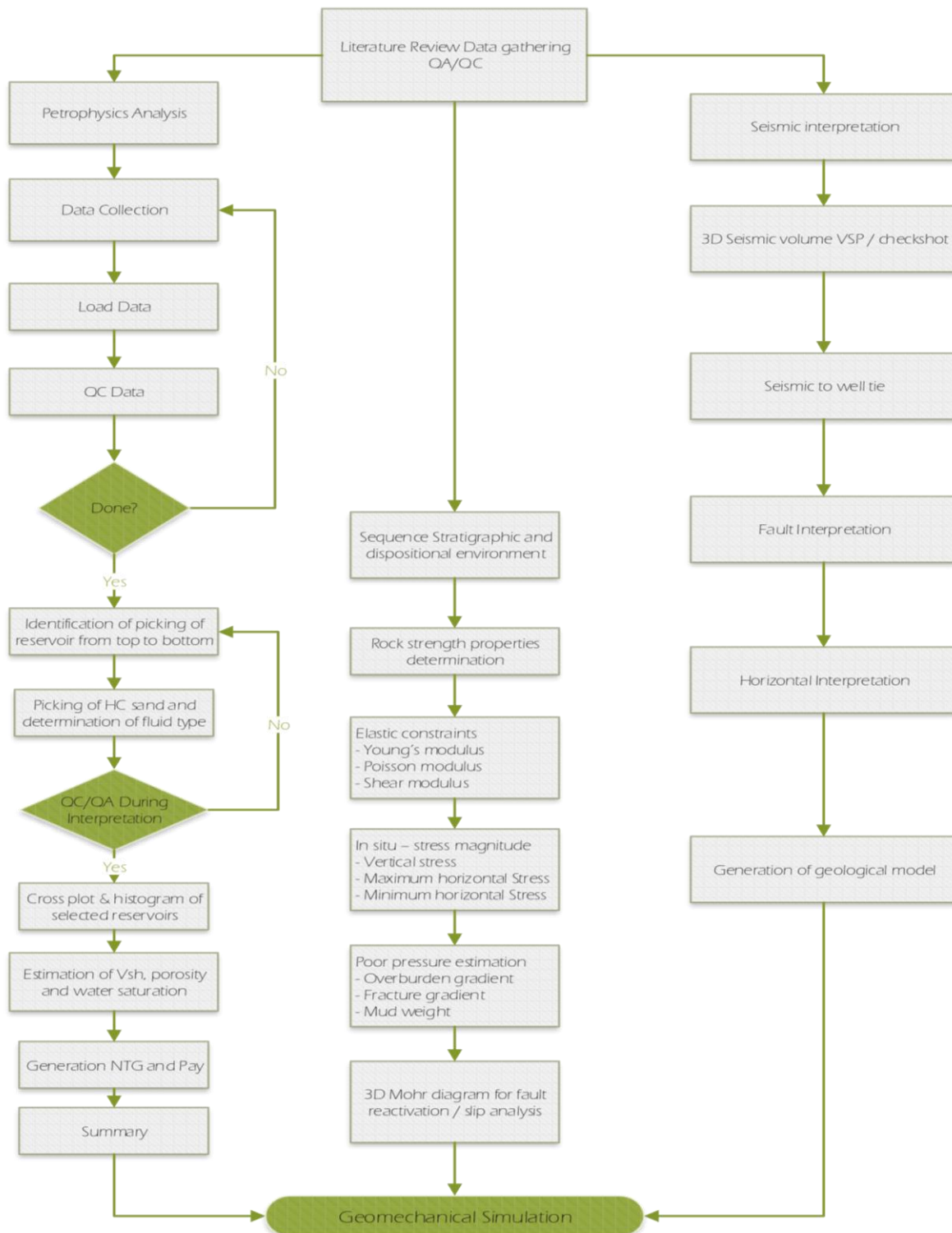


**Figure 3.1. Workflow design**

### **3.2.1 Procedures to carry out this analysis**

#### **a) Seismic interpretation analysis.**

Detailed 3D seismic interpretation using the appropriate software (i.e. Schlumberger Petrel for comprehensive seismic interpretation workflow, both structural & stratigraphic) was employed. This includes: The loading of available data (seismic and logs) to the software, generation of synthetic seismogram to determine the horizons or picks of interest to be interpreted on the seismic profile, fault and horizon interpretation, calculation of heaves, creation of fault polygons and zapping/interpolation/smoothing of horizons, generation of depth converted contour maps, volumetric estimation and generation of geo-models, determination of fault trends, extent and direction as well as delineation of stratigraphy of the area using seismic stratigraphic approach.

#### **b) Petrophysical parameters valuation from well logs for reservoir characterization**

Detailed petrophysical evaluations of sediments of the Basin will be carried out, such evaluations included: Estimation of sand thicknesses with a view to producing an isopach map and determine areas with good sand development, estimation of sand/shale percentages, estimation of total and effective porosities, estimation of water and hydrocarbon saturation, delineation of possible hydrocarbon-bearing sands and also water, oil and gas contacts, estimation and comparison of porosity, permeability, water saturation, hydrocarbon saturation in and across the well(s) using the available wireline logs, determination of the lithology and geometry of the sand units with a view to correlating them, estimation of shale volume content, bulk volume water, hydrocarbon pore volume/thicknesses, Net pay flag, cross plots of variable parameters, such as the different porosity logs to determine mineral/ lithologic compositions of the sand units, estimation of Gas Production Index (GPI) to determine intervals with good gas potential.

#### **c) Lithology/Stratigraphic Evaluated from well logs for depositional environment.**

Detailed sequence stratigraphic/ sedimentological analysis includes: The correlation of sequences, systems tracts and parasequence from both seismic profiles and field studies, facies analysis and identification/description of lithofacies units, depositional environments and stratigraphic sequences, textural and compositional analyses of sandstone particles and microscopy to determine mineralogical composition, porosity, maturity, provenance and effect of diagenesis on the

sandstone, interpretation of faunal abundance and/or diversity and trends of parasequence thickening and thinning .

#### **d) Geomechanical parameters evaluation from well logs using poroelastic theory**

Detailed geomechanical evaluation of the reservoir parameters shall be carried out. This will include: Estimation of the elastic properties such as shear/rigidity modulus, elastic modulus, bulk and matrix moduli, bulk and grain compressibility, Poisson's ratio and Biot's coefficient from well logs, inelastic properties determination: fracture gradient, rock strength, (uniaxial compressive strengths) , tensile and cohesive strengths, and frictional angle, overburden (vertical stress) calculation and the magnitudes of minimum and maximum horizontal stresses estimation using poroelastic formulation, lithology delineation, pore pressure estimation, onset sand production prediction estimation and construction of a 3D Mohr diagram.

### **3.3 Geomechanical properties estimation**

The principle of elasticity examines the relationship existing between the forces applied to a rock material and its responses to changes in shape and size (Timur, 1987). Upon the removal of the forces acting on rock sample, it returns to its original shape and size, in elastic, Isotropic, homogeneous solid. Therefore, the theory of elasticity assumes a linear relationship between stress and resulting strain, provided the force or load is not large enough to cause permanent deformation (Economides and Nolte, 2000). This implies that all strain recovers when the deforming force is removed. The coefficient of proportionality is called Young's modulus. Subjecting a rock sample to a deforming force shortens or expands it (Timur, 1987).

#### **3.3.1 Elastic property of rock and their definition**

The property of a rock that describes or defines its ability to resist permanent deformation or slightly deformed under the action of applied force is known as the elastic properties of that given rock. These properties include shear modulus, bulk modulus, young's modulus and Poisson's ratio (Serra, 1984). The reciprocal of bulk modulus is known as compressibility. Knowledge of these elastic properties is very crucial for well engineering development because their determination

helps to predict the behavior of rock with regards to the applied for as an approximation of the rock behavior (Economides and Nolte, 2000). Various established relationships exist between these elastic constants or coefficients. Timur (1987) defines and expressed these relations as follows;

- i. Young's Modulus (E) defines the ratio of tensile or compressive stress to the resultant strain. It is a strength modulus, expressed as:

$$E = \frac{\sigma_x}{\varepsilon_x} = \frac{F/A}{\Delta L/L} \quad (3.1)$$

Where  $\sigma_x$  is the applied stress,  $\varepsilon_x$  is the corresponding elongation,  $l$  is the original length,  $\Delta L$  change in diameter.  $F/A$  is the force per unit area.

Bulk Modulus (K) describes or defines the response of an object to the change in volume under hydrostatic pressure or compression. In other words, it is the coefficient of proportionality between stress and volumetric strain during a hydrostatic test. It is a compressibility modulus, is expressed as:

$$K = \frac{P}{\Delta v/v} = \frac{F/A}{\Delta v/v} \quad (3.2)$$

where,  $P$  is the pressure,  $\Delta v$  is the change in volume,  $v$  is the original volume.

- ii. Shear Modulus (G) It is a rigidity modulus defined as the ratio of shearing stress to shear strain, expressed mathematically as:

$$G = \frac{\text{Shear Stress}}{\text{Shear Strain}} = \frac{\tau}{\gamma} \quad (3.3)$$

- iii. Poisson's ratio ( $\nu$ ) describes the measure of the geometric change of shape or the ratio of the lateral change (contraction) to longitudinal dilation. It is a plastic modulus, expressed as:

$$\nu = \frac{\Delta d/d}{\Delta l/l} \quad (3.4)$$

where,  $\Delta d$  is the change in diameter,  $d$  is the original diameter of cylindrical core sample

For isotropic linear elastic medium, there are four established elastic parameters which are not independent of one another, (Economides and Nolte, 2000; Timur, 1987) and anyone of these can be articulated in terms of two others. i.e. the shear modulus  $G$  and bulk modulus  $K$  then an expression can be written as a function of Young's modulus,  $E$  and Poisson's ratio,  $\nu$  (Tiab and Donaldson, 2012; Timur, 1987; Serra, 1984) and so on and so forth. See example below;

$$G = \frac{E}{2(1+\nu)} \quad (3.5)$$

$$K = \frac{E}{3(1-2\nu)} \quad (3.6)$$

### 3.3.2 In-situ stress measurement of mechanical properties

The frequently used indirect method for the determination of mechanical properties of rock is the sonic (acoustic) and bulk density log measurements through wireline tools (Jones *et al.*, 1992). Acoustic waves propagate mechanical energy. This is the only petrophysical sonde (tool) that responds to mechanical (elastic) properties of a formation. This is because its records parameters linked with the transmission of sound waves in a given formation (Timur, 1987; Serra 1984). Two types of waves are utilized, they are: compressive and shear waves for estimation of elastic constants of a formation (Timur, 1987), thus measures the speed of propagation of compressive and shear waves in a wellbore as well as their characteristics (Economides and Nolte, 2000). Acoustic wave speed propagated in a formation can be estimated with the aid of the time it takes to travel through a certain thickness of the formation (Timur, 1987).

Acoustic wave propagation in rocks depend on structural framework of grain, and pores, rock matrix composition, temperature, porosity pore pressure and overburden (Timur, 1987). The passage of compressive (P-wave) and shear (S-wave) characterized by particular kind of particle movement through the earth stresses the rock and induces a strain which is proportional to the applied stress. The P-wave caused the rock to change in volume while the S-wave caused the rock to change in shape (Domenico and Danbom, 1986). Hence, the velocity of compressional and shear wave depends on elastic constant of rock. Compressive wave ( $V_P$ ) has a particle motion that is parallel to its direction of propagation sometimes called longitudinal wave. This wave travels

through liquid, gas and solid and has a constant velocity for a given material (Sheriff and Geldart, 1995). Shear wave ( $V_s$ ) has particle motion, which is perpendicular to the propagation of the wave, sometimes called transverse waves. It does not travel through fluid, i.e. gas and liquid but only solid because it lacks attractive forces between molecules (Timur, 1987). Precise measurements of compressional and shear wave velocities for mechanical properties description and analyses using established models predict the capability of sand or rock strength to withstand imposed forces due to overburden weight or fast pressure depletion (Tixier, Loveless and Anderson, 1975).

### 3.3.3 Geophysical tools for the determination of mechanical properties

Acoustic log or sonic log is a continuous record versus depth of the specific time required for a compressed wave to traverse a given distance of formation adjacent to the borehole. The acoustic tool contains a transmitter and two receivers (**Figure 3.2**). When the transmitter is energized, at a rate of 10 to 20 Hertz, the sound wave enters the formation from the mud column, travels through the formation and is reflected back to the receivers through the mud column. Formation velocity (travel time,  $\Delta t$ ) is determined using the differences in arrival times at the two receivers. The system has circuits to compensate for hole size changes or any tilting of tool. The fundamental measurement recorded on the sonic log is interval travel time; this is the reciprocal of interval velocity (Asquith and Gibson, 1982). This parameter is recorded in microseconds per foot. Acoustic travel time can be expressed as:

$$\Delta t = \frac{10^6}{v} \mu s/ft \quad \text{and}$$

$$v = \frac{1 \times 0.3048}{\Delta t \times 10^6} \text{ m/s} \quad (3.7)$$

where,  $v$  is velocity (m/s) and  $\Delta t$  is the sonic interval transit time in  $\mu s/ft$ .

Acoustic travel time normally fall between  $40 \mu s/ft$  and  $200 \mu s/ft$ , which corresponds to velocity readings of 5,000 to 25,000 ft/s as shown in **Table 3.1**.

**Table 3.1.** Sonic interval transit time and velocities for different matrices (lithologies)

Common	$V_{ma}$ (ft/sec)	$\Delta t_{ma}$ ( $\mu$ sec/ft)	$\Delta t_{ma}$ ( $\mu$ sec/ft) commonly used
Sandstone	18,000 to 19,500	55.5 to 51.0	55.5 to 51.0
Limestone	21,000 to 23,000	47.6 to 43.5	47.6
Dolomite	23,000 to 26,000	43.5 to 38.5	43.5
Anhydrite	20,000	50.0	50.0
Salt	15,000	66.7	67.0
Casing (Iron)	17,500	57.0	57.0

(Schlumberger, 1972)

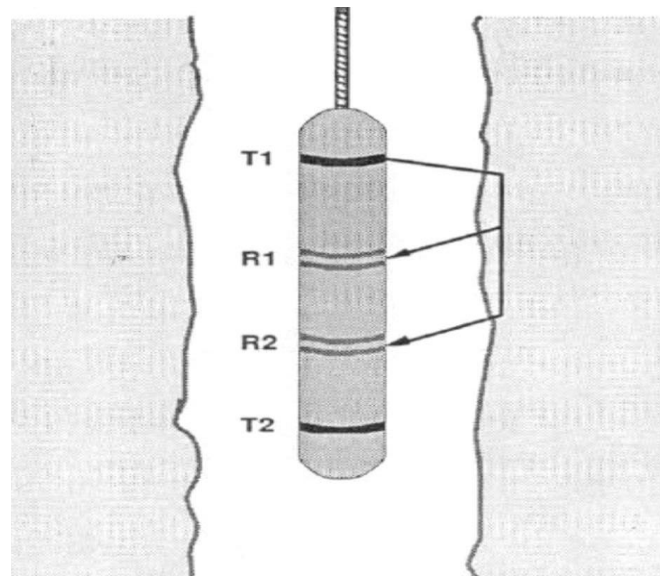


**Figure 3.2.** The Sonic Logging Tool. (Martey, 2000).

The acoustic travel time in a formation depends upon lithology (formation type) and porosity. In general terms, the denser or consolidated a formation is, the lower the travel time,  $\Delta t$ . An increase in travel time indicates an increase in porosity.

- a. Wyllie average equation for uncompacteds sands is given by (Asquith and Gibson, 1982) as:

$$\phi_{sonic} = \frac{\Delta t_{log} - \Delta t_{ma}}{\Delta t_{fl} - \Delta t_{ma}} \times \frac{I}{C_p} \quad (3.8)$$

$$\text{where } C_p = \frac{\Delta t_{sh} \times C}{100}$$

where:  $\phi_{sonic}$  = sonic derived porosity, fraction,  $\Delta t_{log}$  = sonic log reading of formation,  $\mu s/ft$

$\Delta t_{max}$  = Interval transit time of formation/matrix material,  $\Delta t_{fl}$  = interval transit time of fluid ( $189\mu s/ft$  corresponding to a fluid velocity of about 5300ft/s),  $C_p$  = empirical correction factor/compaction factor,  $\Delta t_{sh}$  = transit time of adjacent-shale  $C$  = a constant which is normally 1.0 (Asquith and Gibson, 1982).

**Density log:** The density tool measures the number of electrons that is related to the true bulk density of the formation, using a pad mounted chemical source of gamma radiation which emits medium energy gamma rays of about 66 MeV (Geoservices, 2004; Asquith and Gibson, 1982). At each collision with formation electrons, some energy is lost. This collision is (known as Compton scattering), thereby affecting the amount of gamma rays being detected at the receivers. The receivers are two shielded gamma ray detectors (known as Geiger counters which automatically compensate for mud cake and small borehole irregularities). Density response is based on rock matrix, porosity and pore fluids in their relative proportions (**Figure 3.3**).

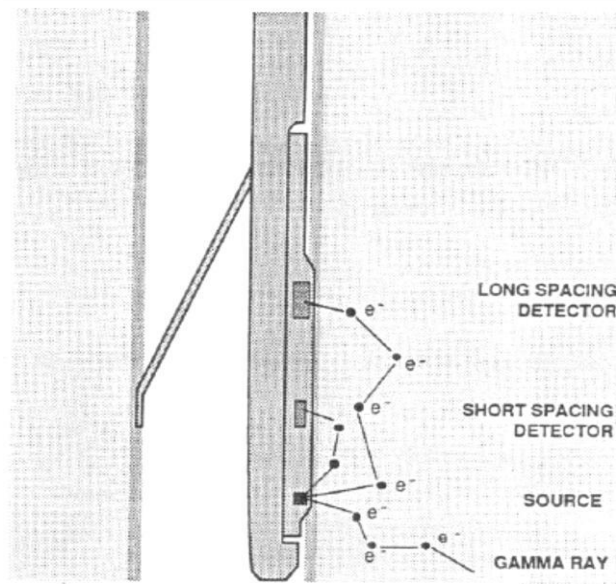


**Figure 3.3.** Formation density tool (Martey, 2000).

The petroleum industry assumes that electron density is equal to bulk density; therefore, the number of gamma rays counted at the detectors can be directly related to the bulk density of the formation. Since density is defined as the ratio of mass to volume with units in grams per cubic centimeter (gm/cc). Most gamma are counted in porous or low-density formation (Timur, 1987; Serra, 1984). As formation density increases (porosity decreases), fewer gamma rays are counted since most mineral densities are known **Table 2.1**, and the pore fluids densities are known as 1.1, 1.0 and 0.7 g/cc for salt, fresh mud and gas respectively. Porosity can be computed from the given equation (Asquith and Gibson, 1982) as:

$$\Phi_D = \frac{\rho_{ma} - \rho_b}{\rho_{ma} - \rho_f} \quad (3.9)$$

where:  $\Phi_D$  = density derived porosity,  $\rho_b$  = density log reading (formation bulk density),  $\rho_f$  = average density of the saturated fluid, and  $\rho_{max}$  = density of the matrix material.

Density log consists of RHOB and DRHO i.e formation bulk density ( $\rho_b$ ) and bulk density correction. DRHO is applied to RHOB due to the presence of mud cake and it is used as a log quality control.

### **3.3.4 Determination of elastic constants from Petrophysical logs**

In the absence of core samples for laboratory testing to obtain geomechanical parameters for solving related geomechanical problems associated with drilling, well design and production management. There are numerous empirical relations established which relate rock strength to measured parameters derived from petrophysical logs (Zoback, 2007). These relations are based on the fact that, many factors affecting rock strength also affect elastic moduli and other petrophysical parameters. Most established empirical relation for determination of rock strength from geophysical logs utilize P-wave and S-wave velocity and Young modulus (E) derived from  $V_p$  and density data (Zoback, 2007).

The determinations of elastic properties are possible from mechanical properties log (sonic) which in turn are used to estimate the formation strength for well engineering. The mechanical properties logs give a quantitative means for the identification of sedimentary rocks that are strong enough to produce hydrocarbon without producing sand (Tixier, Loveless and Anderson, 1975). The correction of dynamic elastic modulus calculated from sonic and density logs, necessitated the elastic properties of a formation to be categorized as static or dynamic modulus, depending on the way they were determined in the laboratory or in the field. The elastic properties derived from experiments conducted in the laboratory on core are called static constant; whereas, the elastic properties determined or estimated using acoustic log and sometimes ultrasonic wave velocities on core in the laboratory or indirect measurement through well logging techniques are called dynamic constant (Oluyemi, 2007).

Well logging utilizes empirical relations for its derivative of elastic constants. Poor laboratory and inadequate process coupled with the parameters used for the calculations of elastic properties are the main reason for the difference observed between static and dynamic properties. Static and dynamic constants' values in an ideal elastic material are constants and linearity concept is obeyed. However, in friable sand (unconsolidated sand), the reverse is the case, as the dynamic constant values are constantly higher than static constant values at low confining stress. Rocks at low confining stress have nonlinear stress-strain relationships (Serra, 1984) while at high confining stresses rock behavior is more linear or elastic hence, both static and dynamic constants have

correlation (Jones *et al.*, 1992). Tixier, Loveless and Anderson (1975) concluded that in practice, dynamic constants from wire line logs when evaluating friable sand gives better results than static because the measurement are made under in situ conditions and fairly represent the confining stress in the formation of interest.

For the determination of Young modulus and Poisson's ratio, a good reliable measurement for density, compressional and shear wave velocity are desirable (Economides and Nolte, 2000). For intervals where the shear velocity is not present or missing, a synthetic model travel times can be used for the estimation of compressional and shear wave (Simm and Bacon, 2014). However, care should be taken. Gartner's relation is handy in the transformation of sonic or density logs for the purposes of replacing missing sections. Because, in many rocks, compressional velocity and bulk density have a positive relationship, so that as velocity increases so density increases. Gartner *et al.* (1974) developed a copy (series of brine- saturated lithology dependent relation of the form;

$$\rho = dV_p^f \quad (3.10)$$

where,  $\rho$  is the density,  $V_p$  is the P-wave velocity,  $d$  is a magnitude constant and  $f$  is the shape constant.

Bai and Li (2012) demonstrated that because of the intense need for interpretation of mechanical properties of rock formation,  $V_P$  can also be derived from density using Gardner's method as:

$$V_p = 357.346 \times \rho^4 \quad (3.11)$$

where 357.346 is Gardner coefficient.

In addition, Castagna *et al.* (1985) demonstrated that in the absence of shear log in old wells, shear velocity needs to be predicted from log measurement since generally there is a strong lithology dependent, and basically pressure independent; optimistic correlation between compressional and shear velocity had been established from collection of data sets.

Therefore, Greenberg and Castagna (1992) defined four empirical equations which give good trends for predicting  $V_s$  occurring in brine bearing lithologies as follows:

$$\text{Sandstone} \quad : \quad V_S = 0.8042 V_P - 0.8559 \quad (3.12)$$

$$\text{Limestone} \quad : \quad V_S = 0.0551V_P^2 + 1.016V_P - 1.0305 \quad (3.13)$$

$$\text{Dolomite} \quad : \quad V_S = 0.58321V_P - 0.07775 \quad (3.14)$$

$$\text{Shale} \quad : \quad V_S = 0.7697V_P - 0.86735 \quad (3.15)$$

where,  $V_S$  and  $V_P$  are in km/s.

However, due to the significant variation that can occur using empirical relations for  $V_S$  prediction in different sandstone lithologies  $V_S$  could be higher than that predicted by the sand line (Sim and Bacon, 2004; Smith, 2011) including clean quartz and glauconitic sands. Therefore, Murphy *et al.* (1993) developed an equation for clean sand prediction as  $V_S = 0.802V_P - 0.75$ .

### ***Young's modulus***

The strength modulus was estimated from acoustic log reading of the travel time of compressional and shear waves using empirical relations for its computation expressed as;

$$\text{Young's modulus (E)} = \frac{\rho_b \times 1000 \times V_S^2 \times (3V_P^2 - 4V_S^2)}{(V_P^2 - V_S^2) \times 10^6} \quad \text{unit in MPa} \quad (3.16)$$

where  $\rho_b$ ,  $V_S$ , and  $V_P$  have their usual meaning (Omar 2015)

### ***Shear modulus***

The rigidity modulus was estimated from bulk density  $\rho_b$  of the formation and acoustic shear velocity  $V_s$  through the empirical relation given by (Omar, 2015) as:

$$\text{Shear modulus (G)} = \rho_b \times 1000 \times V_s^2 \quad \text{unit in Pascal} \quad (3.17)$$

### ***Bulk Modulus***

Compressibility modulus can be calculated from the Young's modulus and Poisson's ratio coefficient through the empirical relation given by (Economides and Nolte, 2000; Timur, 1987) as:

$$K = \frac{E}{3(1-2\nu)} \quad \text{unit in Pascal or MPa} \quad (3.18)$$

### *Poisson's ratios*

The plastic modulus was computed from acoustic measurements of the compressional wave  $V_P$  and shear wave  $V_S$  velocities using the empirical equation by (Omar, 2015) expressed as:

$$\text{Poisson's ratio } (\nu) = \frac{V_p^2 - 2V_s^2}{2(V_p^2 - V_s^2)} \quad \text{dimensionless unit} \quad (3.19)$$

## **3.4 In-situ stress estimation**

Understanding of the in-situ stress magnitudes and their directions existing at depth in the subsurface have lot of applications in petroleum geomechanics. This comprehension assists in predicting and solving geomechanical related issues such as sand production determination, estimation of fracture gradient, casing design, compaction, subsidence, fault reactivation, and rock failure investigations (Maleki *et al.* 2014; Addis and Yassir, 1996; Oyenyin, 2015). This is because reservoir rocks/formations are under constant forces either from tectonic forces, gravitational, geological process resulting to fault or folds, diapirs and mechanical contracts (Oluyemi, 2007; Oyenyin, 2015).

Stress states are characterized by three principal in-situ stresses namely vertical or overburden stress, principal maximum horizontal stress and minimum horizontal stress (Economides and Nolte, 2000). The orientations of these stresses depend on the normal, thrust and strike-slip fault regimes (stress regimes). These stresses are estimated from geophysical logs in this study. It is beneficial to recognize these stresses to address geomechanical reservoir description for development.

### **3.4.1 Vertical stress determination**

The vertical or overburden stress is the stress acting on the reservoir formation due to the load of the overlying beds in normal faulting regimes (Jones *et al.*, 1992; Abdideh and Ahmadifar, 2013)

They act in downward direction. This stress is computed as an integral of the rock density to the depth of interest from density log using equation (2.9) expressed as (Jones *et al.*, 1992). Vertical stress

$$\sigma_v = \int_0^h \rho g h$$

For onshore, the vertical or overburden stress is calculated by the expression given by (Omar, 2015) as:

$$\sigma_v = \rho \times 1000 \times g \times depth(h) \times 0.3048 \times 0.000145037738 \text{ (psi) or MPa.}$$

where  $\sigma_v$  is the vertical stress;  $\rho$  is the formation bulk density read off from density log,  $g$  is acceleration due to gravity and  $h$  is the depth of interest.

### 3.4.2 Minimum horizontal stress determination ( $Sh_{min}$ )

Successive field development requires an accurate petroleum geomechanics evaluation for the understanding of the minimum horizontal stress which is essential for the assessment of sand production, hydraulic fracturing, fault reactivation and wellbore stability (Jamshidian *et al.*, 2017). The minimum horizontal stress can be estimated or measured from two techniques namely, indirect or direct methods from field data such as wireline logs through (viz) empirical correlations and well tests; leak of test (LOT) conducted in prior wells and from core data respectively (Jamshidian *et al.*, 2017; Abdideh and Ahmadifar, 2013). It is very important to note that, tectonic stress and pore pressure caused and controlled the variations in magnitudes and orientations of the minimum horizontal stress  $Sh_{min}$  in sedimentary basins (Adewole and Healy, 2013). The study area has been reported to be over pressured, therefore, this inform the empirical relation to be applied. In this study the minimum horizontal stress was evaluated using the proposed Ahmed *et al.* (1991) equation given as:

$$S_{hmin} = \frac{\nu}{(1-\nu)} (\sigma_v - \alpha P_p) + \alpha P_p \quad \text{unit in MPa} \quad (3.20)$$

where:  $\sigma_v$  is the overburden stress,  $\nu$  is the Poisson's ratio,  $P_p$  is the pore pressure,  $\alpha$  is the Biot's constant and  $Sh_{min}$  is the minimum horizontal stress.

The Biot's constant can be estimated from the (Schlumberger, 1985) expression given as:

$$\alpha = 1 - \frac{K_b}{K_r} = 1 - \frac{C_r}{C_b} \quad (3.21)$$

where:  $K_b$  is the bulk modulus of the material,  $K_r$  is the bulk of the rock constituents,  $C_r$  is the matrix compressibility and  $C_b$  is the rock bulk compressibility. The computation of compressibility from  $\rho_b$ ,  $\Delta t_c$  and  $\Delta t_s$  of bulk rock and matrix.

The coefficient of earth pressure at rest  $K_o$  can be computed from the expression given by (Economides and Nolte, 2000) as:

$$K_o = \frac{\nu}{(1-\nu)} \quad (3.22)$$

It can also be written in terms of effective stress when two principal stresses are equal in horizontal plane as:

$$K_o = \frac{\sigma'_h}{\sigma'_v} \quad (3.23)$$

Where:  $\sigma'_v$  is the vertical effective stress,  $\sigma'_h$  is the minimum horizontal effective stress and  $K_o$  is the matrix or earth pressure coefficient at rest accounting for vertical stress at depth.

### 3.4.3 Maximum horizontal stress determination ( $Sh_{max}$ )

Among the three in situ principal stresses used to define the full stress tensors existing at depth explained in this study, the most difficult to estimate is the maximum horizontal stress ( $SH_{max}$ ) tensors (Adewole and Healy, 2013; Maleki *et al.*, 2014). Its determination depends on the comprehensive knowledge of the pore pressure, minimum horizontal stress, vertical stress, static Young's modulus and Poisson's ratio (Maleki *et al.*, 2014; Jamshidian *et al.*, 2017). There are numerous empirical relations that exist which can be used to estimate maximum and minimum stress (Zoback, 2007) but in this study the following relations equations 3.20-3.24 were used.

The estimation of the magnitudes of the major and minor principal stresses (i.e maximum and horizontal) were calculated from using (Ostadhassan *et al.*, 2012; Holbrook *et al.*, 1993) Poroelastic model expressed as:

$$S_{hmax} = \frac{\nu}{(1-\nu)} (\sigma_v - \alpha P_p) + \alpha P_p + \frac{E_{sta}}{(1-\nu^2)} \varepsilon_y + \nu \varepsilon_x \quad \text{unit in MPa} \quad (3.24)$$

where:  $\nu$  is Poisson's ratio,  $\sigma_v$  is the vertical or overburden stress,  $P_p$  pore pressure,  $\alpha$  is Biot constant,  $E_{sta}$  is the static Young's moduli,  $\varepsilon_x$  and  $\varepsilon_y$  are strain at maximum and minimum horizontal stress directions (Maleki *et al.*, 2014). The deformation (strain) in the maximum and minimum horizontal directions is given by (Kidambi and Kumar, 2016) equation as:

$$\varepsilon_x = \frac{\sigma_v \times \nu}{E_{sta}} \times \left( \frac{1}{1-\nu} - 1 \right) \quad (3.25)$$

$$\varepsilon_y = \frac{\sigma_v \times \nu}{E_{sta}} \times \left( 1 - \frac{\nu^2}{1-\nu} \right) \quad (3.26)$$

To obtain the Young's modulus static constant from the dynamic constant, the dynamic moduli must be converted using the relation established by (Seyed and Aghighi, 2015) expressed as:

$$E_{stat} = 0.731 \times E_{dyn} - 2.337 \quad (3.27)$$

where 0.731 and 2.337 are Seyed and Aghighi constants obtained from laboratory experiment on core and applied for static correction of elastic constant.

#### 3.4.4 Pore pressure Estimation

According to Schlumberger glossary of terms (2018), the pressure exerted by a column of fluid or water in the pore spaces from earth surface or sea level through the formation's depth is called pore pressure or formation pressure. When this pressure is at equilibrium that is it act equally in all direction with respect to the principal stresses the formation is said to have hydrostatic pressure. This is computed in this study using equation (2.8) expressed by Jones *et al.* (1992) and (Omar, 2015) relation as follows:

$$P_p = \int_0^h \rho_f g h$$

or

$$P_p = 1 \times 1000 \times g \times \text{depth } (h) \times 0.3048 \times 0.0001450378 \text{ (Psi)} \quad (3.28)$$

where,  $g$  is the acceleration due to gravity,  $P_p$  is the pore pressure,  $h$  is the depth.

### 3.4.5 Stress (Pressure/depth) gradients

#### i. Overburden gradient estimation

Knowledge of overburden gradient is necessary in oil field operation and development. It is meant for the evaluation of formation pressure and for calculation of fracture gradient (Geoservices, 2004; Addis and Yassir, 1996). In this study, the overburden gradient is computed by averaging density derived from wireline density log over the intervals or depth of interest using the expression of (Omar, 2015) relation as follows:

$$\text{Overburden gradient (OVBG)} = \frac{\sigma_v}{h} \text{ Psi/ft} \quad (3.29)$$

where,  $\sigma_v$  is the vertical stress,  $h$  is the depth.

#### ii Fracture gradient estimation (FG)

To avoid the unprecedented incident of formation fracturing and opening of pre-existed fault and fissures which result to very expensive and catastrophic lost circulation issue in a wellbore, accurate prediction of formation fracture gradient is required (Zhang and Yin, 2017; Tiab and Donaldson, 2012). It is very important to note that rocks Poisson's ratio, overburden stress gradient and pore pressure are the main factors influencing fracture pressure gradient (Zhang and Yin, 2017; Tiab and Donaldson, 2012). The choice of methods to be used for the calculation of this fracture gradient differs in the oil and gas industry as there is no consensus method. Some pore pressure specialists adopt the use of minimum stress gradient for fracture estimation while others employed

fracture initiation pressure gradient or maximum leak off tests (Zhang and Yin, 2017). This can be estimated according to Tiab and Donaldson (2012) as:

$$FG = \frac{1}{D} \times \frac{\nu}{(1-\nu)} (\sigma_v - \alpha P_p) + \alpha P_p \quad (3.30)$$

where,  $FG$  is the fracture gradient,  $D$  is the depth,  $P_p$  is the pore pressure,  $\sigma_v$  is the overburden pressure,  $\nu$  is the Poisson's ratio and  $\alpha$  is the Biot constant.

### iii Pore pressure gradient estimation (PG)

The pressure gradient is calculated by dividing the pore pressure at any given point in a formation by the corresponding depth.

$$PG = \frac{PF}{Depth} = \frac{1 \times 1000 \times g \times depth (h) \times 0.3048 \times 0.0001450378}{Depth} (Psi) \quad (3.31)$$

## 3.5 Rock strength determination

Rock strength defines the peak stress level at which rock sample fails. Rock strength depends on the strength of intact rock and strength of rock discontinuities. Therefore, understanding the stress distribution and redistribution is essential for well planning (Economides and Nolte, 2000; Jumikis, 1983).

### 3.5.1 Unconfined Compressive strength (USC)

Rock strength can be measured by unconfined compressive strength (UCS), that is, the peak value of stress that can be withstood by rock before its failure (deformation) when subjected to compressive force with no radial stress or lateral constraint (Goodman, 1989). There are several types of tests conducted for UCS but the most widely used tests are uniaxial compressive and triaxial compressive tests. Prior understanding of the characteristic of failure model as applicable to rock strength requires certain and capable failure criterion to be applied. Knowledge of strength of rock is essential for construction and design of drilling, production and secondary recovery

program for reservoir development (Sylvester and Lader, 2015). It aids proper simulation of the reservoir based on the availability of geomechanical data.

Mechanical properties and behavior of rock strength depends on elastic moduli values at the interval of interest. The UCS of the study field can be estimated from geophysical logs through the empirical relations established for the Niger delta by Salawu, Sanaee and Onabanjo (2016). These correlations are between UCS and formation slowness, Poisson's ratio, and Young's modulus for upper Agbada formation. They are:

$$UCS = 1 \times 10^6 \times \Delta t^{-2.664} \quad (3.32)$$

$$UCS = 0.2017 \times \nu^{-3.162} \quad (3.33)$$

$$UCS = 0.3966 E + 1.1956 \quad (3.34)$$

where E is the young modulus of Niger Delta, UCS is the unconfined compressive strength of rock in the Niger Delta,  $\nu$  is the Poisson's ratio in the Niger Delta and  $\Delta t$  is the formation slowness or interval transit time in the Niger Delta.

### 3.5.2 Cohesive strength

Cohesion is not a measurable physical quantity although it expresses rock strength. Sometimes unconfined compressive strength is referred to as cohesive strength since it describes the linear model or failure envelope line demonstrated by Mohr criterion in terms of the intercept made with the ordinate axis, when the minimum principal stress is zero, i.e.  $\sigma_3 = 0$  related to shear stress in soil mechanics (Jaeger, Cook and Zimmerman, 2007). As a result, the linearized failure line of Mohr can be expressed as

$$\tau = s_o + \sigma_n \mu \quad (3.35)$$

where;  $\tau$  is the shear stress,  $s_o$  is cohesive strength of soil,  $\mu$  is the coefficient of friction and  $\sigma_n$  is the effective normal stress (Zoback, 2007).

### 3.5.3 Tensile strength ( $T_o$ )

Tensile strength reflects the punching or flexural failure of a thin bed of overlying weak material that is, it depicts failure under tension (where a weak bed underlies a layer of stiffer rock) (Willie, 1999). Tensile testing is not usually conducted and rarely acceptable in the plan of structures because tensile strength of fractured rock is efficiently zero. However, direct testing in clean tension gives the most consistent results. The Brazilian test is also conducted for tensile strength determination (Oluyemi, 2007).

Again, this not also used in geomechanics for failure analysis because of its magnitude being set at one-tenth of the  $C_o$  which is the average value. When comparing  $C_o$  to unconfined compressive strength its value is lower than to UCS (Serra, 1986). This makes its usefulness unimportant coupled with the fact that stress at depth is not tensile except caused by induce hydraulic tensile failure. Tensile failure occurs due to the application of biaxial stress (Tiab and Donaldson, 2012). In situ rock strength is expressed by (Schlumberger, 1985) as:

$$T_o = \frac{C_o}{12} \quad \text{and} \quad C_o = 12 T_o \quad (3.36)$$

where:  $C_o$  is the cohesive strength =  $\frac{5(V_p-1)}{0.5(V_p)}$  (Abijah and Tse, 2016) (3.37)

## 3.6 Failure Mechanisms

Knowledge of failure mechanism requires the application of well-matched failure criterion. Failure is caused by the stresses identified as effective stresses experienced by the rock structure. Failure mechanism describes the simplified models for which rock fails and depicts the real behavior of rocks under applied forces. These criteria utilize mathematical relations for observed behavior of rock deformation which is valid for Isotropic rock. Three main failure mechanisms mode have been reported and observed in uniaxial and triaxial test (Zoback, 2007; Fjaer *et al.*, 2008). They are shear failure, tensile failure and pore collapse (Fjaer *et al.*, 2008). Other mechanisms are creep, plastic failure and cohesive failure. During drilling phase, shear and tensile failure mechanisms are extensively used for wellbore stability analysis (Economides and Nolte, 2000).

### 3.6.1 Shear failure mechanism

The existence of excessive shear stress along some planes in a rock sample or reservoir causes fracture and fault development (Fjaer *et al.*, 2008) along the failure plane in which two sides of the plane are in relative motion due to one another in a frictional procedure. Frictional force at play depends on the attractive force acting to keep the bodies in motion together. Thus, failure occurs due to the actualization of the critical shear stress called  $\tau_{max}$  which depend on the normal stress acting over the failure plane (Fjaer *et al.*, 2008) it can be expressed as:

$$\tau_{max}=f(\sigma^I) \quad (3.38)$$

This equation in a  $\tau - \sigma^I$  plane describes stable region from unstable region (Fjaer *et al.*, 2008).

The Tresca criterion for shear failure is expressed as:

$$\tau_{max} = \frac{1}{2}(\sigma_1 - \sigma_3) \quad (3.39)$$

The above equation (3.39) shows that rock yield when the critical shear stress is attained.

### 3.6.2 Tensile failure mechanism

This is caused by excessive tensile stress occurrence because of the effective tensile stress across some plane in the rock exceeding the tensile strength of the formation. It is a characteristic property of any given rock (Fjaer *et al.*, 2008). Tensile strength of sedimentary formations is too low. It is localized and inhomogeneous due to its failure pattern which splits along few fault/fracture planes. Tensile failure criterion which specified conditions and identified failure surface in principal stress ( $\sigma^I$ ) space is written as:

$$\sigma^I = -T_0 \quad (3.40)$$

But, for homogeneous rock, the conditions for tensile failure is fulfilled at the lowest principal stress  $\sigma_3$ . The tensile failure criterion becomes

$$\sigma_3 = -T_0 \quad (3.41)$$

### 3.7 Failure criteria

The empirical relation for rock failure criteria is the expressions of physical hypotheses. This implies that they are obtained from experiments conducted. These criteria identify how in situ stress, temperature, time and other factors influence strength of rock (Jumikis, 1983). We use failure criteria to determine if a rock will yield, flow, buckle, crush, crack or else give way in services (Goodman, 1989). All failure criteria are dependent on effective stresses.

#### 3.7.1 Mohr Criterion

To appraise rock failure or fracture (i.e. when there is a complete loss of cohesion), the mechanical conditions which ascertain its failure was first investigated by Coulomb and Navier (1960) whose study considered the state of failure as shear failure (Jumikis, 1983). In 1900 Mohr reviewed the work of Coulomb and Navier and incorporated the maximum shear theory as the basis of his failure criterion (Yona and Warkentin, 1975). The Mohr theory considered shear failure across a plane and provides a relationship between shear and normal stresses acting on the plane of failure (Goodman, 1989; Zoback, 2007; Pollard and Fletcher, 2005) as:

$$\tau = f(\sigma)$$

where,  $\tau$  is shearing stress along the plane of failure; and,  $\sigma$  is the normal stress transverse the plane. The following are the assumptions of the above relation (Amadei 2007):

- i. The tensile and compressive strengths of the rock are unequal.
- ii. Failure occurs when there is equalization between maximum shear stress  $\tau_{max}$  and shear strength of a given rock. In other words, failure takes place when the Mohr envelope is tangential to the Mohr circle and failure also depends on the major and minor applied principal stresses (Amadei, 2007).

#### 3.7.2 Mohr Coulomb Failure Criterion

According to Fjaer (2008) Mohr Coulomb criterion is an expansion of the Mohr criterion. Mohr criterion assumes the reality of a shear curve envelope (Jumikis, 1983). The Mohr Coulomb

criterion is an empirical equation which relates the shear strength to normal stress. That is, the resistance of a rock to fail in shear to the contact forces and friction, to the cohesion that exist among grains (Jaeger and Cooke, 1979; Aadnoy and Looyeh, 2011). In other words, it states that the maximum shear stress  $\tau_{max}$  at which failure occur is equal to the sum of cohesion  $S_o$ , normal stress  $\sigma_n$  and coefficient of friction  $\phi$  acting on the failure plane. This criterion characterizes rock behavior in terms of  $C_o$  or  $S_o$  and internal friction.

Mohr Coulomb theory seeks to predict the plane on which failure or sliding occurs. Thus, the M-C criterion is a linear shear of Mohr failure line (Zoback, 2007; Aadnoy and Looyeh, 2011; Goodman, 1989) given as:

$$\tau = S_o + \sigma_n \mu$$

where,  $\tau$  is the shear stress,  $\sigma_n$  is the effective normal stress acting on the grains,  $S_o$  is the intrinsic shear strength of the rock,  $\mu$  is the coefficient of internal friction ( $\tan \phi$ ); where  $\phi$  is the angle of surface sliding (Amadei, 2007; Aadnoy and Looyeh, 2011).

Mohr Coulomb failure criterion describes rock behavior in the middle range of compressive stress where failure takes place along two conjugate planes at an angle  $\theta = \frac{\pi}{4} - \frac{\phi}{2}$  with respect to  $\sigma_1$  being parallel to  $\sigma_2$ , where  $\theta$  is the angle between the normal to the failure plain or envelop and the direction of  $\sigma_1$ .

Because of its well explained and established concepts in simple terms, using few parameters which can be obtained from laboratory experiment necessitated its wide usage as failure criterion within the industry (Oyeneyin, 2015; Oluyemi, 2007).

### 3.8 Cost and Limitation of the study

The technique used in this study can be deployed in the absence of core data to derive elastic constants. Coring is known to be expensive and cannot be acquired in every well drilled. Especially, in the Niger Delta only few wells had been cored. Hence, in the absence of core plugs, the use of dynamic elastic constants was estimated from geophysical logs since acoustic and density logs which are mechanical logs were run as part of the open-hole logging suite at a

reasonable cost (drilling cost). Therefore, wireline techniques could provide a practical, cost effective method to estimate geomechanical and petrophysical properties. Provided the calculations made from acoustic and density logs yield accurate estimate of in situ stress and petrophysical properties where proper adjustment due to drilling fluid is accounted for. The advantages of this method include; good representative of the confining stress in the reservoirs, dynamic measurements obtained from wireline logs provide continuous curves that reveal changes and trends throughout the well penetrated than cores retrieved from the reservoir provides discrete point properties. Core provide the ground truth and more direct method of determining rock strength than logging, but precautions are essential.

The followings challenges were found in this study. They are:

- 1) Fracture orientation data for Wabi field was not made available for construction of the Mohr circle model.
- 2) Leak off test (LOT), a test conducted to know the formation integrity, mini and micro fracture data were not provided for comparing stress information obtained from well logs.
- 3) The Niger delta basin lack necessary subsurface stress information.
- 4) Did not have access to Schlumberger wellbore software for prediction of fracture properties (i.e. cohesion and fracture angle) in Wabi.
- 5) Above all, core samples data from Wabi field was not given for laboratory testing of elastic constants and to validate information obtained from wireline logs. Hence, the results herein are obtained from wireline logs only.

## CHAPTER 4

### Result presentation and discussion

This section deals with the report of this study's findings and discussion of the analyses of Wabi field data available from two wells named Wabi 5 and Wabi 11. These two wells were chosen because of the availability of mechanical elastic logs (i.e. sonic and density) logs in them. However, petrophysical analyses were made in all the wells in the study field. The assumption made in this study was that the reservoir rock is isotropic that is, the material exhibits a perfectly linear stress-strain relationship.

#### 4.1. Data sources (inventory)

Wabi field data inventory was done to identify the availability of petrophysical tools recorded in each of the four wells which penetrated the formation of interest in the study area. These data availability check seeks to know the well with the complete sets of petrophysical tools run in them, for reservoir characterization and geomechanical parameters estimation, **Table 4.1**. This table shows data sources denoted as Y (Yes) and N (No) which signifies their availability or not. Logs suites available in this study are resistivity, density, neutron, gamma ray and sonic logs. Sequel to this inventory only Wabi 5 and Wabi 11 had the complete set of tools for geomechanical characterization. However, all the tools available in other Wabi wells are still of importance in use for petrophysical characterization. Among these data the most significant for this study are sonic and density logs because their combination gives an insight into the in-situ stress state and mechanical behavior of rocks especially rock strength (Tiab and Donaldson, 2012; Tixier, Lovely and Anderson, 1987).

Apart from the tools listed above, other data such as DST/RFT, master logs, X-ray scan of core and seismic data) were provided or made available for this study based on the original aim and objectives conceived (i.e to characterize Wabi reservoirs for development). However, slight changes were made which alter the available data to suit this present study. Therefore, most of the analyses done in this study are based on empirical correlation through petrophysical techniques and tools.

#### 4.1.1 Regional correlation

To have the knowledge of the field of study, regional correlation was made. The logs used for this correlation were gamma ray and resistivity logs. The correlation was done along dip where strike (i.e. crossline captures reservoir variation in space. For the sake of analyses and comparisons, two reservoirs intervals of were chosen as ‘shallow’ denoted as (A) and ‘deep’ denoted as (B) reservoirs. Wabi field well log correlation provides detailed stratigraphic analyzing of hydrocarbon reservoir in the study area. Beside the lithology log (i.e. gamma ray), resistivity logs were used to identified constrained at the reservoir intervals.

**Table 4.1.** Data inventory for this study (data sources).

WABI Well Logs Data Availability Check: Comments and Observations											
		LITHOLOGY LOGS			RESISTIVITY LOGS			POROSITY LOGS			HYDROCARBON TYPING
WELLS/ LOGS UNIT		GAMMA RAY LOG (GR)	SPONTANEOUS POTENTIAL LOG (SP)	CALIPER LOG (HCAL/CALI/SCAL )	DEEP RESISTIVITY (LLD/AHT190/SEDP )	MEDIUM RESISTIVITY (SEMP)	SHALLOW RESISTIVITY (LLS/AHT10/MFSL/SESP/SEXP)	DENSITY LOG (RHOZ/RHOB /SBD2/ HDBO)	NEUTRON LOG (APLC/NPHI/TNPL /TPNL)	SONIC LOG (DTP/DTS)	GAS - OIL DIFFERENTIATION LOGS
		GAPI	MV	IN	OHMM	OHMM	OHMM	KCAM3	VV	USM	
WABI 05	M	Y	N	Y	Y	N	Y	Y	Y	Y	RHOZ/ APLC
WABI 11	M	Y	Y	Y	Y	N	Y	Y	Y	Y	RHOB / NPHI
WABI 06	M	Y	N	Y	Y	Y	Y	Y	Y	N	SBD2/ TPNL
WABI 07	M	Y	N	Y	Y	Y	Y	Y	Y	N	HDBQ/ TNPL
<b>LEGENDS</b>											
Y	YES										
N	NO										

Chronostratigraphic surfaces typified by maximum flooding surfaces (MFS) and sequence boundary (SBs) were also used for regional correlation as shown in **Figure 4.1**. In the Niger Delta, the base of the youngest deposit (Benin Formation) is used as surface boundaries for correlation exercise (Rider, 1986). As a norm, the gamma ray (GR) is used to delineate lithology based on radioactive content of a formation with high counts indicating shale and low counts indicating sand/sandstone (Rider, 1986; Asquith and Gibson, 1982). The resistivity log was used as quality control. This correlation result shows that Wabi field reservoirs thickened from the North-East to South-West (NE-SW). This implies that Wabi reservoir pinches out in the North east direction this

gives rise to water injection well placement for enhancement of hydrocarbon recovery in Wabi field.

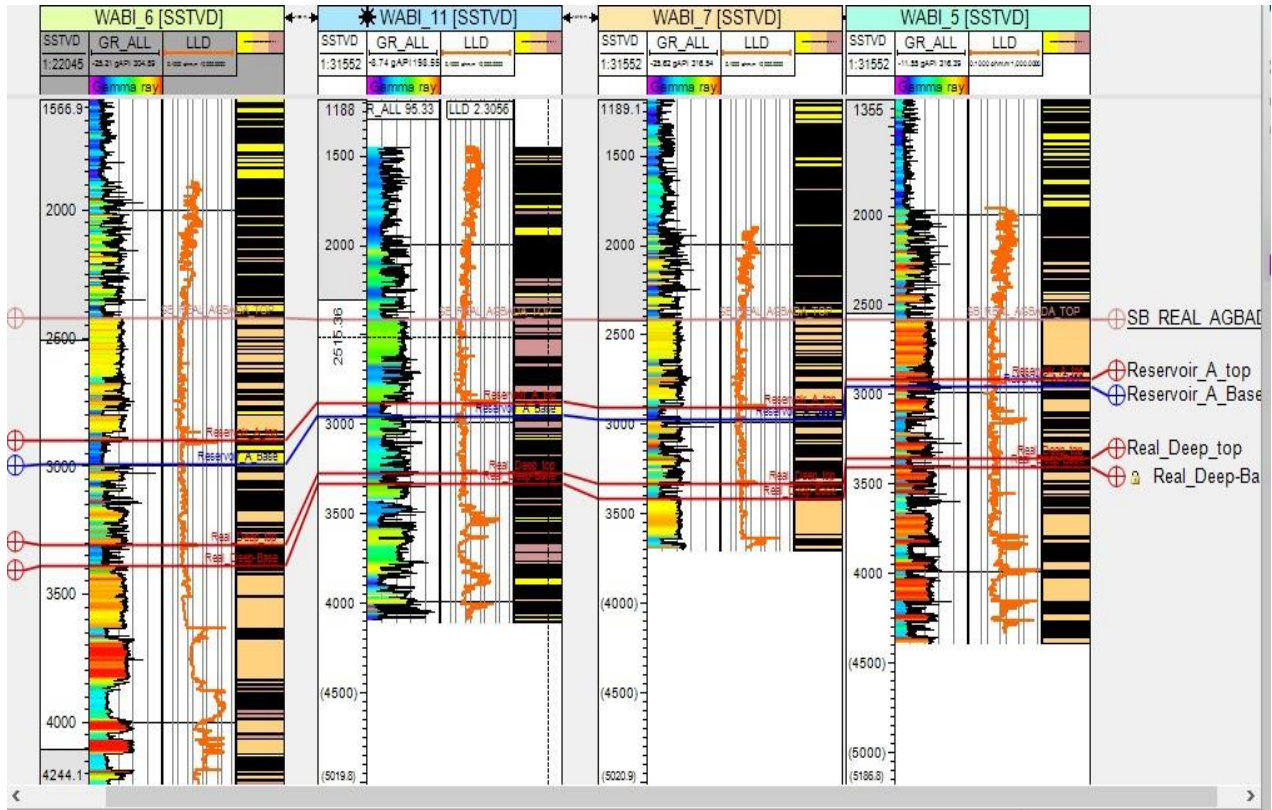


Figure 4.1. Regional correlation panel for Wabi field.

#### 4.1.2 Depositional environment

From sequence stratigraphic analysis two depositional environments were identified in Wabi field as Channel and Tidal flat setting to deltaic plain environment. This confirms with the dominant depositional environments identified in the Niger Delta (Schlumberger, 1985).

#### 4.1.3 Reservoir delineation for sand production/failure

The study field is a mature field in the onshore Niger Delta which needs to be upgraded for commercial production of hydrocarbon therein. This onshore field was investigated for the

common unconsolidated problem known as sand production found in most tertiary young formation (Otti and Woods, 2005). No drilling data report was provided to verify the likelihood of sanding. This drilling report would have partially identified geomechanical problems before hand to know the mechanical properties and strength of the formation penetrated. In this study, the identification of weak formations liable to have geomechanical issues was investigated and evaluated (Tixier, Lovely and Anderson, 1987). To evaluate the formation's likelihood for geomechanical problems, several established failure criteria were employed. In this study three (3) failure criteria were used to recognize the existence of geomechanical related issues in Wabi field as follows:

i) **Rock harness is described by Brinell hardness number (BHN):** This is the ratio of applied force on an indenter to the depth of indentation (Tiab and Donaldson, 2012). The delineation of the intervals of interest from Wabi 10 and 11 master log descriptions of lithology shows that the formation is loosely consolidated. The Wabi formation geologic age ranges from Oligocene to Miocene (Weber and Daukoru, 1985). Based on the BHN classification, this formation has some cementing materials and moderately cemented which resulted in weak unconfined compressive strength of the formation. When there is grain to grain stress increase coupled with erosion and changes in fluid saturation, the cement bond is broken and permits geomechanical issue occurrence (Oyeneyin, 2015), **Appendix C and D.**

ii) **Depth criterion:** This criterion has been documented in several literatures on sand production prediction in the Niger delta region (Abiola *et al.*, 2014) using depth range to define the compaction and strength of a formation. The established depth range is 10,000 ftss and well deeper than 10000ftss. The former indicated that wells drilled and completed within 10,000 ftss are prone to sand production, whereas the latter demonstrates that wells drilled and completed deeper than 10,000ftss have lesser sand production problem. Therefore, a trend can be shown for both cases that compaction increases onshore-ward (i.e. upward) implying that unconsolidation increases downward towards offshore where we have young depobelts (depocenters).

iii) **Sonic log criterion:** Acoustic or slowness ( $D_{TP}$  and  $D_{TS}$ ) profiles were used to differentiate consolidation from unconsolidated formation to identify formation that would produce sanding. This criterion used an established threshold to distinguish unconsolidated from consolidated

formation (Chang Zoback and Khaksar, 2006; Tixier Loveless and Anderson, 1975). Sonic transit time in sedimentary basin which measures the compressional wave greater than 110  $\mu$ s/ft and less than 90  $\mu$ s/ft were used as strength indicator for the characterization of the formation as unconsolidated and consolidated respectively **Figures 4.2-4.6** as well as lithology identification using  $V_P/V_S$  ratio (Chang Zoback and Khaksar, 2006).

In addition, interpretation of caliper log showed that Wabi field has related geomechanical problems to be addressed for safe hydrocarbon infill drilling and exploitation (Abdideh and Ahmadifar, 2013; Maleki *et al.*, 2014). The description of X-ray scanned of core from Wabi 05 confirmed that the reservoir has numerous fractures or induced fractures caused by moving core barrels to laboratory, indicated orientation of strike and dip on cores, showed that core plugs have been taken for further analysis such as special core analysis or routine core analysis **Figure 4.7**. The lithology of Wabi is seen as alternation of sand, sandstone and shale popularly known as shaly sand sequence. Its lithology description is as follows: White-rose, colorless, transparent – translucent, sub-angular-sub-rounded, fine-coarse, glauconites, calcareous- dolomites cement in sand and sandstone reservoirs while in shale it is grey-dark, indulated, silty, locally graded to siltstone and fissile **Appendix C**.

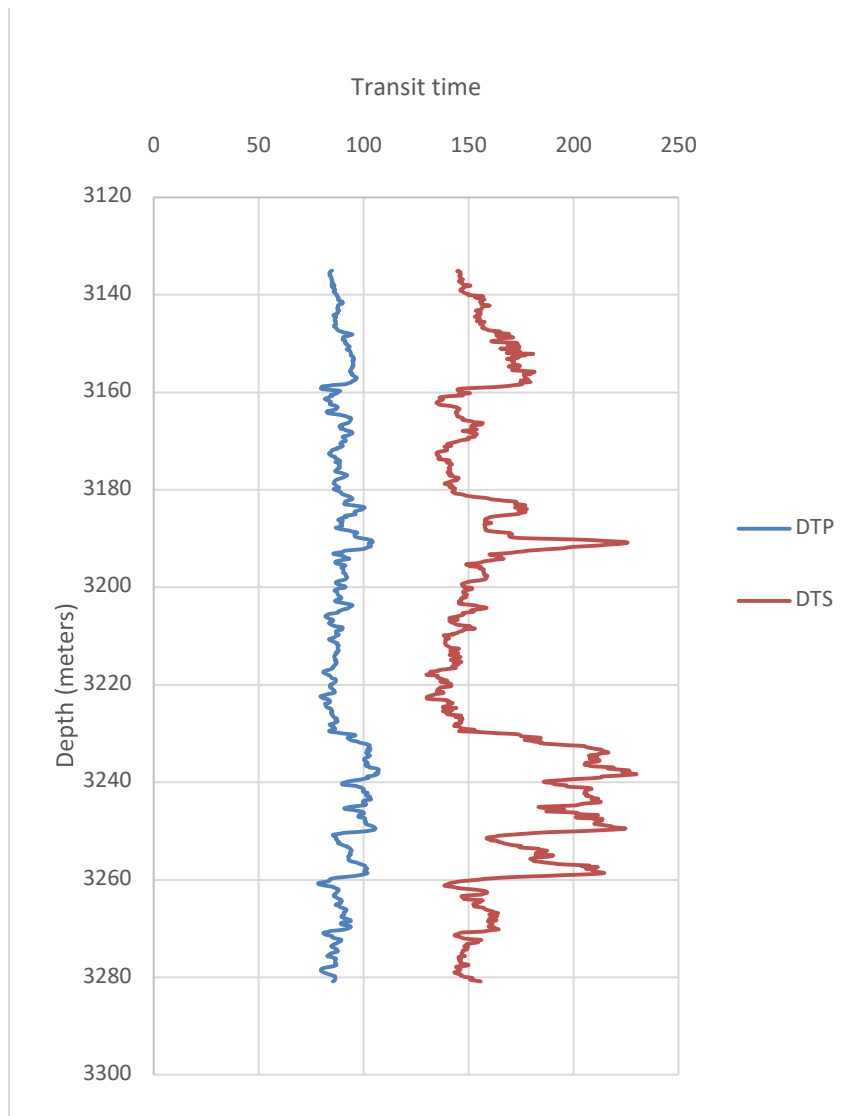


**Figure 4.2.** Slowness ( $D_{TP}$  and  $D_{TS}$ ) profile for Wabi 5A reservoir. Where  $D_{TP}$  is the P-wave travel time and  $D_{TS}$  is the S-wave travel time

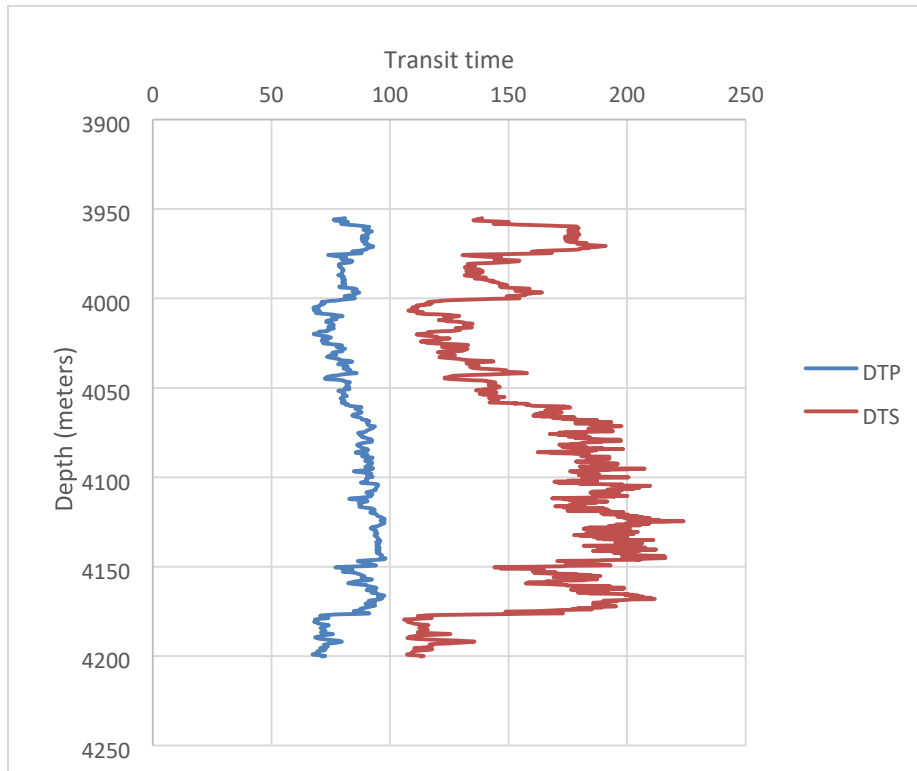


**Figure 4.3.** Slowness profile for Wabi 5B reservoir

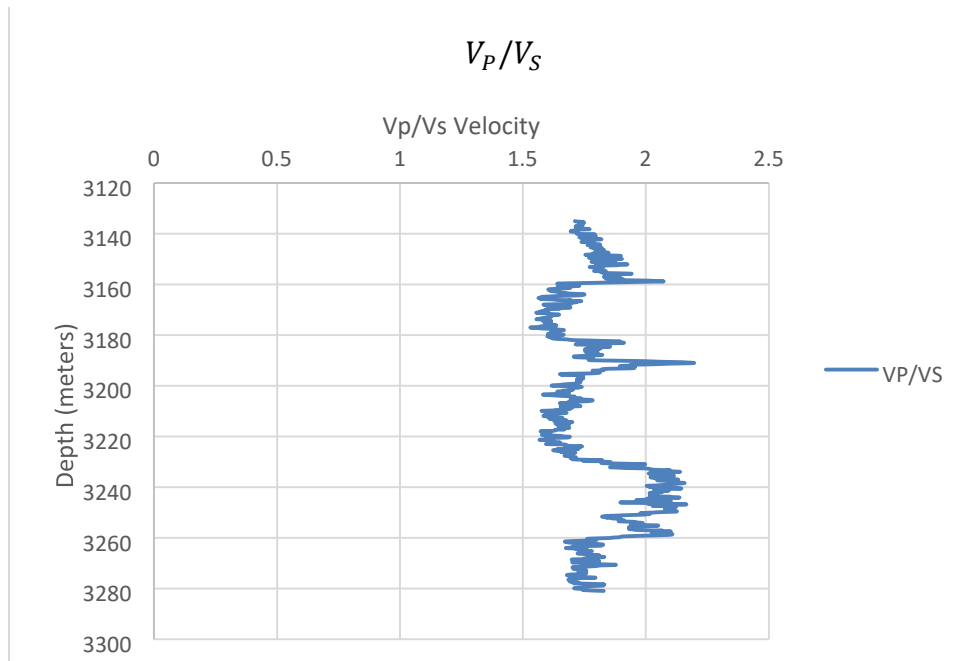


**Figure 4.4.**  $V_P/V_S$  profile for lithology delineation of Wabi 5A reservoir.

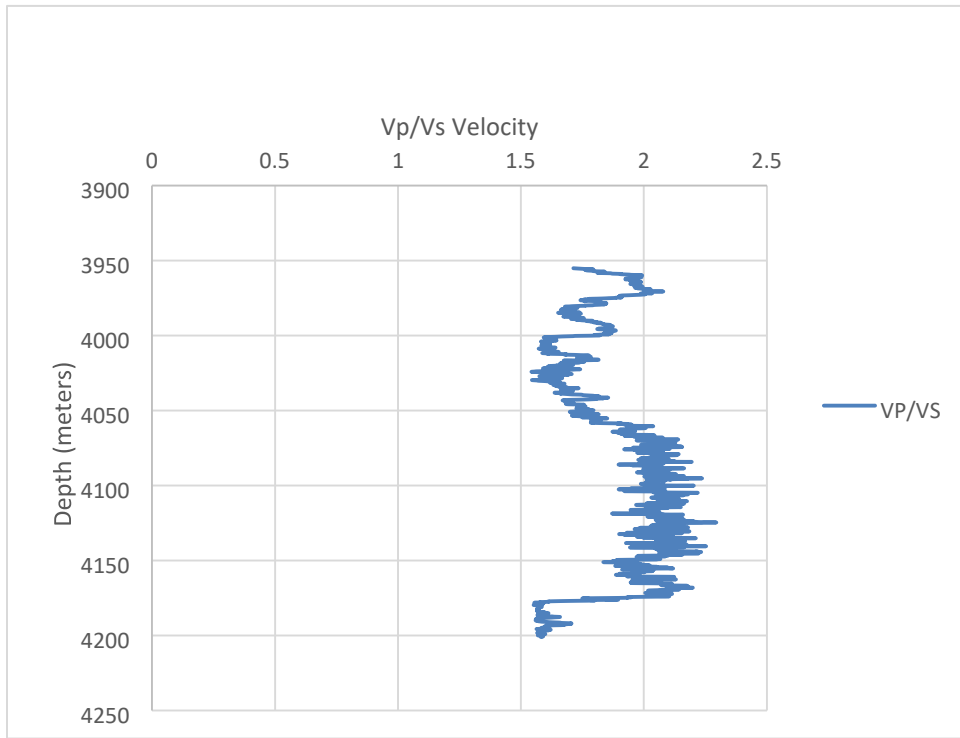


**Figure 4.5.**  $V_P/V_S$  profile for lithology delineation Wabi 5B reservoir

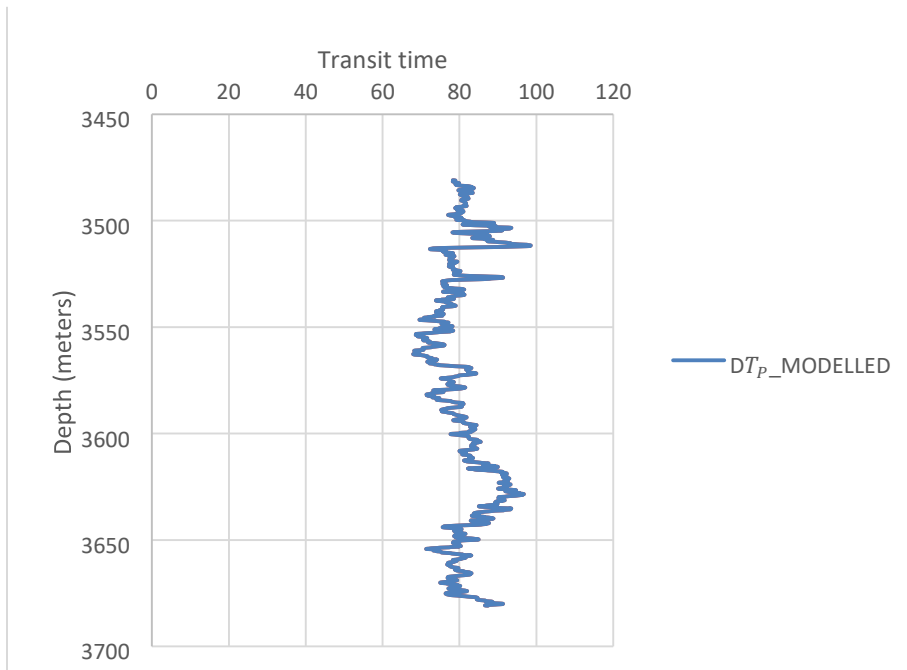


**Figure 4.6.** Interval transit time for lithology delineation in Wabi 11 Reservoir.

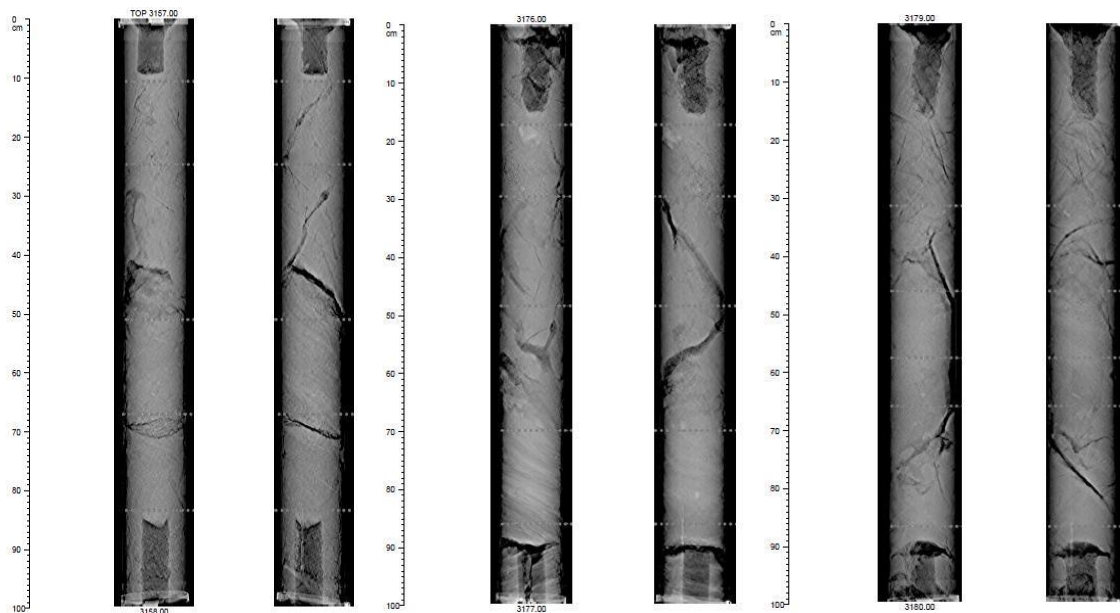


**Figure 4.7.** X-ray computerized tomography scan of core showing cracks (or induce fractures) for Wabi 05 well.

#### 4.2 Petrophysical evaluation analysis

The basic steps for evaluation is aided by well log data collected from Total Exploration and Production Nigeria in LAS file format. The log data was loaded into interactive petrophysics software 3.6, QC/QA was carried out, identification of reservoirs of interest, picking reservoir top and base, pick hydrocarbon sand and determined fluid type, QC/QA interpretation, cross plot and histogram of reservoirs, calculates volume of shale/clay, porosity, water saturation, generate net to gross pay, summary of parameters and reporting.

The composite wireline log consists of gamma ray, density, resistivity, sonic, neutron and PEF acquired by oil servicing company (Schlumberger) during the drilling phase of the wells were analyzed. Petrophysical evaluation was done in this study to know the reservoir quality and hydrocarbon potential of Wabi field for completion and development design. Reservoir quality and petrophysical properties are essential for both hydrocarbon potential estimation and enhancement of recovery in depleted reservoir for selection of best layers for hydraulic fracturing (Abdideh and Ahmadifar, 2013; Woehrl *et al.*, 2010). The summary of petrophysical analyses of Wabi field are shown in **Tables 4.2-4.8**. The petrophysical and geomechanical properties of the reservoir of

interest include: porosity, fluid saturation, lithology, bulk density, compressional and shear velocities, fluid contacts, net to gross, net pay, clay volume, pore pressure, overburden stress, maximum, minimum horizontal stress were all derived from geophysical wireline logs. These petrophysical properties may have influence on the mechanical properties (rock strength). The influence they may have depends on their intrinsic composition of the rock masses (Dusseault, 2011). For consolidated formation, the composition increases the mechanical properties while for unconsolidated formations, the composition lowers the mechanical properties of the rock (Oluyemi, 2007). In other words, these compositions also show the capability of the rock to withstand stress (Economides and Nolte, 2000).

#### **4.2.1 Reservoir delineation and petrophysical characterization**

Wabi field has stacked multiple reservoirs, although only two intervals were chosen for this study as shallow and deeper reservoir (Zorasi, 2017). These intervals were identified based on the following logs; gamma ray (GR) in track 3, resistivity in track 4, density (RHOB) in track 5, neutron (NPHI) log in track 5 and sonic log in track 6. This is known as basic qualitative interpretation shown in **Figures 4.8-4.9**. Combination of lithology and porosity logs (i.e Gamma ray and Neutron-density) were used for identification of oil and gas bearing zones. Gamma ray respond to radioactive content of Wabi which helps to differentiate shales from sand and carbonates that have low radioactive content. See section 3.2.1 and **Figure 3.1** for the workflow that led to **Figure 4.8**.

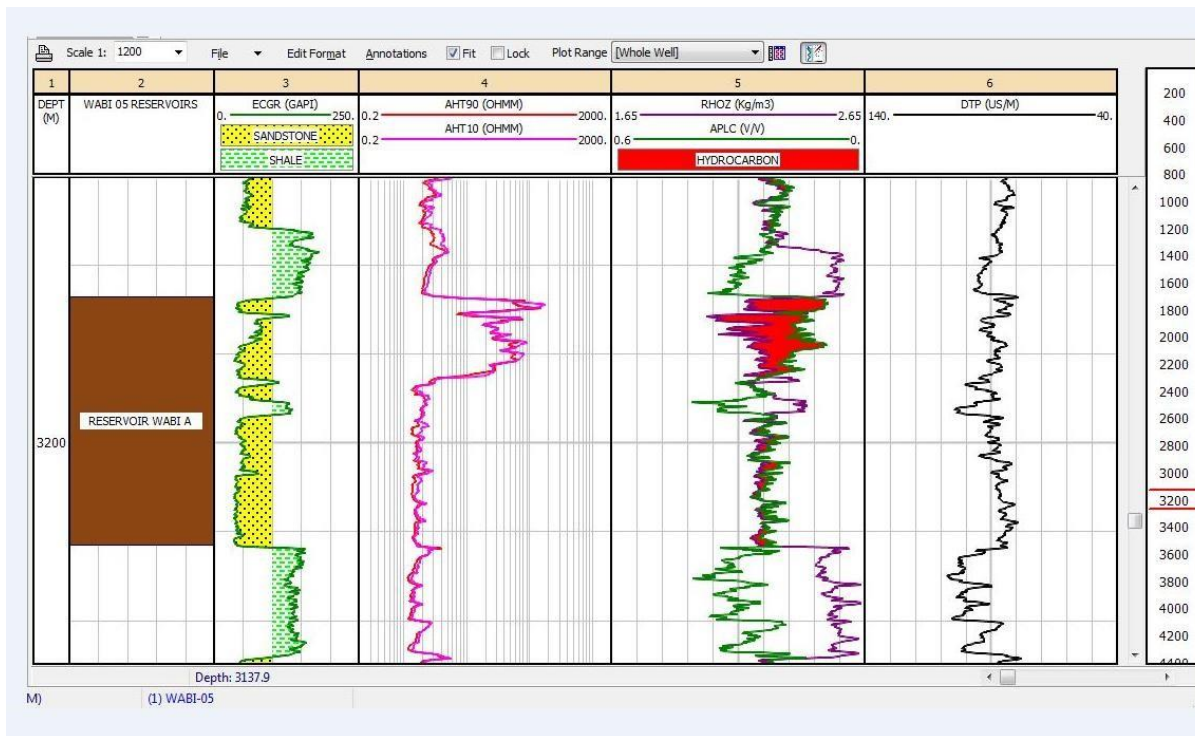


Figure 4.8a. Wabi 5A reservoir delineation (The log suit consists of track1-6).

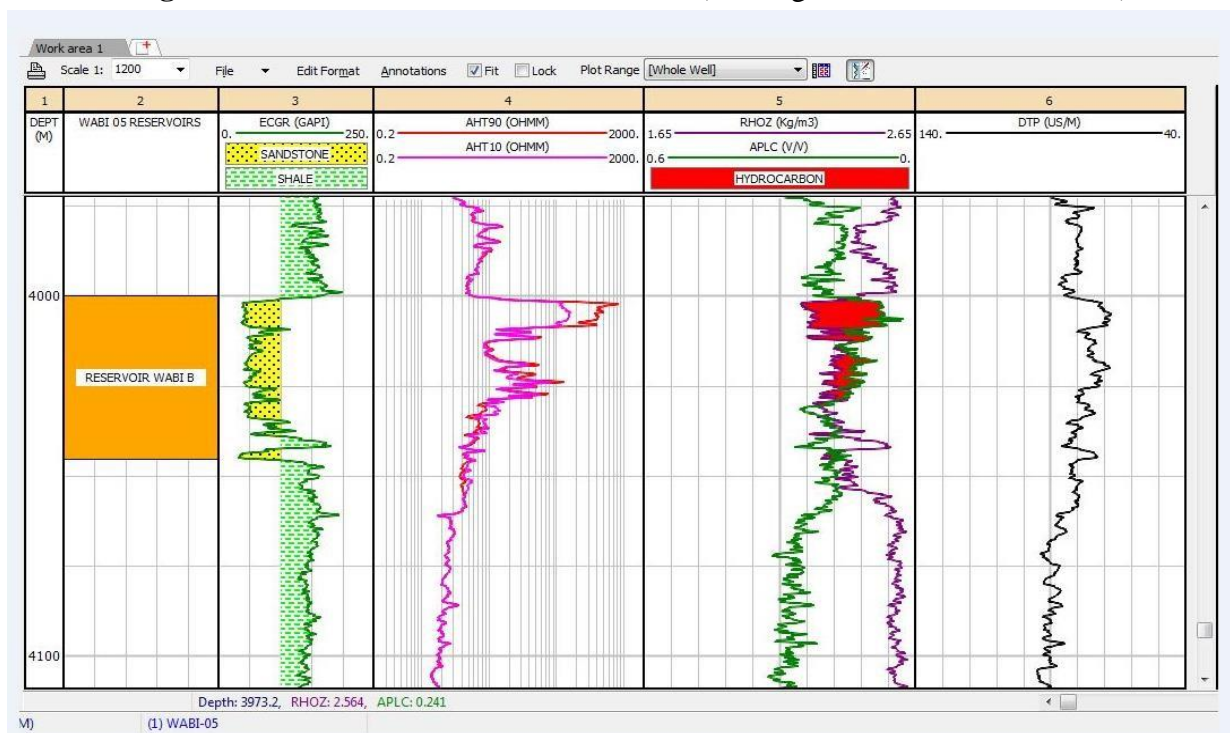


Figure 4.8b. Wabi 5 B reservoir delineation.

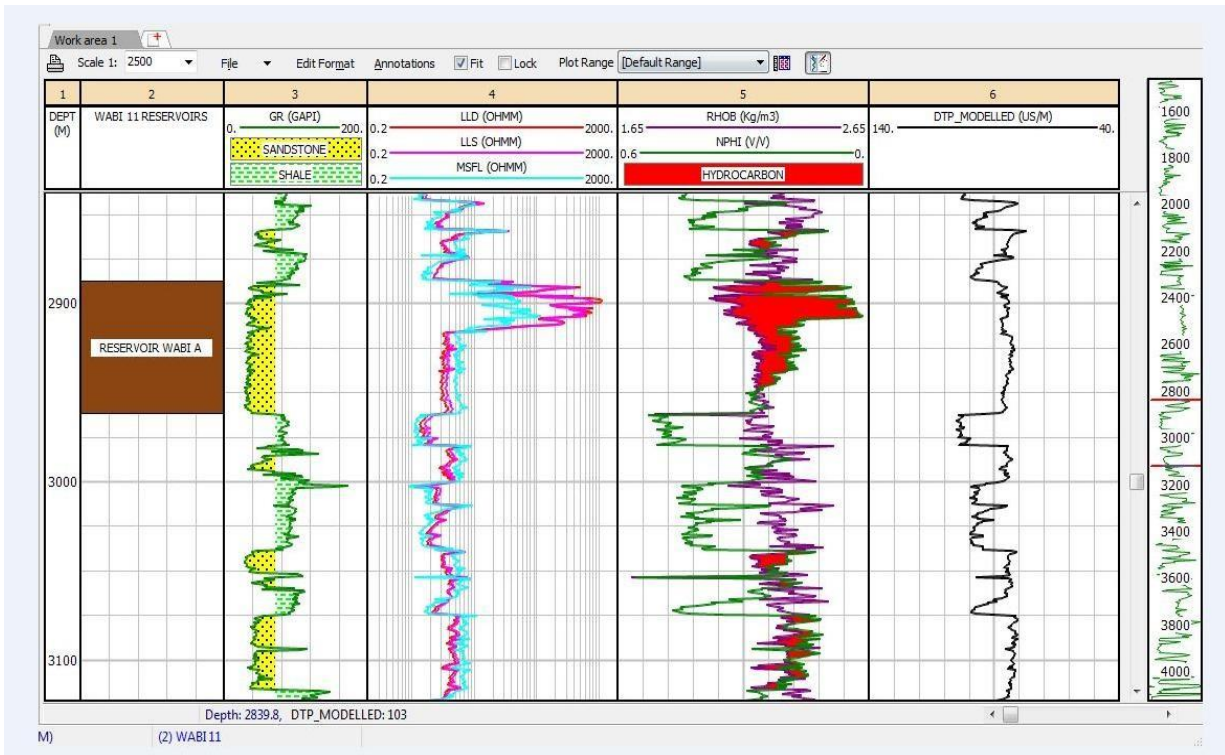


Figure 4.9a. Wabi 11 A reservoir delineation.

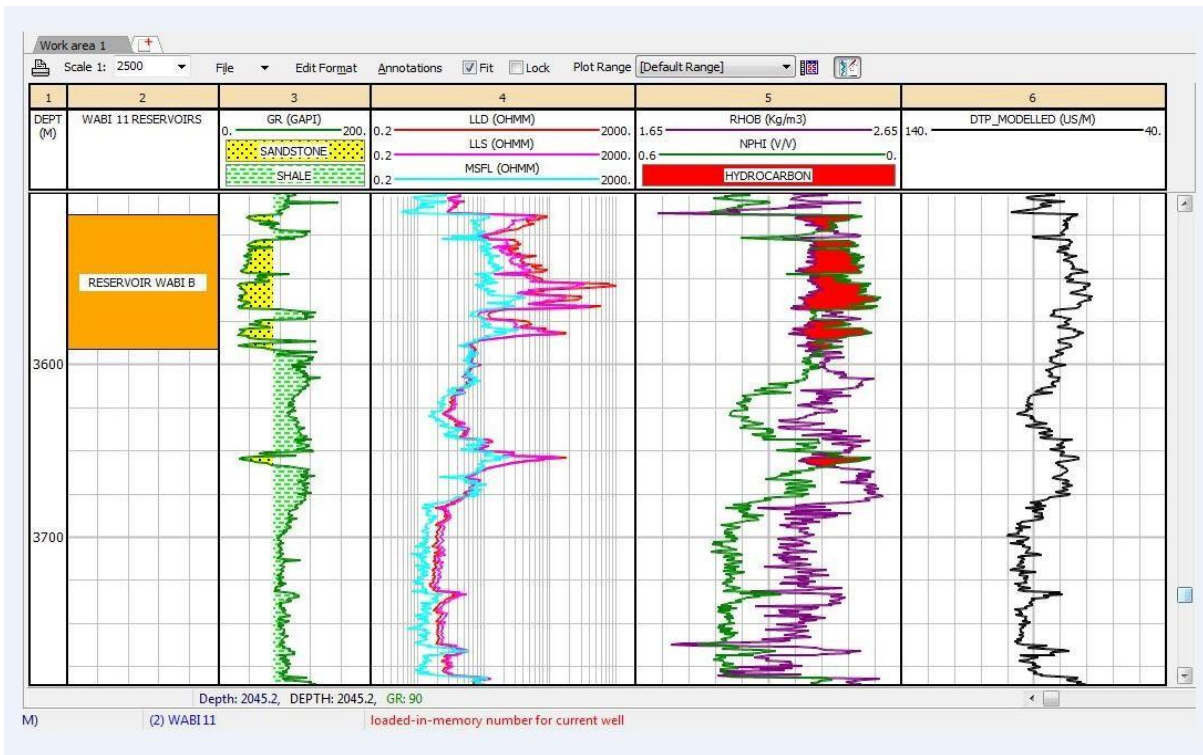
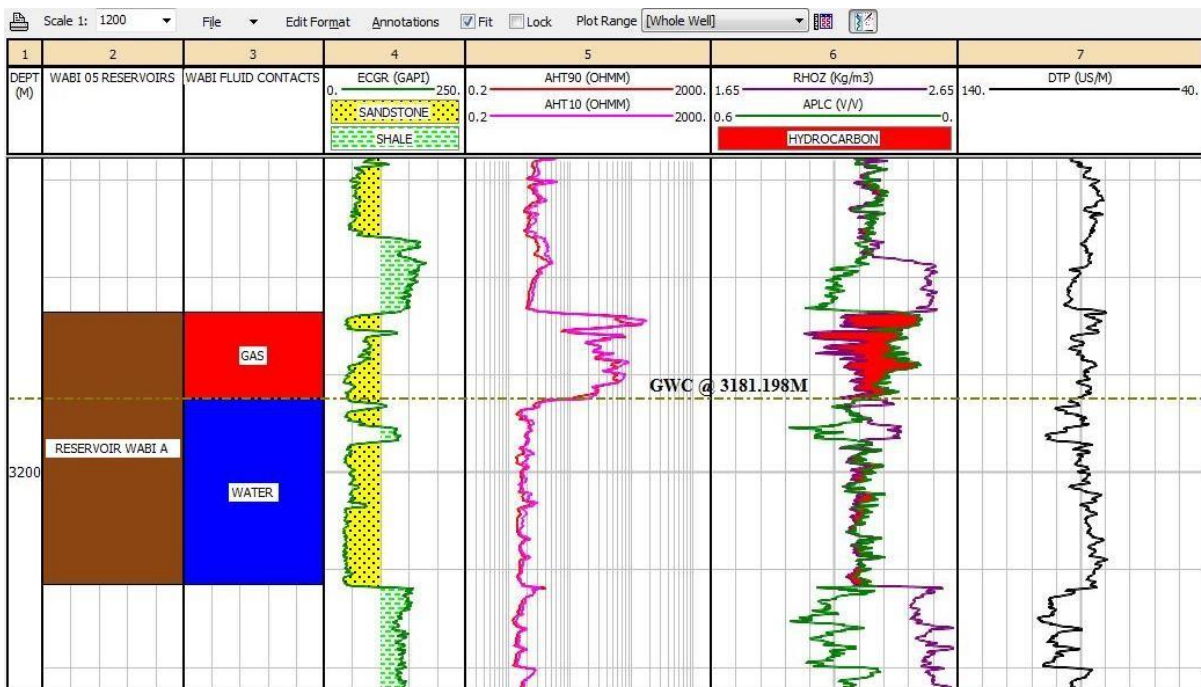


Figure 4.9b. Wabi 11B reservoir delineation.

#### 4.2.2 Reservoir Analysis for hydrocarbon types and fluid contacts

The predictable methods for fluid contact identification consist of interpretation of pressure gradients due to fluid density differences in the reservoir hydrostatic column **Figures 4.10-4.11**. The figures below show the various fluid type and contacts for WABI 05, 06, 07 and 11. The interpretation of wireline logs which involves the use of representative models to characterize logs responses due to formation parameters is known as qualitative characterization (Etu-Efeotor, 1997; Rider, 1990). This was employed for lithology delineation, hydrocarbon differential (i.e. oil or gas), fluid contact and well correlation (Asquith and Gibson, 1982). Meanwhile gamma ray, neutron and density logs were used to delineate reservoirs and hydrocarbons bearing zones in Wabi 5, 6, 7 and 11. The summary of the fluid types and contact for WABI field are showed in **Table 4.2-4.8**.



**Figure 4.10a.** Wabi 5A fluid contact analysis.

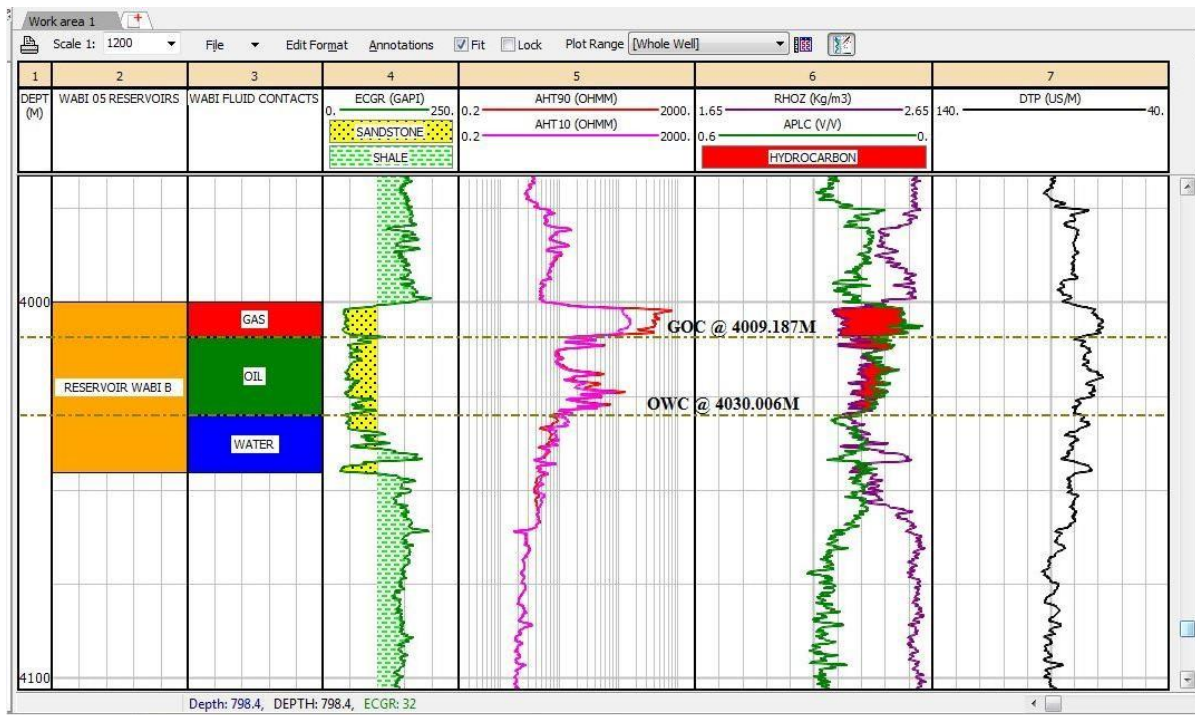


Figure 4.10b. Wabi 5B fluid contact analysis.

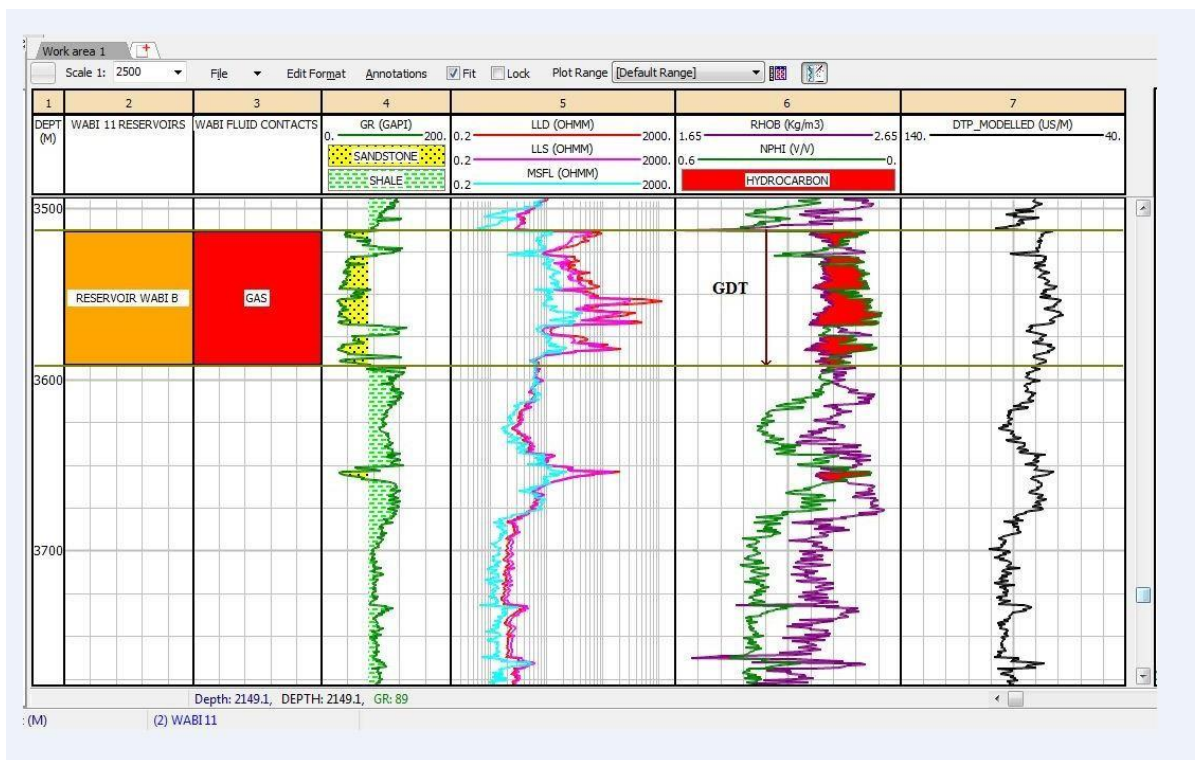
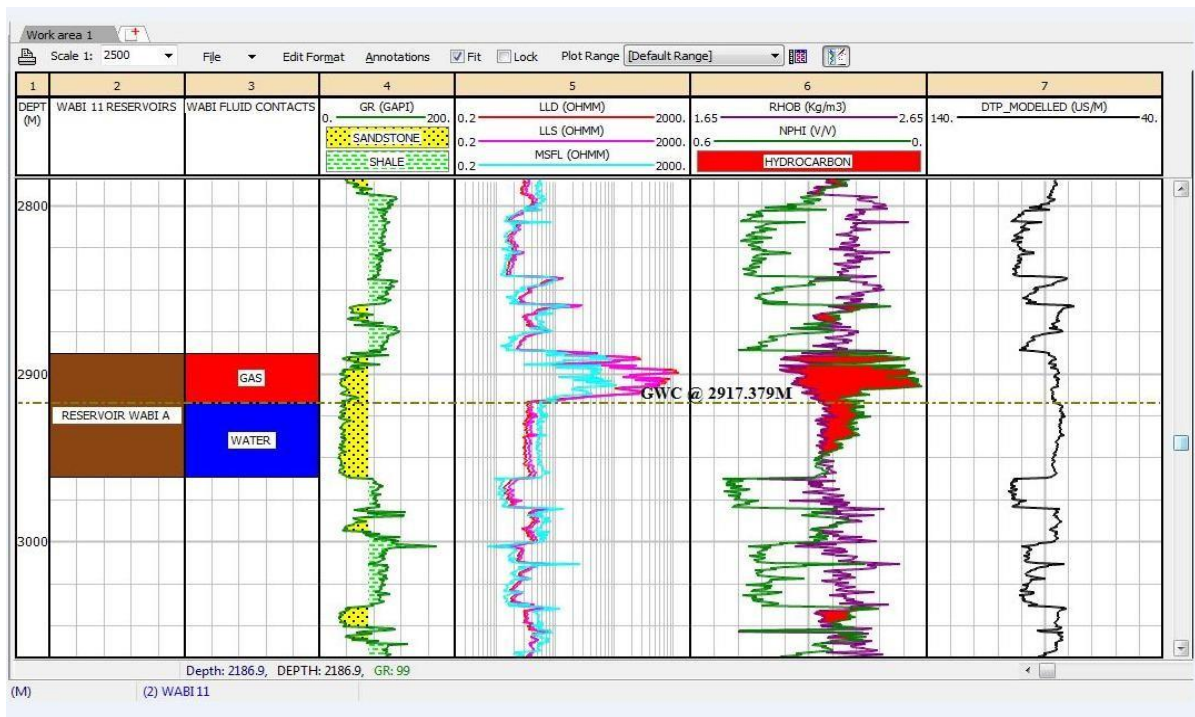


Figure 4.11a. Wabi 11 fluid contact analysis



**Figure 4.11b.** Wabi 11B fluid contact analysis.

### 4.2.3 Quantitative analysis

The qualitative interpretation involves the use of models which represent the characteristic log responses to formation parameters while the quantitative interpretation involves the use of mathematical models and relations which give identical values of the log response to the formation parameters (Etu-Efeotor, 1997). The follows are the step by steps evaluation of petrophysical results.

#### *i) Neutron log*

The neutron tool response is primarily dominated by the "Hydrogen Index". The replacement of liquid by gas reduces the hydrogen index. Therefore, gas bearing reservoirs have low, apparent neutron porosities. Modeling and experimentation have shown that the effect of gas on neutron logs is greater than would be expected by considering only hydrogen index considerations. Also, shale, lithology and neutron absorbing trace elements all have influence on the neutron response. For these reasons, confident hydrocarbon differentiation, lithology and porosity determination were made when neutron data is used in combination with another log information (density).

### *ii) Density log*

In porous formations, the difference between the bulk density as measured by the tool in a water filled system compared to a water plus oil filled system is very small. However, if gas is present in the pore space, the measured bulk density can be significantly less than in a liquid filled system. This is the basis for hydrocarbon differentiation using the density tool and when used in combination with a neutron log usually provides reliable results in Wabi field.

### *iii) Sonic log*

The gas effect on the acoustic velocities is a complex process; and surprisingly the most significant effect that occur in the low gas saturation range. In general, gas in the pore space results in a decrease in compressional velocity i.e. longer transit time and attenuation of the compressional wave. This commonly leads to cycle skipping in compressional velocity tools. The modern array devices do not, in general, suffer from this problem as compressional velocities are derived from the wave form correlations rather than arrival picks. Gas bearing zones can be identified by a tendency for the sonic to shift to the left due to the slowing of the compressional wave. Thus, in gas bearing intervals, the parting between the sonic and resistivity readings are greater than in oil bearing intervals (Zaki, 1994).

### *iv) Porosity calculation*

The available porosity logs for Wabi Wells are Neutron, Density and Sonic. The density log was used to calculate porosities in the entire reservoirs. The matrix and fluid density used are respectively 2.648 g/cm and 1.1 g/cm, respectively. The calculated porosities are effective and total porosities of the reservoirs. Effective porosities are less than the total porosity in decimal. The ratio of interconnected pore volume to the bulk volume of a material defines the effective porosity. The interconnected pore volume or void space in a rock contributes to fluid flow or permeability in a reservoir **Figures 4.12-4.13**.

### *v) Calculating net pay with cutoffs*

The thickness of rock that contributes to economically feasible production with today's technology describes the net pay. Net pay is obviously a moving target since technology, prices, and costs vary

almost daily (Zorasi, 2017). Hence, tight reservoirs or shaley zones that were bypassed in the past are now prospective pay zones due to new technology and continued demand for hydrocarbons. Net pay is determined by applying appropriate cutoffs values to reservoir properties so that unproductive or uneconomic layers are not counted (Zorasi, 2017). Cumulative reservoir properties, after appropriate cut off are applied to provide information about the pore volume (PV), hydrocarbon pore volume (HPV) and flow capacity (KH) of a potential pay zone. These values are used to calculate hydrocarbon in place recoverable reserves and productivity of wells (Asquith and Gibson 1982). Cut – Off used for this interpretation are: Volume of shale (Vsh) = 0.4, Effective porosity (PHIE) = 0.15, Water saturation (SW=0.5).

*vi) Fluid saturation calculation*

The fraction or percentage of pore space that is occupied by water called water saturation was calculated for the reservoirs of the WABI wells using the formula for hydrocarbon saturation as follows:

$$S_H = 1 - S_W \text{ (decimal) or } S_H = 100 - S_W \text{ (\%)} \quad (\text{Asquith and Gibson, 1982}).$$

Where,  $S_H$  = Hydrocarbon Saturation;  $S_W$  = Water Saturation,  $S_H = S_O$  or  $S_g$  where  $S_O$  is Oil Saturation and  $S_g$  is Gas Saturation.

The formula used in calculating this water saturation parameter was Juhasz (1981) and Waxman Smith (1968):

$$\frac{1}{R_t} = \left( \frac{v_{cl}^{1.4}}{\sqrt{R_{cl}}} + \frac{\phi_e^{m/2}}{\sqrt{a R_w}} \right)^2 S_w^n$$

where,

$\phi_e$  - Effective porosity

$R_t$  - Resistivity of uninvaded zone or true resistivity.

$V_{Sh}$	-	Volume of shale
n	-	Saturation exponent
$R_W$	-	Resistivity of formation water
$S_W$	-	Water saturation
$R_{Sh}$	-	Resistivity of adjacent shale

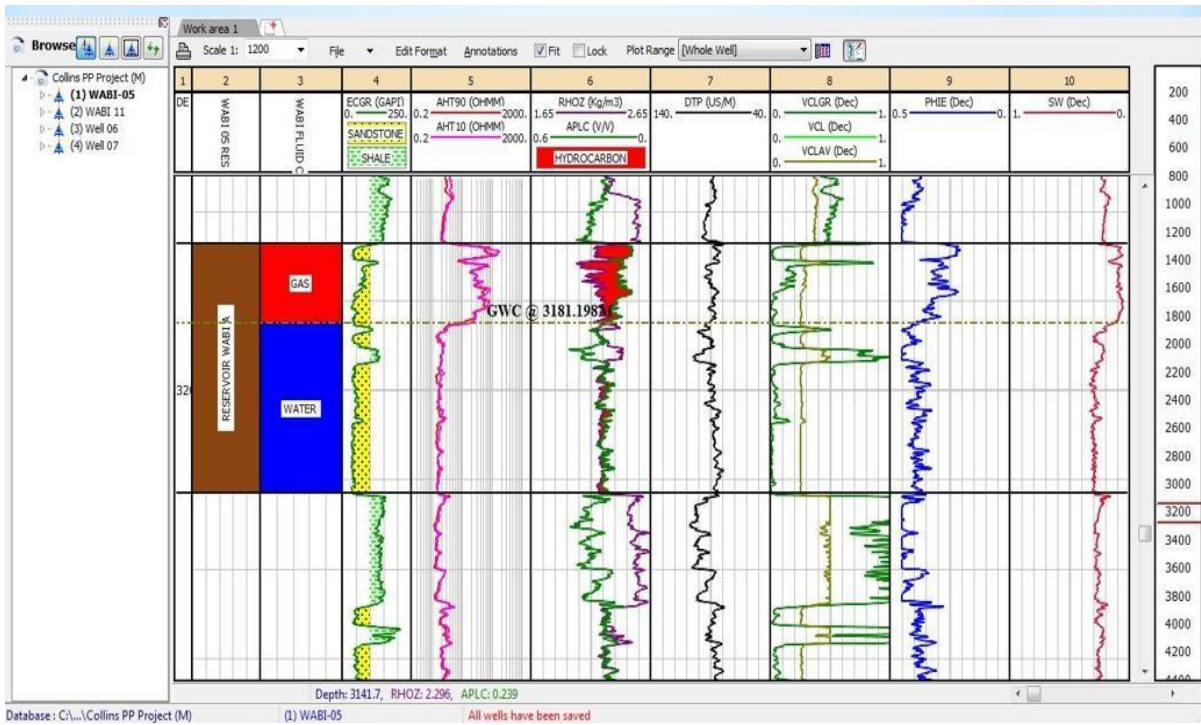


Figure 4.12a. Wabi 5 A quantitative analysis.

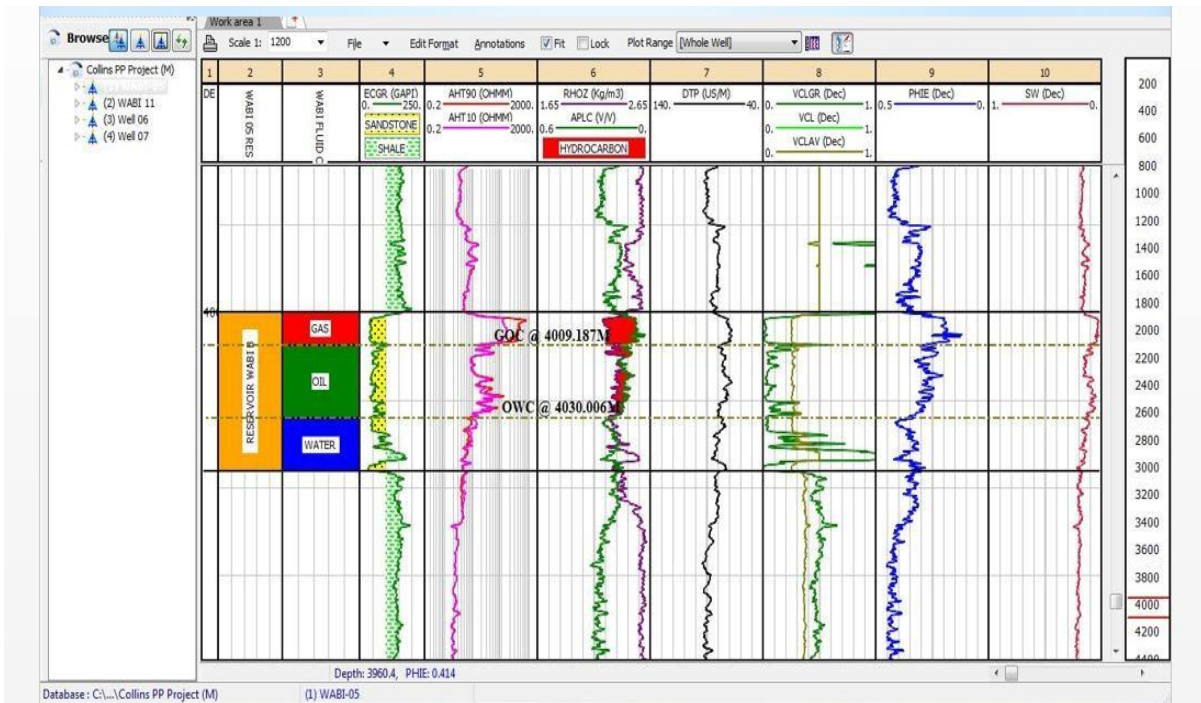


Figure 4.12b. Wabi quantitative analysis.

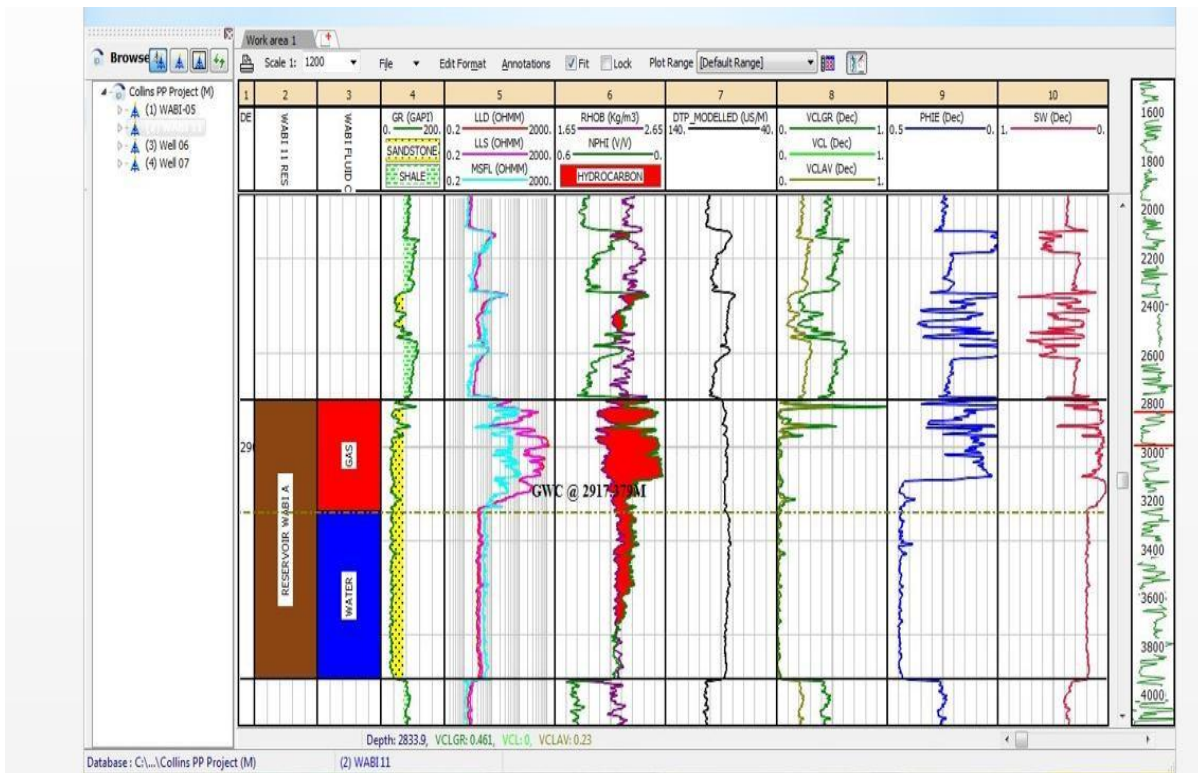


Figure 4.13a. Wabi 11A quantitative analysis.

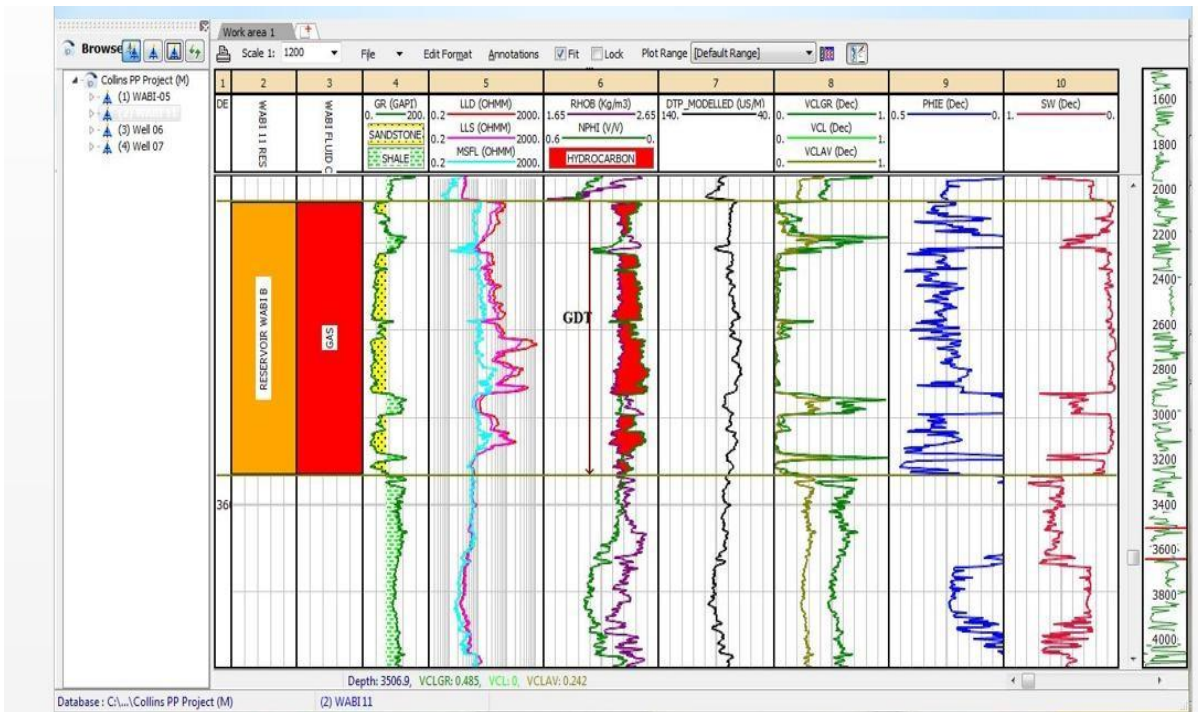
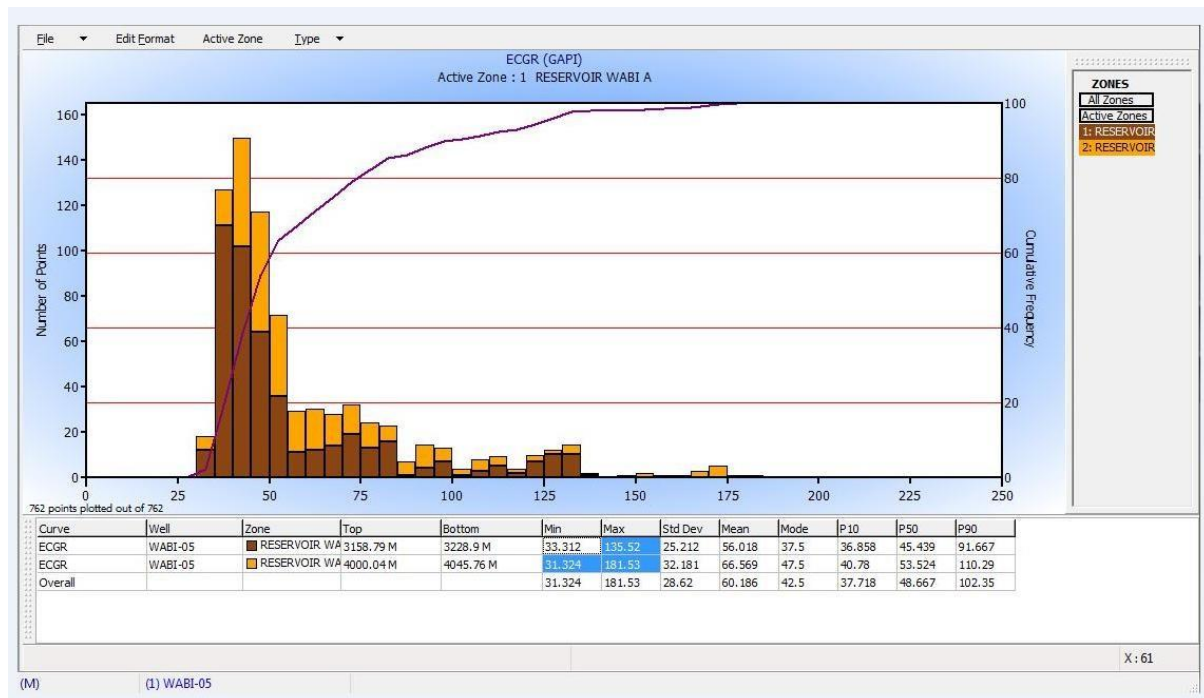


Figure 4.13b. Wabi 11B quantitative analysis.

vii) *Volume of shale calculation*

The volume of shale was calculated for the reservoirs in four wells (WABI-05, 11, 06, and 07 respectively). The method used in calculating the volume of shale was the one prescribed by Larionov (1969) for Tertiary rocks (unconsolidated formation). In interactive petrophysics (IP 3.6), it is called young rock. It gives accurate result of volume of shale in shaly sandstone. It is used more in wells explored for Niger Delta Basin Fields, in which our WABI Wells falls under such basin. The linear response is first calculated and then followed by the nonlinear response. The GRmin and GRmax are derived from the histogram plot of each of the reservoirs in the well drilled, while the GRlog is derived from the gamma ray log reading from the interval of interest, **Figures 4.8-4.9. Figures 4.16-4.17** show the cross plots which confirm the lithology of the chosen intervals as sandstone with slight intercalation of shale.



**Figure 4.14.** Wabi 5 histogram.

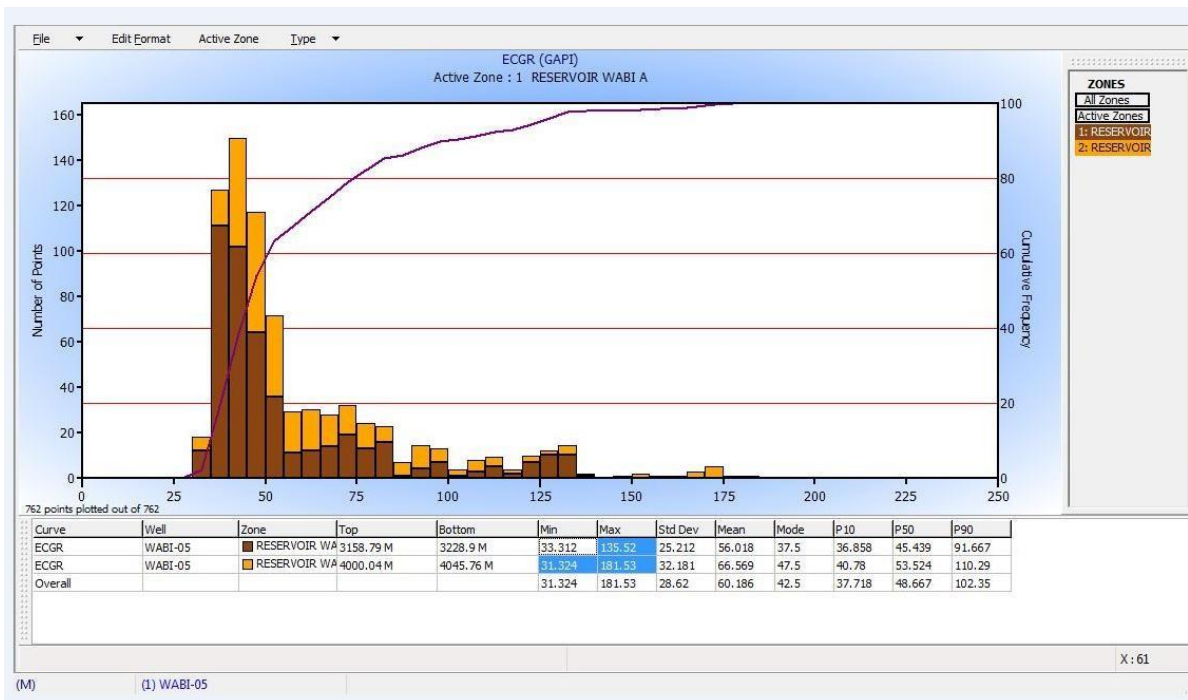


**Figure 4.15.** Wabi 11 histogram.

### Viii) Cluster Analysis

Cross plotting techniques are very robust for classification of lithology and fluid type using log responses. Cross plotting of rock properties from petrophysical logs is one of the convenient and proficient techniques to look at two rock properties and their attributes. Therefore, prove decisively which rock properties and their attributes will be supportive to differentiate gas in a particular reservoir. Crossplot analysis was carried out to establish Wabi rock properties / attributes that described and differentiates the reservoir and hydrocarbon content. The cross plot of Neutron log versus Density colour coded with gamma ray in **Figure 4.16-4.17** discriminates the reservoirs into shale, brine sands, oil sands and gas sands. This was realized when cursor is moved on reservoir intervals on log section and the cross plot equally highlighted same for confirmation of similar result. Hence, cross plots were used to visually recognize or detect anomalies that may result to hydrocarbon presence or other fluids and lithologies.

The **tables 4.2-4.8** showed the summary of Petrophysical analyses results of Wabi field.

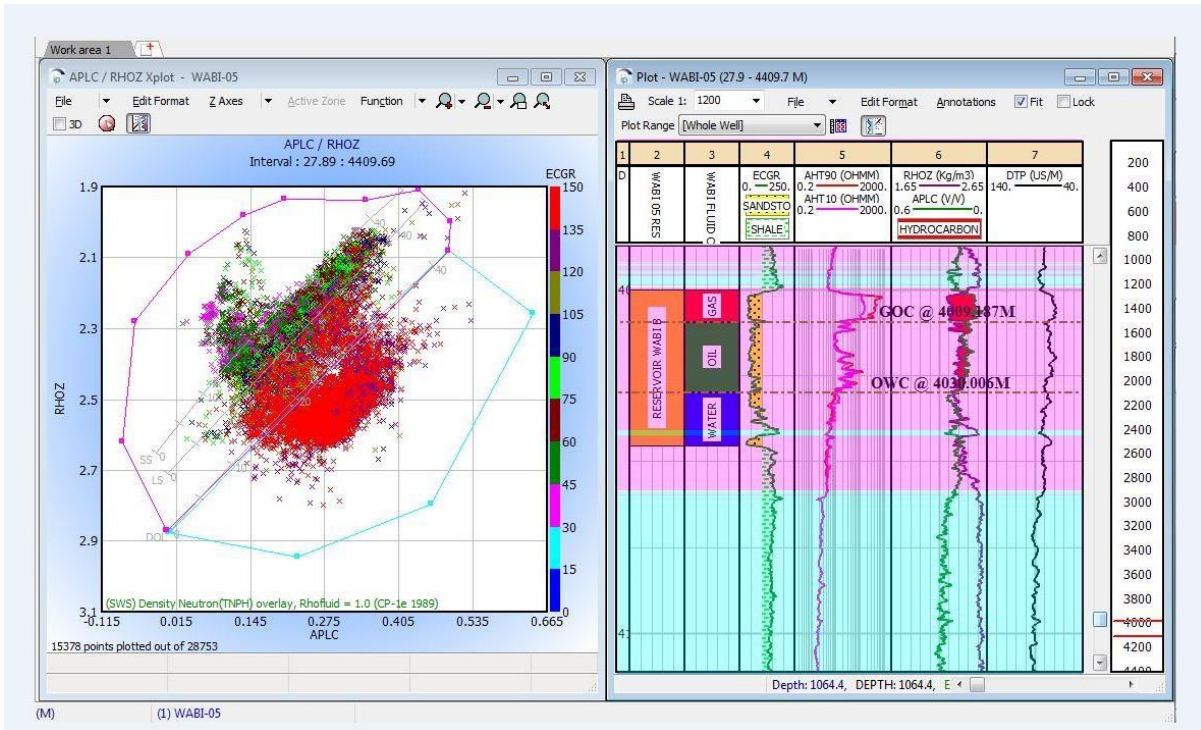


Figure 4.16a. Wabi 5A Lithology cross plot showing cluster interval of interest.

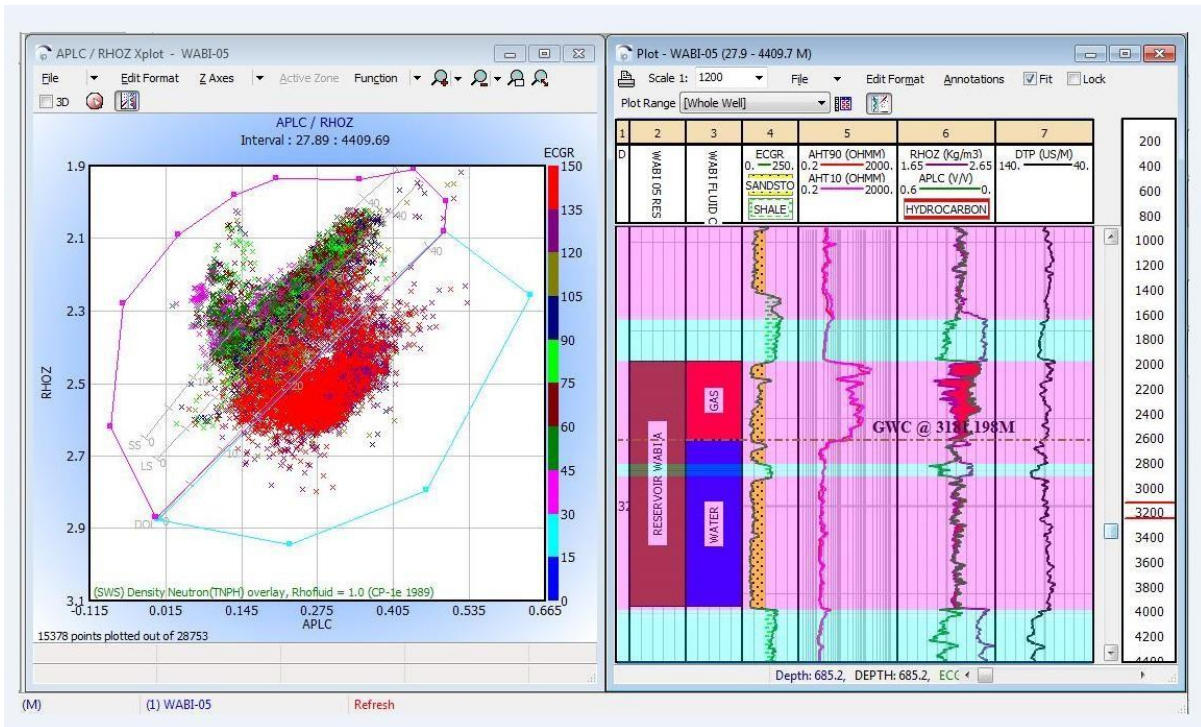
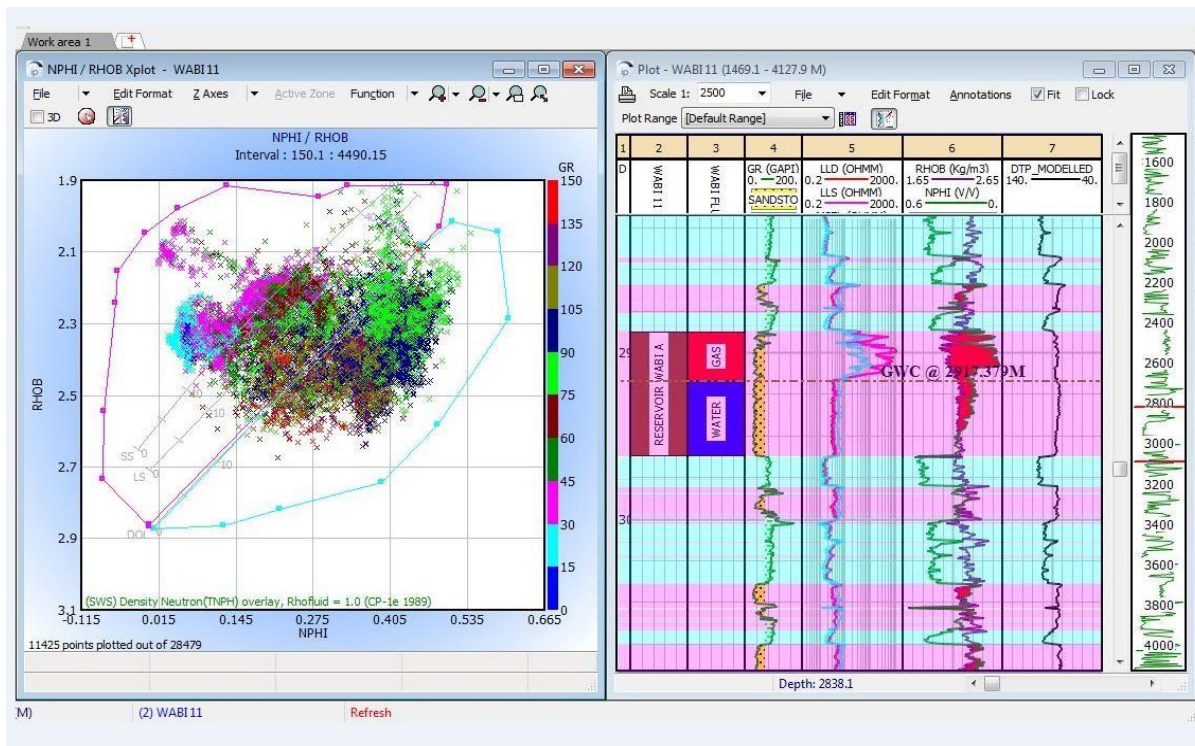


Figure 4.16b. 5B lithology cross plot.



**Figure 4.17.** Wabi 11 Lithology cross plot.

The petrophysical results of Wabi field based on interactive petrophysics software are discussed in chapter 5. The discussion addresses the part of the Thesis objectives.

**Table 4.2: Summary report on identification of reservoirs of interest in Wabi wells**

<b>WELL</b>	<b>RESERVOIRS</b>	<b>TOP MD (M)</b>	<b>BOTTOM MD (M)</b>
WABI 05	RESERVOIR WABI A	3158.795	3228.899
WABI 05	RESERVOIR WABI B	4000.043	4045.763
WABI 11	RESERVOIR WABI A	2887.661	2962.185
WABI 11	RESERVOIR WABI B	3513.263	3591.597
WABI 06	RESERVOIR WABI A	3887.862	3997.286
WABI 06	RESERVOIR WABI B	4053.216	4078.972

**Table 4.3: Summary table for Wabi wells showing fluid type and the fluid contacts.**

WELL	RESERVOIRS	TOP MD (M)	BOTTOM MD (M)	HYDROCARBON FLUID TYPE	FLUID CONTACT
WABI 05	RESERVOIR WABI A	3158.795	3181.198	GAS	GWC @ 3181.198M
		3181.198	3228.899	WATER	
WABI 05	RESERVOIR WABI B	4000.043	4009.492	GAS	GOC @ 4009.492M  OWC @ 4030.066M
		4009.492	4030.066	OIL	
		4030.066	4045.763	WATER	
WABI 11	RESERVOIR WABI A	2887.661	2917.379	GAS	GWC @ 2917.379M
		2917.379	2962.185	WATER	
WABI 11	RESERVOIR WABI B	3513.263	3591.597	GAS	GDT

**OWC:** Oil – Water Contact  
**GDT:** Gas Down- To  
**GWC:** Gas – Water Contact  
**GOC:** Gas – Oil Contact.

**Table 4.4: Summary table for Wabi wells showing fluid type and the fluid contacts.**

WELL	RESERVOIRS	TOP MD (M)	BOTTOM MD (M)	HYDROCARBON FLUID TYPE	FLUID CONTACT
WABI 06	RESERVOIR WABI A	3887.862	3997.286	GAS	GDT
WABI 06	RESERVOIR WABI B	4053.216	4078.972	GAS	GDT
WABI 07	RESERVOIR WABI A	2915.26	2931.9	GAS	GWC @ 2931.9M
		2931.9	2984.144	WATER	
WABI 07	RESERVOIR WABI B	3340.76	3365.1	GAS	GWC @ 3364.078M
		3365.1	3429.61	WATER	

**GWC:** Gas – Water Contact,     **GDT:** Gas Down- To

**Table 4.5: Average summary report on WABI 05 Well (Quantitative)**

<b>WABI 05 RESERVOIRS</b>	<b>RESERVOIR WABI A</b>	<b>RESERVOIR WABI B</b>
SAND TOP (M)	3158.795	4000.04
SAND BOTTOM (M)	3228.899	4045.763
Thinnest Interval Thickness (M)	4.72	0.46
Thickest Interval Thickness (M)	36.73	33.22
Gross Sand / Thickness (M)	70.10	45.72
Net Thickness (M)	64.39	43.05
Net to Gross (N / G)	0.918	0.942
Hydrocarbon Type	GAS / WATER	GAS/OIL/WATER
Fluid Contact	GWC @ 3181.198M	GOC @ 4009.492M; OWC @ 4030.066M
Volume of Shale (Vshale)	0.055	0.068
Total Porosity (PHIT)	0.358	0.288
Effective Porosity (PHIE)	0.340	0.269
Water Saturation (SW)	0.231	0.117
Hydrocarbon Saturation (Sh)	0.769	0.883
Water Saturation in the Invaded/Flushed zone (Sxo)	0.186	0.106
Bulk Volume Water (BVW)	0.0686	0.0283

**Table 4.6: Average summary report on WABI 11 well (Quantitative)**

<b>WABI 05 RESERVOIRS</b>	<b>RESERVOIR WABI A</b>	<b>RESERVOIR WABI B</b>
SAND TOP (M)	2887.661	3513.263
SAND BOTTOM (M)	2962.185	3591.597
Thinnest Interval Thickness (M)	0.15	0.15
Thickest Interval Thickness (M)	53.8	53.8
Gross Sand / Thickness (M)	74.52	78.34
Net Thickness (M)	58.60	64.47
Net to Gross (N / G)	0.786	0.823
Hydrocarbon Type	GAS / WATER	GAS
Fluid Contact	GWC @ 2917.379M	GDT
Volume of Shale (Vshale)	0.031	0.057
Total Porosity (PHIT)	0.419	0.273
Effective Porosity (PHIE)	0.2411	0.343
Water Saturation (SW)	0.167	0.076
Hydrocarbon Saturation (Sh)	0.833	0.924
Water Saturation in the Invaded/Flushed zone (Sxo)	0.196	0.1737
Bulk Volume Water (BVW)	0.0246	0.0247

**Table 4.7: Average summary report on WABI 06 Well (Quantitative)**  
**WABI 05 RESERVOIRS                      RESERVOIR WABI A    RESERVOIR WABI B**

Sand top (m)	3887.862	4053.216
Sand bottom (m)	3997.286	4078.972
Thinnest Interval Thickness (M)	0.15	0.61
Thickest Interval Thickness (M)	78.33	10.82
Gross Sand / Thickness (M)	109.42	25.76
Net Thickness (M)	103.86	20.19
Net to Gross (N / G)	0.949	0.784
Hydrocarbon Type	GAS	GAS
Fluid Contact	GDT	GDT
Volume of Shale (Vshale)	0.070	0.077
Total Porosity (PHIT)	0.2226	0.2845
Effective Porosity (PHIE)	0.2065	0.2723
Water Saturation (SW)	0.0288	0.053
Hydrocarbon Saturation (Sh)	0.9712	0.947
Water Saturation in the Invaded/Flushed zone (Sxo)	0.0288	0.053
Bulk Volume Water (BVW)	0.0056	0.014

**Table 4.8: Average summary report on WABI 07 Well (Quantitative)**

<b>WABI 05 RESERVOIRS</b>	<b>RESERVOIR WABI A</b>	<b>RESERVOIR WABI B</b>
SAND TOP (M)	2915.26	3340.76
SAND BOTTOM (M)	2984.144	3429.61
Thinnest Interval Thickness (M)	5.79	19.51
Thickest Interval Thickness (M)	49.53	28.96
Gross Sand / Thickness (M)	68.88	88.85
Net Thickness (M)	65.68	48.46
Net to Gross (N / G)	0.954	0.545
Hydrocarbon Type	GAS / WATER	GAS / WATER
Fluid Contact	GWC @ 2931.9M	GWC @ 3365.1M
Volume of Shale (Vshale)	0.0452	0.0698
Total Porosity (PHIT)	0.4428	0.44
Effective Porosity (PHIE)	0.4397	0.43
Water Saturation (SW)	0.1661	0.1467
Hydrocarbon Saturation (Sh)	0.8339	0.8533
Water Saturation in the Invaded/Flushed zone (Sxo)	0.168	0.1491
Bulk Volume Water (BVW)	0.0734	0.0639

### 4.3 Seismic interpretation of Wabi field.

3D seismic vintage in Seg Y data format of this study area was among the data set collected from Total E&P Nigeria for review and interpretation. This seismic volume was QC/QA before It was loaded for detailed 3D seismic interpretations using the appropriate Geology and Geophysics (G&G) software, (i.e. Petrel) a ‘Schlumberger trademark’ for comprehensive seismic interpretation workflow, structural and stratigraphic interpretation. The generation of synthetic seismogram to determine the horizons or picks of interest to be interpreted on the seismic profile, fault and horizon interpretation, generation of depth converted contour maps and generation of structural model were carried out (Illo, 2015) as shown in **Figure 4.18a**. The 3D seismic interpretation of WABI field involved fault picking and correlation, which was done to establish the regional structural framework of the field. The seismic section is characterized by low to high amplitudes that continues and terminates at faulted zones. Two major faults and one minor fault were identified in Wabi as F1 and F2 **Figure 4.18b**. One of the main aims for this interpretation was to identify the stress regime existing in Wabi field based on normal, strike-slip and reverse (Anderson, 1951; Zoback, 2007) to know the appropriate model to be used for the estimation of in situ stress magnitudes and directions.

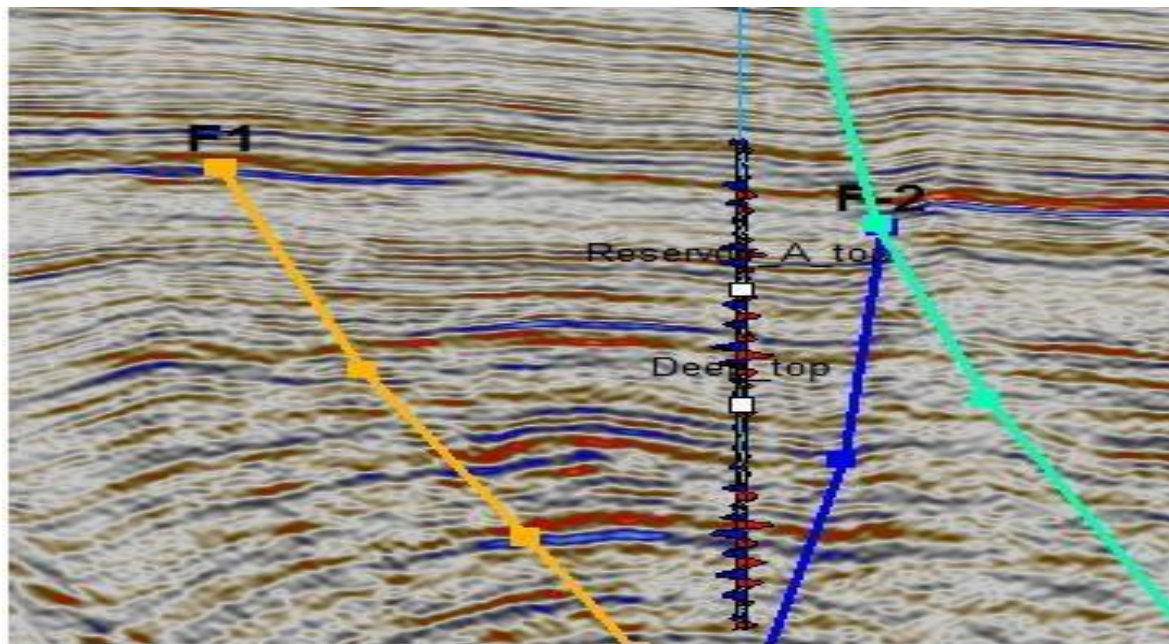


**Figure 4.18a.** Seismic section with Fault and Horizon interpretation on a scale of 1:25,000.

**Figure 4.18b** shows the structural fault system in the study area. These faults compartmentalized the reservoir into three blocks as block A, block B and block C. This block compartmentalization was also captured in time slice as shown in **Figure 4.19**. Block A does not have any well control and block C was not considered in this study because it is plagued with poor data quality. Therefore, the focus of this research is on block B which has four wells that has penetrated into it. The dominant structural trap style in Wabi field is the synthetic growth fault system (F1, F3, F4) with a subtle antithetic fault captured at down deep reservoir which localized within NE section of block B.

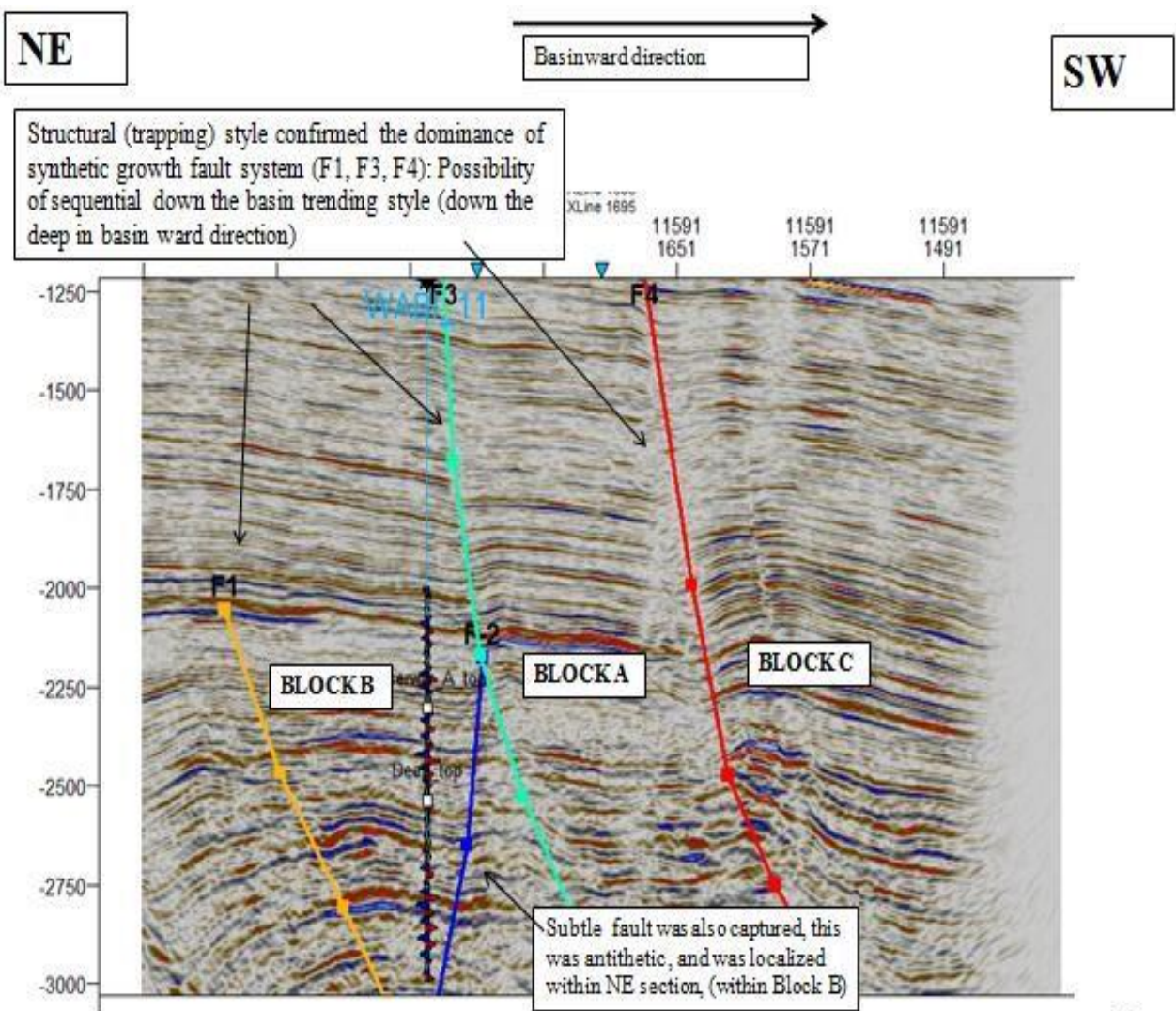


**Figure 4.18b.** Fault system of the field.

Growth fault is initiated by the rapid sand deposition along the Delta edge on top of under compacted clay. This resulted in the development of large number of syn-sedimentary gravitational faults. Growth faults tend to envelop local depocenters at their time of formation.

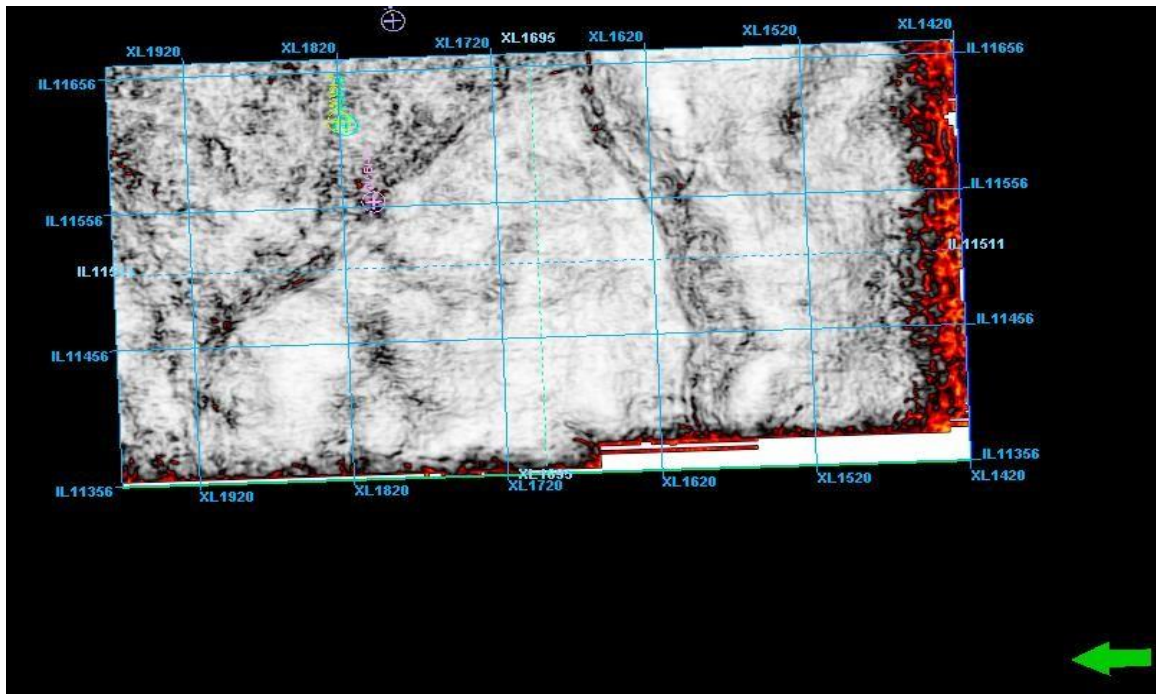


**Figure 4.19.** Wabi field broken into 3 major blocks (map captured at 2.212 sec).

#### 4.3.1 Time structural Map

Seed grid exercise was carried out for the chosen tops of the reservoir picked as shallow and deep. These pickings were used to generate a seed grid. The grid is the outcome of pickings done in both inline and cross line at 10 inline and cross line intervals which forms grids used for time structured map of Wabi field **Figure 4.20**. This structured map can be converted from time to depth map as seen in structural framework of the field through velocity modeling. Velocity modeling in this study employs two methods: the polynomial and the instantaneous velocity vs depth (i.e VoK). But the method with the least residual value was chosen for the conversion from time-depth map (Zorasi, 2017).

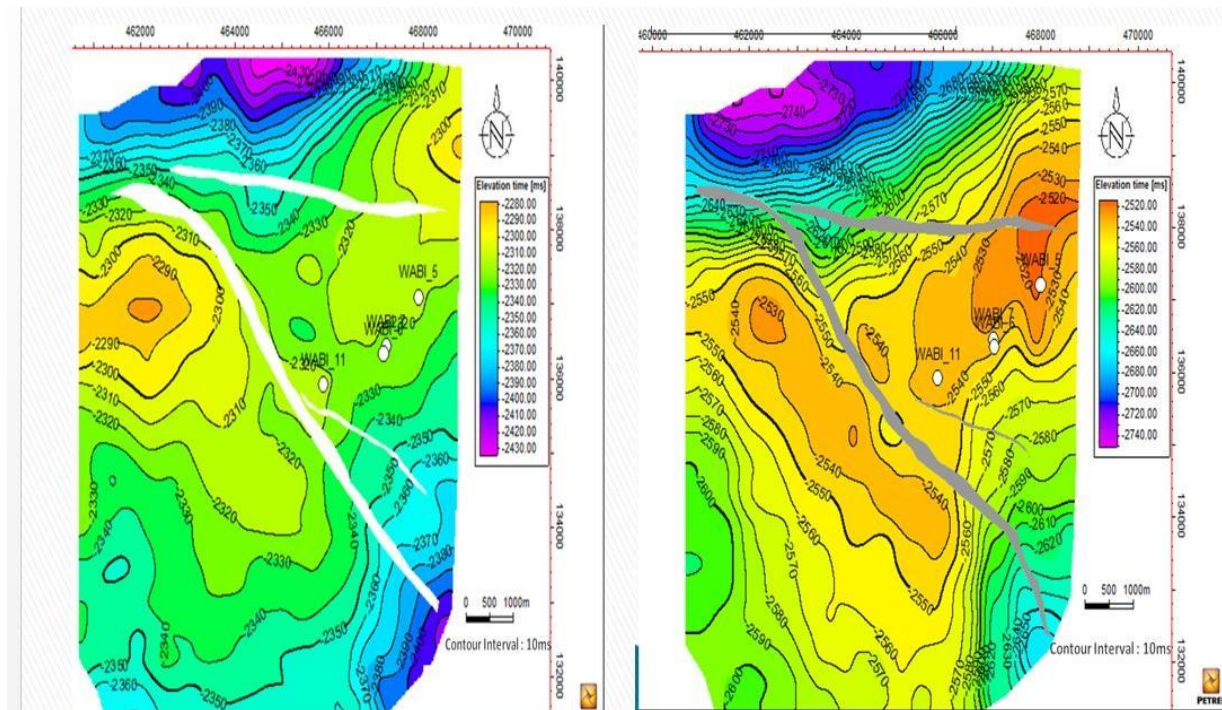


**Figure 4.20.** Time structural Maps for Shallow and Deep reservoir with interval of 10m

### 4.3.2 Structural Analysis

The structural interpretations done in this study were executed on 3D seismic volume where faults picked are intended to show the structural framework/pattern in Wabi field (Illo, 2015). Two major faults were picked, as shown in **Figures 4.21-4.22**. Structural modeling involves three operational phases. Static modeling entailed two approaches namely: structural and petrophysical modeling. The structural modeling entailed fault modeling, pillar gridding horizon layering and zonation. This is the first requirement for building a 3D model (Bessa, 2004). Fault modeling done in this research assured the compartmentalization of the reservoirs into two-unit blocks tagged as block A and blocks B, **Figure 4.18b**. The pillar gridding aided in the fragmentation of reservoir into unit cells denoted as (I J K) whose dimension are 50 m by 50 m by 0.6m **Figure 4.21**. This enables accurate scale sampling of the field. These three operations are integrated into one 3D model or grid which represents the structural framework (**Figure 4.22**) of the study intervals of interest upon which all other models could be built (Bessa, 2004).

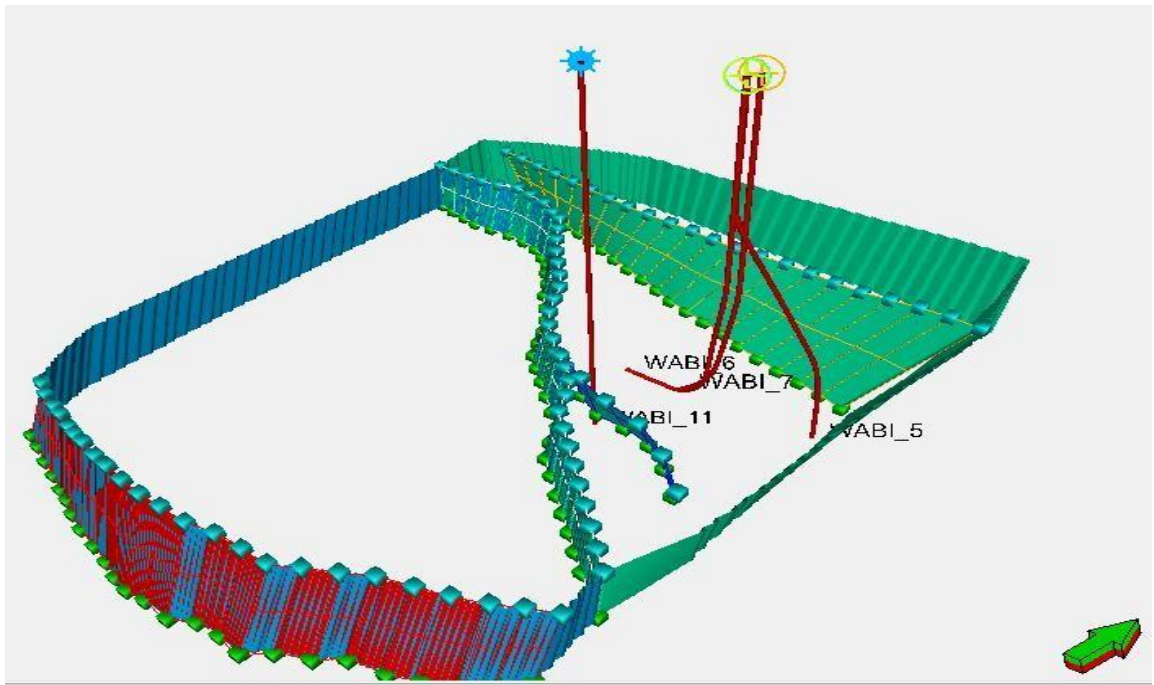


**Figure 4.21.** Pillar gridding of Wabi field showing well trajectories.

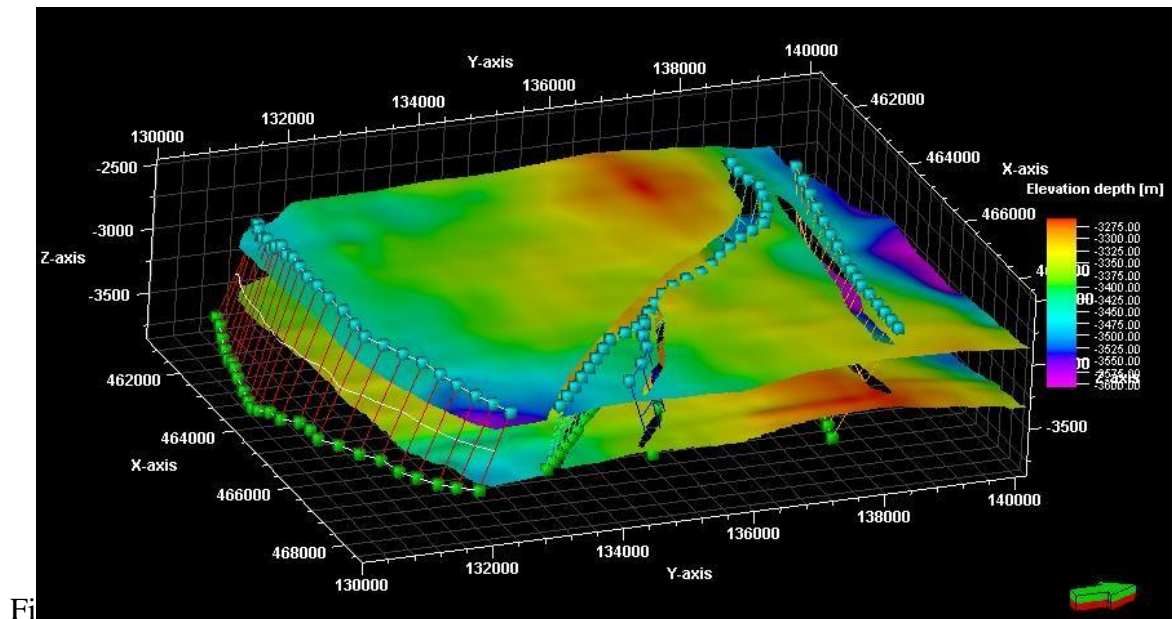


**Figure 4.22.** Structural framework.

#### 4.4 Stress distribution from geologic map of seismic section

The seismic section showing fault interpretation and structural map were used for the identification of stress regime in the Wabi field as normal faulting following the Andersonian classification of faults regime (Zoback, 2007). Therefore,  $S_v \geq S_H \geq S_h$ , this implies that the application of the Uniaxial Elastic –Strain Model for the field is valid. The type of growth fault found in Wabi field is known as antithetic growth which is associated with the detached stress regime (Bell, 1993). More importantly, stress regime may vary from bed to beds as reported by Warpinski (1989) whereas in some cases maximum and minimum horizontal stress measured in the same stress regime have shown approximately equal values (Avasthi *et al.*, 1991). Rosepiller (1979) studies confirmed that maximum horizontal stress is closer to minimum horizontal stress than to overburden stress due to ambiguity in unknown tensile strength in Cotton Valley East Texas. This is the discrepancies that may result in estimating stress regimes in this study (Bell, 1996), **Figure 4.23**. Therefore, it is advisable to use the geologic map of the study field to identify the appropriate regimes (Katahara, 1996). The tectonic setting, history and structural maps provided the insight of order of principal stresses.

##### 4.4.1 Stress directions

According to the work done by Abija and Tse (2016), using borehole breakout data and multiarm (4 and 6 arms) caliper logs from Wabi 10 and 11, shows the maximum horizontal stress is in the directions of ENE-WSW, NNW-SSW and NW-SE. These directions indicated the existence of multiple sources of stress in Wabi field. Adewole and Healy (2013) pointed out that Northern Niger delta is an inhomogeneous basin with different sources of stress. The direction of the maximum stress, ENE-WSW is orientated parallel to the fracture zone. Fractures are caused by tectonic stresses. The existing strike of the fractures normally coincides with the orientation of the faults in a region (Schlumberger, 1989), while the NE –SW is orientated towards the basin fault, known as the major lines of weak spot separating the North from South (Abija and Tse, 2016; Eze *et al.*, 2011). Hence, principal stress orientations are controlled by geological forces and anisotropy of rocks.

#### 4.4.2 Magnitudes of principal stresses

The principal stress magnitudes were estimated from petrophysical logs in this study using the UES model equation 3.24-3.26. The following parameters were the inputs required for the determination of vertical, maximum and minimum horizontal stresses; they are elastic constants, bulk density, Biot constant and pore pressure. Other relevant data to obtain these stresses were not given. Hence, stress magnitudes are only estimated values using geophysical logs. The first approach here was to know the stress regimes which have been demonstrated in *Section 4.3*. This was followed by the assumption that in a homogeneous and tectonically relaxed basin which the Niger Delta is one, the two principal horizontal stresses should be equal that is  $\sigma_2 = \sigma_3$  (Maleki *et al.*, 2014; Abdideh and Ahmadifar, 2013). But the presence of an active fault or tectonic activity invalidates the above assumption. Hence, both horizontal stresses will not be equal, and the tectonic term is required to be added to the UES model. The estimated magnitudes of the three principal stresses: overburden or vertical,  $S_v$  maximum or major  $S_H$  and minimum or minor  $S_h$  are shown in **Figures 4.23-4.24**. In some intervals they conform to the normal stress regime classification while in other cases there is stress anisotropy found from bed to bed caused by tectonic or other sources. This gives the significant differences observed in maximum and minimum horizontal stresses (Katahara, 1996). In the presence of tectonic stresses, to have an accurate stress profile, tectonic term  $\sigma_{tect}$  must be included or added to the conventional UES model (Song, 2012). The empirical relation for tectonic terms is given as:

$$\sigma_{tect} = S'_h - \frac{\nu}{1-\nu}(S_v - \alpha_{pp}) - \alpha_{pp} \quad (4.1)$$

Where  $S'_h$  is the measured minimum stress from closure pressure from testing analysis (Song, 2012). The tectonic term called tectonic stress can be computed by subtracting the estimated stress from petrophysical log and from the measured minor horizontal stress value. The shift in stress profile to match with the direct measured value can be express by the relation given by (Song, 2012) as follows:

$$S_h = \frac{\nu}{1-\nu}(S_v - \alpha_{pp}) + \alpha_{pp} + \sigma_{tect} \quad (4.2)$$

However, no Leak off test (LOT) or other means of direct measured minimum stress was given. Therefore, tectonic term was not used in the estimation. In summary, in-situ stress state is a paramount property of a rock for fracture design because it determines the mechanical failures of a wellbore and its evaluation is essential for injection or infill well drilling design and planning.

The maximum and minimum horizontal stresses are the intermediate and least stresses acting on the formation horizontally as confined stress/pressure. In other words, it defines the stiffness of the rock (Goodman, 1989). As the rock stiffness increases, horizontal stress reduces. Thus, it is known as a criterion of failure. In a normal faulting system, these stresses are orthogonal to each other (Economides and Nolte, 2000). The knowledge of these stresses is vital as they influence rock failure; especially, brittle materials fail due to the presence of stress.

The stress profile estimated and their model (Figures 4.23-4.24) shows that the stress at the intervals of shallow reservoir depth (3140 m to 3280 m) signifies that the vertical stress is greater than the maximum horizontal stress while the maximum horizontal stress in turn is greater than the minimum horizontal stress ( $\sigma_v > \sigma_H > \sigma_h$ ) (Zoback, 2007). This trend conforms with the normal fault regime described by Anderson 1951 and the deduction made from seismic interpretation also confirms the study area to be normal fault (Maleki *et al.*, 2014). However, at some intervals between 3230m to 3260m and 3605m to 3605m, the maximum horizontal and vertical stresses are equal  $\sigma_H = \sigma_v$  and maximum horizontal stress is greater than vertical stress  $\sigma_H > \sigma_v$  at down deep reservoir respectively due to mechanical anomalies in elastic properties of rocks (Bell, 1996) obtained from analysis of principal stresses.

The existence of wide variations in the present-day stress magnitudes and orientations at some intervals (beds) in Wabi field is as a result of the presence of anisotropy media (Kozloski *et al.*, 2011) caused by mechanical rock contrasts (Bell, 1996). Confining stresses (i.e. maximum and minimum horizontal) cause compression in a reservoir. This rock failure in tension or shear depends on the differential stress  $\Delta\sigma = \sigma_v - \sigma_h$ . Hence, low differential stress causes tensile failure while high differential stress causes shear failure (Wilson and Cosgrove, 1982).

It is obvious from the stress model that the stresses acting in Wabi field are not in equilibrium or hydrostatic state for example  $\sigma_v \neq \sigma_H \neq \sigma_h$  the balance of these stresses are caused by tensional or compressional. Therefore, when these in situ stresses are great enough and exceed the formation strength, the rock which they are acting on rupture (Wilson and Cosgrove, 1982). Rock fails as a result of multiple deep-seated processes taking place and not dependent on only a single dynamic action.

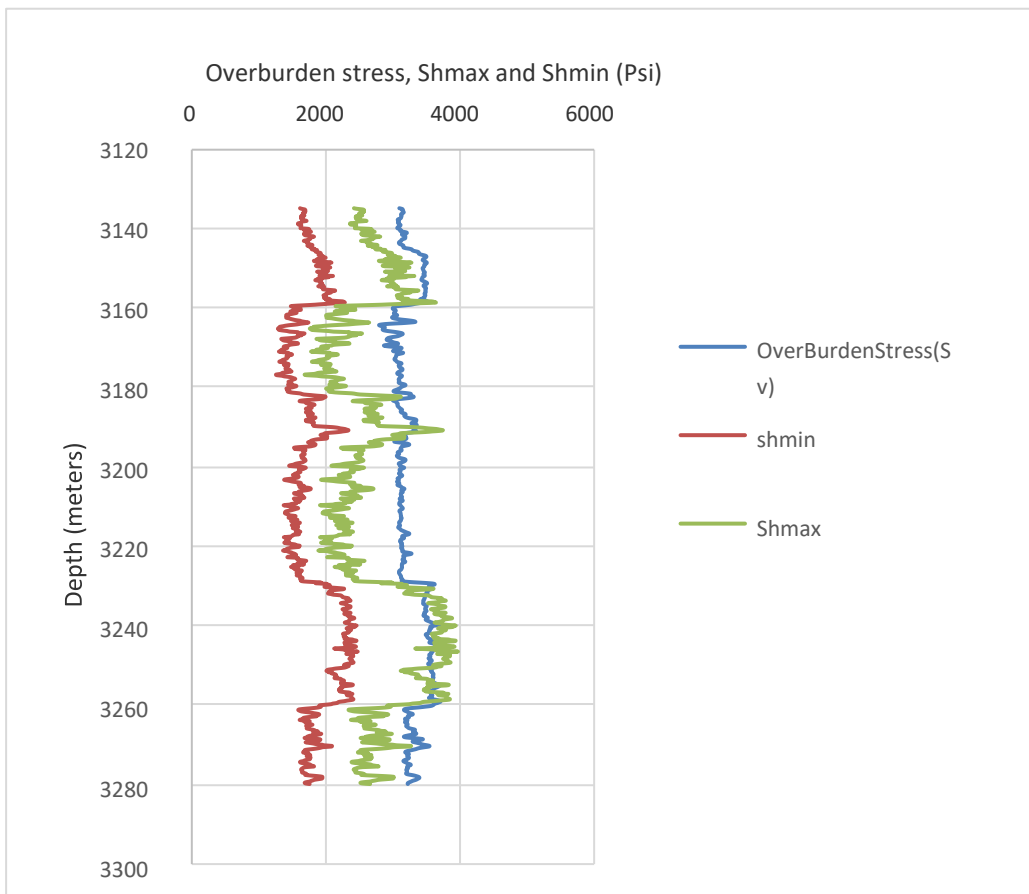


**Figure 4.23a.** Estimated stress profile model for Wabi 5 shallow reservoir.

where overburden stress is the effective stress  $\sigma_v$ ,  $Sh_{max}$  is maximum horizontal stress,  $Sh_{min}$  is minimum horizontal stress. The rock type in Wabi field is sand and shaly sand sequence.

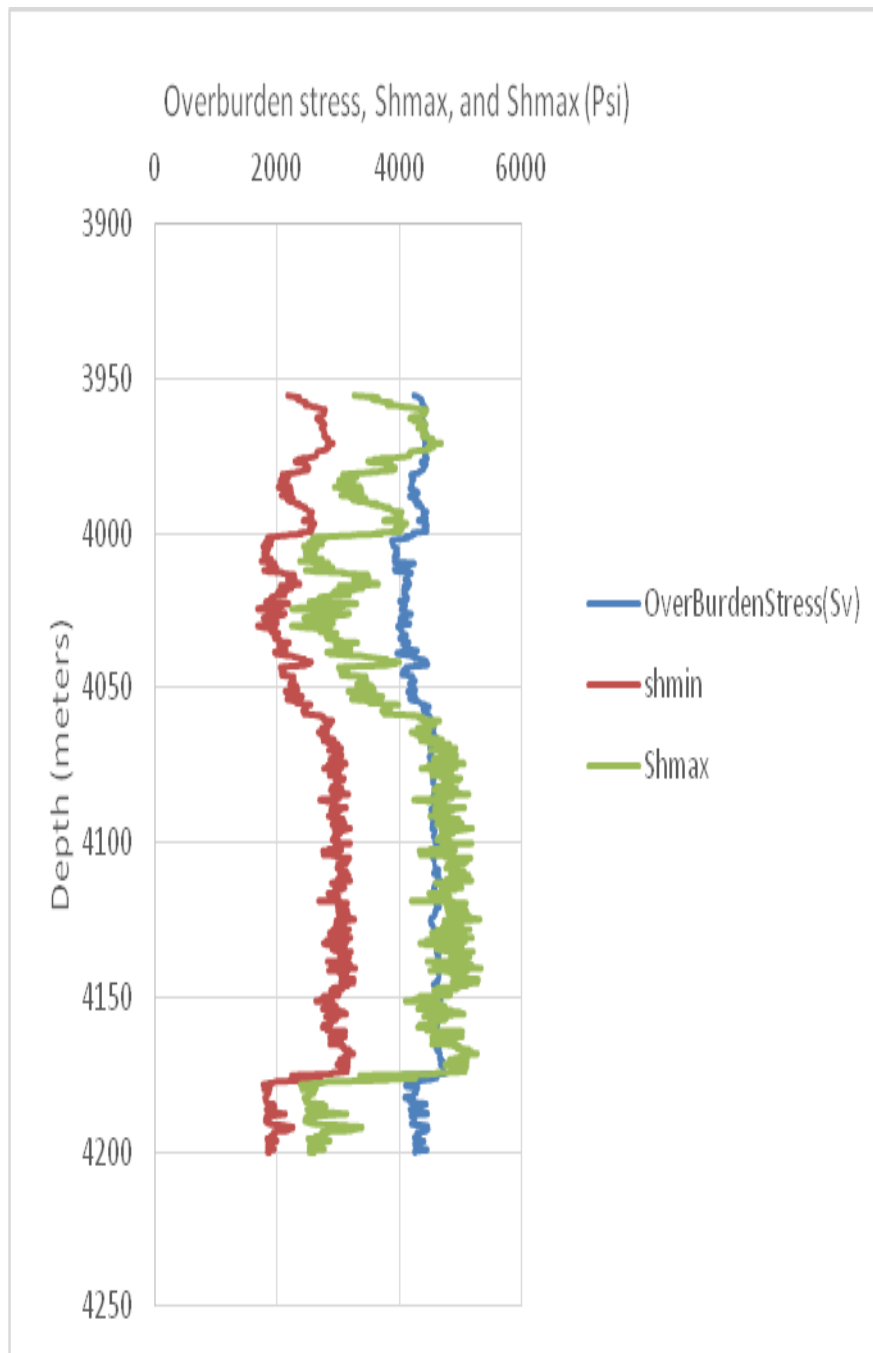


**Figure 4.23b.** Estimated stress profile model for Wabi 5 deep reservoir.

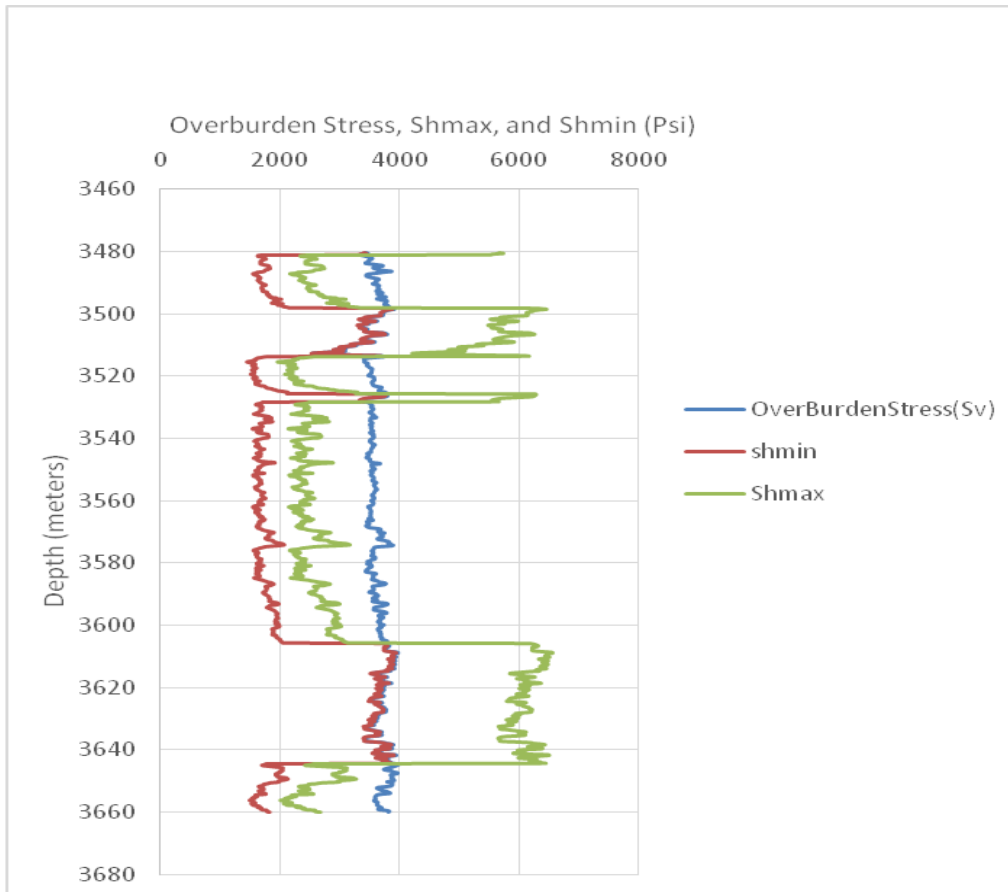


**Figure 4.24.** Estimated stress profile model for Wabi 11 reservoir.

where overburden stress is the effective stress  $\sigma_v$ ,  $Sh_{max}$  is maximum horizontal stress,  $Sh_{min}$  is minimum horizontal stress

#### 4.4.3 Pore pressure and overburden gradient

Fracture gradient, pore pressure and overburden stress gradient were computed using equations (3.29 -3.31). These are required parameters used for prediction of safe drilling mud weight window for well bore stability, completion and infill drilling operations (Zhang and Yin, 2017). **Figures 4.25-4.26** show the fracture gradient, pore pressure gradient and overburden gradient predicted for the study area. The equivalent mud weight used for drilling Wabi field as provided by oil servicing company tools Repeat formation tester RFT and drilling stem test DST ranges from 1.0516-1.366648 g/cm<sup>3</sup> and 1.04032-1.127057 g/cm<sup>3</sup>, respectively. Hence, the downhole mud weight must

be greater than the pore pressure gradient to avoid wellbore collapse, pressure kicks and fluid influx in the section of an open hole (Zhang and Yin, 2017). On the other hand, if the downhole mud weight is greater than the formation fracture gradient of the phase to be drilled, fracturing may occur, and this may lead to mud losses into the formation. The selection of downhole mud weight to be lower than a given threshold would result to shear failure and when it is higher than the higher threshold, tensile failure would occur (Zhang and Yin, 2017; Abdideh and Ahmadifar, 2013).

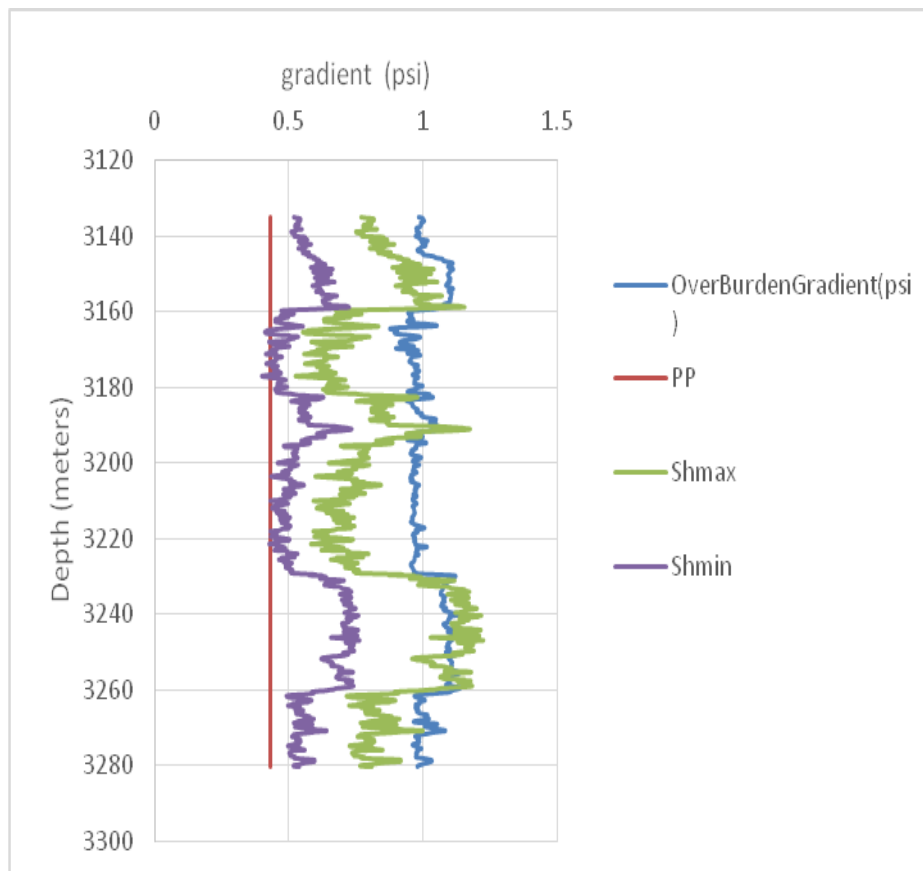


**Figure 4.25a.** Pore pressure gradient/stress gradient for Wabi 5 Shallow reservoir. where  $P_p$  is the formation's pore pressure

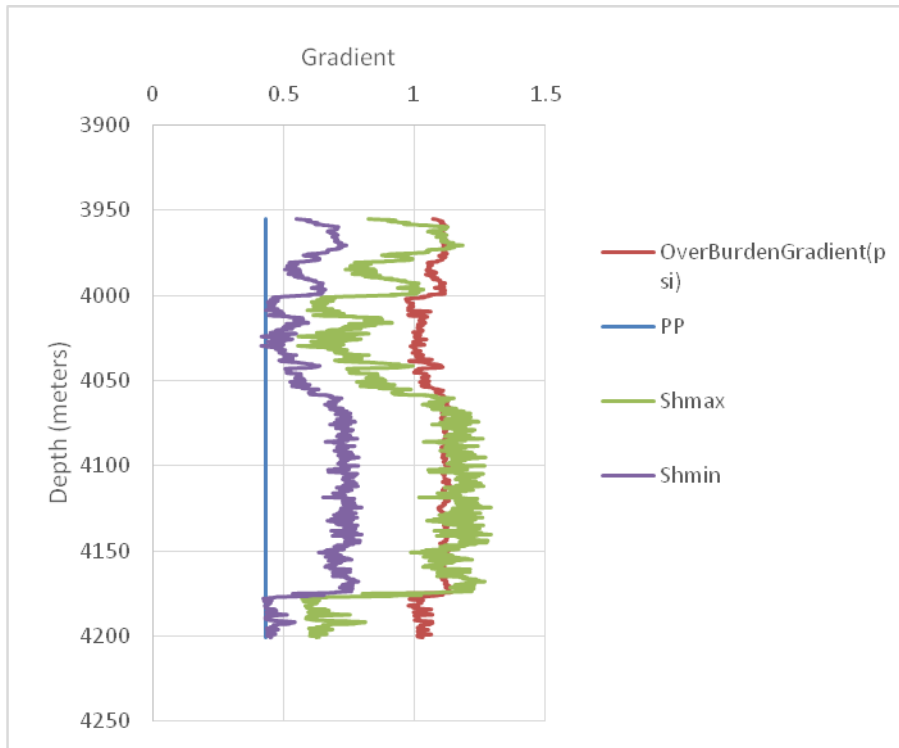


**Figure 4.25b.** Pore pressure gradient/stress gradient for Wabi 5 Deep reservoir.

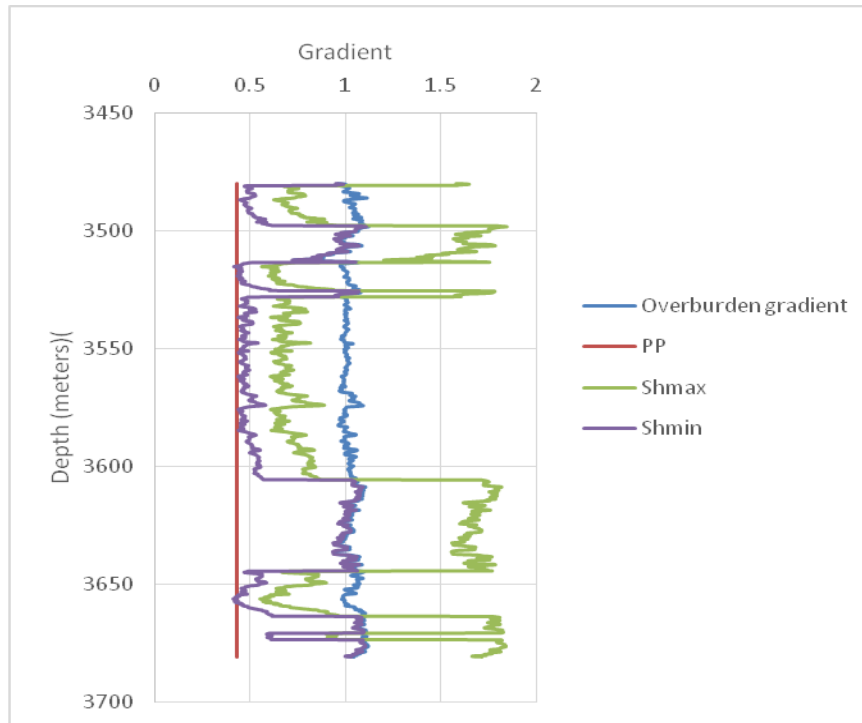


**Figure 4.26.** Pore pressure gradient/stress gradient for Wabi 11 reservoirs.

## 4.5 Mechanical properties estimation from well logs

The Mechanical properties of Wabi field were derived from Petrophysical logs. These properties are: Elastic constants (i.e Young's modulus, Shear modulus, Bulk modulus and Poisson's ratio), rock strength, pore pressure and in situ stresses. Relevant poroelastic empirical correlations were used for the estimation of these geomechanical parameters for Wabi field characterization, and development of oil and gas resources therein. These geomechanical parameters are function of acoustic measured compressional and shear velocities and density measurements in the formation of interest which are in turn used to compute Young's modulus and Poisson's ratio using dynamic elastic poroelastic equation (Fjaer *et al.*, 2008) for linear and quasi-elastic behavior of rock. These constants were then converted to static constant through the proposed relation by Seyed and Aghighi (2015).

### 4.5.1 Young's modulus of Wabi field

The transverse acoustic waves in the formation enable the measurements of both fast rate strain and small amplitude deformation incident. The measured modulus is known as Young's dynamic constant and it is measured in situ through the petrophysical tools under ambient temperature and pressure conditions. **Figures 4.27-4.28** shows the various calculated Young's modulus profile within the intervals of interest. In this study correlation proposed by Seyed Sajadi and Aghighi (2015) i.e  $E_s = (0.73 \times E_d - 2.2.337)$  and  $E_{s2} = 0.7 \times E_d$  were used to convert the dynamic to static Young's Modulus. Where  $E_s$  is static elastic and  $E_{s2}$  is second static elastic correction applied. A decrease in Young modulus is linked with deformation of the formation and an increase in the Young's modulus shows high or strong UCS. A rock remains unbroken as far as the deviatoric stress in the formation remains below yield stress/strength of the formation. But the rock deformed as far as the deviatoric stress is higher than the yield strength. Strong grain to grain bond depends on type of cementation materials (Goodman, 1989; Wilson and Cosgrove, 1982). The presence of significant clay content also increases the unconfined compressive strength in a sandstone formation whereas an increased siltstone and sandstone reduces the formation strength (Oluyemi, 2007).

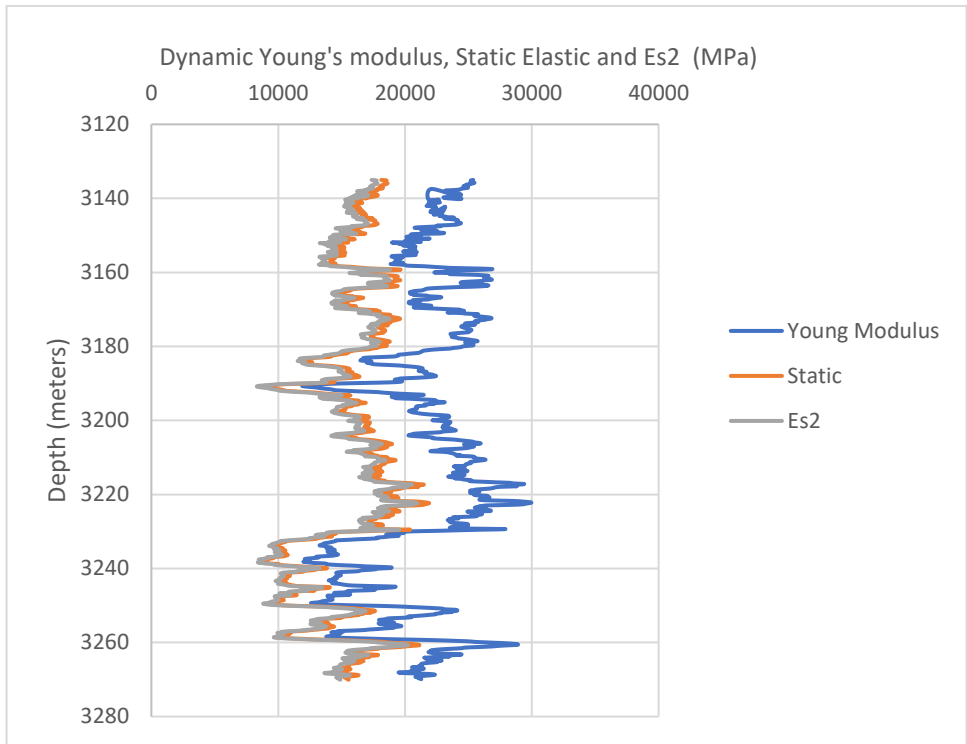


**Figure 4.27a.** UCS derived from Young's modulus for Wabi 5 Shallow reservoir.

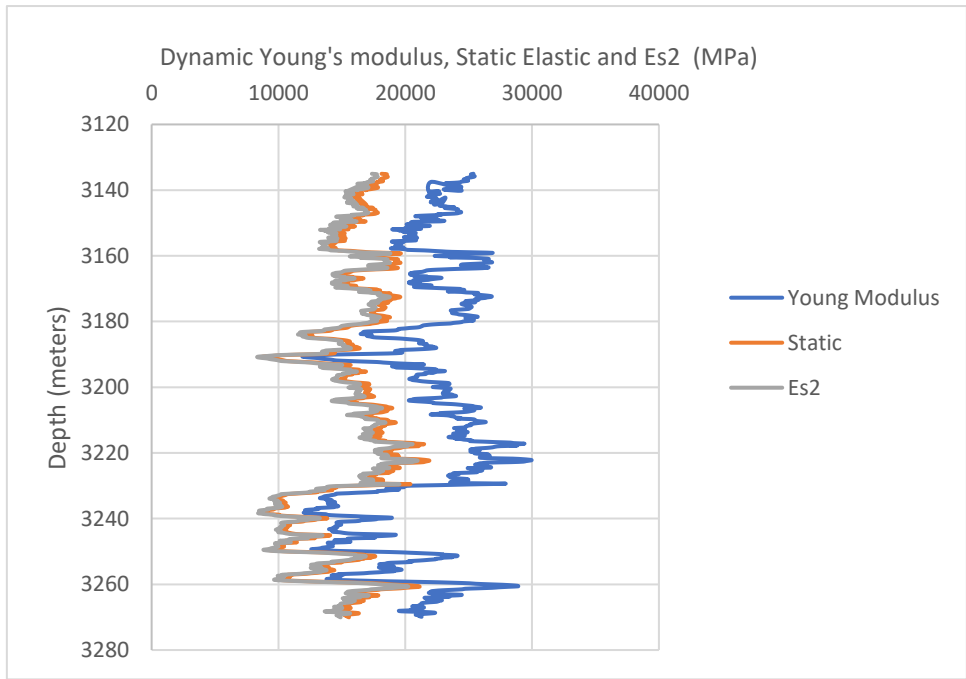


**Figure 4.27b.** UCS derived from Young's modulus for Wabi 5 deep reservoir.

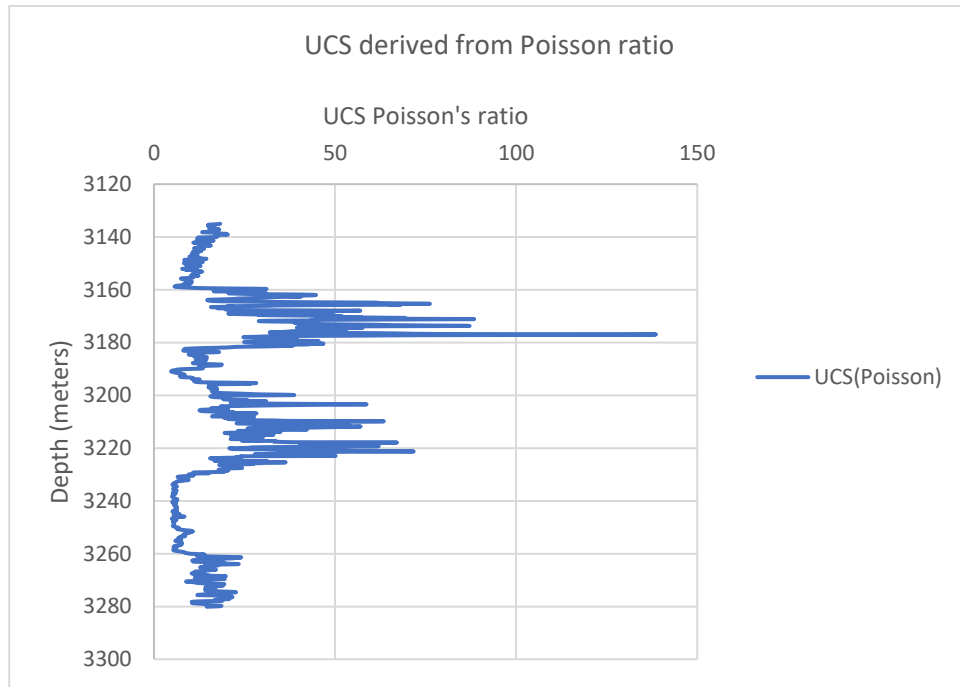


**Figure 4.28a.** UCS derived from Poisson’s ratio for Wabi 5 shallow reservoir.

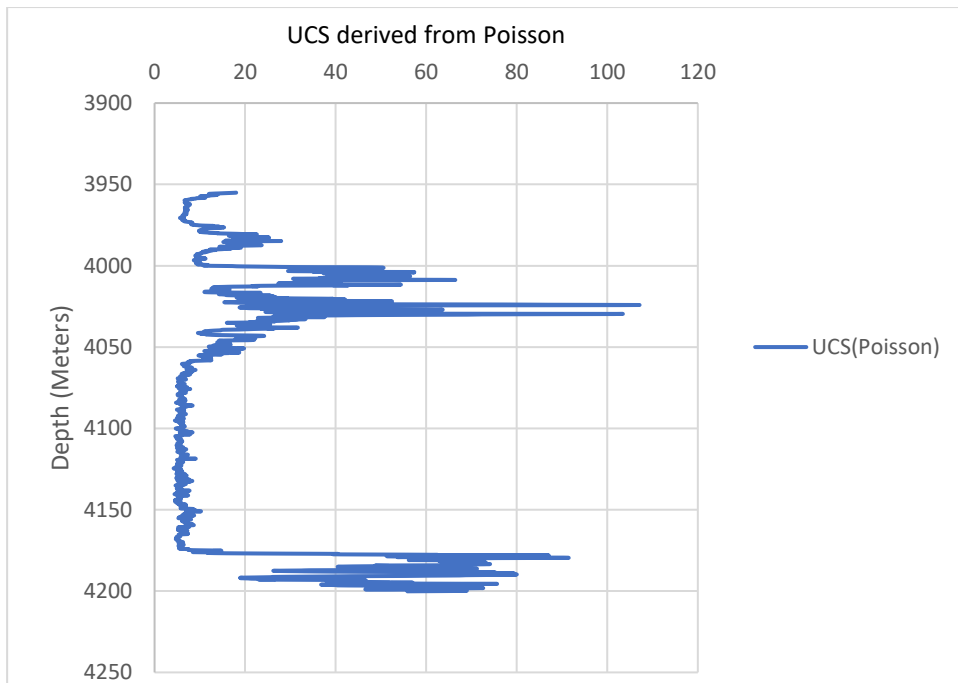


**Figure 4.28b.** UCS derived from Poisson’s ratio for Wabi 5 Deep reservoir.

#### 4.5.2 Poisson's ratio of Wabi field

Acoustic logs are displayed as slowness ( $\Delta t$ ) which is the reciprocal of velocity. Slowness of compressional is denoted as  $\Delta t_c$  and Slowness of shear wave denoted as  $\Delta t_s$ . The ratio of compressional and shear waves defines the Poisson's ratio ( $\nu$ ) and this ratio provides additional information about the formation's lithology. Poisson's ratio describes the ability of the formation's material to shorten parallel to overburden (vertical) stress with equivalent elongation in the minimum principal stress direction **Figures 4.29a-4.29b**. Poisson ( $\nu$ ) have values between 0.00 and 0.5. This implies that ( $\nu$ ) value range of 0.05 signifies very hard and rigid rocks and 0.45 for soft poorly consolidated rocks. Thus, high Poisson's ratio shows that the material is subject to deformation which results into volume change. Consequent to the above analysis of Poisson's ratio, the more ductile a material becomes the more its Poisson ratio will increase because of lateral expansion relative to longitudinal contractions and on the other hand, the more brittle a material becomes the less the Poisson ratio.

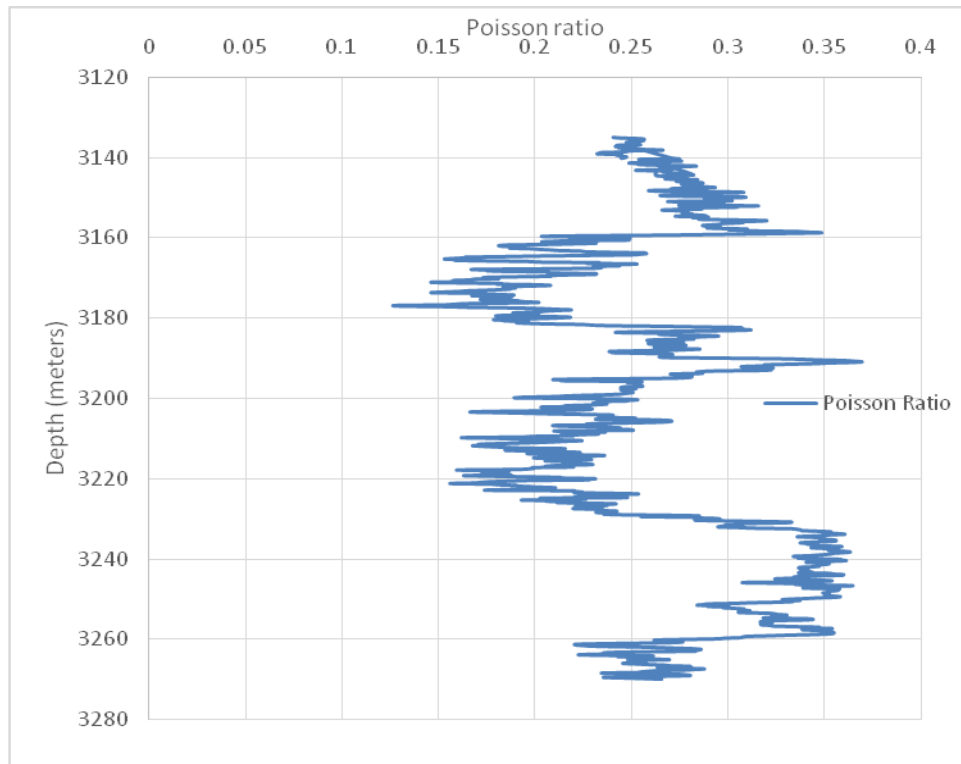


**Figure 4.29a.** Poisson's ratio in Wabi 5 for Shallow reservoir.

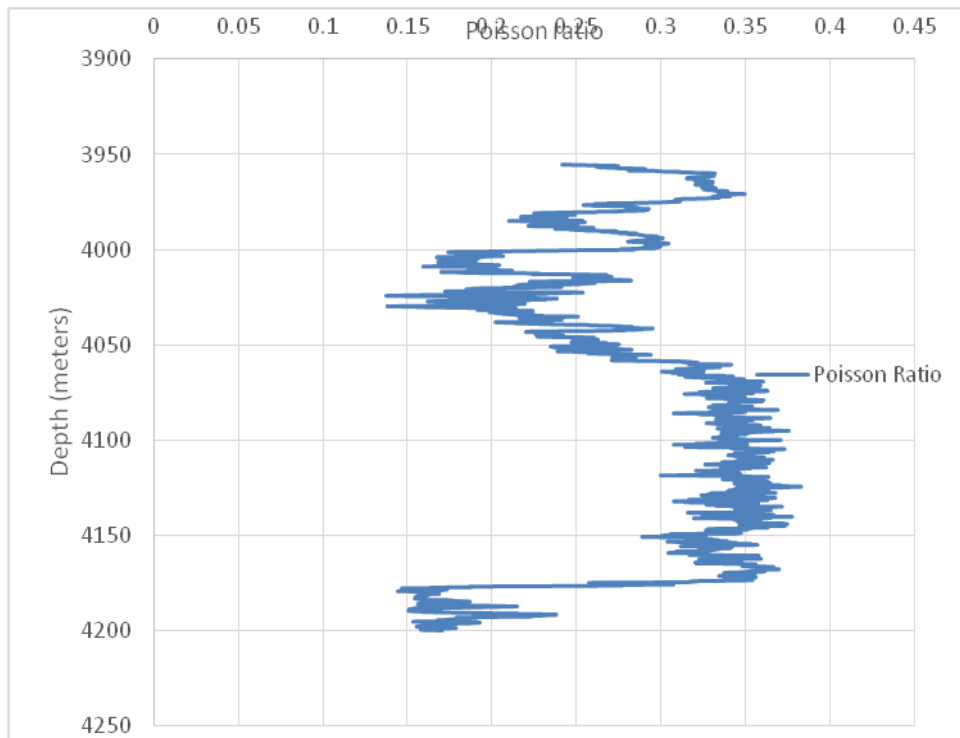


**Figure 4.29b.** Poisson's ratio in Wabi 5 for Deep reservoir.

For incompressible material,  $\nu$  is 0.5. This means that the minimum value of Poisson's ratio is 0.0 and its theoretical maximum is 0.5. Most rocks have a Poisson's ratio between 0.2-0.35 (Tiab and Donaldson, 2012; Jumikis, 1983). Thus, the reservoirs of interest have an average Poisson ratio between 0.18- 0.35 indicating moderate consolidation formation in the area of study. This result conforms with most sandstone formations in terms of Poisson's ratio.

#### **4.5.3 Unconfined compressional strength (UCS)**

The parameters used to obtain unconfined compressive strength (UCS) were derived from density and sonic log (i.e. compressional and shear wave velocities) using an empirical correlation for the computation of Poisson's ratio and dynamic Young's modulus (Najibi *et al.*, 2017). The dynamic young's modulus is converted to static constants to obtain a continuous UCS of Wabi field. Three empirical relations derived for the Niger delta basin which permits the use of Young's modulus value, Poisson's ratio and compressional transit time or velocity were adopted from the studies of Salawu, Sanaee and Onabanjo (2017) for the determination of UCS.

The application of the Young's modulus values to estimate UCS gives a better estimate of the rock strength, because its dynamic values were converted to static value, **Figures 4.27-4.28**. The application of slowness ( $\Delta_{tc}$ ) with values greater than 100  $\mu\text{s}/\text{ft}$  or low velocities  $V_p < 3000 \text{ m}/\text{s}$  for the estimation of unconfined compressive strength gives a lower result meaning that it under predict the UCS. The above velocity is an indication of a poorly (weak) sedimentary rock (Chang, Zoback and Khaksar, 2006). Although, the transit time derived equation for the Niger delta values were not used in this study. Finally, the application of Poisson's ratio for the estimation of UCS of Wabi field gives a relatively good UCS, **Figure 4.29**.

#### **4.5.4 Influence of rock strength**

Wabi formation of interest with high  $K_o$  value that is, the coefficient of earth pressure at rest which varies with depth indicates stiff layers with concentration of stress and low value indicates soft layers that have more strain (deformation). The use of  $K_o$  is applicable only when there is no lateral compliance/compaction (Jones *et al.*, 1992).

The porosity of Wabi field within the reservoir intervals are summarized in **Tables 4.2-4.8**. High porous formation with porosity values of 45-35% reduces the young's modulus (Herwanger and Koutsabeloulis, 2011). Thus, intervals with high porosities are soft formation and are prone to reservoir compaction during the productive stage of the field's life. In these intervals the ratio between dynamic to static elastic young's modulus is high. Hence, sand control program should be designed to mitigate this geomechanical problem from cutting down only production which may eventually lead to loss of the wells (Herwanger and Koutsabeloulis, 2011). Pressure maintenance should be anticipated to reinstate reservoir compaction caused by depletion or pressure drawdown. For low porosity intervals, the observed difference between the dynamic to static elastic is negligible.

#### **4.5.5 Fracture and Fault stability Analysis**

Most formations in the crustal region of the vertical composition of the earth contain several structural imperfections and a number of planes of weaknesses known as rock defects (Jumikis, 1983). Rock formations are therefore prevented from exhibiting perfect elasticity due to the

presence of these rock defects. Therefore, rocks are often characterized to be inelastic. According to the work of Morris, Ferrill and Henderson (2014) defined slip tendency as surface that may fault, fracture or rupture in a stress field and relate it to the ratio of shear stress to the normal stress including the orientation of the maximum determined shear stress. They summarized that slip occurs on pre-existing fracture and fault plane when the determined shear stress equals or exceeds the frictional resistance to sliding (i.e. shear strength).

#### 4.5.6 3D Mohr Analytical diagram

Accurate assessment of the orientation of faults, fracture and failure envelope of Wabi field depends on the magnitude of the in situ stress state for fault reactivation and possible breach of cap rock integrity (Adewole, 2013). This analysis involves the computation of the shear and normal stresses acting on an arbitrary oriented faults in 3D (Zoback, 2007). To address this geometrical problem, it should be noted that the directions of the three principal stresses are not aligned normally to our North-East down coordinate system (Schmitt, 2014; Allmendinger *et al.*, 2012) where these stress state can be resolved into a vector acting on the plane of weakness. One of the simplest approaches to solving this problem is the utilization of 3D Mohr diagram, refer **Appendices (A-B)**. The 3D Mohr diagram is valuable for representing fault stability in the subsurface formation (Zoback, 2007). In this study, the values of the average three principal stresses in descending order of magnitude,  $\sigma_1, \sigma_2$  and  $\sigma_3$  were used to determine the 3D Mohr circles (Zoback, 2007). Faults are represented by a point, situated in the space between  $\sigma_1$  and  $\sigma_2$  and  $\sigma_2$  and  $\sigma_3$  of the smaller Mohr circle defined as the differential stress or deviatoric stress  $\Delta\sigma$  **Appendix (A and B)**, and the greater Mohr circle is defined by the difference between  $\sigma_1$  and  $\sigma_3$ . Also, from this 3D Mohr circle diagram, the shear stress can be determined.

According to Bell (1996) and Schmitt (2014), dry rock fails according to the proposed Mohr Coulomb criterion equation. But in the subsurface our formation rock is porous in the reservoir intervals and contains pore fluids. Therefore, the failure criterion in this case differs from that of the dry rock. The Terzaghi equation for effective stress is very crucial in the explanation of pore

pressure and effective stress for the analysis of rock failure (Schmitt, 2014). The principal stresses must be replaced by effective stress (Twiss and Moores, 1992; Schmitt, 2014; Bell, 1996) as:

$$\sigma_{eff} = (\sigma_i - P_p)$$

where, the subscript i, is overburden stress, maximum horizontal (H) or Minimum horizontal stress (h),  $\sigma_{eff}$  is the effective stress and  $P_p$  is the pore fluid pressure.

It is obvious that most formations in the crust are already wrecked and exhibit available plane of weakness that support slip and ruptures if the appropriate conditions are in place. **Appendices (A-B)** show shallow and deep reservoirs of Wabi 05. Appendices (a) and (b) represent the undisturbed or virgin state of the effective stress before pore fluid pressure is agitated (Schmitt, 2014). The 3D Mohr diagram and its failure envelope represent the potential plane of weakness in differing orientations for the field of study. For convenience, we assume that cohesion C is approximately zero because as sliding occurs, it vanishes (Timmerman, 1982; Schmitt, 2014). Exploitation of hydrocarbon from Wabi field overtime would induce changes in the formation pore pressure which resulted in depletion of the reservoir pressure. This decrease reduces the impact of slip in the formation of interest. Thus, it caused the virgin stress state of the Mohr circle at hydrostatic state to be shifted to the right (i.e. away from the failure envelope) leading to reservoir compaction due to the consequences of large effective stress alternation (Schmitt, 2014; Nacht *et al.*, 2010). It is important to note that this does not affect cohesion rather it affects only the rock frictional strength by reduction and subject the formation to be weaker (Zoback, 2007). The continuous modification of the stress state by decrease in pore fluid pressure keeps Wabi field formation stronger (Schmitt, 2014).

On the other hand, when enhancement recovery injection of fluid is done, hence, increasing the pore fluid pressure which decreases the effective normal stresses of the formation on the fault plane and resulted or culminated in shifting of the virgin state of the Mohr circle to the left (Bell, 1996; Schmitt, 2014). As the formation pore pressure keeps increasing due to injection of fluid and necessitates further shifting of the Mohr circle to the left till it intercept the failure envelope of the rock mass when slip or the rock fail under favorable conditions (i.e. fault reactivation on pre-existing fault plane) (Schmitt, 2014; Nacht *et al.*, 2010; Streit and Hillis, 2004; Bell, 1996). The

point at which the shifted Mohr circle touches the failure line, the shear strength and shear stress of the formation are equal (minimum). This point is known as the plane of maximum obliquity (Zoback, 2007). Thus, two zones are demarcated from the failure line as unstable and stable zone. If the combination of the effective normal and shear stresses falls under the failure line, then the formation is stable, and the shear strength of the formation is greater than the shear stress of the formation (Jaeger, Cook and Zimmerman, 2007). But when the plot of effective normal stresses and shear stresses exceeds the failure envelope, the shear strength of the rock is lesser than the shear stress and the rock mass fail or slip. This analysis is known as the slip tendency analysis (Morris, Ferill and Henderson, 2014; Streit and Hillis, 2004). The failure line properties (i.e cohesion  $C$  and frictional angle  $\phi$ ) when varied update all available display interactively on the Mohr circle (Twiss and Moores, 1992) and describe rock stability and instability.

## CHAPTER 5

### Summary, Conclusion and Recommendations

#### 5.1 Summary of Research

This chapter summarizes and concludes the entire investigations carried out and recommends areas for further studies to be executed to have good petrophysical and geomechanical representation of Wabi field. Also, some mitigation strategies are mentioned to avoid severe damage that could be caused by sand production in the future of the field.

The Niger Delta is an unconsolidated formation with naturally fractured reservoirs cause by loose sands. These have posed major challenges for operators both multinational and indigenous companies in developing their reserves. This unconsolidation also affects drilling, completion, production and enhancement programmes. Therefore, the need to understand this naturally fracture reservoir is one of the reasons that necessitated this research to look out the geomechanical properties of Wabi field.

The field of study is a mature brown onshore field located at North-West of Port Harcourt, Rivers State, Nigeria. The motivation for this study is sequel to the call by the Federal Government of Nigeria for release and allocation of Marginal fields to indigenous oil and gas Companies. The meanings of Marginal field and its characteristics have been detailed in previous chapter 1. The operator of this field concluded to farm into this block for hydrocarbon potential evaluation and to evaluate any possible geomechanical related issues the field may have for its upgrading and development. This anticipation was made to boost the Nigerian economy and increasing energy supply needed across the country.

This study adopted empirical correlations and best company practices for the investigation of the study area. The following data set (i.e. Petrophysical wireline logs, Seismic data, DST/RFT, core picture from Wabi) were collected for the Petrophysical and Geomechanical analyses for risk assessment to enable mitigation strategy design for Wabi field. The elastic properties of reservoir rocks derived from log data were bulk modulus ( $K_b$ ), shear modulus ( $G$ ) and Poisson's ratio ( $\nu$ ). Young modulus ( $E$ ) is subsequently, evaluated from shear modulus and Poisson's ratio. The

strength of the reservoir rock was expressed in terms of Uniaxial compressive strength (UCS) through a calibration with core laboratory.

Good knowledge of the mechanical properties of reservoir rocks is an important component of pre-production investigations for both reservoirs. This would facilitate the design and implementation of an economic development program for Wabi field. Consequently, this research provides an understanding of Wabi reservoir description for optimal development plan and management.

The mechanical properties log provides a quantitative means for identifying sands that are strong enough to produce oil and gas without any form of sand control. The method is based on a correction of in situ strength with the dynamic elastic moduli computed from sonic and density logs. The assumption made in this study was that the reservoir rock is isotropic this implies that the material exhibits a perfectly linear stress-strain relationship.

## **5.2 Conclusion**

The ultimate objective of this research was to have detailed Petrophysical and Geomechanical characterization of Wabi field in the Niger Delta province for hydrocarbon potential determination and geomechanical related problems which include in-situ rock stress, modulus of elasticity, formation porosity, leak off coefficient and Poisson's ratio determination to ensure that proper well planning/stable wellbore is achieved while we explore for more hydrocarbon reserves for commercial exploitation. This study helps to mitigate against reservoir reactivation for injection project and management of reservoir compaction and subsidence which could occur as we produce from the reservoirs.

Table 4.2-4.8 shows the summary of Petrophysical analyses carried out in Wabi field. Table 4.2 showed the identification of reservoirs intervals from Top to bottom known as the reservoir thickness. Tables 4.3-4.4 showed the type of hydrocarbon fluid identified and their contacts levels between gas and water (GWC), gas and oil contact (GOC) and oil water contacts. Table 4.5 showed various petrophysical properties these include reservoir thickness (net pay sand), net to gross,

hydrocarbon types, fluid contact, sand top and bottom, gross sand thickness, volume of shale, porosity, effective porosity, water saturation, hydrocarbon, bulk volume water.

Wabi 5 well had average net sand thickness of 64.39m and 43.05m, effective porosity of 0.34 to 0.269, water saturation 0.231 and 0.117 and hydrocarbon saturation of 0.769 and 0.883 for shallow and deeper reservoir. Low water saturation means that the reservoir has more hydrocarbon in place. The hydrocarbon present in Wabi 5 is Gas. Wabi 11 had average net sand thickness of 58.60m and 64.47m for shallow and deeper reservoir, effective porosity of 0.2411 and 0.343, water saturation of 0.167 and 0.076 hydrocarbon saturation 0.833 and 0.924. Hydrocarbon type is Gas. Wabi 6 had average net thickness of 103.86m and 20.19m, effective porosity 0.2065 and 0.2723, water saturation 0.0288 and 0.053 and hydrocarbon saturation 0.9712 and 0.947. Wabi 7 had net sand thickness of 65.68m and 48.46m, effective porosity of 0.4397 and 0.43, water saturation of saturation 0.1661 and 0.1467 and hydrocarbon saturation as 0.8339 and 0.8533. Hydrocarbon type Gas.

Consequently, Wabi field has good reservoir quality for oil and gas production. The field is identified as a gas field and production of gas from all wells could be harmonize to production manifold for subsequent transportation to various customers such as Nigeria Liquefied Natural Gas (NLNG), Indorama, and Gas turbine stations) that need it for sale and power supply. In terms of the first well to be produced, the asset manager would start with reservoirs with the highest reserves and has huge thickness before producing from the reservoir with lower reserves (i.e Wabi 06,07,05 and 11) respectively is the order of producing if commingling is not allowed by DPR.

In order to address the aim and objectives of geomechanical characterization, two reservoir intervals were picked at each well and from a total of four wells drilled in Wabi field. These wells are: Wabi 5, Wabi 6, Wabi 7 and Wabi 11. The petrophysical analyses at the reservoir intervals ranges from top to bottom as follows: 3158.795 m - 3228.899 m, 4000.04 m - 4045.763 m, 3887.862 m - 3997.286 m, 4053.216 m - 4078.972 m, 2915.26 m - 2984.144 m, 3340.76 m - 3429.61 m, 288.661 m 2962.185 m, 3513.263 m – 3591.597 m, respectively. The reservoir qualities in terms of the total and effective porosity were as follows: 0.358-0.340 and 0.288- 0.269, 0.2226 – 0.2065 and 0.2723- 0.053, 0.4428 -0.4397 and 0.44-0.43, and 0.419-0.2411 and 0.273-0.343, respectively. These porosities are good for storage and transmissivity of hydrocarbon. Also,

the hydrocarbon saturation for the respective intervals are 0.769 and 0.883, 0.9712 and 0.947, 0.8339 and 0.8533 and 0.833 and 0.924. These intervals are good for shallow reservoir development because of the significant volume of hydrocarbon estimated therein.

Only two wells were used for the geomechanical properties investigation of Wabi field because of the availability of sonic log in them, these were Wabi 5 and Wabi 11). However, the sonic  $V_p$  modeled log for Wabi 11 showed errors within the intervals of interest, therefore only Wabi 5 and few sections of Wabi 11 results are displayed in this study. The intervals considered for Geomechanical rock properties of Wabi field ranges from 3160 m - 3230 m, 4000 m – 4050 m and 3510 m – 3650 m for Wabi 5 and 11, respectively.

Young's moduli (E) of the field are 23199.21 Psi, 33679.68 Psi, and 24.87 Psi while UCS ranging between 23153.00 Psi, 33053.69 Psi. UCS derived from Poisson's ratio is 29.90 Psi, 28.650 Psi and 31.31.59 Psi. The UCS obtained with Young modulus parameter showed that the rock formation has the capacity to withstand external forces and shown high strength against rock failure. Poisson's average ratio ranges between 0.2258, 0.21570 and 0.29935 meaning that, there is small variation in volume of rock. Hence, this study shows Poisson's ratio of 0.18- 0.35 which indicates that the reservoir is stable.

The studied reservoirs show high porosity with poor cementation this signifies its vulnerability to deformation. Although, it is in the consolidated region in the Niger Delta. Therefore, the ratio of dynamic to elastic constant, that is, Young's modulus constant is between 10 MPa to 20 MPa. It is obvious that, rock strength decreases with increasing porosity with variation in  $C_0$  between porosity of 30-35%.

For pore pressure prognosis in case of drilling further wells in Wabi field, the mud window for the field can be designed since the drilling equivalent mud weight ranges between 1.05163 g/cm<sup>3</sup>- 1.366642 g/cm<sup>3</sup> and 1.010686 g/cm<sup>3</sup>-1.127057 g/cm<sup>3</sup>. Mud weight must be greater than the pore pressure gradient and less than the fracture gradient for the avoidance of wellbore instability, fluid influx and pressure kicks in an open hole drilled.

From this study, the average in situ stress principal stresses are:  $\sigma_1 = 3112.65$  Psi,  $\sigma_2 = 2356.63$  Psi,  $\sigma_3 = 1607.80$  Psi in shallow reservoir and in deep reservoir;  $\sigma_1 = 4409.29$  Psi,  $\sigma_2 = 4115.27$  Psi,

$\sigma_3 = 2639.04$  for Wabi 5. While for Wabi 11 they are;  $\sigma_1 = 3617.90$  Psi,  $\sigma_2 = 3709.42$  Psi,  $\sigma_3 = 2375.85$  Psi. These in situ stress trends indicated normal faulting regime in Wabi field, however, rock anisotropy exists in some parts of the reservoir thereby causes different stress regime existence. Where any small difference between  $\sigma_3$  and  $\sigma_2$  will affect stress orientation and fracture propagation design in Wabi field, if the need arises. The estimated hydrostatic pressure  $P_P$  are; 1384.37 Psi, 1732.95 Psi and 1520.68 Psi.

The estimated principal stresses and pore pressures above were used to construct 3D Mohr diagram for Wabi field. The Mohr diagram for the interval of interest at hydrostatic pressure indicated that the reservoirs are stable as the combined normal effective and shear stresses are below the failure envelope, but as exploitation activities progresses, it would reduce the effective stress and the reservoir would be compacted leading to subsidence. On the other hand, increasing pore fluid pressure by injection of fluid would cause fault reactivation and fracturing of the reservoirs at both chosen depth as shown in 3D Mohr diagram for this study (Appendices A-B).

The estimation of the mechanical behavior of the rock mass was done to understand the formation's properties to mitigate what will cause risk to Wabi reservoir either during exploitation or recovery phases. This is essential for stimulation and completion design to prevent fault reactivation, fracturing of the reservoir and subsidence.

Addressing the technical challenges that would be faced for development of Marginal and Brownfield in the Niger Delta and elsewhere requires a generic workflow and integrated solution as demonstrated in this study. Therefore, geomechanical analysis play an important role in a field life spanning from exploration, appraisal, and development to production of hydrocarbon to prevent the risks and boost daily crude production required in our today's energy demand.

In summary, the followings conclusions are made: Wabi field has pockets of potential hydrocarbon reserves at different intervals with good reservoir qualities to enhance its development for production. Also, rock strength estimation in this field shows that the reservoir is stable; however, production of hydrocarbon from these zones may lead to subsidence in the future. To mitigate for this futuristic event reservoir pressure maintenance should be planned for.

### 5.3 Recommendations

After a careful study and analysis of data collected, the following recommendations are made:

1. Active sand control methods such as screens, slotted liners and gravel pack completion designed is recommended for the study area.
2. Proper pressure maintenance should be planned for the longevity of the reservoir.
3. Lack of appropriate data from Oil and Gas industry is highly needed to better understand the phenomena that may trigger or induce Seismicity or subsidence in the study area.
4. Fracture data from Wabi field alongside rock mechanical properties from Laboratory testing should be used for the construction of the 3D Mohr diagram and compare with the model obtained in this study.
5. The results presented in this study were based on log derived, to serve as representative values of the geomechanical properties of the field. Thus, further studies should be conducted in the area using laboratory core testing for geomechanical properties to validate results.
6. More information from exploration to development phases of the reservoirs are needed as major input to understand the physics and geomechanics of the in-situ stresses for reappraisal, well completion, and accurate predictive model and for development strategy.
7. Pressure information from leak of test (LOT), mini and micro fracture test from Wabi field should be used to validate the result in this study.
8. Type of drilling fluid used for Wabi field drilling should be specified for its usage for further analysis of stress effect.
9. This study focuses on macro-mechanical rock properties of Wabi field; therefore, further studies should be conducted on micromechanical properties as this may focus more on the initiation and propagation of failure or fracture in Wabi field.
10. Also, further studies should be carried out in respect to temperature conditions of the field and its effect on the rock properties.
11. Finally, to predict real time sanding issue in the field, simulation study must be done. This is what my PhD research will be focusing on.

## REFERENCES

- AADNOY, B.S. and LOOYEH, R., 2011. *Petroleum rock mechanics. drilling operations and well design*. Elsevier, Amsterdam: Gulf Professional Publishing.
- ABDIDEH, M. and AHMADITFAR, A., 2013. Predication of geomechanical modeling and selection of suitable layer for hydraulic fracturing operation in oil reservoir (South West of Iran). *European Journal of Environmental and Civil Engineering*.
- ABDIDEH, M. and FATHABADI, M.R., 2013. Analysis of stress field and determination of safe mud window in borehole drilling. Case study: South West Iran. *Journal of Petro. Production Tech. Springer*, 3, pp.105-110.
- ABIJA, F.A. and TSE, A, C., 2016. Geomechanical evaluation of an onshore oil field in the Niger Delta, Nigeria. *Journal of Applied Geology and Geophysics*, 4(1). pp.99-111.
- ABIJA, F.A. and TSE, A. C., 2016. In-situ stress magnitude and orientation in an onshore field Eastern Niger Delta: Implications for directional drilling. *SPE-184234MS*.
- ABIOLA, S.O., NWABUEZE, V.O., OKORO, F.O. and AJIENKA, J.A., 2014. Review of sand production from oil well completions across depositional environments in the Niger Delta. *SPE- 172484-MS*.
- ADAMU, M.A., AJIENKA, J.A. and IKIENSIKIMA, S.S., 2013. Economics analysis on the development of Nigeria offshore marginal fields using probabilistic approach. *Advances in Petro. Explo. and Dev.*, 6(1), pp. 11-21.
- ADDIS, M.A. LAST, N. and YASSIR, N.A., 1996. Estimation of horizontal stresses at depth in faulted Regions and their relationship to pore pressure variation. *SPE*.
- ADDIS, M.A., LAST, N.C., and YASSIR, N.A., 1994. The estimation of horizontal stress at depth in faulted regions and their relationship to pore pressure variations. *Eurorock '94, Balkema, Rotterdam*. pp. 887 – 895.
- ADDIS, M.A., LAST, N.C., and YASSIR, N.A., 1996. Estimation of Horizontal Stresses at Depth in Faulted Regions and their Relationship to Pore Pressure Variations. *SPE Res. Eva. and Eng.*, 11(1), pp.11-18. *SPE-28140-PA*. available from: <http://dx.doi.org/10.2118/ 28140-PA>.
- ADETOBA, L.A., 2008. The Nigeria marginal field development initiative-issues and challenges. *Society of Petroleum Engineers*, 119709 Abuja, Nigeria.
- ADEWOLE, E.O. and HEALY, D., 2013. Quantifying in-situ horizontal stress in the Niger Delta basin. Nigeria. *Journal of Engineering Technology*, 2(3), pp.88.
- ADEWOLE, E.O., 2013. *Overpressure in the Northern Niger Delta Basin, Nigeria mechanical, probability and classification*. Ph.D. thesis, University of Aberdeen.

AHMED, U., MARKLEY, M.E., CRARY, S.F., 1991. Enhanced in-situ stress profiling with micro fracture, core and sonic logging data. *SPE Form. Eval.* 6(02). 243-251.

AJAYI, O., 2017. Marginal field bid rounds. *IJALP oil and gas*. Available from: <https://www.olaniwunajayi.net/wp-content/uploads/2017/89/FG-TO-OPEN-BIDROUNDS-FOR-30-MARGINAL-OIL-FIELDS-pdf>.

AL-AMJMI, A.M., SULTAN, Q.U. and ZIMMERMAN, R.W., 2006. Stability analysis of deviated boreholes using the Mogi-Coulomb failure criterion, with application to some oil and gas reservoir. *International Association of Drilling Contractors/SPE*.

ALLEN, J.R.L., 1965. Late quaternary Niger Delta and adjacent areas: Sedimentary environments and Lithofacies. *Bull. Ameri. Asso. Petro. Geolo.*

ALLMENDINGER, R.W., 2015. Modern Structural Practice: A structural geology laboratory manual for the 21<sup>st</sup> Century. Available from: <http://www.geo.cornell.edu/geology/faulty/RWA/structure-lab-manual>.

ALLMENDINGER, R.W., CARDOZO and FISCHER, D. M., 2012. *Structural geology algorithms*. London: Cambridge University Press.

ALMISNED, O.A. 1995. *A model for predicting sand production from well logging data*. PhD thesis. University of Oklahoma, USA.

AMADEI, B. 2007. Suggested methods for rock characterization, testing and monitoring. *Springer*. Amsterdam.

ANDERSON, E.M. (1951). The dynamic of faulting and dyke formation with application of Britain. Edinburgh Oliver and Boyd.

ARCHER, S. and RASOULI, V., 2012. A log-based analysis to estimate mechanical properties and In situ stresses in a shale gas well in North Perth Basin. *Transaction on Engineering Sciences*. 81, pp. 163-173.

Asquith, G. and Gibson, C., 1982. *Basic Well log analysis for geologists*. The American Association of Petroleum Geologists. Methods in Exploration Series Number 3.

AVASTHI, J.M., NOLEN-HOEKSEMA, R.C., and ELRAAA, A.W.M., 1991. In situ stress evaluation in the McElroy Field, West Texas. *SPE Formation Evaluation*, pp. 301308.

AVBOVBO, 1978. Tertiary lithostratigraphy of Niger Delta. *American association of Petroleum Geologists Bulletin*, 62 (2), 295-300.

AYDIN, A., 1978. Small faults formed and deformation bands in sandstone. *Pure and Applied Geophysics*, 16, pp.913-930.

BAI, M. and LI, G., 2012. A comprehensive approach on determining correlation between sonic and density log measurements from the Gulf of Guinea of Mexico and North Sea fields for improved reservoir descriptions. *SPE-152195*.

BAKER HUGES INTEQ 1996.*Geological Procedures Workbook*. Training and Development Houston U.S.A.

BALARABE, T. and ISEHUNWA, S., 2017. Evaluation of sand production potential using well logs. *SPE-189107*.

BARTON, C.A. and ZOBACK, M.D., 1994. Stress perturbations associated with active faults penetrated by boreholes: Possible evidence for near-complete stress drop and a new technique for stress magnitude determination. *Journal of Geophysics Researchers*, Vol. 99, pp. 9373-9390.

BAULAC, J., GROSDIDIER, E. and BOUTET, 1986.*Biostratigraphical study of Wabi 10*. Direction exploration division richer ches et application on geologie Laboratoire etablissement de Boussens.

BOSSIOUNI, ZAKI. 1994.*Theory, Measurement and Interpretation of well logs*. Society of Petroleum Engineers Inc.

BECKER, A., BLUMLING, P. and MULLER, W.H., 1987. Recent stress field and neotectonics in the Eastern Jura mountains, Switzerland. *Tectonophysics*, Vol. 135, pp. 277-288.

BELL J.S., 1993. Attached and detached in situ stress regime in sedimentary basins: *European Association of Petroleum Geoscientist and Engineers*. 5<sup>th</sup> Conference and Technical Exhibition. Stavanger, Norway. 7 – 11. June 1993, Extended Abstracts of papers F046.

BELL, 1996. "Applications of stress measurements". *Geoscience Canada*, 23(3), pp. 135-153.

BELL, 1996. In situ stresses in Sedimentary rocks (Part 1): Measuring technique. *Geoscience Canada*, 23(2), pp. 85-100.

BELL, J.S., and Babcock, E. A., 1986. The stress regime of the Western Canadian basin and implication for hydrocarbon recovery. *Canadian Petroleum Geology, Bulletin*, Vol. 34, pp. 364-378.

BENETITOS, C., RECCA, V., SACCHI, Q. and VERGA, F., 2015. How to approach subsidence evaluation for marginal fields. A case history. *The Open Petroleum Engineering, Journal*, 8, 214-234.

BESSA, F., 2004. *Reservoir characterization and reservoir modeling in the northwestern part of Hassi Messaoud field Algeria*. PhD. Thesis. University of Hamburg, Germany.

BIDOGOLI, M.N. and JING, L., 2014. Anisotropy of strength and deformation ability of fractured rocks. *Journal of Rock Mechanics and Geotechnical Engineering*, 6, 156164.

BIENIAWSKI, Z.T., 1974. Estimating the strength of rock materials. *Journal of South African Institution of Mining and Metallurgy*, 312-320.

BIOT, M.A., 1941. General theory of three-dimensional consolidation. *Journal of Applied Physics*, 12, 155 – 164.

BIOT, M.A., 1956a. "General solutions of the equations of elasticity and consolidation for a porous material". *Journal of Applied Mechanics*. 23, 1, 91-96.

CARBOGNIN, L., GATTO, P., MOZZI, G. and GAMBOLATI, G., 1978. Land subsidence of Ravenna and its similarities with the Venice case, Proc. of engineering foundation. *Conf. on evaluation and prediction of subsidence*, New York, 254-266.

CARNEGIE, A., THOMAS, M., EFNIK, M. S., HAMAWI, M., AKBAR, M. and BURTON, M., 2002. An advanced method of determining in situ reservoir stresses: wireline conveyed micro-fracturing. In *Abu Dhabi International Petroleum Exhibition and Conference*. Society of Petroleum Engineers.

CASTAGNA, J.P., BATZLE, M.L. and EASTWOOD, R.L., 1985. Relationships between compressional wave and shear wave velocities in clastic silicate rocks. *Geophysics*, 50, 571-581.

CERVENY, K., DAVIS, R., DUDLEY, R. F., KAUFMAN, P., KNIPE, R. and KRANTZ, B., 2004. Reducing uncertainty with fault seal analysis. Available from: [www.slb.com/2/media/file/.../04-faultsealanalysispdf](http://www.slb.com/2/media/file/.../04-faultsealanalysispdf)

CESARO, M., CHEUNG, P., ETCHECOPAR, A. and GONTALINI, M., "Shaping up to stress in the Apennines, "Italy 2000: Value Added Reservoir Characterization (*Well evaluation conference, Italy*) Schlumberger 1997.

CHANG, X., ZOBACK, M.D. and KHAKSA, A., 2006. Empirical relations between rock strength and physical properties in Sedimentary rocks. *Jour. of Sci. and Engineering*, 5(1), pp. 223-237.

CHIN, L.Y., and RAMOS, G.G., 2002. Predicting volumetric sand production in weak reservoirs. *Society of Petroleum Engineering* - 78169-MS.

DAFFAUT, K. and LANDRO, M., 2006. Vp/Vs ratio differential stress and rock consolidation of comparison between rock models and time -lapse AVO data. Society *CREWES research report* (9).

DARVISH, H., NOURI-TALEGHANI, M., SHOKROLLAHI, A. and TATAR, A., 2015. Geomechanical modeling and selection of suitable layer for hydraulic fracturing operation in an oil reservoir (South West of Iran). *Journal of African Earth Sciences*, III, 409-420.

DASSAULT, 2015. Systemes Simulia: Reservoir Geomechanics. Available from: [file:///E:/Geomechanics/whitepaper-reservoir geomechanics.pdf](file:///E:/Geomechanics/whitepaper-reservoir%20geomechanics.pdf).

DASSEAULT, M., 2011. Lecture slides: Petroleum in the value chain: Available from: [file:///e:/Geomechanics/a intro to Geome.pdf](file:///e:/Geomechanics/a%20intro%20to%20Geome.pdf).

DAVATZES, N. C., and A. AYDIN, 2005, Distribution and nature of fault architecture in a layered sandstone and shale sequence: An example from the Moab fault, Utah, in R. Sorkhabi and Y. Tsuji, eds., *Faults, fluid flow, and petroleum traps: AAPG Memoir 85*, p. 153–180

DEPARTMENT OF PETROLEUM RESOURCES (DPR), 1999. Available from: *DPR website*.

DETOURNAY, E. and CHENG, A.H.D., 1993. Fundamentals of Poroelasticity in comprehensive Rock Engineering, J. A Hudson, ed., Pergamon, Oxford 113 – 171.

DOUST, H. and OMATSOLA, E., 1990. Niger Delta, in Edwards, J. D. and Santogrossi, P.A., eds., *Divergent/passive Margin Basins, AAPG Memoir 48: Tulsa, American Association of Petroleum Geologists*, pp. 239-248.

DUAN, K., KNOK, C.Y. and THAM, L.G., 2014. Micromechanical Analysis of the failure Process of brittle rock. *International Journal for Numerical and Analytical Methods in Geomechanics*, 39, pp. 618-634.

DUSSEAULT, M.B., 2011. Geomechanical challenges in petroleum reservoir Exploration. KSCE. *Journal of Civil Engineering*, 15(4), pp. 669-678.

ECONOMIDES, M.J. and NOLTE, K., 2000. *Reservoir Simulation*. 3<sup>rd</sup> Edition. Chichester: John Wiley and Sons Ltd.

ECONOMIDES, M. J., HILL, A.D., ECONOMIDES, C. and ZHU, D., 2013. *Petroleum Production Systems*. Prentice Hall. Pearson Education. USA.

ECONOMIDES, M.J., WATTERS, L.T. and DUNN-NORMAN, S., 1998. *Petroleum well construction*: John Wiley & Sons Ltd.

ETU-EFEOTOR, J.O., 1999. *Fundamental of petroleum geology*. Jeson services.

ETU-EFFEOTOR, J.O., 1997. Manual of Petroleum Geology. Manuscript edn. Nigeria: Uniport.

EVAMY, B.D., HAREMBOURE, J., KAMERLING, P., KNAAP, W.A., MOLLOY, F.A. and ROWLANDS, P.H., 1978. Hydrocarbon habitat of Tertiary Niger Delta. *American Association of Petroleum Geologists Bulletin*, Vol. 62, pp. 277-298.

EVANS, K.F., ENGELDER, T. and PLUMB, R.A., 1989. Appalachian stress study 1. A detailed description of in situ stress variations in Devonian shales of the Appalachian Plateau. *Journal of Geophysical Research*, 94, pp. 7129-7154.

EZE, G. L., SUNDAY, V. N., UGWU, S. A., UKO, E. D. and NGAH, S. A., 2011. Mechanical model for Nigerian interpolate Earth tremors. Available from: <https://earthzine.org/2011/.../Mechanical-model-for- Nigeria.int...>

FANG, Z. and KHAKSAR, A., 2011. Complexity of mini fracture tests and implecations for in-situ horizontal stresses in coalbed methane reservoir. *In International Petroleum Technology Conference.*

FEE, D.A. and O'DEA, J., 1986. *Technology for developing marginal offshore oil fields.* London and New York: Elsevier Applied Science Publishers

FERRILL, D.A., WINTERLE, G., WITMEYER, D., SIMS, S., COLTON, A., ARMSTRONG and A.P. MORRIS., 1999. Stress rock strains groundwater at Yacca Mountain, Nevada. *Geological society of America today*, 9, 1-8.

FERRILL, D.A.A.P., MORRIS, D.W. SIMS, D.G. WAITING and S. HASEGAWA, 2005. Development of synthetic layer dip adjacent to normal faults in R. Sorkhabi and Y. Tsuji, eds., *Fault, fluid flow and petroleum traps. AAPG Memoir 85*, 125-138.

FOWLES, J., and BURLEY, S.D., 1994, Textural and permeability characteristics of faulted, high porosity sandstones: *Marine Petroleum and Geology*, v. 11, p. 608– 623

FJAER, E., HOLT, R.M. HORSRUD, P., RAAEN, A.M. and RISNES, R., 2008. *Petroleum related rock mechanics* (2<sup>nd</sup> edition). Amsterdain Elsevier.

GARDNER, G.H.F, GARDNER, L.W. and GREGORY, A.R., 1974. Formation velocity and density: the diagnostic for stratigraphic traps. *Geophysics*, 39, 770–780.

GEOSERVICES, 2004. Lecture slide: Competence assurance system. Quantitative pressure detection. Presented at Port Gentile Gabon.

GHOLAMI, R. AADNOY, B., RASOULI, V. and FAKHAN, N., 2016. An analytical model to predict the volume of sand during drilling and production. *Journal of Rock Mechanics and Geotechnical Engineering* 8, 4, pp. 521-532.

GODMUNDSSON, A., 2011. *Rock fractures in geological process.* Cambridge.

GOODMAN, R.E., 1989. *Introduction to Rock mechanics second edition.* New York: John Wiley & Sons.

GREENBERG, M.L. and CASTAGNA, J.P., 1992. Shear wave velocity estimation in porous rocks: Theoretical formulation, preliminary verification and applications. *Geophysical Prospecting*, 40, 195-209.

GUTIERREZ, M., 1996. The role of geomechanics in reservoir simulation. *Society of Petroleum Engineers.*

HAACK, R. C., SUNDARARAMAN, P., DIEDJOMAHOR, J. O., XIAO, H., GANT, N. J., MAY, E. D. and KELSCH, K., 2000. Niger Delta Petroleum Systems, Nigeria, In M.R.

Mello and B. J. Katz, eds., Petroleum Systems of South Atlantic Margins, *AAPG Memoir* 73, pp. 213 – 231

HAMID, O., OMAIR, A. and GUIZADA, P., 2017. Reservoir geomechanics on carbonates. *SPE- 183704-MS*.

HAN, G. and DUSSEAULT, M.B., 2005. Strength variation with deformation in unconsolidated rock after water breakthrough. *SCA2002- 22*

HAZZARD, J. F. and YOUNG, R.P., 2000. Micromechanical modeling of cracking and failure in brittle rocks. *Journal of Geophysical Research*, Vol. 105, B7, pp. 16, 683-16, 697.

HEGAZY, M. and LAKMIKANTHA, M.R., 2014. Geomechanics: a new star in the horizon to change the fortunes in E&P projects. *SPE*. Doi: 10: 2118/169914 – MS

HEIDBACH, O., TINGAY, M., BARTH, A., REINECKER, J., KURFEB, D. and MÜLLER, B., 2008. The World Stress Map database release 2008. doi:10.1594/GFZ.WSM.Rel2008.

HERWANGER, J. and KOUTSABELOULIS, N., 2011. *Seismic Geomechanics*. "How to build and calibrate Geomechanical models using 3D and 4D seismic data". Netherlands: EAGE publication.

HIBBELER, J. and RAC, P., 2005. Simplifying hydraulic fracturing theory and practice. In *SPE 97311, SPE Annual Technical conference and exhibition*, Dalas, Texas, USA.

HILLIS, R.R., MILDREN, S.D., PIGRAM, C.J. and WILLOUGHBY, D.R., 1997. Horizontal Stress Orientation in the Australian North West Continental Shelf: Stress Rotation Associated With a Convergent Plate Boundary. *Tectonics*, 16(2), pp. 323335.

HOEDEMAN, G., 2015. Multi-scale Geomechanics. How much model complex is enough? *Society of Petroleum Engineering -177634-MS*.

HOLBROOK, P.W., MAGGIORI D.A., 1993. Real time pore pressure and fracture gradient evaluation in all sedimentary lithologies. In: *Proceedings of Offshore European Conference. Aberdeen, Scotland, SPE: 1993*. Paper SPE 26791.

HOWARD, K.A. and JOHN, B.E., 1987. Crustal extension along a roof system of imbricate low angle fault: Colorado River extensional corridor, California and Arizona.

HUBBERT, M.K and RUBEY, W.N., 1959. Role of fluid Pressure in Mechanics of overthrust faulting. *Bull. Geol. 502. Ame.* 70, 115 – 205.

HUBBERT, M.K. and WILLIS, D.G., 1957. Mechanics of hydraulic fracturing. *Petro. Trans. AIME*, 210, 153- 163.

HUCKA, V. and DAS, B., 1974. Brittleness determination of rocks by different methods. *International Journal of Rock Mechanics and Mining Science and Geomechanics Abstracts*.

HUDSON, J.A and HARRISON, J.P., 2000. *Engineering rock mechanics: an introduction to the principles*. UK: Elsevier Science Ltd.

HUDSON, J.A.,and HARRISON, J.P. and 1997. *Engineering rock mechanics. An introduction to the principles.First edition*. London: Elsevier.

HUGO, H.E. and IAN, R., 2014. NAPE Lecture slides: Addressing the challenges in Nigerian development and brown-fields wireline logging advances. *NAPE* Port Harcourt.

ILLO, C.A., 2015. *Reservoir characterization in Fanito Oil field: An integration of seismic and petrophysical log data in the onshore Niger Delta Nigeria*. MSc Thesis. University of Nsukka.

JAEGER, J.C. and COOK, N.G., 1979. *Fundamental of Rock mechanics*. 3<sup>rd</sup> ed. London: Chapman and Hall.

JAEGER, J.C., COOK, N.G.W. and ZIMMERMAN, R.W., 2007. *Fundamentals of rock mechanics*. Fourth edition. USA: Blackwell publishing.

JAMSHIDIAN, M., ZADEH, M.M., HADIAN, M., NEKOEIAN, S. and Zadeh, M.M., 2016. Estimation of minimum horizontal stress, Geomechanical modeling and hybrid neural Network based on Conventional well logging data: A case study. *Geosystem Engineering*, 20(2), pp.88-103.

JONES M.E., LEDDRA, M.J., GOLDSMITH, A.S. and EDWARDS, D., 1992. The Geomechanical Characteristics of Reservoirs and Reservoir Rocks, Health and Safety Executive - Offshore Technology Report. London: HMSO Books.

JUMIKIS, A.R., 1983. *Rock Mechanics*.2<sup>nd</sup> edition. Germany: Trans Tech Publications.

KACHI, T.H., YAMADA, K., YASUHARA, M., FUJIMOTO, S., HASEGAWA, S.I. and, R. SORKHABI., 2005. Fault-seal analysis applied to the Erawan gas-condensate field in the Gulf of Thailand, In F. Sorkhabi and Y. Tsuji, eds., *Faults, fluid flow and petroleum traps*. *AAPG memoir*, 85, 59-78.

KANG, Y,YU. M. MISKA, S. and TAKACH, N., 2009. Wellbore stability: A critical review and introduction to DEM. *SPE* 124669.

KATAHARA, K.W., 1996. Estimation of in situ stress profiles from well logs. *SPNLA 37<sup>TH</sup> Annual logging symposium*.

KIDAMBI, T., KUMAR, G.S., 2016. Mechanical earth modeling for a vertical well drilled in a nationally fracture light carbonate gas reservoir in the *Persian Gulf*. *Journal of Petro. Sci. Eng.*, 141, 38-51.

KIM, A., 2012. Sand control mechanism and its impact on mature fields. Available from: <https://halliburtonblog.com/sand-control-mechnaism> and its impact on mature fields.

KONIETZKY, H.H., ISMAEL, M.A., and FREIBERG, B., 2017. Failure Criteria for rocks. Geotechnical institute Available from: [https://tufreiberg/.../gt/.../23\\_Failure\\_Criteria\\_rocks.pdf](https://tufreiberg/.../gt/.../23_Failure_Criteria_rocks.pdf).

KOZLOWSKI, K.A., FIDAN, M., DONALD, A., SHOTLON, P., NIELSEN, H., ANDERSON, N. AND JOCKER, J., 2011. Overburden characterization for geomechanics and geophysical applications in the Ekofisk Field. A North sea case study. SPNLA 52<sup>nd</sup> Annual logging symposium.

KULASINGA, R., BEGGS, D. and COHEN, J., 2014. *Marginal fields in Nigeria: recent development. Available from: https://www.denton.com....2014.*

LANGHI, L., 2014. Lecture slide: Geomechanics for reservoir and beyond. Available from: <https://www.sut.org/wp-content/uploads/2014/07/Langhi-reservoirGeomechanics-WEB-APPROVED,onsite.pdf>.

LARIONOV, V.V., 1969. Radiometry of boreholes in (Moscow: Nedra).

LAWRENCE, S. R., Monday, S. and Bray, R., 2002. Regional Geology and Geophysics of the Eastern Gulf of Guinea (Niger Delta to Riomuni): *The Leading Edge*, Vol. 21, pp. 1112 – 1117.

MAGNENENT, V., Cornet, F.H. and Fond, C., 2007. A Nontectonic origin for the present-day stress field in the Paris basin (France). *Journal of Geophysical research. Solid earth* 122, pp. 9313-9327.

MAJIDI, R., EDWARDS, S., ZHANG, J., SANT, R. and LAST, N., 2015. Drilling depleted sands. Geomechanics, challenges and mitigations. *SPE- 174741-MS*.

MALEKI, S., MORADZADEH, A., RIABI, R.G. and SADAGHZADEH, F., 2014. Comparison of several different methods of in situ stress determination. *International Journal of Rocks Mechanics and Mining Science*. 7, 395-404.

MARTEY, A.O., 2000. Lecture Note: Petrophysics for Shell intensive training programme univation.

MCDERMOTT, C. and KOLDITZ, 2005. Geomechanical model for fracture deformation under hydraulic, mechanical and thermal loads. *Hydrogeology. Journal*. 14, 485-498.

MERKI, P.J., 1972. Structural geology of the Cenozoic Niger delta, *Proceedings of African Geology Conference*, Ibadan, Nigeria 1972, Ibadan University Press, pp. 635-646.

MOCKORCIAKOVA, A. and PANDULA, B. (2003). Study of the relation between the static and dynamic moduli of rocks. *Metalurgija*, 42 (1), 37-39.

MORRIS, A., FERRILL, D.A. and HENDERSON, D.B., 1996. Slip-tendency analysis and fault reactivation. *The Geological Society of America*. Vol. 24-5, pp. 275-278.

MURPHY, W., REISCHER, A. and HSU, K., 1993. Modulus decomposition of compressional and shear velocities in sand bodies. *Geophysics*, 58, 227-239.

NACHT, P.K., DE-OLIVERIA, M.F.F., ROEL, D.M. and COSTA, A.M., 2010. Investigation of geological fault reactivation and opening. *Asociacion Argentina de Mecanica computacional*, Vol. 29, pp. 8689-8697.

NAJIBI, A.R., GHATOORI, M., LASHKARIPOUR, G.R., and ASEF, M.R., 2017. Reservoir Geomechanical modeling: In-situ stress, pre pressure, and mud design. *Journal of Petroleum Science and Engineering*, 151, pp. 31- 39.

NEW CROSS PETROLEUM LIMITED, 2010: Fate of Nigeria's marginal fields. Available from: <http://www.newcrosspet.com/fate-of-Nigeria-marginal-fields>.

NOROUZI, S., BAGHBANAN, A. and KHANI, A., 2013. Investigation of grain size effects on Micro/Macromechanical properties of intact rock using voronoi element – discrete element method approach. *Particulate Science and Technology*, 31: 507-514.

NORRIS, A., 1992. On the correspondence between Poroelasticity and thermoelasticity, *J. Appl. Phys.*, 71, 1138-1141.

NOURI, A., VAZIRI, H., BELHAY, H., ISLAM, R., 2003. Effect of volumetric failure on sand production in Oil-wellbore : *SPE Asia Pacific Oil and Gas conference and Exhibition*. Jakarta, Indonesia. Society of Petroleum Engineering.

OFFIA, U.S., 2011. Development and management of Marginal field in the Niger Delta basin: Opportunities and challenges. *Petro.Tech. Dev. Jour.*, 1(1), pp.1-9.

OJO, A.O., ADEPELUMI, A.A. and OJO O.A., 2019. Abnormal pressure detection using integrated Approach in Oluku Field, East Niger-Delta, Nigeria. *Journal of Geography, Environment and Earth Science International*, 9(3), pp. 1-11.

OLUYEMI, G.F., 2007. *Intelligent grain size profiling using neural network and application to sand potential prediction in real time*. PhD Thesis. Robert Gordon University. Aberdeen.

OMAR, I., 2015. Reservoir geomechanics lecture slides. Stanford University. Available from: <https://lagunita.Stanford.edu/Course v1...about>.

OSISANYA, S.O., 2010. Practical guidelines for predicting sand production". *SPE 136980*, paper presented at the 34th Annual SPE International Conference and Exhibition held in Tinapa, Calabar, Nigeria.

OSTADHASSAN, M., ZONG, Z. and ZAMRIAN, S., 2012. Geomechanical modeling of an anisotropic formation-Bakken: Case study. 46<sup>th</sup> US Rock

Mechanics/Geomechanics Symposium American Rock Mechanics Association.

OTTI, P.E. and WOOD, J.D., 2005. *World Oil: Modern sandface completion practices Handbook*. Houston Texas: Gulf Publishing Company.

OYENEYIN, B., 2015. *Integrated sand management for effective hydrocarbon flow assurance*. Amsterdam: Elsevier.

POLLARD, D.D. and FLETCHER, R.C., 2005. *Fundamental of structural Geology*. Cambridge and New York: Cambridge University Press.

RAJABI, M., TINGAY, M. and HEIDBACH, O., 2016. The present-day state of tectonic stress in the Darling Basin, Australia: Implications for exploration and production. *Marine and petroleum geology*, 77, pp. 776-790

RASOULI, V., PALLIKATHEKATHI, Z.J. and MAWULI, E., 2011. The influence of perturbed stresses near faults on drilling strategy: A case study in Blacktip field, North Australia. *Journal of Petroleum Science and Engineering*, 76, pp.37-50.

RATH, J.S., ARGUELLO, J.G., STONE, C.M. and SOBOLIK, S.R., 2009. Evaluating the present in-situ stress state for the Richton, MS Strategic Petroleum reserve site using geomechanical analysis. *Publication*.

RIDER, M.H. 1986. *The Geological interpretation of well log*. John Wiley and Sons. New York.

ROSEPIER, M.J., 1979. Determination of principal stress and confinement of hydraulic fractures in cotton vale. In *SPE- 8405-MS, SPE Annual Tech. Conf. and Exh. Las Vegas, NV: SPE*.

SALAWU, B.A., SANAE, R. and ONABANJO, O., 2017. Rock compressive strength: a correlation from formation Evaluation data for the Niger Delta. *AAPG/SEG*. Nairobi Kenya.

SCHLUMBERGER, 1989. *Log Interpretation Principles/applications*. Houston Texas, U.S.A: Schlumberger education services.

SCHLUMBERGER, 1972. *Log interpretation: Principles*. Schlumberger.

SCHLUMBERGER, 1985. *Well Evaluation Conference*. Nigeria.

SCHLUMBERGER, 2018. Oilfield Glossary [Homepage of Schlumberger Limited], [Online]. Available: <http://www.glossary.oilfield.slb.com> [May/08, 2018].

SCHLUMBERGER, 2017. Geomechanics of reservoir management. Available. <http://www.slb.com/.../geomechanics/reservoir-management.as>

SCHMITT, D.R., 2014. Basic geomechanics for induced seismicity: A Tutorial focus article coordinated by Mostafa Naghizadeh/ Fereidoon Vasheghani. *CSEG Recorder*, pp. 24-28.

SCHNEIDER, T., 1985. *Bohrlochrandausbreuche in norddeutschen bohrungen und ihm bezichung zum regionalen spannungsfeld-beobachtung und theorie*. Diploma Thesis. University of Karlsruhe, Germany.

SENGUPTA, et al., 2011. Building a seismic-driven 3D geomechanical model in a deep carbonate reservoir. *SEG Annual meeting*.

SERRA, O., 1986. *Fundamentals of well log interpretation volume 2*. Interpretation of logging data. Amsterdam: Elsevier science publishers.

SERRA, O., 1984. *Fundamentals of well log interpretation*, the acquisition of logging data. Amsterdam Elsevier: Science Publishers.

SEYED SAJADI, S. and AGHIGHI, M.A., 2015. Building and analyzing geomechanical model of Bangestan reservoir in Kopal oil field, Iranian. *Journal of Mining Engineering*, 10, 21-34.

SHERRIF, R. and GELDART, L. 1995. *Exploration Seismology*. Cambridge University Press.

SHORT, K.C. and STAUBLE, A.J., 1967. Outline of geology of Niger Delta. *American Association of Petroleum Geologists Bulletin*, 51, pp. 761-779.

SIMM, R. and BACON, M., 2014. *Seismic Amplitude: An interpreter's Handbook*. Cambridge University Press United Kingdom.

SIMS, D.W., MORRIS, A.P., FERRILL, D.A., and SORKHABI, R., 2005. Extensional fault system evolution and reservoir connectivity. In R. Sorkhabi and Tsuji eds. *Faults, flow and petroleum traps: AAPG Memoir*, 85, 79-93.

SINHA, B.K., WANG, J., KISRRA, S., LI, J., PISTRE, V, BRATTON, T. and SANDERS, M., 2008. Estimation of Formation stress using borehole Sonic data. *SPWLA Annual Logging Symposium*, Edinburgh, Scotland.

SMITH, T., 2011. Practical seismic petrophysics: The effective use of 'log data for seismic analysis. *The leading Edge*, 30-1128-1141.

SOCIETY OF PETROLEUM ENGINEERING, 2016. The role of geomechanics in conventional and unconventional reservoir performance and management. Available [www.spe.org/events/16fsap/docs/16FSAR-Application-Brochure.pdf](http://www.spe.org/events/16fsap/docs/16FSAR-Application-Brochure.pdf).

SONG, L., 2012. Minimum horizontal stress profile from logging data for Montney Formation of North East Britain Columbia. *SPE* 162233

SORKHABI, B. and TSUJI, Y., 2015. Faults, fluid flow and petroleum traps. In Japan oil, gas and metals national corporation. *AAPG Memoir* 85.

SORKHABI, R. and S. HASEGAWA, S., 2005. Fault zone architecture and permeability distribution in the Neogene classics of northern Sarawak (Min Airport Road out crop),

Malaysia, In R. Sorkhabi and Y. Tsuji, eds. Faults, fluid flow and petroleum traps. *AAPG Memoir 85*, 139-157.

SORKHABI, R. and TSUJI, Y., 2005. The place of faults in petroleum traps, in R. Sorkhabi and Y. Tsuji, eds. Faults, fluid flow and petroleum traps. *AAPG Memoir 85*, pp. 1-31.

SOROUGH, H., 2013. Discover a career in Geomechanics. *Society of Petroleum Engineers. SPE-0313-015-TWA*.

STREIT, J.E. and HILLIS, R.R., 2004. Estimating fault stability and sustainable fluid pressures for underground storage of CO<sub>2</sub> in Porous rock. *Journal of Energy*, 29, pp, 1224-1450.

SYGALA, A., BUKOWSKA, M., and JANOSZEK, T., 2013. High temperature versus geomechanical parameters of selected rocks. The present state of research. *Journal of Sustainable Mining*, Vol. 12, 4, pp. 45- 51.

SYLVESTER, O. and JOHN-LANDER, I., 2015. Comparative study of rock strength and petrophysical properties derived from core and log data. *International Journal of Current Engineering and Technology*. Vol. 5, 2, pp. 900-906.

TAHERI, E., SADRNEJAD, S.A. and GHESEMZADEH, H., 2005. Multiscale geomachanical model for a deformable oil reservoir with surrounding rock effects. *International Journal of Multi-scale Computational Engineering*, 13 (6), 533-559.

TERZAGHI, 1923. K. VAN: "De Berechnung der Durchlassig-Keitszitter des Tones aus dem verlauf de Hydrodynamischen Spannungserscheinungen: Sitzungsber., Akad, Wiss., *Wien Math. Natuwiss: KL*, 132, 105-124.

TIAB, D. and DONALDSON, E.C., 2012. *Theory and practice of measuring reservoir rock and fluid transport properties*. 3<sup>rd</sup> edition. Amsterdam: Gulf Professional Publishing.

TIMMERMAN, E.H., 1982. Practical reservoir Engineering: Methods for analyzing output from equations and computers. Oklahoma: Pennwell Publishing Company Tulsa.

TIMUR, A., 1987. Acoustic logging chapter 51. In H.B., Bradley. Edition-in-chief petroleum engineering Hand-Book. *Society of Petroleum Engineers*, 51-1-51-52.

TINGAY, M., 2009. States and origin of present day stress fields in sedimentary basins. DOI: 10.1071/ASEG 2009ab 037.

TINGAY, M., MULLER,B., REINECKER, J., HEIDBACH, O., WENZEL, F. and FLEKENSTEIN, P., 2006. Understanding tectonic stress in the oil patch: the world stress map project. *The Leading Edge*, pp.1276-1282.

TINGAY, M.R.P., HILLIS, R.R., MORLEY, C.K., SWARBRICK, R.E. and OKPERE, E.C., 2003a. Variation in vertical stress in the Baram Basin, Brunei: tectonic and geomechanical implications. *Marine and Petroleum Geology*, 20(10), pp. 1201-1212.

TINGAY, M.R.P., MULLER, B., REIMAKER, J. and HEIDBACH, O., 2005. State and original of the present day stress field in sedimentary basins. New results from the world stress map project. *American Rock Mechanics Association ARMA/USRMS*, 061048.

TIXIER, M.P. LOVELESS, G.W. and ANDERSON, R.X., 1975 Estimation of the formation strength from the mechanical properties log. *Journal of Petroleum Technology*, 27, 283-293.

TUNIO, S.Q., TUNIO, A.H., GHIRANO, N.A and EL ALDAWY, Z.M., 2011. Comparison of different enhanced oil recovery techniques for better oil productivity. *Intern. Jour. of Appl. Sci. and Tech.*, 1(5), pp. 143-153.

TUTTLE, M.L.W., BROWN Field M.E. and CHARPENTIER, R.R., 1999. The Niger Delta petroleum system. Niger Delta province, Nigeria Cameroon and Equatorial Guinea Africa, U.S. Geological survey open-file Report-95-50H, 3.1P. Available <https://pubs.usgs.gov/of/1999/ofr-99=0050/.../chapter.A.html>

TWISS, R. J. and MOORES, E. M. 1992. *Structural Geology*. New York: W. H. Freeman and Company.

UDEBHULU, D.O. and OGBE, D.O., 2015. Mechanistic model for predicting sand production: A case Study of Niger Delta Wells. *Society of Petroleum Engineer* 178279-MS.

UZORCHUKWU, M.I., 2016. *Critical Evaluation of the correlations used for estimating geomechanical properties for the Niger Delta*. MSc Thesis, African University of Science and Technology.

VERNER, K., 2007. The Mapping of geological structure. Czech geological survey in Prague. Available from: [https://www.krystof-verner.com/structure\\_geology\\_and\\_tectonics.pdf](https://www.krystof-verner.com/structure_geology_and_tectonics.pdf).

WARPINSKI, et al., 1993, N.R., LORENZ, J.C. BRANAGAN, P.T. MYAL, F.K. and GALL, B.L. "Examination of cored Hydraulic Fracture in a deep gas well". *Paper SPE. 22876, SPE Formation Evaluation*, 8, 3, 150-158.

WARPINSKI, N.R., 1989. Elastic and Viscoelastic calculation of stresses in sedimentary basins. *SPE*- 522- 530.

WARPINSKI, N., and TEUFEL, L., 1989. Insitu stresses in low permeability, nonmarine rocks. *Journal of Petroleum Technology*, 41, 405-414.

WEBER, K. J. and DAUKOU, E. M., 1975. Petroleum geology of the Niger Delta: *Proceedings of the Ninth World Petroleum Congress*, Vol. 2, Geology: London, Applied Science, pp. 210-221.

WEBER, K.J., 1987. Hydrocarbon distribution patterns in Nigerian growth fault structures controlled by structural style and stratigraphy. *Journal of Petroleum Science and Engineering*, 1, pp. 91-104.

WEBER, R.J., 1971. Sedimentological aspects of oil fields in the Niger Delta. *Geology magazine*, 105. pp. 386-389.

WHITEMAN A., 1982. Nigeria: its petroleum ecology resources and potential. London, Graham and trotman.

WILLIS, R. B. FONTAINE, J., PAUGH, L., GRIFFIN, L., 2005. Geology and geometry: a review of factors affecting the effectiveness of hydraulic fracturing. *In SPE Eastern Regional meeting; Morgantown, W.V., SPE 97993*.

WILSON, G. and COSGROVE, J.W., 1982. *Introduction to small scale geological structures*. George Allen and Unwin Publishers Ltd.

WOEHL, B., PEI, J. and REMER, J., 2010. Comparison of methods to derive rock mechanical properties from formation evaluation logs. *American Rock Mechanics Association, ARMA*, 10-167.

WYLLIE, D.C.K., 1999. *Foundations on Rock* 2<sup>nd</sup> edition. Chapman and Hall.

XIAO, X., JENAKUMA, T., ASH, C., BUL, H. and FAKUNLE, O., 2016. An integrated workflow combining seismic inversion and geomechanics modeling-Bonga field, offshore Nigeria. *Offshore Tech. Conference*. Houston Texas.

XIE, H., and GAO, F., 2000. The mechanics of cracks and a statistical strength theory for rocks. *International Journal of Rock Mechanics and Mining Sciences*, 37, pp. 477

YALE, D.P., 2003. Fault and Stress magnitude controls on variations in the orientation of in-situ stress. Fracture and in-situ stress characterization of hydrocarbon reservoirs. M. Ameen. London. *Geological Society*, 209, 55-64.

YAMADA, Y.H., OKAMURA, Y. T. and TSUNEYAMA, F., 2005. Analog models of faults associated with salt doming and wrenching: Application to offshore United Arab Emirates, In R. Sorkhabi and Y. Tsuji, eds., *Faults, fluid flow and petroleum traps: AAPG Memoir*, 85, 95-106.

YAMADA, Y.H. and MATSUOKA, T., 2005. Digital sand box modeling using distinct element method. Applications to fault tectonics, in R. Sorkhabi and Y. Tsuji, eds. *Faults, fluid, flow and petroleum traps: AAPG Memoir*, 85, 107-123.

YANA, R.N. and NAERKENTIN, B.P., 1975. *Developments in Geotechnical Engineering soil properties and behavior*. Amsterdam, Oxford New York: Elsevier Scientific Publishing Company.

YASSIR, N.A. and BELL, J.S., 1994. Relationship between Pore Pressure Stresses, and present day Geodynamics in Scotian Shelf, Offshore Eastern Canada: *America Association of Petroleum Geologists, Bulletin*, Vol. 78, pp.1863 – 1880.

ZHANG, J.J., RAI, C.S. and SANDERGELDS, 2000. Mechanical strength of reservoir materials. Key information for sand prediction. *SPE Reservoir Eval. & Eng.* 3(2), 127-131.

ZHANG, J., and YIN, S., 2017. Fracture gradient Prediction: An overview and an improved method. *Petroleum Science*, 14: pp. 720 – 730.

ZHOU, B., FRASER, S., BORSARU, M., AIZAWA, T., SLIWA, R. and HASHIMOTO, T., 2005. New approaches for rock strength. Estimation from geophysics logs. Available at [http://www.suncohi.co.jp/tech\\_topics/technology/...../002\\_/pdf](http://www.suncohi.co.jp/tech_topics/technology/...../002_/pdf)

ZIMMERMAN, R.W., KUMAR, S. and BODVARSSON, G.S., 1991. Lubrication theory analysis of the permeability of Rough- walled fractures. *Int. J. rock Mech.*, 28, 325 – 331.

ZOBACK, M.D. and ZOBACK M.L., 1991. Tectonic stress field of North America and relative plate motions, In SLEMMONS, D. B., ENGDAHL, E. R., ZOBACK, M. D. and BLACKWELL, D.D., eds., *Neotectonic of North America, Decade map volume 1: Geological Society of America*, Boulder, Colorado, pp. 339-366.

ZOBACK, M.D. and ZOBACK, M.B., 2002. Stress in the Earth's lithosphere. *Encyclopedia of Physics Science and Technology*. Third edition, Vol. 16, pp. 143153.

ZOBACK, M.D., 2016. Reservoir Geomechanics: In situ stress and rock mechanics applied to reservoir process. Course overview. Stanford University (online-lecture1-overview-2016%20Zoback. pdf.

ZOBACK, M.L., Zoback, M.D. et al, 1989. Global patterns of tectonic stress. *Nature*, 341, 291-298.

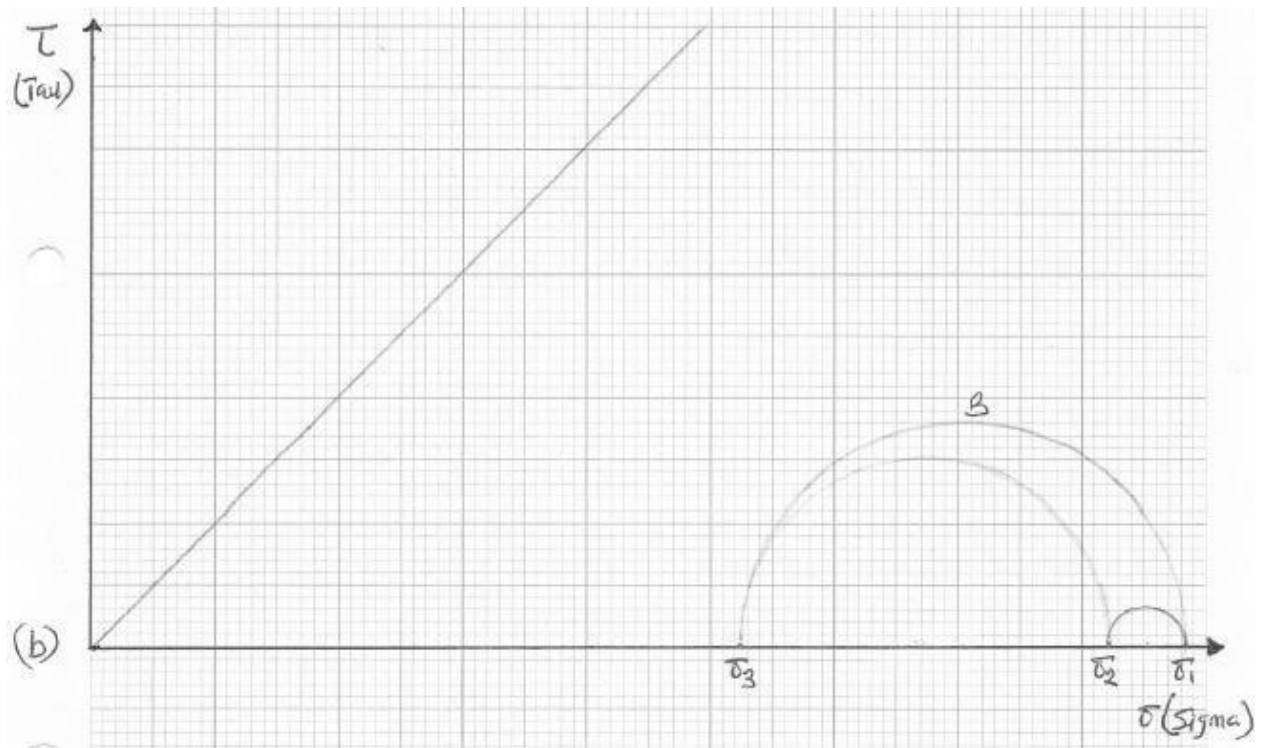
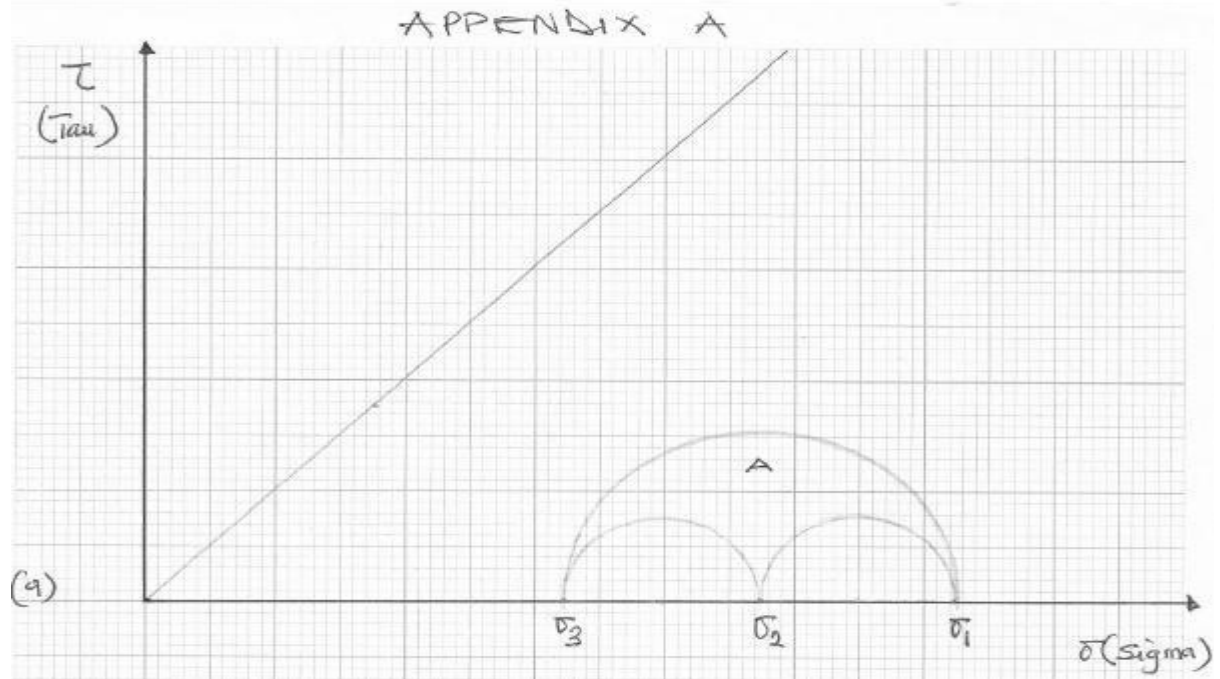
ZOBACK, M.D., 2007. *Reservoirs Geomechanics*. New York, U.S.A: Cambridge University press.

ZOBACK, M.D., MOOS, D. AND MASTIN, L., 1985. "Well bore breakouts and in situ stress, "*Journal of Geophysics Research*, 90, No. B7, 5523-5530.

ZOCCARATO, C. BAU, D., BATHAZZI, FERRONATO, M., GAMBOLATI, G., MANTICA, S. and TEATINI, P., 2016. On the importance of the heterogeneity assumption in the characterization of reservoir geomechanical properties. *Geophys. Journal International*, 209, 47-58.

ZORASI, C.B., ADOOH, L.S.K, DAMABEL, B.C., TANEN, R. and AL ABBADD, A., 2017. Waterflood forecast between injectors and producers pattern for maximum hydrocarbon recovery in depleted reservoirs. *International Jour. of Eng. and Modern Tech.*, 3(2) pp.14-32.

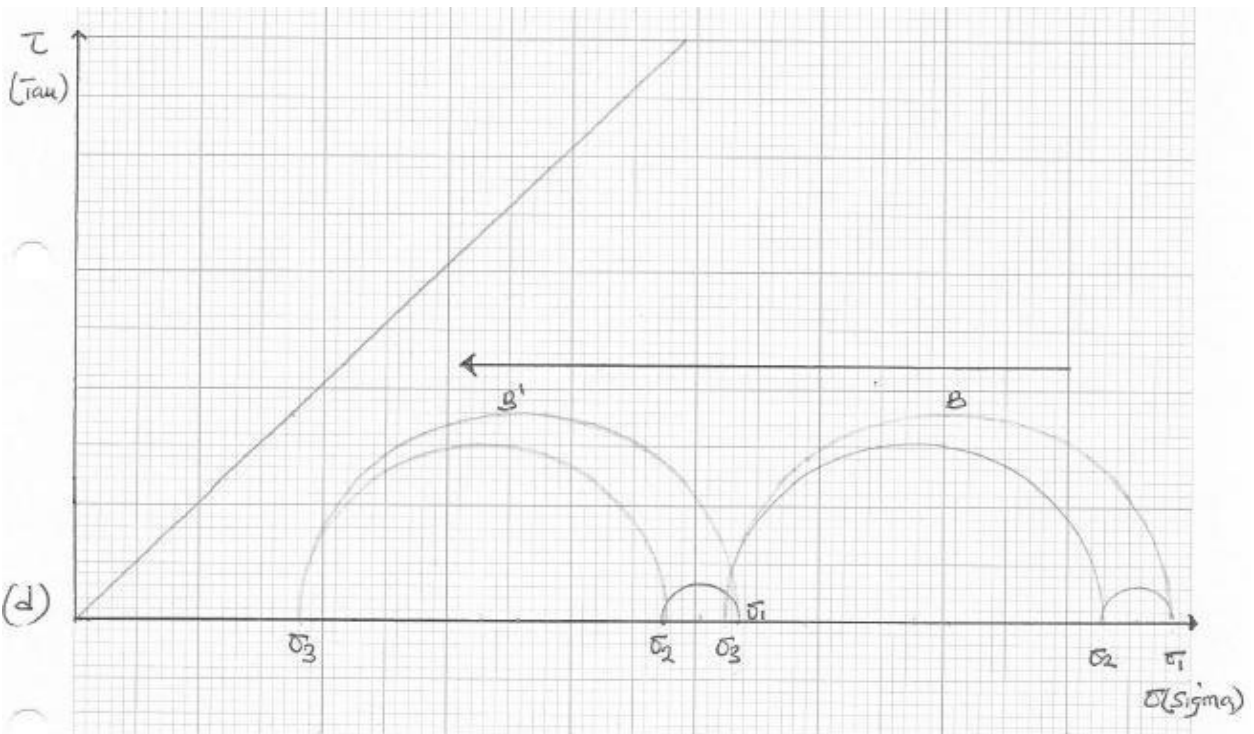
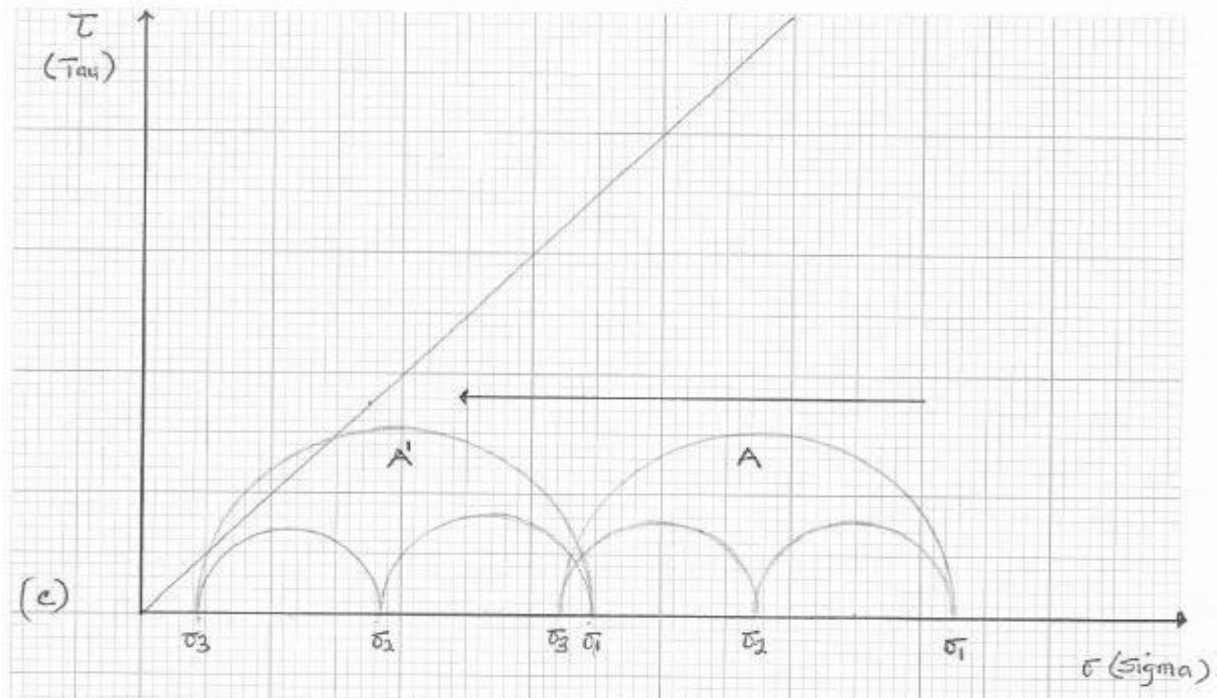
ZORASI, C.B., EKINE, A.S. and NWANKWO, C.N., 2017. *Reservoir characterization for the Development of a Marginal (Wabi) Field in the North Central Niger Delta*. PhD Thesis Unpublished, University of Port Harcourt Nigeria.



3D Mohr diagram construction for Wabi 05 stability of Wabi field for development design

Appendix B

APPENDIX B

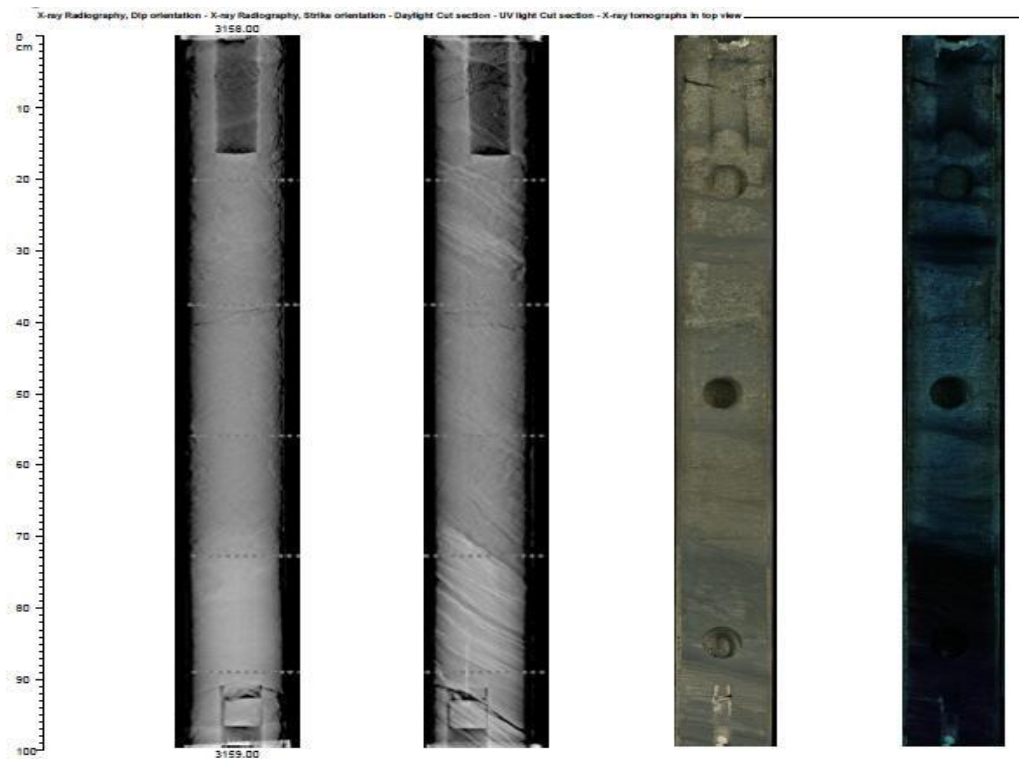


3D Mohr diagram construction for Wabi 05 showing movement of Mohr circle for injectivity scenarios

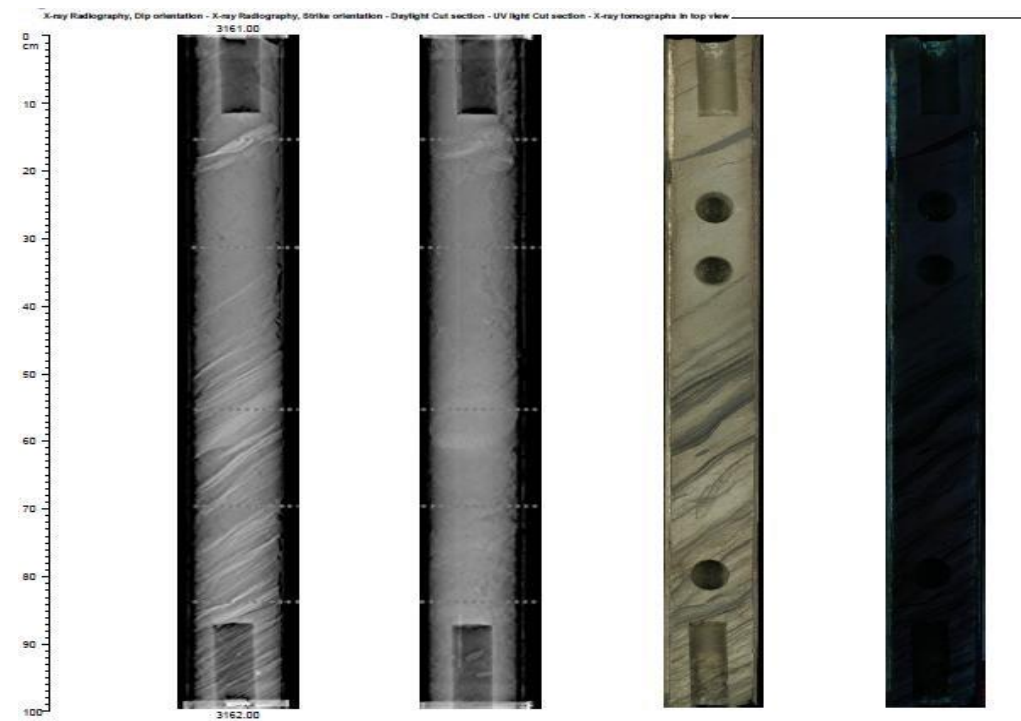
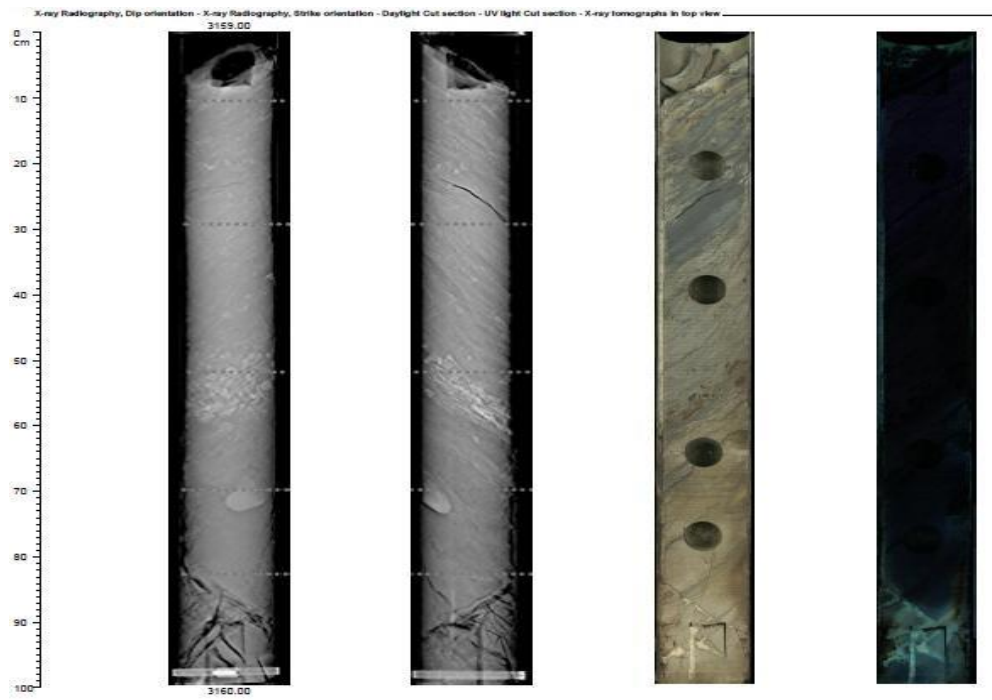
Appendix C    1                    2                    3                    4



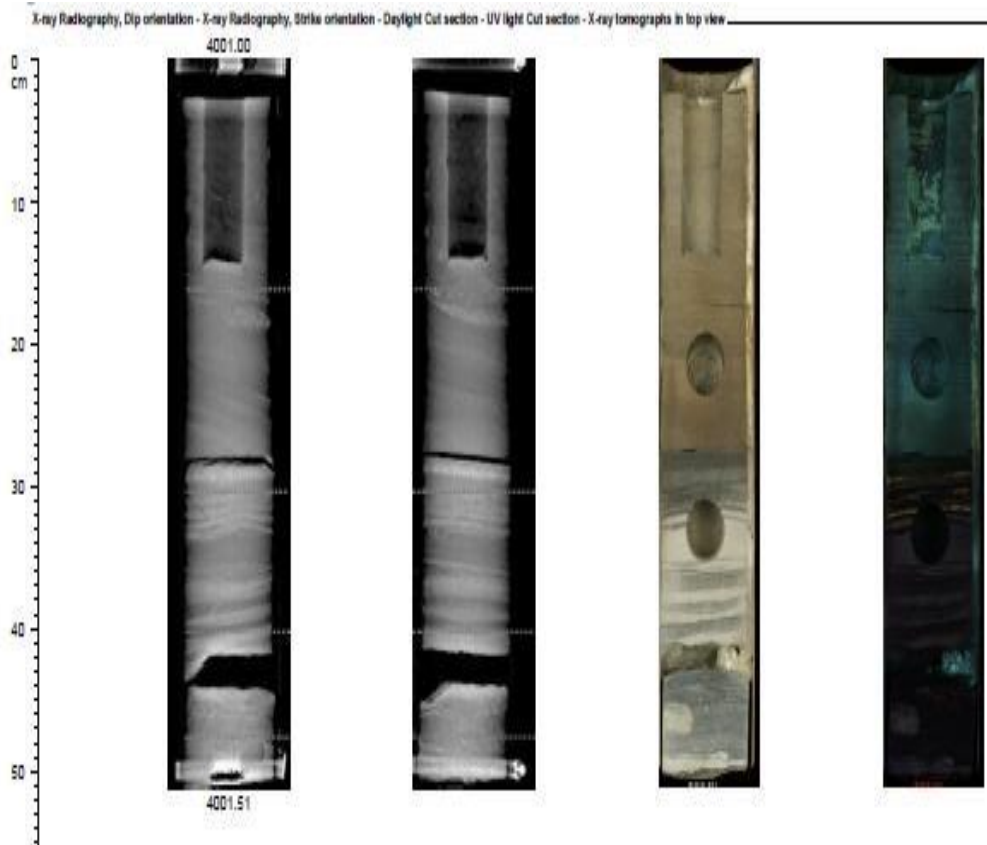
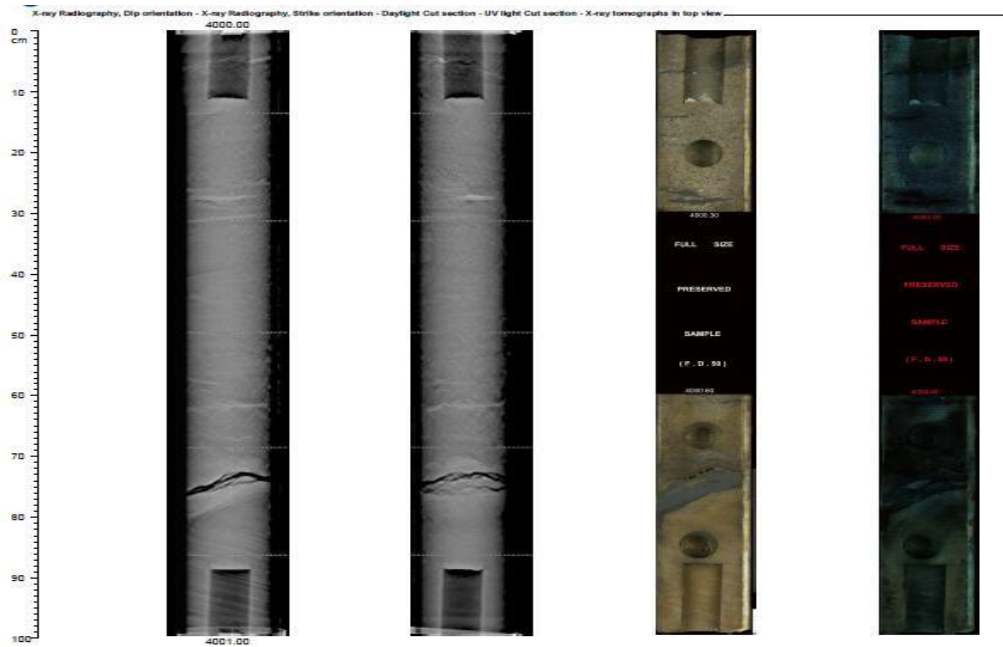
1&2): X-ray radiography showing dip and strike orientations,3.)Daylight cut and 4.) UV light cut section



1&2): X-ray radiography showing dip and strike orientations,3.)Daylight cut and 4.) UV light cut section



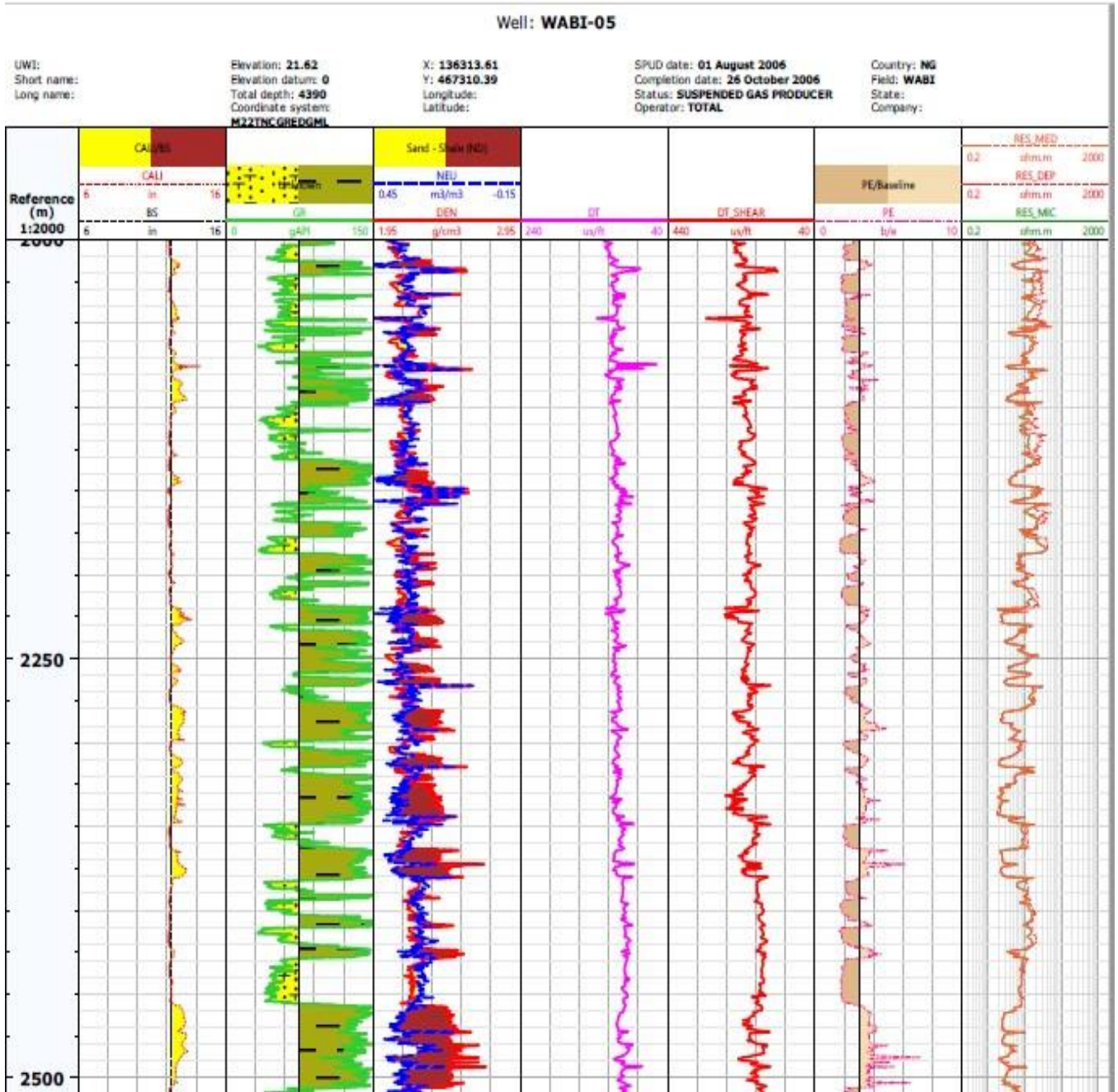
Core sections of Shallow reservoirs interpreted in this study

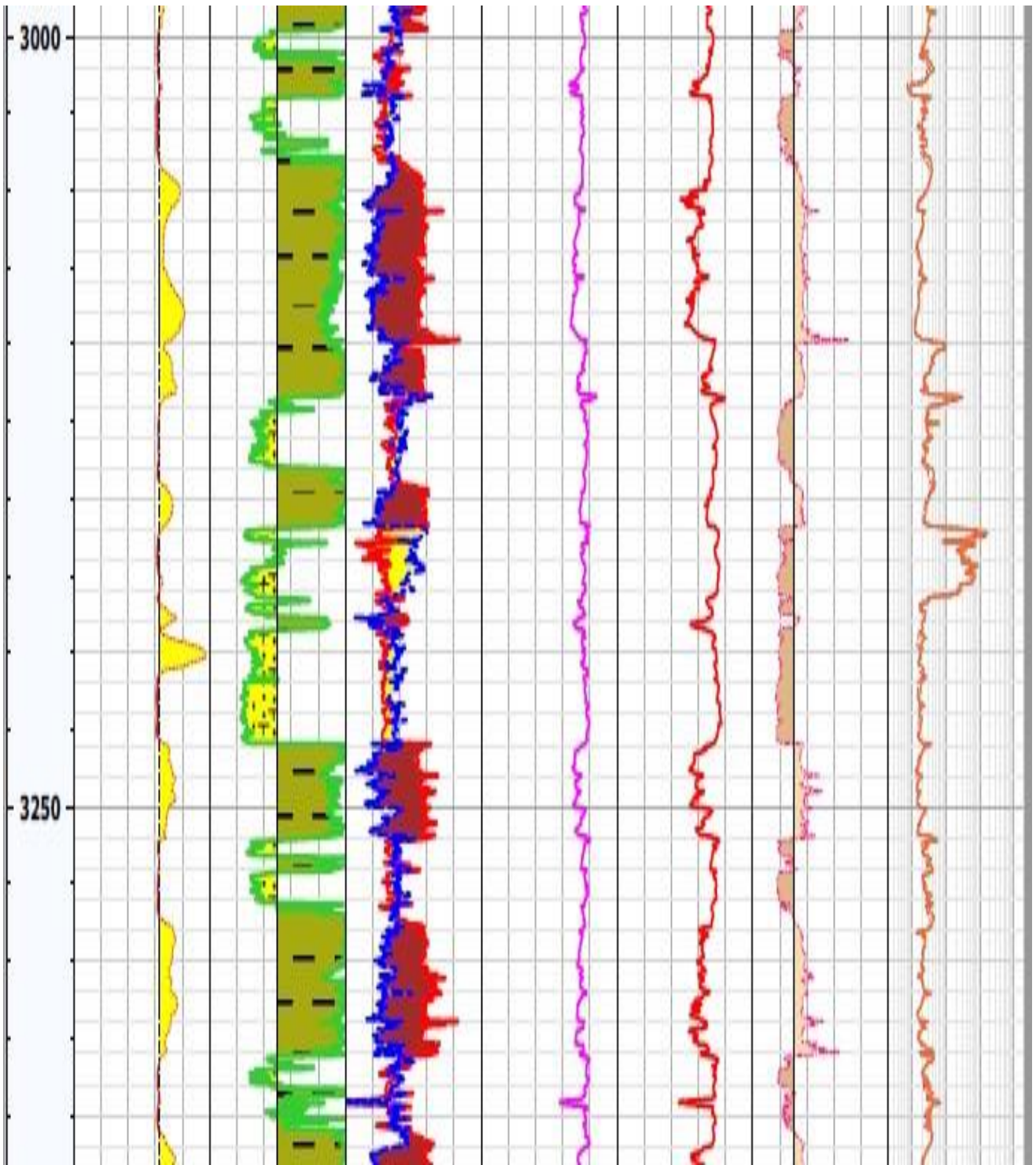




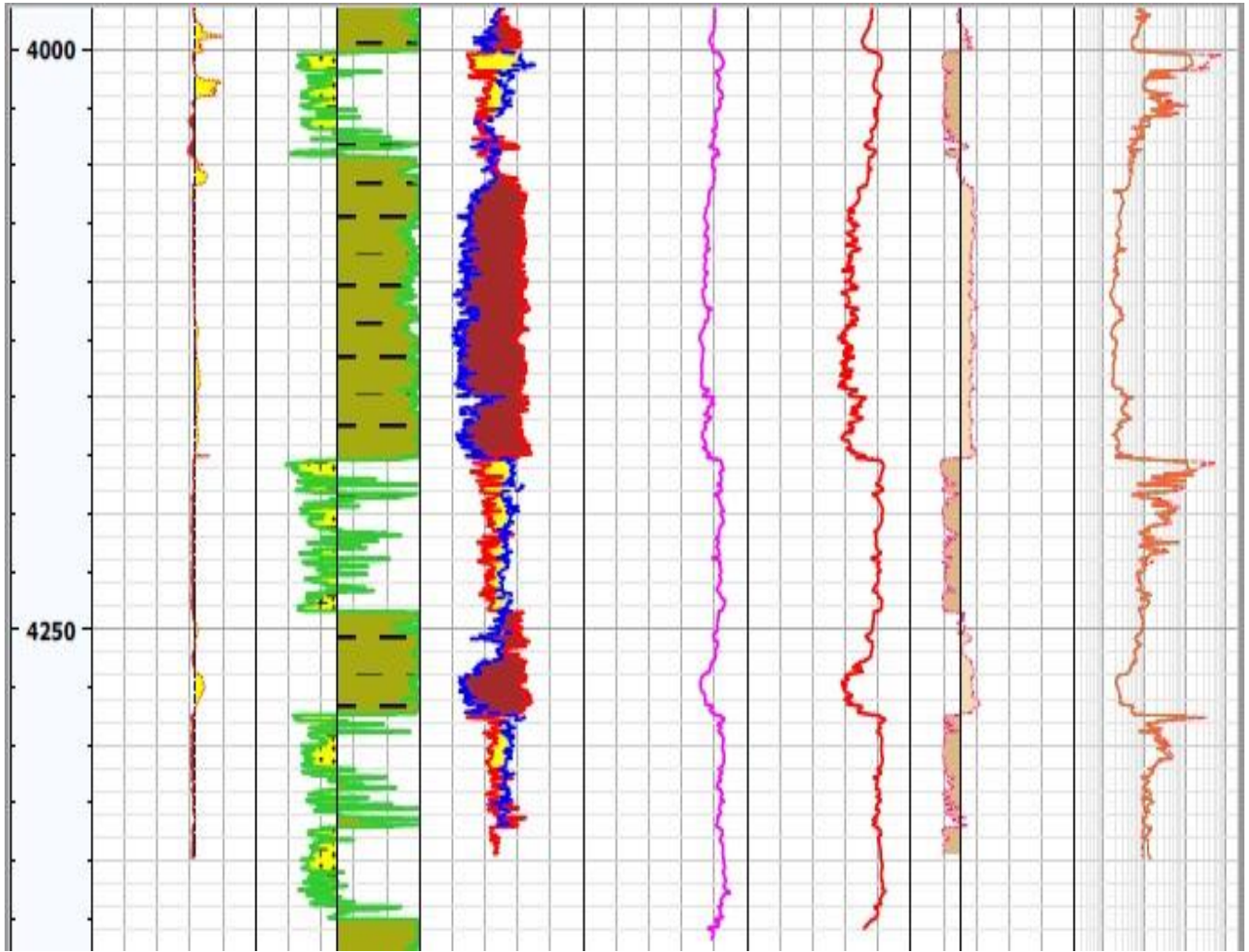
Core sections of deep reservoir interpreted in this study

# Appendix D





Well log showing Shallow reservoir from which mechanical properties were evaluated



Well log showing Deep reservoir from which mechanical properties were evaluated.

### Equations used for calculation and few examples for illustration

1.  $V_p = \frac{1}{\Delta t \text{ compression}} = \frac{1 (ft) * 0.3048}{\Delta t (\mu s) \times 10^6} = \frac{30480}{\Delta t}$
2.  $V_s = \frac{304800}{\Delta t \text{ shear}}$
3. *Poisson's Ratio* ( $\nu$ ) =  $\frac{V_p^2 - 2V_s^2}{2(V_p^2 - V_s^2)}$
4. *Shear Modulus* ( $G$ ) =  $\rho \left( \frac{g}{cc} \right) \times 100 \times V_s^2 \left( \frac{m^2}{s^2} \right)$   
 $= \frac{kg}{m^3} \cdot \frac{m^3}{s^3} = \text{Pascal} = \frac{\text{Pascal}}{10^6} = \text{MPa}$
5. *Young Modulus* ( $E$ ) =  $\frac{\rho(g/cc) \times 100 \times V_s^2 \times (3V_p^2 - 4V_s^2)}{(V_p^2 - V_s^2)}$   
 $= \frac{kg}{m^3} \cdot \frac{m^2}{s^3} = \left( \frac{m^2}{s^2} / \frac{m^2}{s^2} \right) = \text{Pascal}$

$$E = 2G (1 + \nu) \text{ Pascal}$$

$$6. \text{ Porosity } \emptyset = \frac{\rho_{matrix} - \rho_{log}}{\rho_{matrix} - \rho_{fluid}}$$

Where  $\rho_{log}$  is the bulk density

$\rho_f$  is the density of the pore fluid

$\rho_{ma}$  is the density of the sedimentary reservoir matrix

$$7. \text{ Overburden stress } (S_v) = \rho \cdot g \cdot z$$

$$= \int_0^z \rho g^z$$

where  $z$  is the depth

$\rho$  is the density

$g$  is acceleration

$$8. \text{ Overburden stress gradient} = \frac{\text{overburden stress}}{\text{depth}} = \frac{S_v}{z} \text{ in } \frac{\text{Psi}}{\text{ft}}$$

$$9. \text{ Hydrostatic Pore pressure } (P_p) = \rho \cdot g \cdot h$$

Where  $\rho$  is the density of the formation (g/cc)

$g$  is acceleration due gravity (m/s<sup>2</sup>)

$h$  is the depth in (feet)

$$10. \text{ Pascal} = \frac{N}{m^2} = \frac{kg}{m \cdot s^2}$$

$$\rho \cdot g \cdot h = \frac{g}{cm^3} \times 1000 \times \left[ \frac{kg}{m^2} \right] \cdot \left[ \frac{m}{s^2} \right] \cdot ft \times 0.3048 (m)$$

$$= \left[ \frac{kg}{m \cdot s^2} \right] \text{ Pascal}$$

$$11. \text{ Mega Pascal (MP}_a\text{)} = 10^6 \text{ Pascals} = 10 \text{ Bars} = 145.037738 \text{ Psi}$$

$$\text{Pascals} = 0.000145037738 \text{ Psi}$$

UCS correlation developed for the Niger Delta region used in this study

$$12. UCS = 0.2017 \times V^{-3.162}$$

$$13. UCS = 0.3966E + 1.1956$$

### Examples of calculation done

$$\text{At depth } 3135.024 \quad \Delta t_c = 84.8668 \mu s/ft$$

$$\Delta t_s = 145.1772 \mu s/ft$$

$$\rho_b = \rho_{log} = 2.2685 \text{ g/cc}$$

$$V_p = \frac{304800}{84.8668 \times 10^6} = 3591.51 \text{ m/s}^2$$

$$V_s = \frac{304800}{145.1772 \times 10^6} = 2099.503228 \text{ m/s}^2$$

$$\text{Poisson's ratio } (0) = \frac{(3591.51)^2 - 2(2099.50)^2}{2(3591.51)^2 - (2099.503228)^2} = 0.245$$

$$\text{Shear Modulus (G)} = 2.2685 \times 1000 \times (2099.503228)^2 = 9.9987E + 19$$

$$\text{Young Modulus (E)} = 2.2685 \times 1000 \times (2099.503228)^2 - (3591.51)^2 -$$

$$\frac{4(2099.503228)^2}{(3591.51)^2 - (2099.503228)^2} = 24807.13649 \text{ MPa}$$

$$\text{Porosity } \emptyset = \frac{2.648 - 2.2685}{2.648 - 1.1} = 0.245 \text{ no unit.}$$

$$\begin{aligned} \text{UCS (Young Modulus)} &= 0.3966 \times (2480.13649) + 1.1956 \\ &= 9839.70593 \text{ MPa} \end{aligned}$$

$$\text{Overburden stress } (S_v = \sigma_1) = 2.2109 \times 100 \times 9.8 \times 3135 \times 0.3048 \times 0.00014503778 = 3002.83627 \text{ Psi}$$

$$\text{Overburden gradient} = \frac{3002.83627}{3135} = 0.957836 \text{ Psi}$$